

# FEM-BEM procedures for elastoplastic thermo-viscoplastic contact problems

Von der Fakultät für Mathematik und Physik  
der Gottfried Wilhelm Leibniz Universität Hannover  
zur Erlangung des Grades  
Doktor der Naturwissenschaften  
Dr. rer. nat.

genehmigte Dissertation

von

Dipl.-Math. Sergey Geyn

geboren am 08.05.1981 in Tula

2007

Referent: Prof. Dr. E. P. Stephan, Gottfried Wilhelm Leibniz Universität Hannover  
Korreferent: Prof. Dr. G. Starke, Gottfried Wilhelm Leibniz Universität Hannover  
Tag der Promotion: 01.02.2007

## Abstract

The main goal of this thesis is the extension and improvement of existing methods for describing and solving thermo-mechanical problems involving the contact of bodies, plastic behavior as well as hypoelasto-viscoplasticity, which have an application in machining and metal forming processes. Besides the finite element method (FEM) also the boundary element method (BEM) and the FEM/BEM coupling are investigated as discretization procedures.

In Chapter 1 the quasistatic two-body elastoplastic contact problem with Coulomb friction is discretized using the FE/FE, BE/BE, and FE/BE coupling methods. The incremental loading procedure with Newton iterations on each time step is analyzed. Linearizations of the frictional contact and the plasticity terms as well as a description of the solution algorithms are given. As a further approach we also investigate a domain decomposition method, whereas the transmission conditions between elastic and plastic part in the work piece are incorporated via Lagrange multipliers. Furthermore additionally the distribution of temperature is modelled by a two-field approach. The above procedures are used to simulate benchmark problems in metal forming.

In Chapter 2 the quasistatic one-body hypoelasto-viscoplasticity problem subjected to the Hart's model, describing large viscoplastic and small elastic deformations, is discretized with FE and BE methods in space, using an updated Lagrange approach for the discretization in time. Here a fix point procedure on each time step is used. An explicit integration procedure of the constitutive material equations as well as a description of the solution procedure are given.

Furthermore, the thermo-mechanical two-body hypoelasto-viscoplasticity contact problem with Coulomb friction is discretized with FE/BE in space and with finite differences in time employing the updated Lagrange approach. This approach can be applied to simulate metal chipping.

Our numerical algorithms are implemented as a library within the scientific package `maiprog`s and are written in Fortran 95.

The numerical computations are realized using different discretization procedures for benchmark problems providing comparable results for FE, BE and FE/BE coupling methods.

**Key words.** FE/BE coupling, finite elements, boundary elements, frictional contact, penalty, Hart's model, updated Lagrange, large deformations

## Zusammenfassung

Das Hauptziel dieser Dissertation ist die Erweiterung und Verbesserung der vorhandenen Methoden für die Beschreibung und das Lösen thermomechanischer Probleme, welche den Kontakt der Körper, das Plastizitätsverhalten sowie das hyperelastischviskoplastische Verhalten einschließen. Anwendungsgebiete dieser Probleme findet man bei der Metallbearbeitung, zum Beispiel bei der Umformung und bei Zerspanprozessen. Die unterschiedlichen Diskretisierungsverfahren, d.h. Finite-Elemente-Methode (FEM) und Rand-Elemente-Methode (BEM) bzw. deren Kopplung, angewendet auf die oben genannten Modellprobleme, werden untersucht.

Im Kapitel 1 wird das quasistatische Kontaktproblem von zwei elastoplastischen Körpern mit Coulombscher Reibung mit FE/FE-, BE/BE- und FE/BE- Kopplungs-Methoden diskretisiert. Es wird das inkrementelle Lastverfahren mit Newtonschen Iterationen in jedem Zeitschritt verwendet. Zudem wird die Linearisierung des Kontakt- und Plastizitätsanteils angegeben und das Lösungsverfahren beschrieben. Eine Gebietszerlegungsmethode wird untersucht, wobei die Transmissionsbedingungen zwischen dem elastischen und dem plastischen Gebiet des Werkzeuges über Lagrange-Multiplikatoren eingearbeitet sind. Zudem ist die Verteilung der Temperatur mit dem two-field Verfahren modelliert. Die oben genannten Verfahren werden verwendet, um die Benchmark-Probleme bei Zerspanprozessen zu simulieren.

Im Kapitel 2 wird das quasistatische Einkörper-Problem mit dem hyperelastischviskoplastischen Stoffgesetz, welches mit dem Hartschen Modell beschrieben ist, mit FE- sowie mit BE- Methoden im Raum diskretisiert. In der Zeit wird die auf dem aktualisierten Lagrange-Verfahren basierende explizite finite Differenzen Methode angewendet. In jedem Zeitschritt wird eine Fixpunktiteration durchgeführt. Ein Verfahren zur expliziten Integration der konstitutiven Materialgleichungen sowie die Beschreibung der Lösungsverfahren werden gegeben.

Das thermomechanische hyperelastischviskoplastische Zweikörper Kontaktproblem mit Coulombscher Reibung wird mit FE/BE im Raum und mit finiten Differenzen bezüglich der Zeit diskretisiert. Die Referenzkonfiguration wird nach jedem Zeitschritt gemäß des aktualisierten Lagrange'sche Verfahrens erneuert.

Die numerischen Algorithmen sind als interne Bibliothek innerhalb des Softwarepaketes `maipros` in Fortran 95 realisiert.

Die numerischen Berechnungen für die verschiedenen Diskretisierungsverfahren liefern vergleichbare Ergebnisse.

**Schlagerworte:** FE/BE-Kopplung, Finite Elemente, Randelemente, Reibungskontakt, Penalty, Hartmodell, updated Lagrange, große Verformungen

# Acknowledgments

It is a great pleasure for me to thank my advisor, Prof. Dr. Ernst P. Stephan, for inspiring me to work in this area. I am very grateful to him for his intensive guidance during my work, for helpful discussions and important remarks. Also I would like to thank PD Dr. Matthias Maischak for his support and help in the programming. His software package `maiprogs` became a basis for the implementation of the numerical experiments, presented in the thesis.

Furthermore, I would like to give my thanks to the members of our working group in the Institute of Applied Mathematics, Gottfried Wilhelm Leibniz University of Hanover, for the friendly and stimulating atmosphere.

This thesis was supported by the *DFG grant no. STE 573/5-1* and *DFG grant no. STE 573/7-1*.

Hanover, December 2006

Sergey Geyn



# Contents

<b>Introduction</b>	<b>13</b>
<b>1 Elastoplastic contact problems. Small deformations</b>	<b>17</b>
1.1 Weak and penalty formulations . . . . .	17
1.2 Discretization and solution procedure (incremental loading) . . . . .	30
1.2.1 FEM/FEM . . . . .	30
1.2.2 BEM/BEM . . . . .	34
1.2.3 FEM/BEM . . . . .	39
1.3 Linearizations of contact and elastoplasticity . . . . .	40
1.4 Contact functional investigation . . . . .	48
1.5 A Newton-type method for two-body elastoplastic contact with friction .	57
1.6 Newton-like iterations for two-body elastoplastic contact with friction . .	65
1.7 Numerical simulations . . . . .	72
1.8 FEM/BEM domain decomposition for frictional contact . . . . .	82
1.8.1 Weak formulations . . . . .	83
1.8.2 Discretization . . . . .	86
1.8.3 Linearization . . . . .	87
1.8.4 Numerical simulations . . . . .	91
1.9 FE/BE coupling for thermoelastic contact problems . . . . .	92
1.9.1 Weak formulation . . . . .	95
1.9.2 Operator splitting, discretization and solution procedure . . . . .	98
1.9.3 Numerical simulation . . . . .	99
<b>2 Hypoelasto-viscoplasticity. Large deformations</b>	<b>103</b>
2.1 The equilibrium equation . . . . .	103
2.2 Hart's constitutive equations for hypoelasto-viscoplasticity . . . . .	106
2.3 Time integration . . . . .	108
2.4 Updated Lagrange approach . . . . .	110
2.5 A boundary element method for hypoelasto-viscoplasticity . . . . .	111
2.5.1 Integral operators . . . . .	111
2.5.2 Discretization . . . . .	117
2.5.3 Benchmarks . . . . .	118
2.5.4 Implementation . . . . .	121
2.5.5 Discretization with finite elements . . . . .	124

2.6	Boundary element and finite element procedures for metal chipping . . .	125
2.6.1	Viscoplastic thermomechanical coupling . . . . .	125
2.6.2	Benchmarks . . . . .	128
<b>3</b>	<b>Appendix</b>	<b>133</b>
3.1	Implementation . . . . .	133
3.1.1	Boundary operators and volume potentials . . . . .	133
3.1.2	Hypoelasto-viscoplasticity . . . . .	140
	<b>Bibliography</b>	<b>143</b>



# List of Figures

1.1	Admissible region of traction . . . . .	48
1.2	Elastic and plastic regions of penetration . . . . .	48
1.3	FE/FE: deformed mesh . . . . .	73
1.4	FE/FE: $\ \boldsymbol{\varepsilon}^p\ $ . . . . .	73
1.5	FE/BE: deformed mesh . . . . .	73
1.6	FE/BE: $\ \boldsymbol{\varepsilon}^p\ $ . . . . .	73
1.7	FE/FE, FE/BE: $\ \boldsymbol{\varepsilon}^p\ $ . . . . .	74
1.8	Characteristic points . . . . .	75
1.9	Geometry . . . . .	75
1.10	incremental loading of $u_y$ at segment $\overline{(-2, -3), (2, -3)}$ . . . . .	75
1.11	FE/FE: deformed mesh . . . . .	76
1.12	FE/FE: $\ \boldsymbol{\varepsilon}^p\ $ . . . . .	76
1.13	FE/BE: deformed mesh . . . . .	76
1.14	FE/BE: $\ \boldsymbol{\varepsilon}^p\ $ . . . . .	76
1.15	BE/BE: deformed mesh . . . . .	76
1.16	BE/BE: $\ \boldsymbol{\varepsilon}^p\ $ . . . . .	76
1.17	FE/FE, FE/BE, BE/BE: $\ \text{dev } \boldsymbol{\sigma}\ $ . . . . .	77
1.18	FE/BE: $\ \text{dev } \boldsymbol{\sigma}\ $ for different mesh sizes . . . . .	77
1.19	Error of $\ \text{dev } \boldsymbol{\sigma}\ $ . . . . .	77
1.20	$\ \text{dev}[\boldsymbol{\sigma}]\ $ at $X_1 = (-1, -1)$ . . . . .	78
1.21	$\ \text{dev}[\boldsymbol{\sigma}]\ $ at $X_2 = (-1, -1.1)$ . . . . .	78
1.22	$\ \text{dev}[\boldsymbol{\sigma}]\ $ at $X_3 = (1, -1.1)$ . . . . .	78
1.23	$\ \text{dev}[\boldsymbol{\sigma}]\ $ at $X_4 = (1, -1)$ . . . . .	78
1.24	$\ \text{dev}[\boldsymbol{\sigma}]\ $ at $X_5 = (0, -1.75)$ . . . . .	78
1.25	$\ \text{dev}[\boldsymbol{\sigma}]\ $ at $X_6 = (-1, -1.5)$ . . . . .	78
1.26	$\ \text{dev}[\boldsymbol{\sigma}]\ $ at $X_7 = (-1, -2.5)$ . . . . .	79
1.27	$\ \text{dev}[\boldsymbol{\sigma}]\ $ at $X_8 = (1, -1.5)$ . . . . .	79
1.28	$\ \text{dev}[\boldsymbol{\sigma}]\ $ at $X_9 = (1, -2.5)$ . . . . .	79
1.29	$\ \text{dev}[\boldsymbol{\sigma}]\ $ at $X_{10} = (0, -1)$ . . . . .	79
1.30	$\ \text{dev}[\boldsymbol{\sigma}]\ $ at $X_{11} = (0, -2)$ . . . . .	79
1.31	$\ \text{dev}[\boldsymbol{\sigma}]\ $ at $X_{12} = (0, -3)$ . . . . .	79
1.32	$u_x$ at $X_1 = (-1, -1)$ . . . . .	80
1.33	$u_x$ at $X_2 = (-1, -1.1)$ . . . . .	80

1.34	$u_x$ at $X_3 = (1, -1.1)$	80
1.35	$u_x$ at $X_4 = (1, -1)$	80
1.36	$u_x$ at $X_5 = (0, -1.75)$	80
1.37	$u_x$ at $X_6 = (-1, -1.5)$	80
1.38	$u_x$ at $X_7 = (-1, -2.5)$	81
1.39	$u_x$ at $X_8 = (1, -1.5)$	81
1.40	$u_x$ at $X_9 = (1, -2.5)$	81
1.41	$u_x$ at $X_{10} = (0, -1)$	81
1.42	$u_x$ at $X_{11} = (0, -2)$	81
1.43	$u_x$ at $X_{12} = (0, -3)$	81
1.44	The model geometry	82
1.45	deformed mesh	93
1.46	$\ \boldsymbol{\varepsilon}^p\ $	93
1.47	$x$ -component of the displacement: $u_x$	93
1.48	$y$ -component of the displacement: $u_y$	93
1.49	$\ \text{dev } \boldsymbol{\sigma}\ $	93
1.50	$\sigma_{xx}$	93
1.51	$\sigma_{xy}$	93
1.52	$\sigma_{yy}$	93
1.53	16 increments of 2nd tangent cycle	100
1.54	End of simulation	101
2.1	Flow chart. Hart's model regularization	109
2.2	FEM-BEM comparison ( $\sigma_{xx}$ )	119
2.3	FEM-BEM comparison ( $\sigma_{yy}$ )	119
2.4	Convergence of BEM approach	119
2.5	Convergence of FEM approach	119
2.6	FEM (after 50 second simulation)	120
2.7	BEM (after 30 second simulation)	121
2.8	Flow chart. BEM discretization	123
2.9	Flow chart. FEM discretization	124
2.10	Model problem	127
2.11	Metal chipping	131

# List of Tables

1.1	Material data . . . . .	73
1.2	Contact parameters . . . . .	73
2.1	Material data . . . . .	118



# Introduction

Based on the work by Wriggers and Miehe [51], Peric and Owen [40], and Costabel and Stephan [23, 24] we introduce finite element (FE), boundary element (BE) and FE/BE coupling procedures for friction contact problems in elastoplasticity. In our approach we use the radial return algorithm (see Simo and Hughes [43], Simo and Miehe [44]) for both plastification of the material and contact. Here, we study small deformations and therefore can model the linear elastic parts by standard BEM with the linear elastic fundamental solution. Our numerical results demonstrate clearly that pure FEM, pure BEM and FE/BE coupling approaches give relevant numerical simulations.

The framework of Glowinski [28] supplies an abstract and a numerical (FE) analysis for nonlinear variational problems. The work of Eck and Jarušek [26] provides existence and regularity results for the static one body contact problem with Coulomb friction. The existence, uniqueness and regularity results for boundary value problems of the plastic flow theory are given in the book by Korneev and Langer [34]. This work also provides foundations for FE analysis of quasistatic plastic flows. Existence, uniqueness and stability results are obtained in the work of Han and Reddy [29] for the one body associated elastoplastic problem. Moreover, they prove the convergence results for discrete versions. The work of Blaheta et. al. [5, 6, 2] is devoted to the investigation of convergence of discretized problems, namely convergence of the Newton and Newton-like methods for FE discretization of the one body associated elastoplasticity problem.

For the theoretical background of the boundary integral equations and the Galerkin boundary element methods (BEM) for linear problems we refer to the book of Sauter and Schwab [42]. The coupling technique of boundary element method and finite element methods are described in work by Stephan [48], Carstensen and Stephan [15]. In the works of Brebbia et. al. [9, 13, 10, 11] one can find extension of the boundary element techniques for solving nonlinear elastoplastic problems. These approaches are based on the heuristical collocation method. An application of the boundary element method to elastoplastic unilateral contact problems with friction was suggested by Polizzotto and Zitto [41]. Theoretical and numerical investigations for the one-body quasistatic elastoplastic problem are done by Alberty [1]. Theoretical and numerical investigations of the time-discretized one-body quasistatic elastoplastic problem with a non-penetration contact constraint are done by Zarrabi [53].

Based on the series of papers by Mukherjee [39], Chandra and Mukherjee [16, 17, 18] we

introduce finite element, boundary element and FE/BE coupling procedures for metal-forming and metal chipping. As in [30, 32, 31] we consider Hart's constitutive model, which describes hypoelasto-viscoplasticity [4]. We use the updated Lagrange approach in order to pose the equilibrium equation of the media, i.e. the equilibrium equation of the body and constitutive conditions on the time interval  $(t, t + dt)$  are given employing the pure Lagrange approach with the reference configuration coinciding with the actual one taken at time  $t$ . Discretizing the problem in time one obtains the set of problems at discrete time points  $t_n$ , whereas the mesh has to be updated corresponding to the updated Lagrange description as soon as the new actual configuration is known.

This thesis is organized as follows. In **Chapter 1** we consider two-body contact problems in elastoplasticity with and without friction and present solution procedures based on finite element and boundary element methods. We formulate the weak elastoplastic contact problem in Section 1.1 and derive its penalty approximation. We discretize the penalty weak formulation in time as well as in space in Section 1.2.

The predictor-corrector solution procedure for the elastoplastic contact problem is considered in Section 1.1. The radial return mapping algorithm is used to handle both contact conditions and plastification. We describe in detail a segment-to-segment contact discretization, which allows also to model friction.

The linearization of contact and plastic terms in the equilibrium equation is derived in Section 1.3. In Section 1.2 we provide the FEM/FEM, BEM/BEM and FEM/BEM, respectively, discretization procedures of two-body elastoplastic frictional contact (Problem 1.1.4). In Section 1.4 we extend the return mapping algorithm for elastoplasticity, which is carried out in [5] in order to investigate the contact return mapping algorithm. In Section 1.5 we prove the convergence of the Newton method introduced in Section 1.2 for elastoplasticity with frictional contact using the results obtained in Section 1.4 and in [5]. In Section 1.6 we extend the Newton-like iterations introduced in [6] onto elastoplasticity with frictional contact. Using the results obtained in Section 1.4 and in [6] we prove the convergence of extended Newton-like iterations. The approaches given cover small deformations. Numerical simulations in Section 1.7 demonstrate the wide applicability of our approaches described in Sections 1.2.1, 1.2.2, 1.2.3. In Section 1.8 we extend the coupling procedures introduced in Section 1.2. We decompose one body (that is subjected to the elastoplastic material law) into a purely elastic domain and an elastoplastic domain. Using Lagrange multipliers (cf. [49]) on the interface boundary we obtain a coupling formulation. Section 1.8.4 is devoted to the FE-BE-FE (elastic body is discretized with BE; elastoplastic body is decomposed into 2 subdomains, the linear elastic is with FE, whereas the elastoplastic with BE) simulations of our approaches given in Section 1.8.1. In Section 1.9 we consider a two-body thermo-elastic frictional contact problem, as in Sections 1.2, 1.8 the contact conditions are regularized using the penalty method. We end up Section 1.9 with Subsection 1.9.3, where we present the numerical simulation of the solution procedure introduced in Section 1.9.2.

In **Chapter 2** we consider the application of Hart's model for hypoelasto-viscoplasticity to contact problems. We start by providing a theoretical background of a continuum mechanic description of large deformations (Section 2.1) as well as Hart's constitutive equations (Section 2.2). The integration of the material law is done via an explicit finite difference scheme in time in Section 2.3. We apply the updated Lagrange approach in Section 2.4. Employing the update Lagrange approach we derive in Section 2.5 the space discretization using BE discretization of the problem posed in Section 2.1 under Hart's material law, which is integrated in time in Section 2.3. In Section 2.5.3 we present a numerical simulation: stretching a square plate. The problem is discretized using FE and BE methods. In Section 2.6 we consider a two-body contact problem under Hart's constitutive conditions coupled with heat conduction. In Section 2.6 we pose the thermo-mechanical weak formulation in rate form. In Section 2.6.2 we present two benchmark problems: in Example 1 we consider FEM-BEM coupling for one a body problem; in Example 2 we consider the metal chipping process using FEM-BEM coupling, whereas the work tool is discretized with BE and work piece with FE in space. The work tool in our simulation is supposed to be purely elastic.

The appendix is devoted to the implementation of the boundary integral operators, the volume potentials as well as the finite element method for large deformations.





# 1 Elastoplastic contact problems.

## Small deformations

We consider two-body contact problems in elastoplasticity with and without friction and present solution procedures based on finite elements and boundary elements. The radial return mapping algorithm is used to handle both contact conditions and plastification. We describe in detail a segment-to-segment contact discretization which allows also to treat friction. The approaches given cover small deformations. Numerical benchmarks demonstrate the wide applicability of our approaches.

Following Costabel and Stephan [23, 24] we introduce boundary element and FE/BE coupling procedures for friction contact problems in elastoplasticity. We consider associated von Mises plasticity as described e.g. in [43]. We perform incremental loading in connection with Newton method and radial return for the contact problem formulated as the penalty method we consider all three cases: pure FEM simulation, pure BEM simulations and simulations with FEM/BEM coupling. In all cases we show convergence for the Newton scheme by extending the analysis of Blaheta [5] (which was done for FEM simulations of plasticity) to contact problems. As a further solution procedure we use a domain decomposition method splitting the regions under the investigation into elastic and plastic parts and use Lagrangian multipliers on the interface and then again apply incremental loading. Our numerical experiments for benchmarks problems show comparable results for FEM and BEM simulations. Furthermore, we consider a staggered scheme where we consider an elastic material under heating leading to a difference scheme for the heat equation and the FE-BE discretizations of the elastic contact, which is included in the above formulations.

### 1.1 Weak and penalty formulations

We consider two deformable elasto-plastic bodies  $A$  and  $B$  occupying Lipschitz domains  $\Omega^A, \Omega^B \subset \mathbb{R}^2$  in the small deformation formulation. They can be disjoint or touch each other along their boundaries. We denote one body as 'slave' ( $B$ ), the other as 'master' ( $A$ ). The choice is symmetric, i.e. we can change notations vice versa. This concept is essential for the treatment of contact conditions. We assume, that the boundary of the

domain  $\Omega^i$ , ( $i = B, A$ ) consists of 3 disjoint parts: a part with prescribed displacements  $\Gamma_D^i$ , one with prescribed tractions  $\Gamma_N^i$  and a part  $\Gamma_C^i$  - zone of probable contact, i.e.  $\Gamma^i = \partial\Omega^i = \overline{\Gamma}_D^i \cup \overline{\Gamma}_N^i \cup \overline{\Gamma}_C^i$ . Define  $\Sigma^i := \Gamma_N^i \cup \Gamma_C^i$ . We admit the bodies to have some micro-interpenetration in the contact zone, which allows us to construct contact conditions. Let  $\mathbf{x}^B, \mathbf{x}^A \in \mathbb{R}^2$  be the coordinates of the corresponding bodies. We parameterize the master surface by the natural parameter  $\zeta^A$  and slave surface with  $\zeta^B$ .

Next, we introduce some function spaces needed for the formulation of the elastoplastic contact problem. We define the space of stresses

$$S := \{ \boldsymbol{\tau} \mid \boldsymbol{\tau} \in \mathbb{R}_{sym}^{3 \times 3} \}, \quad \text{where } \mathbb{R}_{sym}^{3 \times 3} := \{ \boldsymbol{x} \in \mathbb{R}^{3 \times 3} \mid \forall i, j = 1, 2, 3 \ x_{ij} = x_{ji} \}, \quad (1.1)$$

$$\mathbf{S}(\Omega) := \{ \boldsymbol{\tau} \mid \boldsymbol{\tau} : \Omega \rightarrow S. \forall i, j \in \overline{1, 3} \ \tau_{ij} \in L^2(\Omega) \}, \quad (1.2)$$

the space of plastic strains

$$Q_0 := \{ \boldsymbol{\varepsilon} \mid \boldsymbol{\varepsilon} \in S. \ \text{tr } \boldsymbol{\varepsilon} = 0 \}, \quad \text{where } \text{tr } \boldsymbol{\varepsilon} := \varepsilon_{ii}, \quad (1.3)$$

$$\mathbf{Q}_0(\Omega) := \{ \boldsymbol{\varepsilon} \mid \boldsymbol{\varepsilon} : \Omega \rightarrow S. \forall i, j \in \overline{1, 3} \ \varepsilon_{ij} \in L^2(\Omega). \ \text{tr } \boldsymbol{\varepsilon} = 0 \ \text{a.e. in } \Omega \}, \quad (1.4)$$

the spaces of internal variables

$$\mathbf{M}^i := \{ \boldsymbol{\mu} \mid \boldsymbol{\mu} \in \mathbb{R}^{m_i} \} \quad (1.5)$$

$$\mathbf{M}^i(\Omega) := \{ \boldsymbol{\mu} \mid \boldsymbol{\mu} : \Omega \rightarrow \mathbb{R}^{m_i}. \forall j \in \overline{1, m_i} \ \mu_j \in L^2(\Omega) \}, \quad (1.6)$$

the space of admissible generalized stresses  $(\boldsymbol{\tau}, \boldsymbol{\mu})$

$$\mathcal{P}^i := \{ (\boldsymbol{\sigma}, \boldsymbol{\chi}) \in S \times M^i \mid \phi_{pl}^i(\boldsymbol{\sigma}, \boldsymbol{\chi}) \leq 0 \}, \quad (1.7)$$

$$\mathcal{P}^i(\Omega^i) := \{ (\boldsymbol{\sigma}, \boldsymbol{\chi}) \in \mathbf{S}(\Omega^i) \times \mathbf{M}^i(\Omega^i) \mid \phi_{pl}^i(\boldsymbol{\sigma}, \boldsymbol{\chi}) \leq 0 \ \text{a.e. in } \Omega^i \}, \quad (1.8)$$

the space of generalized strains  $(\boldsymbol{\varepsilon}^p, \boldsymbol{\xi})$

$$K^i := \{ (\boldsymbol{\varepsilon}^p, \boldsymbol{\xi}) \in Q_0 \times M^i \}, \quad (1.9)$$

$$\mathbf{K}^i(\Omega^i) := \{ (\boldsymbol{\varepsilon}^p, \boldsymbol{\xi}) \in \mathbf{Q}_0(\Omega^i) \times \mathbf{M}^i(\Omega^i) \}. \quad (1.10)$$

Here we have used a notation  $\overline{1, m} := \{n\}_1^m$  to define a set of integers from 1 to  $m$ . Now we give the elastoplastic in its strong form

**Problem 1.1.1.** *For given time interval of interest  $(0, T)$ , given friction coefficient  $\mu_f \in [0, 1/2)$ , displacements  $\hat{\mathbf{u}}^i : [0, T] \rightarrow (H^{1/2}(\Gamma_D^i))^2$ , boundary traction  $\hat{\mathbf{t}}^i : [0, T] \rightarrow (H^{-1/2}(\Gamma_N^i))^2$ , volume forces  $\hat{\mathbf{f}}^i : [0, T] \rightarrow (H^{-1}(\Gamma_N^i))^2$ , free energy scalar functions  $\psi^i(\boldsymbol{\varepsilon}^{ie}, \boldsymbol{\xi}^i)$ ,  $\psi^i : S \times M^i \rightarrow \mathbb{R}_+$  and their decompositions  $\psi^i(\boldsymbol{\varepsilon}^{ie}, \boldsymbol{\xi}^i) = \psi^{ie}(\boldsymbol{\varepsilon}^{ie}) + \psi^{ip}(\boldsymbol{\xi}^i)$ , scalar yield function for elastoplasticity  $\phi_{pl}^i(\boldsymbol{\sigma}^i, \boldsymbol{\chi}^i)$ ,  $\phi_{pl}^i : S \times M^i \rightarrow \mathbb{R}$  and initial values  $(\mathbf{u}^i(0), \boldsymbol{\varepsilon}^{ip}(0), \boldsymbol{\xi}^i(0)) = (\mathbf{0}, \mathbf{0}, \mathbf{0})$  we consider the following elastoplastic contact problem*

with contact boundary  $\Gamma_C$ :

Find  $(\mathbf{u}^i, \boldsymbol{\varepsilon}^{ip}, \boldsymbol{\xi}^i) : [0, T] \rightarrow (H^1(\Omega^i))^2 \times S(\Omega^i) \times M^i(\Omega^i)$  satisfying the classical formulation for the elastoplastic frictional contact problem:

$$\left. \begin{aligned} -\operatorname{div} \boldsymbol{\sigma}^i &= \hat{\mathbf{f}}^i && \text{in } [0, T] \times \Omega^i, \\ \mathbf{u}^i &= \hat{\mathbf{u}}^i && \text{on } [0, T] \times \Gamma_D^i, \\ \mathbf{t}^i &= \hat{\mathbf{t}}^i && \text{on } [0, T] \times \Gamma_N^i, \end{aligned} \right\} \text{in } [0, T] \times \Omega^i, \quad i = A, B, \quad (1.11)$$

$$\left. \begin{aligned} \mathbf{n}^A \cdot (\mathbf{n}^A \cdot \boldsymbol{\sigma}^A) &= \mathbf{n}^B \cdot (\mathbf{n}^B \cdot \boldsymbol{\sigma}^B) =: \sigma_N, \\ &\text{if } u_N^{AB} = g, \text{ then } \sigma_N < 0, \\ \boldsymbol{\sigma}^A \cdot \mathbf{n}^A - \sigma_N \mathbf{n}^A &= -(\boldsymbol{\sigma}^B \cdot \mathbf{n}^B - \sigma_N \mathbf{n}^B) =: \boldsymbol{\sigma}_T \\ \sigma_T &:= \boldsymbol{\sigma}_T \cdot \mathbf{e}^A, \\ &\text{if } |\sigma_T| < \mu_f |\sigma_N|, \text{ then } u_T = 0, \\ &\text{if } |\sigma_T| = \mu_f |\sigma_N|, \text{ then } \exists \lambda_C \geq 0 : u_T^{AB} = -\lambda_C \sigma_T \end{aligned} \right\} \text{on } [0, T] \times \Gamma_C, \quad (1.12)$$

$$\left. \begin{aligned} \boldsymbol{\varepsilon}^i(\mathbf{u}^i) &= \boldsymbol{\varepsilon}(\mathbf{u}^i) = 1/2(\nabla \mathbf{u}^i + (\nabla \mathbf{u}^i)^T), \\ \boldsymbol{\sigma}^i &= \frac{\partial \psi^{ie}}{\partial \boldsymbol{\varepsilon}^{ie}}, \\ \boldsymbol{\chi}^i &= -\frac{\partial \psi^{ip}}{\partial \boldsymbol{\xi}^i}, \\ \exists \lambda_p^i \geq 0 \quad \dot{\boldsymbol{\varepsilon}}^{ip} &= \lambda_p^i \frac{\partial \phi_{pl}^i}{\partial \boldsymbol{\sigma}^i}, \\ \dot{\boldsymbol{\xi}}^{ip} &= \lambda_p^i \frac{\partial \phi_{pl}^i}{\partial \boldsymbol{\chi}^i}, \\ \lambda_p^i &\geq 0, \phi_{pl}^i \leq 0, \lambda_p^i \phi_{pl}^i = 0, \\ &\text{when } \phi_{pl}^i = 0, \text{ then } \lambda_p^i \geq 0, \dot{\phi}_{pl}^i \leq 0, \lambda_p^i \dot{\phi}_{pl}^i = 0 \end{aligned} \right\} \text{in } [0, T] \times \Omega^i, \quad i = A, B, \quad (1.13)$$

where  $\boldsymbol{\sigma}^i$  denotes the stress tensor,  $\boldsymbol{\varepsilon}^{ip}$  denotes the plastic part of the strain in the domain  $\Omega^i$ ,  $u_N^{AB}$  denotes the jump of the normal displacement  $u_N^i := \mathbf{u}^i \cdot \mathbf{n}^A$  and  $u_T^{AB}$  stands for the jump of the tangential displacement  $u_T^i := \mathbf{u}^i \cdot \mathbf{e}^A$  through  $\Gamma_C$ , namely

$$\begin{aligned} u_N^{AB} &:= u_N^A - u_N^B \equiv \mathbf{u}^A \cdot \mathbf{n}^A + \mathbf{u}^B \cdot \mathbf{n}^A, \\ u_T^{AB} &:= u_T^A - u_T^B \equiv \mathbf{u}^A \cdot \mathbf{e}^A + \mathbf{u}^B \cdot \mathbf{e}^A, \end{aligned}$$

denoting with  $\mathbf{n}^A, \mathbf{e}^A$  the outer normal and tangential unit vectors to  $\Gamma_C^A$ . with the gap function  $g : \Gamma_C \subset \mathbb{R}^2 \rightarrow \mathbb{R}_{\geq 0}$  describing the initial distance between the two bodies in normal direction,  $\mu_f$  - coefficient of friction.

Introducing the dissipation functions  $D^i : K^i \rightarrow \mathbb{R} \cup \{+\infty\}$

$$D^i(\dot{\boldsymbol{\varepsilon}}^{ip}, \dot{\boldsymbol{\xi}}^i) := \sup \left\{ \dot{\boldsymbol{\varepsilon}}^{ip} : \boldsymbol{\sigma}^i + \dot{\boldsymbol{\xi}}^i : \boldsymbol{\chi}^i \mid (\boldsymbol{\sigma}^i, \boldsymbol{\chi}^i) \in \mathcal{P}^i \right\}. \quad (1.14)$$

Then the equivalent form of plastic constraints (1.13) is

$$\left. \begin{aligned} \boldsymbol{\varepsilon}^i(\mathbf{u}^i) &= \boldsymbol{\varepsilon}(\mathbf{u}^i) = 1/2(\nabla \mathbf{u}^i + (\nabla \mathbf{u}^i)^T), \\ \boldsymbol{\sigma}^i &= \frac{\partial \psi^{ie}}{\partial \boldsymbol{\varepsilon}^{ie}}, \\ \boldsymbol{\chi}^i &= -\frac{\partial \psi^{ip}}{\partial \boldsymbol{\xi}^i}, \\ (\dot{\boldsymbol{\varepsilon}}^{ip}, \dot{\boldsymbol{\xi}}^i) &\in \text{dom } D^i, \\ (\boldsymbol{\sigma}^i, \boldsymbol{\chi}^i) &\in \partial D^i(\dot{\boldsymbol{\varepsilon}}^{ip}, \dot{\boldsymbol{\xi}}^i), \end{aligned} \right\} \text{ in } \Omega^i, \quad i = A, B. \quad (1.15)$$

*Remark 1.1.1.* Later we will use specific representations of the free energy function.

1. Elastic behavior:

$$\psi^e(\boldsymbol{\varepsilon}^e) := \frac{1}{2} \boldsymbol{\varepsilon}^e : \mathbb{C} : \boldsymbol{\varepsilon}^e, \quad (1.16)$$

where  $\mathbb{C} : \mathbb{R}_{sym}^{3 \times 3} \rightarrow \mathbb{R}_{sym}^{3 \times 3}$  is the elastic Hooke's tensor. In case of isotropic, homogeneous media it is completely defined by two Lamé constants  $\lambda, \mu > 0$ , such that

$$\boldsymbol{\sigma} = \frac{\partial \psi^e}{\partial \boldsymbol{\varepsilon}^e} = \mathbb{C} : \boldsymbol{\varepsilon}^e = \lambda \mathbf{1} \text{tr } \boldsymbol{\varepsilon}^e + 2\mu \boldsymbol{\varepsilon}^e. \quad (1.17)$$

2. Plastic behavior:

- for a purely elastic body we do not have any yield function and set

$$\psi^p(\boldsymbol{\xi}) := 0. \quad (1.18)$$

- von Mises plasticity with linear isotropic hardening ( $\boldsymbol{\xi} = \{\xi\}, \boldsymbol{\chi} = \{\chi\}$ )

$$\psi^p(\xi) := \frac{1}{2} k_2 \xi^2. \quad (1.19)$$

The yield function is

$$\phi_{pl}(\boldsymbol{\sigma}, \chi) := \|\operatorname{dev} \boldsymbol{\sigma}\| - \sqrt{\frac{2}{3}}(\sigma_Y - \chi), \quad (1.20)$$

where the given constants  $\sigma_Y > 0$  and  $k_2 > 0$  are the yield stress and the isotropic hardening parameter, respectively.

- von Mises plasticity with linear kinematic hardening

Internal variable in this situation is nothing more than plastic strain

$$\boldsymbol{\xi} = \boldsymbol{\varepsilon}^p. \quad (1.21)$$

$$\psi^p(\boldsymbol{\varepsilon}^p) := \frac{1}{2}k_1\|\boldsymbol{\varepsilon}^p\|^2. \quad (1.22)$$

The yield function is

$$\phi_{pl}(\boldsymbol{\sigma}, \boldsymbol{\chi}) := \|\operatorname{dev} \boldsymbol{\sigma} + \boldsymbol{\chi}\| - \sqrt{\frac{2}{3}}\sigma_Y, \quad (1.23)$$

where the given constants  $\sigma_Y > 0$  and  $k_1 > 0$  are the yield stress and the kinematic hardening parameter, respectively.

- von Mises plasticity with combined linear kinematic / isotropic hardening

We denote for clearness the internal variables

$$\boldsymbol{\xi} = (\boldsymbol{\varepsilon}^p, \alpha) \quad (1.24)$$

and the conjugate forces

$$\boldsymbol{\chi} = (\boldsymbol{a}, \vartheta). \quad (1.25)$$

Then the plastic free energy function is

$$\psi^p(\boldsymbol{\varepsilon}^p, \alpha) := \frac{1}{2}k_1\|\boldsymbol{\varepsilon}^p\|^2 + \frac{1}{2}k_2|\alpha|^2 \quad (1.26)$$

and the yield function is

$$\phi_{pl}(\boldsymbol{\sigma}, \boldsymbol{\chi}) := \|\operatorname{dev} \boldsymbol{\sigma} + \boldsymbol{a}\| - \sqrt{\frac{2}{3}}(\sigma_Y - \vartheta), \quad (1.27)$$

where the given constants  $\sigma_Y > 0$ ,  $k_1 > 0$ ,  $k_2 > 0$  are the yield stress and the kinematic and isotropic hardening parameters.

Taking into account Remark 1.1.1 we write formally the plastic part of the free energy

function as

$$\psi^p = \frac{1}{2} \boldsymbol{\xi} : \mathbb{H} : \boldsymbol{\xi}, \quad (1.28)$$

where  $\mathbb{H} = \begin{pmatrix} k_1 \mathbf{I} & 0 \\ 0 & k_2 \end{pmatrix}$  for von Mises plasticity with linear isotropic/kinematic hardening.

We write in the sequel  $\mathbf{t}_C := \sigma_{\mathcal{N}} \mathbf{n}^A + \sigma_{\mathcal{T}} \mathbf{e}^A$  for the boundary traction and use the space of displacement test functions

$$\mathbf{V}_0(\Omega^i) := \left\{ \mathbf{u} \in [H^1(\Omega^i)]^2 \mid \mathbf{u}|_{\Gamma_D^i} = 0 \right\} \quad (1.29)$$

and the space of displacement ansatz functions

$$\mathbf{V}_D(\Omega^i) := \left\{ \mathbf{u} \in [H^1(\Omega^i)]^2 \mid \mathbf{u}|_{\Gamma_D^i} = \hat{\mathbf{u}} \right\}. \quad (1.30)$$

Next, we introduce some bilinear forms which are used in the weak formulations of Problem 1.1.1:

$$\begin{aligned} \bar{a} : \mathbf{S}(\Omega^i) \times \mathbf{S}(\Omega^i) &\rightarrow \mathbb{R}, & \bar{a}(\boldsymbol{\sigma}^i, \boldsymbol{\tau}^i) &:= \int_{\Omega^i} \boldsymbol{\sigma}^i : (\mathbb{C}^i)^{-1} : \boldsymbol{\tau}^i d\Omega, \\ b : \mathbf{V}_0(\Omega^i) \times \mathbf{S}(\Omega^i) &\rightarrow \mathbb{R}, & b(\mathbf{v}^i, \boldsymbol{\tau}^i) &:= \int_{\Omega^i} \boldsymbol{\varepsilon}(\mathbf{v}^i) : \boldsymbol{\tau}^i d\Omega, \\ c : \mathbf{M}(\Omega^i) \times \mathbf{M}(\Omega^i) &\rightarrow \mathbb{R}, & c(\boldsymbol{\chi}^i, \boldsymbol{\mu}^i) &:= \int_{\Omega^i} \boldsymbol{\chi}^i \cdot (\mathbb{H}^i)^{-1} \boldsymbol{\mu}^i d\Omega, \\ (\cdot, \cdot)_{\Omega^i} : [H^{-1}(\Omega^i)]^2 \times [H^1(\Omega^i)]^2 &\rightarrow \mathbb{R}, & (\mathbf{f}^i, \boldsymbol{\eta}^i)_{\Omega^i} &:= \int_{\Omega} \mathbf{f}^i \cdot \boldsymbol{\eta}^i d\Omega, \\ \langle \cdot, \cdot \rangle_{\Gamma^i} : [H^{-1/2}(\Gamma^i)]^2 \times [H^{1/2}(\Gamma^i)]^2 &\rightarrow \mathbb{R}, & \langle \mathbf{t}^i, \boldsymbol{\eta}^i \rangle_{\Gamma^i} &:= \int_{\Gamma^i} \mathbf{t}^i \cdot \boldsymbol{\eta}^i d\Gamma, \\ l(t) : H^1(\Omega^i) &\rightarrow \mathbb{R}, & \langle l(t), \boldsymbol{\eta}^i \rangle &= (\hat{\mathbf{f}}^i(t), \boldsymbol{\eta}^i)_{\Omega^i} + \langle \hat{\mathbf{t}}^i(t), \boldsymbol{\eta}^i \rangle_{\Gamma_N^i}. \end{aligned}$$

In order to obtain the weak form of Problem 1.1.1 we proceed as follows. Testing the first equation in (1.11) with some test function, integrating by parts, employing the boundary conditions and adding the result for  $i = A, B$  we obtain the weak form of the equilibrium equation:

$$\sum_{i=B,A} b(\boldsymbol{\eta}^i, \boldsymbol{\sigma}^i(t)) - \langle \mathbf{t}_C(t), \boldsymbol{\eta}^A - \boldsymbol{\eta}^B \rangle_{\Gamma_C} = \sum_{i=B,A} \langle l(t), \boldsymbol{\eta}^i \rangle, \quad (1.31)$$

From the system (1.13) it follows that

$$\dot{\boldsymbol{\sigma}}(\mathbb{C}^i)^{-1} : (\boldsymbol{\tau}^i - \boldsymbol{\sigma}^i) - \dot{\boldsymbol{\chi}} : (\mathbb{H}^i)^{-1} (\boldsymbol{\mu}^i - \boldsymbol{\chi}^i) \geq 0, \quad \forall (\boldsymbol{\tau}^i, \boldsymbol{\mu}^i) \in \mathcal{P}^i, \quad (1.32)$$

and the corresponding weak form is

$$\int_{\Omega^i} \dot{\boldsymbol{\sigma}}(\mathbb{C}^i)^{-1} : (\boldsymbol{\tau}^i - \boldsymbol{\sigma}^i) d\Omega - \int_{\Omega^i} \dot{\boldsymbol{\chi}} : (\mathbb{H}^i)^{-1}(\boldsymbol{\mu}^i - \boldsymbol{\chi}^i) d\Omega \geq 0, \quad \forall (\boldsymbol{\tau}^i, \boldsymbol{\mu}^i) \in \mathcal{P}^i. \quad (1.33)$$

Then the weak formulation of Problem 1.1.1 reads:

**Problem 1.1.2.** *Given time interval  $(0, T)$ , given friction coefficient  $\mu_f \in [0, 1/2)$ , displacements  $\hat{\mathbf{u}}^i : [0, T] \rightarrow (H^{1/2}(\Gamma_D^i))^2$ , boundary traction  $\hat{\mathbf{t}}^i : [0, T] \rightarrow (H^{-1/2}(\Gamma_N^i))^2$ , volume forces  $\hat{\mathbf{f}}^i : [0, T] \rightarrow (H^{-1}(\Omega^i))^2$ , free energy scalar functions  $\psi^i(\boldsymbol{\varepsilon}^{ie}, \boldsymbol{\xi}^i)$  and their decompositions  $\psi^i(\boldsymbol{\varepsilon}^{ie}, \boldsymbol{\xi}^i) = \psi^{ie}(\boldsymbol{\varepsilon}^{ie}) + \psi^{ip}(\boldsymbol{\xi}^i)$ , scalar yield function for elastoplasticity  $\phi_{pl}^i(\boldsymbol{\sigma}^i, \boldsymbol{\chi}^i)$ , initial values  $(\mathbf{u}^i(0), \boldsymbol{\sigma}^i(0), \boldsymbol{\chi}^i(0)) = (\mathbf{0}, \mathbf{0}, \mathbf{0})$ , contact boundary  $\Gamma_C$ : find  $(\mathbf{u}^i, \boldsymbol{\sigma}^i, \boldsymbol{\chi}^i, \mathbf{t}_C) : [0, T] \rightarrow \mathbf{V}_D(\Omega^i) \times \mathbf{S}(\Omega^i) \times \mathbf{M}(\Omega^i) \times \mathbf{H}^{-1/2}(\Gamma_C)$ , such that:*

$$\sum_{i=B,A} b(\boldsymbol{\eta}^i, \boldsymbol{\sigma}^i(t)) - \langle \mathbf{t}_C(t), \boldsymbol{\eta}^A - \boldsymbol{\eta}^B \rangle_{\Gamma_C} = \sum_{i=B,A} \langle l(t), \boldsymbol{\eta}^i \rangle, \quad (1.34)$$

$$\bar{a}(\dot{\boldsymbol{\sigma}}^i(t), \boldsymbol{\tau}^i - \boldsymbol{\sigma}^i(t)) + c(\dot{\boldsymbol{\chi}}^i(t), \boldsymbol{\mu}^i - \boldsymbol{\chi}^i(t)) - b(\dot{\mathbf{u}}^i(t), \boldsymbol{\tau}^i - \boldsymbol{\sigma}^i(t)) \geq 0, \quad (1.35)$$

$$\int_{\Gamma_C} \sigma_{\mathcal{N}} \lambda_{\mathcal{N}} d\Gamma \geq \int_{\Gamma_C} \sigma_{\mathcal{N}} u_{\mathcal{N}}^{AB} d\Gamma, \quad (1.36)$$

$$\int_{\Gamma_C} (\sigma_{\mathcal{T}} \lambda_{\mathcal{T}} + \mu_f \sigma_{\mathcal{N}} |\lambda_{\mathcal{T}}|) d\Gamma \geq \int_{\Gamma_C} (\sigma_{\mathcal{T}} u_{\mathcal{N}}^{AB} + \mu_f \sigma_{\mathcal{N}} |u_{\mathcal{T}}^{AB}|) d\Gamma, \quad (1.37)$$

for all  $(\boldsymbol{\eta}^A, \boldsymbol{\eta}^B) \in \mathbf{V}_0(\Omega^A) \times \mathbf{V}_0(\Omega^B) \cap \{\boldsymbol{\eta}^{AB} \leq 0\}$ , for all  $(\boldsymbol{\tau}^i, \boldsymbol{\mu}^i) \in \mathcal{P}^i(\Omega^i)$ , for all  $\lambda_{\mathcal{N}} \in H_-^{1/2}(\Gamma_C)$ ,  $\lambda_{\mathcal{T}} \in H^{1/2}(\Gamma_C)$   $i = B, A$ .

Note, the constraint (1.12) on tractions on the contact boundary is posed in a weak form (1.36), (1.37). The equation (1.34) and the inequality (1.35) are the weak forms of the equilibrium equation and the plastic constitutive conditions in (1.11) and (1.13) respectively, see [29].  $H_-^{1/2}(\Gamma_C)$  is the subspace of the space  $H^{1/2}(\Gamma_C)$  consisting of all negative valued functions.

Next, we consider the contact conditions in more detail following [51]. For every point  $\mathbf{x}^B(\zeta^B, t) \in \Gamma_C^B$  which is in contact with the master we can find the orthogonal projection to the master-side  $\mathbf{x}^A(\bar{\zeta}^A, t) \in \Gamma_C^A$ . The bar over  $\bar{\zeta}$  denotes that the value of the parameter  $\zeta^A$  is subjected to  $\zeta^B$ . We define a penetration function  $g_{\mathcal{N}}$  on the slave surface  $\Gamma_C^B$  by

$$g_{\mathcal{N}}(\zeta^B, t) := \begin{cases} \|\bar{\mathbf{x}}^A - \mathbf{x}^B\| = (\bar{\mathbf{x}}^A - \mathbf{x}^B) \cdot \bar{\mathbf{n}}^A, & \text{if } [\bar{\mathbf{x}}^A - \mathbf{x}^B] \cdot \bar{\mathbf{n}}^A > 0, \\ 0, & \text{if } [\bar{\mathbf{x}}^A - \mathbf{x}^B] \cdot \bar{\mathbf{n}}^A \leq 0. \end{cases}$$

where  $\bar{\zeta}^A(\zeta^B, t)$  is the minimiser of the distance function

$$l(\zeta^A, \zeta^B, t) := \|\mathbf{x}^A(\zeta^A, t) - \mathbf{x}^B(\zeta^B, t)\| \longrightarrow \text{MIN over } \zeta^A$$

for a given slave point  $\mathbf{x}^B(\zeta^B, t)$ . The value  $\bar{\zeta}^A(\zeta^B, t)$  can be obtained by the necessary condition

$$\frac{\partial}{\partial \zeta^A} l(\zeta^A, \zeta^B, t) = \frac{\mathbf{x}^A(\zeta^A) - \mathbf{x}^B}{\|\mathbf{x}^A(\zeta^A) - \mathbf{x}^B\|} \cdot \mathbf{x}_{,\zeta^A}^A(\zeta^A) = 0.$$

With the tangent vector  $\mathbf{a}^A := \frac{\partial \mathbf{x}^A}{\partial \zeta^A}$  we have

$$\frac{\mathbf{x}^A(\zeta^A) - \mathbf{x}^B}{\|\mathbf{x}^A(\zeta^A) - \mathbf{x}^B\|} \cdot \mathbf{a}^A(\zeta^A) = 0,$$

such that  $\frac{\bar{\mathbf{x}}^A(\zeta^B) - \mathbf{x}^B(\zeta^B)}{\|\bar{\mathbf{x}}^A(\zeta^B) - \mathbf{x}^B(\zeta^B)\|} = \bar{\mathbf{n}}^A(\zeta^B)$ , since the unit vector which is orthogonal to the tangential vector of the surface is the normal to the surface.

Let us define the relative tangential displacement  $\mathbf{g}_{\mathcal{T}}$  of some slave point  $\mathbf{x}^B$  at some time step with respect to the previous one by

$$\mathbf{g}_{\mathcal{T}} = (\bar{\zeta}^A - \zeta_0^A) \bar{\mathbf{a}}^A,$$

where  $\bar{\zeta}_0^A$  is the previous natural parameter of the projected material point  $\mathbf{x}^B$  and  $\bar{\zeta}^A$  is the natural parameter of the current projection.

The contact stress is determined by the penetration function and the relative displacements. If  $\mathfrak{g}_{\mathcal{N}}(\mathbf{x}^B) = 0$ , the slave point and the corresponding projection on the master side (if it exists) are not in contact. Then normal and tangential stresses are defined by *outer pressure*, i.e. Neumann data. For example

$$\sigma_{\mathcal{N}} = 0, \quad \boldsymbol{\sigma}_{\mathcal{T}} = 0. \quad (1.38)$$

In case of penetration  $\mathfrak{g}_{\mathcal{N}}(\mathbf{x}^B) > 0$  the normal stress is postulated to be

$$\sigma_{\mathcal{N}} = -\frac{1}{\epsilon_{\mathcal{N}}} \mathfrak{g}_{\mathcal{N}}.$$

Here  $\frac{1}{\epsilon_{\mathcal{N}}}$  is the normal stiffness or penalty factor (see Peric and Owen [40]).

We assume a linear elastic constitutive equation for the tangential contact stress component

$$\mathbf{t}_{\mathcal{T}} = -\frac{1}{\epsilon_{\mathcal{T}}} \mathbf{g}_{\mathcal{T}}^e, \quad \text{with } \mathbf{g}_{\mathcal{T}}^e := \mathbf{g}_{\mathcal{T}} - \mathbf{g}_{\mathcal{T}}^p,$$

where  $\frac{1}{\epsilon_{\mathcal{T}}}$  is the tangential contact stiffness,  $\mathbf{g}_{\mathcal{T}}$  - tangential slip component,  $\mathbf{g}_{\mathcal{T}}^e$  - *elastic* part (microdisplacement describing the stick behavior),  $\mathbf{g}_{\mathcal{T}}^p$  - *plastic* part (frictional slip).



The plastic tangential slip  $\mathbf{g}_T^p$  is governed by a constitutive evolution. Consider an elastic domain  $\mathcal{P}_C := \{\mathbf{t}_C \in \mathbb{R}^2 \mid \phi_C(\mathbf{t}_C) \leq 0\}$  in the space of the contact tangential stress. Here

$$\phi_C = \|\boldsymbol{\sigma}_T\| + \mu_f \sigma_N$$

is the plastic slip criterion function for a given contact pressure  $|\sigma_N|$  with friction coefficient  $\mu_f$ . Define

$$\mathbf{g}_T^p = \begin{cases} 0, & \text{if } \|\frac{1}{\epsilon_T} \mathbf{g}_T\| \leq -\mu_f \sigma_N, \\ \left(1 + \frac{\mu_f \sigma_N}{\|\frac{1}{\epsilon_T} \mathbf{g}_T\|}\right) \mathbf{g}_T, & \text{if } \|\frac{1}{\epsilon_T} \mathbf{g}_T\| > -\mu_f \sigma_N. \end{cases}$$

It yields that

$$\begin{aligned} \mathbf{g}_T^p = 0, & \implies \mathbf{t}_C \in \mathcal{P}_C && \text{macro-stick,} \\ \mathbf{g}_T^p \neq 0, & \implies \mathbf{t}_C \in \partial \mathcal{P}_C && \text{macro-slip.} \end{aligned}$$

The evaluation of that projection is especially simple for polygonal boundaries.

Next we describe the plasticity model, which we have implemented in our numerical experiments, namely the classical  $J_2$  flow theory with isotropic/kinematic hardening [43, 2.3.2] which has two internal plastic variables.  $\alpha$  is the equivalent plastic strain which represents isotropic hardening of the von Mises yield surface. The deviatoric tensor  $\boldsymbol{\beta}$  stands for the center of the von Mises yield surface. We use the  $J_2$ -plasticity model with the following yield condition, flow rule and hardening law.

$$\begin{aligned} \boldsymbol{\eta} &:= \text{dev}[\boldsymbol{\sigma}] - \boldsymbol{\beta}, & \text{tr}[\boldsymbol{\beta}] &:= 0, \\ \phi_{pl}(\boldsymbol{\sigma}, \alpha, \boldsymbol{\beta}) &= \|\boldsymbol{\eta}\| - \sqrt{\frac{2}{3}} K(\alpha), \\ \mathbf{n} &:= \frac{\boldsymbol{\eta}}{\|\boldsymbol{\eta}\|} \\ \dot{\boldsymbol{\epsilon}}^p &= \gamma \mathbf{n}, & (1.39) \\ \dot{\boldsymbol{\beta}} &= \gamma \frac{2}{3} H'(\alpha) \mathbf{n}, \\ \dot{\alpha} &= \gamma \sqrt{\frac{2}{3}}, \end{aligned}$$

where  $\phi_{pl}$  is the yield function,  $K(\alpha)$ ,  $H(\alpha)$  are isotropic and kinematic hardening modulus respectively given by

$$\left. \begin{aligned} H'(\alpha) &= (1 - \theta) \bar{H}, \\ K(\alpha) &= \sigma_Y + \theta \bar{H} \alpha, \end{aligned} \right\} \theta \in [0, 1] \quad (1.40)$$

where  $\sigma_Y, \bar{H} \geq 0$  are material constants.  $\sigma_Y$  is the yield stress. The von Mises yield

surface is given by the yield condition

$$\phi_{pl}(\boldsymbol{\sigma}, \alpha, \boldsymbol{\beta}) \leq 0$$

and the loading/unloading complimentary Kuhn-Tucker conditions are

$$\gamma \geq 0, \quad \phi_{pl}(\boldsymbol{\sigma}, \alpha, \boldsymbol{\beta}) \leq 0, \quad \gamma \phi_{pl}(\boldsymbol{\sigma}, \alpha, \boldsymbol{\beta}) = 0.$$

It is easy to check [43, 2.2.18], that the consistency parameter  $\gamma$  is given by

$$\gamma = \frac{\{\mathbf{n} : \boldsymbol{\varepsilon}\}_+}{1 + \frac{K'+H'}{2\mu}}.$$

Here  $\{u\}_+ := \max\{0, u\}$  is the positive part function. Finally, we define the elastoplastic tangent moduli  $\mathbb{C}^{ep}$  by the following relations

$$\begin{aligned} \dot{\boldsymbol{\sigma}} &= \mathbb{C} : (\dot{\boldsymbol{\varepsilon}} - \dot{\boldsymbol{\varepsilon}}^p) = \mathbb{C}^{ep} : \dot{\boldsymbol{\varepsilon}}, \\ \mathbb{C} &= \kappa \mathbf{1} \otimes \mathbf{1} + 2\mu \left( \mathbf{I} - \frac{1}{3} \mathbf{1} \otimes \mathbf{1} \right). \end{aligned}$$

We obtain

$$\mathbb{C}^{ep} = \kappa \mathbf{1} \otimes \mathbf{1} + 2\mu \left( \mathbf{I} - \frac{1}{3} \mathbf{1} \otimes \mathbf{1} - \frac{\mathbf{n} \otimes \mathbf{n}}{1 + \frac{K'+H'}{3\mu}} \right),$$

where

$$\mathbf{1} = \delta_{ij} \mathbf{e}_i \otimes \mathbf{e}_j, \quad \mathbf{I} = 1/2(\delta_{ik}\delta_{jl} + \delta_{il}\delta_{jk}) \mathbf{e}_i \otimes \mathbf{e}_j \otimes \mathbf{e}_k \otimes \mathbf{e}_l$$

are second order fourth order identity tensors respectively and  $\kappa := \lambda + 2\mu/3$  is the bulk modulus. Note that

$$\mathbb{C} : \boldsymbol{\varepsilon} = \lambda \mathbf{1} \operatorname{tr}[\boldsymbol{\varepsilon}] + 2\mu \boldsymbol{\varepsilon} = \kappa \mathbf{1} \operatorname{tr}[\boldsymbol{\varepsilon}] + 2\mu \operatorname{dev}[\boldsymbol{\varepsilon}]. \quad (1.41)$$

Now we introduce a regularized version Problem 1.1.3 of Problem 1.1.2 (obtained by the penalty method) as well as some discretizations in time. For the regularized version (1.42)-(1.44) we will provide three discretization procedures in space, i.e. FEM-FEM, BEM-BEM, and FEM-BEM in sections 1.2.1, 1.2.2, 1.2.3 respectively, as well as solution algorithms. These solution algorithms are of predictor-corrector type, which is discussed below in abstract form. The idea of regularization is to replace the inequalities (1.36), (1.37) by equations. For this we apply the penalty method (see [50, 35]) and regularize the contact condition (1.12) with the smoothed one (1.44). By this we gain a simplified problem without a Lagrange multiplier neither a convex set of shape functions which lead to saddle point problems or variational inequalities. One has to mention that the differential variational inequalities (1.13) we leave unchanged. Zarrabi provided in [53, Section 5] a regularization method for the associated plastic flow in case of combined

linear isotropic-kinematic hardening.

With penalty parameters  $\epsilon_{\mathcal{T}} > 0$ ,  $\epsilon_{\mathcal{N}} > 0$  we formulate a *penalty regularization* of Problem 1.1.2 as follows:

**Problem 1.1.3.** *Under the same assumptions as in Problem 1.1.2 find  $(\mathbf{u}_{\epsilon}^i, \boldsymbol{\sigma}_{\epsilon}^i, \boldsymbol{\chi}_{\epsilon}^i) : [0, T] \rightarrow \mathbf{V}_D(\Omega^i) \times \mathbf{S}(\Omega^i) \times \mathbf{M}(\Omega^i)$ , such that*

$$\sum_{i=B,A} b(\boldsymbol{\eta}^i, \boldsymbol{\sigma}_{\epsilon}^i(t)) - \langle \mathbf{t}_{\epsilon_C}(t), \boldsymbol{\eta}^A - \boldsymbol{\eta}^B \rangle_{\Gamma_C} = \sum_{i=B,A} \langle l^i(t), \boldsymbol{\eta}^i \rangle, \quad (1.42)$$

$$\bar{a}(\dot{\boldsymbol{\sigma}}_{\epsilon}^i(t), \boldsymbol{\tau}^i - \boldsymbol{\sigma}_{\epsilon}^i(t)) + c(\dot{\boldsymbol{\chi}}_{\epsilon}^i(t), \boldsymbol{\mu}^i - \boldsymbol{\chi}_{\epsilon}^i(t)) - b(\dot{\mathbf{u}}_{\epsilon}^i(t), \boldsymbol{\tau}^i - \boldsymbol{\sigma}_{\epsilon}^i(t)) \geq 0 \quad (1.43)$$

for all  $\boldsymbol{\eta}^i \in \mathbf{V}_0(\Omega^i)$ , and for all  $(\boldsymbol{\tau}^i, \boldsymbol{\mu}^i) \in \mathcal{P}(\Omega^i)$ ,  $i = B, A$ . (1.42), (1.43) are obtained from (1.34), (1.35) by substituting the implicit formula for the traction  $\mathbf{t}_{\epsilon_C}$  on the contact boundary  $\Gamma_C$

$$\mathbf{t}_{\epsilon_C}(t) := -\frac{1}{\epsilon_{\mathcal{N}}}(u_{\mathcal{N}}^{AB} - g)^+ \mathbf{n}^A - \frac{1}{\epsilon_{\mathcal{T}}}\mathbf{g}_{\mathcal{T}}^e(u_{\mathcal{T}}). \quad (1.44)$$

The quantity  $\mathbf{g}_{\mathcal{T}}^e$  is obtained via  $\mathbf{g}_{\mathcal{T}} = u_{\mathcal{T}}^{BA} \mathbf{e}^A$  as follows. With  $\mathcal{F} := \mu_f \frac{1}{\epsilon_{\mathcal{N}}} |u_{\mathcal{N}}^{BA} - g|$  we set  $\mathbf{g}_{\mathcal{T}}^p = 0$  if  $\|\frac{1}{\epsilon_{\mathcal{T}}}\mathbf{g}_{\mathcal{T}}\| \leq \mathcal{F}$  and take  $\mathbf{g}_{\mathcal{T}}^e = \mathbf{g}_{\mathcal{T}}$ . Otherwise we set  $\mathbf{g}_{\mathcal{T}}^p = \left(1 - \frac{\mathcal{F}}{\|\mathbf{g}_{\mathcal{T}}/\epsilon_{\mathcal{T}}\|}\right) \mathbf{g}_{\mathcal{T}}$  yielding  $\mathbf{g}_{\mathcal{T}}^e = \mathbf{g}_{\mathcal{T}} - \mathbf{g}_{\mathcal{T}}^p$ .

Using the definition of the contact traction 1.208 the definition of its normal  $\sigma_{\mathcal{N}}$  and tangential  $\sigma_{\mathcal{T}}$  components 1.12 we obtain from 1.44 the explicit formulas for  $\sigma_{\mathcal{N}}$ ,  $\sigma_{\mathcal{T}}$

$$\sigma_{\mathcal{N}} := -\frac{1}{\epsilon_{\mathcal{N}}}(u_{\mathcal{N}}^{AB} - g) \mathbf{n}^A \quad (1.45)$$

$$\boldsymbol{\sigma}_{\mathcal{T}} := -\frac{1}{\epsilon_{\mathcal{T}}}\mathbf{g}_{\mathcal{T}}^e(u_{\mathcal{T}}), \quad (1.46)$$

$$\sigma_{\mathcal{T}} := \boldsymbol{\sigma}_{\mathcal{T}} \cdot \mathbf{e}^A. \quad (1.47)$$

Next, we give a time discretization of Problem 1.1.3. Let  $\mathcal{I}_{\Delta t}$  be a partition of the time interval  $(0, T)$  with maximum time step  $\Delta t$ ,  $\mathcal{I}_{\Delta t} := \{(t_{n-1}, t_n)\}_{n=0}^N$ , where  $0 = t_0 < t_1 < \dots < t_{N-1} < t_N = T$ ,  $\Delta t_n := t_n - t_{n-1}$ . For simplicity we will consider a uniform partition of  $(0, T)$  with a time step  $\Delta t$ , i.e.  $t_n - t_{n-1} = \Delta t$ . The time discretization of Problem 1.1.3 reads

**Problem 1.1.4.** *Given friction coefficient  $\mu_f \in [0, 1/2)$ , displacements  $\{\hat{\mathbf{u}}_n^i\}_{n=1}^N \subset (H^{1/2}(\Gamma_D^i))^2$ , boundary traction  $\{\hat{\mathbf{t}}_n^i\}_{n=1}^N \subset (H^{-1/2}(\Gamma_N^i))^2$ , volume forces  $\{\hat{\mathbf{f}}_n^i\}_{n=1}^N \subset (H^{-1}(\Gamma_N^i))^2$ , free energy scalar functions and scalar yield function as in Problem 1.1.3,*

initial values  $(\mathbf{u}_0^i, \boldsymbol{\sigma}_0^i, \boldsymbol{\chi}_0^i) = (\mathbf{0}, \mathbf{0}, \mathbf{0})$ , prescribed contact boundary  $\Gamma_C$ : find  $\{(\mathbf{u}_{en}^i, \boldsymbol{\sigma}_{en}^i, \boldsymbol{\chi}_{en}^i)_n\}_{n=1}^N \subset \mathbf{V}_D(\Omega^i) \times \mathbf{S}(\Omega^i) \times \mathbf{M}(\Omega^i)$ , such that

$$\sum_{i=B,A} b(\boldsymbol{\eta}^i, \boldsymbol{\sigma}_{en}^i) - \langle \mathbf{t}_{\epsilon C n}, \boldsymbol{\eta}^A - \boldsymbol{\eta}^B \rangle_{\Gamma_C} = \sum_{i=B,A} \langle l_n^i, \boldsymbol{\eta}^i \rangle, \quad (1.48)$$

$$\bar{a}(\Delta \boldsymbol{\sigma}_{en}^i, \boldsymbol{\tau}^i - \boldsymbol{\sigma}_{en}^i) + c(\Delta \boldsymbol{\chi}_{en}^i, \boldsymbol{\mu}^i - \boldsymbol{\chi}_{en}^i) - b(\Delta \mathbf{u}_{en}^i, \boldsymbol{\tau}^i - \boldsymbol{\sigma}_{en}^i) \geq 0 \quad (1.49)$$

for all  $\boldsymbol{\eta}^i \in \mathbf{V}_0(\Omega^i)$ , and for all  $(\boldsymbol{\tau}^i, \boldsymbol{\mu}^i) \in \mathcal{P}(\Omega^i)$ ,  $i = B, A$ , where  $\Delta(\bullet)_n := (\bullet)_n - (\bullet)_{n-1}$ .

From now and later on we will use the convention  $\mathbf{u} := (\mathbf{u}^A, \mathbf{u}^B)$ , the notation applies to other variables as well. For convenience we will omit the subscript  $\epsilon$ . The subscript  $n$  denotes the value at time step  $t_n$  and the superscript  $k$  in brackets  $^{(k)}$  denotes the value at the  $k$ -th iteration step. Having in mind that the stress is an implicit function of the displacement,  $\boldsymbol{\sigma}^i \equiv \boldsymbol{\sigma}^i(\boldsymbol{\varepsilon}(\mathbf{u}^i))$ , we write formally

$$\boldsymbol{\sigma}^i(t) = \boldsymbol{\sigma}^i(\boldsymbol{\varepsilon}(\mathbf{u}^i(t)), \boldsymbol{\varepsilon}^{ip}(t)) \approx \boldsymbol{\sigma}^i(\boldsymbol{\varepsilon}(\mathbf{u}^i(t - \Delta t))) + \mathbb{D}^i : \boldsymbol{\varepsilon}(\mathbf{u}^i(t) - \mathbf{u}^i(t - \Delta t)). \quad (1.50)$$

*Remark 1.1.2.*  $\boldsymbol{\sigma}^i(\boldsymbol{\varepsilon}(\mathbf{u}^i(t)))$  This function is globally multi-valued, but locally we can assume it to be a one-to-one mapping.

For our simulation we will take  $\mathbb{D}^i := \frac{\partial \boldsymbol{\sigma}^i}{\partial \boldsymbol{\varepsilon}}(\boldsymbol{\varepsilon}(\mathbf{u}^i(t - \Delta t)))$ , this choice is known as tangent predictor [5, 29].

A *Predictor-Corrector Solution Procedure* for Problem 1.1.4 is:

First we perform the predictor step: Find  $\mathbf{u}_n^{(k)} \in \mathbf{V}$ :

$$\begin{aligned} & \int_{\Omega} \mathbb{D}_n^{(k)}(\boldsymbol{\varepsilon}(\mathbf{u}_n^{(k)}) - \mathbf{u}_n^{(k-1)}) : \boldsymbol{\varepsilon}(\boldsymbol{\eta}) d\Omega - \left\langle \frac{\partial \mathbf{t}_{Cn}^{(k)}}{\partial \mathbf{u}}(\mathbf{u}_n^{(k)}) - \mathbf{u}_n^{(k-1)}, \boldsymbol{\eta}^A - \boldsymbol{\eta}^B \right\rangle_{\Gamma_C} \\ & = -b(\boldsymbol{\eta}, \boldsymbol{\sigma}_n^{(k-1)}) + \left\langle \mathbf{t}_{Cn}^{(k-1)}, \boldsymbol{\eta}^A - \boldsymbol{\eta}^B \right\rangle_{\Gamma_C} + \langle l_n, \boldsymbol{\eta} \rangle. \end{aligned} \quad (1.51)$$

Next we perform the corrector step: Find  $(\boldsymbol{\sigma}_n^{(k)}, \boldsymbol{\chi}_n^{(k)}) \in \mathcal{P}$ :

$$\bar{a}(\Delta \boldsymbol{\sigma}_n^{(k)tr}, \boldsymbol{\tau} - \boldsymbol{\sigma}_{n-1}) + c(\Delta \boldsymbol{\chi}_n^{(k)tr}, \boldsymbol{\mu} - \boldsymbol{\chi}_{n-1}) - b(\Delta \mathbf{u}_n^{(k)}, \boldsymbol{\tau} - \boldsymbol{\sigma}_{n-1}) \geq 0. \quad (1.52)$$

with

$$\boldsymbol{\sigma}_n^{(k)tr} := \boldsymbol{\sigma}_{n-1} + \mathbb{D}_n^{(k)} \boldsymbol{\varepsilon}(\mathbf{u}_n^{(k)} - \mathbf{u}_{n-1}), \quad (1.53)$$

$$\Delta \boldsymbol{\sigma}_n^{(k)tr} := \boldsymbol{\sigma}_n^{(k)tr} - \boldsymbol{\sigma}_n^{(k)}, \quad (1.54)$$

$$\boldsymbol{\chi}_n^{(k)tr} := \boldsymbol{\chi}_{n-1}, \quad (1.55)$$

$$\Delta \boldsymbol{\chi}_n^{(k)tr} := \boldsymbol{\chi}_n^{(k)tr} - \boldsymbol{\chi}_n^{(k)}. \quad (1.56)$$

The abstract predictor-corrector scheme given here is described in detail within a *Solution procedure* (incremental loading) for FEM/FEM discretizations in Section 1.2.1. The predictor step refers to steps (1.a.i)-(1.a.iv) there in the solution procedure mentioned above, whereas the corrector step is performed at step (1.a.v). The corrector step does not depend on the discretization method and is the same for FEM/FEM, BEM/BEM and FEM/BEM approaches.

## 1.2 Discretization and solution procedure (incremental loading)

### 1.2.1 FEM/FEM

We discretize the weak formulation (1.48),(1.49) in space by defining a partition  $\mathbb{T}_h^i$  of the domain  $\Omega^i, i = B, A$  into finite elements and choosing discrete spaces

$${}^h\mathbf{V}_0^i := \left\{ \boldsymbol{\eta}_h \in [H^1(\Omega^i)]^2 \mid \forall \boldsymbol{\epsilon} \in \mathbb{T}_h^i : \boldsymbol{\eta}_h|_{\boldsymbol{\epsilon}} \in \mathcal{R}^1(\boldsymbol{\epsilon}), \boldsymbol{\eta}_h|_{\boldsymbol{\epsilon} \cap \Gamma_D^i} = 0 \right\},$$

where  $\mathcal{R}^1(\boldsymbol{\epsilon})$  denotes linear functions  $\mathcal{P}^1(\boldsymbol{\epsilon})$  in case of a triangular mesh element  $\boldsymbol{\epsilon}$  or bilinear functions  $\mathcal{Q}^1(\boldsymbol{\epsilon})$  in case of a quadrilateral mesh  $\boldsymbol{\epsilon}$ . For brevity we define

$$\begin{aligned} {}^h\mathbf{V}_D &:= {}^h\mathbf{V}_D^B \times {}^h\mathbf{V}_D^A, \\ {}^h\mathbf{V}_0 &:= {}^h\mathbf{V}_0^B \times {}^h\mathbf{V}_0^A. \end{aligned}$$

The discretized version of (1.42) is given by the following procedure (note that (1.43) is incorporated by return mapping): Find  $\mathbf{u}_h = (\mathbf{u}_h^B, \mathbf{u}_h^A) \in {}^h\mathbf{V}_D$ :

$$F^{int}(\mathbf{u}_h, \boldsymbol{\eta}_h) = F^{ext}(\boldsymbol{\eta}_h) \quad \forall \boldsymbol{\eta}_h \in {}^h\mathbf{V}_0, \quad (1.57)$$

where

$$\begin{aligned} F^{int}(\mathbf{u}_h, \boldsymbol{\eta}_h) &:= F_{\mathbf{u}_h}^{int}(\boldsymbol{\sigma}^i, \mathbf{t}_C^i, \boldsymbol{\eta}_h) := \sum_{i=B,A} (\boldsymbol{\sigma}^i, \boldsymbol{\varepsilon}(\boldsymbol{\eta}_h^i))_{\Omega^i} - \langle \mathbf{t}_C^i, \boldsymbol{\eta}_h^i \rangle_{\Gamma_C}, \\ F^{ext}(\boldsymbol{\eta}_h) &:= \sum_{i=B,A} (\hat{\mathbf{f}}^i, \boldsymbol{\eta}_h^i)_{\Omega^i} + \langle \hat{\mathbf{t}}^i, \boldsymbol{\eta}_h^i \rangle_{\Gamma_N^i}, \\ \boldsymbol{\sigma}_h^i &:= \boldsymbol{\sigma}(\mathbf{u}_h^i), \quad \mathbf{t}_C^i := \mathbf{t}_C(\mathbf{u}_h^i). \end{aligned}$$

Furthermore, the functional  $F^{int}(\mathbf{u}, \boldsymbol{\eta})$  depends on  $\mathbf{u}$  whose nonlinear behavior is described by the contact constitutive equations and the constitutive equations for plasticity formulated in Section 1.2 and linearized in Section 1.3. We treat the loading process and a consequent application of loading increments  $(\Delta \hat{\mathbf{f}}^i)_n, (\Delta \hat{\mathbf{t}}^i)_n, (\Delta \hat{\mathbf{u}}^i)_n$ :

$$\begin{aligned} (\hat{\mathbf{f}}^i)_n &= \hat{\mathbf{f}}^i(t_n), \\ (\hat{\mathbf{t}}^i)_n &= \hat{\mathbf{t}}^i(t_n), \\ (\hat{\mathbf{u}}^i)_n &= \hat{\mathbf{u}}^i(t_n), \end{aligned}$$

which define the discrete external load

$$F_n^{ext}(\boldsymbol{\eta}_h) := \sum_{i=B,A} ((\hat{\boldsymbol{f}}^i)_n, \boldsymbol{\eta}^i)_{\Omega^i} + \left\langle (\hat{\boldsymbol{t}}^i)_n, \boldsymbol{\eta}^i \right\rangle_{\Gamma_N^i}$$

in the pseudo-time stepping process. Define the increment-dependent functional spaces

$$\begin{aligned} {}^h\mathbf{V}_{D,n}^i &:= \left\{ \eta_h \in [H^1(\Omega^i)]^2 \mid \eta_h|_e \in \mathcal{R}^1(e), \eta_h|_{e \cap \Gamma_D^i} = (\hat{\boldsymbol{u}}^i)_n \right\}, \\ {}^h\mathbf{V}_{D,n} &:= {}^h\mathbf{V}_{D,n}^B \times {}^h\mathbf{V}_{D,n}^A. \end{aligned}$$

Let  $(\boldsymbol{u}_h)_0$  be the initial displacement state of the body,  $(\boldsymbol{\varepsilon}^p)_0^{(0)}, \alpha_0^{(0)}, \boldsymbol{\beta}_0^{(0)}$  the initial internal variables,  $(\boldsymbol{g}_T^p)_0^{(0)}$  initial tangential macro-displacement and let  $(\hat{\boldsymbol{f}}^i)_0, (\hat{\boldsymbol{t}}^i)_0, (\hat{\boldsymbol{u}}^i)_0$  be the initial load. Usually, the displacement-free state  $(\boldsymbol{u}_h)_0 = 0$  as well as homogeneous internal variables  $(\boldsymbol{\varepsilon}^p)_0^{(0)} = 0, \alpha_0^{(0)} = 0, \boldsymbol{\beta}_0^{(0)} = 0, (\boldsymbol{g}_T^p)_0^{(0)} = 0$  are chosen as initial data. We use the *backward Euler* scheme for both *contact* and *plasticity*. Thus the problem can be reformulated as follows:

Find  $(\Delta \boldsymbol{u}_h)_n \in {}^h\mathbf{V}_{D,n}$ , and therefore the new displacement state  $(\boldsymbol{u}_h)_n = (\boldsymbol{u}_h)_{n-1} + (\Delta \boldsymbol{u}_h)_n$ , stress  $(\boldsymbol{\sigma}^i)_n = \boldsymbol{\sigma}((\boldsymbol{u}_h)_n)$ , contact traction  $(\boldsymbol{t}_{e_C}^i)_n = \boldsymbol{t}_C((\boldsymbol{u}_h)_n)$  such that

$$F_{\boldsymbol{u}_h}^{int}((\boldsymbol{\sigma}^i)_n, (\boldsymbol{t}_{e_C}^i)_n, \boldsymbol{\eta}_h) = F_n^{ext}(\boldsymbol{\eta}_h) \quad \forall \boldsymbol{\eta}_h \in {}^h\mathbf{V}_0, \quad (1.58)$$

where the contact traction is given by (1.44) and the plastic conditions are enforced by the return mapping algorithm described in boxes 1.3.1, 1.3.2.

To solve (1.58) we use the Newton's method. Let  $\mathbf{U}$  be the coefficients of the expansion of  $\boldsymbol{u}_h$  in basis in the discrete space  ${}^h\mathbf{V}_D$ , i.e.  $\boldsymbol{u}_h = \sum_{j=1}^{n_{el}} U^j \psi^j$ . Define

$$F_*^{int}(\mathbf{U}, \boldsymbol{\eta}_h) := F^{int}(\boldsymbol{u}_h, \boldsymbol{\eta}_h).$$

Therefore (1.58) becomes

$$F_*^{int}(\mathbf{U}_n, \boldsymbol{\eta}_h) = F_n^{ext}(\boldsymbol{\eta}_h) \quad \forall \boldsymbol{\eta}_h \in {}^h\mathbf{V}_0.$$

We perform the linearization of  $F_*^{int}(\mathbf{U}_n, \boldsymbol{\eta}_h)$ . Choose the starting value

$$\mathbf{U}_n^{(0)} := \mathbf{U}_{n-1},$$

and introduce the Newton's increment  $\Delta \mathbf{U}_n^{(k+1)}$  to proceed to the next iterate

$$\mathbf{U}_n^{(k+1)} = \mathbf{U}_n^{(k)} + \Delta \mathbf{U}_n^{(k+1)}, \quad k = 0, 1, 2, \dots$$

The Taylor's expansion provides

$$F_*^{int}(\mathbf{U}_n^{(k+1)}, \boldsymbol{\eta}_h) = F_*^{int}(\mathbf{U}_n^{(k)}, \boldsymbol{\eta}_h) + \frac{\partial F_*^{int}(\mathbf{U}_n^{(k)}, \boldsymbol{\eta}_h)}{\partial \mathbf{U}_n^{(k+1)}} \Delta \mathbf{U}_n^{(k+1)}.$$

Now we are on the position to state the algebraic problem. For brevity we define the matrix  $\mathfrak{A}$  and the right hand side vector  $\mathfrak{b}$  by

$$\begin{aligned} \mathfrak{A} &:= \frac{\partial F_*^{int}(\mathbf{U}_n^{(k)}, \boldsymbol{\eta}_h)}{\partial \mathbf{U}_n^{(k)}}, \\ \mathfrak{b} &:= F_n^{ext}(\boldsymbol{\eta}_h) - F_*^{int}(\mathbf{U}_n^{(k+1)}, \boldsymbol{\eta}_h), \quad j = 1, \dots, N \end{aligned}$$

Then the algebraic problem is: Find  $\mathfrak{x} = \Delta \mathbf{U}_n^{(k+1)}$ :

$$\mathfrak{A}\mathfrak{x} = \mathfrak{b}.$$

The whole algorithm can now be formulated as follows.

### Solution procedure

Set initial displacement  $\mathbf{U}_0^{(0)}$ , initial internal variables  $(\boldsymbol{\varepsilon}^p)_0^{(0)}, \alpha_0^{(0)}, \boldsymbol{\beta}_0^{(0)}$ , initial tangential macro-displacement  $(\mathbf{g}_T^p)_0^{(0)}$  and initial loads  $(\hat{\mathbf{f}}^i)_0, (\hat{\mathbf{t}}^i)_0, (\hat{\mathbf{u}}^i)_0$

1. for  $n = 0, 1, 2, \dots$

a) for  $k = 0, 1, 2, \dots$

i. compute the load vector

$$\mathfrak{b} := F_n^{ext}(\boldsymbol{\eta}_h) - F_*^{int}(\mathbf{U}_n^{(k+1)}, \boldsymbol{\eta}_h)$$

ii. if  $\|\mathfrak{b}\|_{l_2} := \sqrt{\mathfrak{b} \cdot \mathfrak{b}} \leq TOL$  goto 2.

iii. compute the matrix  $\mathfrak{A} := \frac{\partial F_*^{int}(\mathbf{U}_n^{(k)}, \boldsymbol{\eta}_h)}{\partial \mathbf{U}_n^{(k)}}$ ,

iv. find the next displacement increment  $\mathfrak{x} = \Delta \mathbf{U}_n^{(k+1)}$  by solving

$$\mathfrak{A}\mathfrak{x} = \mathfrak{b}.$$

v. update the displacement field

$$\mathbf{U}_n^{(k+1)} = \mathbf{U}_n^{(k)} + \Delta \mathbf{U}_n^{(k+1)}$$

and the internal variables  $(\boldsymbol{\varepsilon}^p)_n^{(k+1)}, \alpha_n^{(k+1)}, \boldsymbol{\beta}_n^{(k+1)}, (\mathbf{g}_T^p)_n^{(k+1)}$ . They should satisfy constitutive contact and plastic conditions. We use the return mapping procedure for both contact and plastification. The details will be described below.



## 1.2 Discretization and solution procedure (incremental loading)

b) set  $k = k + 1$ , goto (a)

2. initialize the next pseudo-time step

$$\mathbf{U}_{n+1}^{(0)} = \mathbf{U}_n^{(k)}.$$

3. apply the next load increment

$$\begin{aligned} (\hat{\mathbf{f}}^i)_{n+1} &= \hat{\mathbf{f}}^i(t_{n+1}), \\ (\hat{\mathbf{t}}^i)_{n+1} &= \hat{\mathbf{t}}^i(t_{n+1}), \\ (\hat{\mathbf{u}}^i)_{n+1} &= \hat{\mathbf{u}}^i(t_{n+1}), \end{aligned}$$

if the total load is achieved exit, if not, goto 1.

We discretize both bodies using triangles or quadrilaterals. In general, both meshes do not match on the contact boundary. We also assume, that there is no change of the boundary condition type along one edge. We take continuous piecewise linear approximation of the displacement. Let us consider the structure of the linear system  $\mathfrak{A}\mathbf{x} = \mathfrak{b}$ . After linearization of contact and plasticity terms described below we obtain

$$\begin{pmatrix} A_{\Omega^B}^{pl} & (B_{\Gamma_C^B}^{pl})^T & 0 & 0 \\ B_{\Gamma_C^B}^{pl} & C_{\Gamma_C^B}^{pl} + C^{BB} & -C^{BA} & 0 \\ 0 & -C^{AB} & C^{AA} + C_{\Gamma_C^A}^{pl} & (B_{\Gamma_C^A}^{pl})^T \\ 0 & 0 & B_{\Gamma_C^A}^{pl} & A_{\Omega^A}^{pl} \end{pmatrix} \begin{pmatrix} \mathfrak{x}_{\Omega^B}^B \\ \mathfrak{x}_{\Gamma_C^B}^B \\ \mathfrak{x}_{\Gamma_C^A}^A \\ \mathfrak{x}_{\Omega^A}^A \end{pmatrix} = \mathfrak{b}^{ext} - \mathfrak{b}^{int} + \begin{pmatrix} 0 \\ \mathfrak{b}_{\Gamma_C^B}^B \\ -\mathfrak{b}_{\Gamma_C^A}^A \\ 0 \end{pmatrix},$$

where the finite element matrix

$$\mathfrak{A}^{FEM} := \begin{pmatrix} A_{\Omega^B}^{pl} & (B_{\Gamma_C^B}^{pl})^T & 0 & 0 \\ B_{\Gamma_C^B}^{pl} & C_{\Gamma_C^B}^{pl} & 0 & 0 \\ 0 & 0 & C_{\Gamma_C^A}^{pl} & (B_{\Gamma_C^A}^{pl})^T \\ 0 & 0 & B_{\Gamma_C^A}^{pl} & A_{\Omega^A}^{pl} \end{pmatrix}$$

has a band structure and has no coupling terms between  $\Omega^B$  and  $\Omega^A$ . The index  $^{pl}$  means that the matrix changes due to the plastic terms. For each body ( $i = B, A$ ) the blocks  $A_{\Omega^i}^{pl}$  are generated by testing the test-functions which correspond to the degrees of freedom in the interior of  $\Omega^i$  and its Neumann boundary  $\Gamma_N^i$  against themselves. The blocks  $C_{\Gamma_C^i}^{pl}$  correspond to the testing of test functions, defined on the contact boundary

$\Gamma_C^i$ . The blocks  $B_{\Gamma_C^i}^{pl}$  are generated by testing of test-functions defined in the interior of  $\Omega^i$  and its Neumann boundary  $\Gamma_N^i$  against test-functions, defined on the contact boundary  $\Gamma_C^i$ .

The term  $\mathbf{b}^{ext}$  is constructed by the usual contributions of external volume forces and prescribed tractions on the Neumann boundary part. The terms  $\mathcal{C}^{BB}$ ,  $\mathcal{C}^{BA}$ ,  $\mathcal{C}^{AB}$ ,  $\mathcal{C}^{AA}$ ,  $\mathbf{b}_{\Gamma_C^B}^B$ ,  $\mathbf{b}_{\Gamma_C^A}^A$  describe coupling of the bodies along contact boundary. They are constructed by the linearization of contact integrals.  $\mathfrak{A}^{FEM}$ ,  $\mathbf{b}^{int}$  describe internal behavior of the bodies and reflect, for example, the plastic effects. The computation of these terms is discussed below.

## 1.2.2 BEM/BEM

In order to obtain an integral operator formulation for the equilibrium equation (1.48) of the elastoplastic contact problem Problem 1.1.4 we apply integration by parts and use the Steklov-Poincaré operator (1.60), together with the Newton potential (1.61). For deriving boundary integral formulation we need the following boundary and volume operators:

$$\begin{aligned}
 V\boldsymbol{\varphi}(x) &:= \int_{\Gamma} \boldsymbol{\varphi}(y) \mathcal{G}(x, y) d\Gamma_y && - \text{single layer potential,} \\
 K\mathbf{u}(x) &:= \int_{\Gamma} \mathbf{u}(y) (\mathcal{T}_y \mathcal{G}(x, y))^T d\Gamma_y && - \text{double layer potential,} \\
 K'\boldsymbol{\varphi}(x) &:= \mathcal{T}_x \int_{\Gamma} \boldsymbol{\varphi}(y) \mathcal{G}(x, y) d\Gamma_y && - \text{adjoint double layer potential,} \\
 W\mathbf{u}(x) &:= -\mathcal{T}_x \int_{\Gamma} \mathbf{u}(y) \mathcal{T}_y \mathcal{G}(x, y) d\Gamma_y && - \text{hypersingular integral operator,} \\
 N_0\mathbf{f}(x) &:= \int_{\Omega} \mathbf{f}(y) \mathcal{G}(x, y) d\Gamma_y && - \text{first Newton potential,} \\
 N_1\mathbf{f}(x) &:= \mathcal{T}_x \int_{\Gamma} \mathbf{f}(y) \mathcal{G}(x, y) d\Gamma_y && - \text{second Newton potential,}
 \end{aligned}$$

where the traction operator  $\mathcal{T}$  is given by

$$\mathcal{T}_y \mathcal{G}(x, y) = \sigma_y(\mathcal{G}(x, y))|_{\Gamma} \cdot \mathbf{n}_{\Gamma}.$$

Here  $\sigma_y(\cdot)$  means that  $y$  is treated as an independent variable. The fundamental solution  $\mathcal{G}(x, y)$  of the Lamé operator is

$$\mathcal{G}(x, y) = \frac{\lambda + 3\mu}{4\pi\mu(\lambda + 2\mu)} \left\{ \log \frac{1}{|x - y|} I + \frac{\lambda + \mu}{\lambda + 3\mu} \frac{(x - y)(x - y)^T}{|x - y|^2} \right\} \quad (1.59)$$

It is well-known [22] that  $V, K, K', W$  satisfy the following mapping properties

$$\begin{aligned} V &: \mathbf{H}^{-1/2}(\Gamma) \rightarrow \mathbf{H}^{1/2}(\Gamma), \\ K &: \mathbf{H}^{1/2}(\Gamma) \rightarrow \mathbf{H}^{1/2}(\Gamma), \\ K' &: \mathbf{H}^{-1/2}(\Gamma) \rightarrow \mathbf{H}^{-1/2}(\Gamma), \\ W &: \mathbf{H}^{1/2}(\Gamma) \rightarrow \mathbf{H}^{-1/2}(\Gamma) \end{aligned}$$

all of them are continuous,  $V$  is positive definite on  $\mathbf{H}^{-1/2}(\Gamma)$  and  $W$  is positive semidefinite on  $\mathbf{H}^{1/2}(\Gamma)$ . Where  $\mathbf{H}^s(\Gamma) := [H^s(\Gamma)]^2$ . Note that of course our approach can be extended to 3D problems we only have to take the 3D free space Green's function for the Lamé operator instead of its 2D version 1.59. The positive semidefinite Poincaré-Steklov [14] operator is defined by

$$S := W + (K' + 1/2)V^{-1}(K + 1/2) : \mathbf{H}^{1/2}(\Gamma) \rightarrow \mathbf{H}^{-1/2}(\Gamma) \quad (1.60)$$

and is a so-called Dirichlet-to-Neumann mapping. The volume potential  $N$  can be defined in two ways [27]:

$$N := V^{-1}N_0 \equiv (K' + 1/2)V^{-1}N_0 - N_1. \quad (1.61)$$

We proceed as follows

$$\begin{aligned} &(\boldsymbol{\sigma}^i, \boldsymbol{\varepsilon}(\boldsymbol{\eta}^i))_{\Omega^i} - (\hat{\boldsymbol{f}}^i, \boldsymbol{\eta}^i)_{\Omega^i} \\ &= (\mathbb{C}^i : \boldsymbol{\varepsilon}(\mathbf{u}^i), \boldsymbol{\varepsilon}(\boldsymbol{\eta}^i))_{\Omega^i} - (\mathbb{C}^i : \boldsymbol{\varepsilon}^{ip}, \boldsymbol{\varepsilon}(\boldsymbol{\eta}^i))_{\Omega^i} - (\hat{\boldsymbol{f}}^i, \boldsymbol{\eta}^i)_{\Omega^i} \\ &= (\mathbb{C}^i : \boldsymbol{\varepsilon}(\mathbf{u}^i), \boldsymbol{\varepsilon}(\boldsymbol{\eta}^i))_{\Omega^i} + (\operatorname{div}[\mathbb{C}^i : \boldsymbol{\varepsilon}^{ip}], \boldsymbol{\eta}^i)_{\Omega^i} \\ &\quad - \langle [\mathbb{C}^i : \boldsymbol{\varepsilon}^{ip}] \cdot \mathbf{n}, \boldsymbol{\eta}^i \rangle_{\Sigma^i} - (\hat{\boldsymbol{f}}^i, \boldsymbol{\eta}^i)_{\Omega^i} \\ &= (\mathbb{C}^i : \boldsymbol{\varepsilon}(\mathbf{u}^i), \boldsymbol{\varepsilon}(\boldsymbol{\eta}^i))_{\Omega^i} + (\operatorname{div}[\mathbb{C}^i : \boldsymbol{\varepsilon}^{ip}] - \hat{\boldsymbol{f}}^i, \boldsymbol{\eta}^i)_{\Omega^i} \\ &\quad - \langle [\mathbb{C}^i : \boldsymbol{\varepsilon}^{ip}] \cdot \mathbf{n}, \boldsymbol{\eta}^i \rangle_{\Sigma^i} \\ &= \langle S\mathbf{u}^i, \boldsymbol{\eta}^i \rangle_{\Sigma^i} + \left\langle N(\operatorname{div}[\mathbb{C}^i : \boldsymbol{\varepsilon}^{ip}] - \hat{\boldsymbol{f}}^i), \boldsymbol{\eta}^i \right\rangle_{\Sigma^i} \\ &\quad - \langle [\mathbb{C}^i : \boldsymbol{\varepsilon}^{ip}] \cdot \mathbf{n}, \boldsymbol{\eta}^i \rangle_{\Sigma^i} \\ &\forall \mathbf{u}^i \in \mathbf{V}_D^i, \quad \forall \boldsymbol{\eta}^i \in \mathbf{V}_0^i, \quad i = B, A. \end{aligned}$$

Therefore the domain penalty formulation Problem 1.1.4 can now be rewritten in terms of the boundary and volume integral operators  $S$  and  $N$  respectively: For given  $\hat{\boldsymbol{f}}^i$  and

$\hat{\mathbf{t}}^i$  find  $\mathbf{u}^i \in H^{1/2}$  with  $\mathbf{u}^i|_{\Gamma_D^i} = \hat{\mathbf{u}}$  satisfying

$$\begin{aligned} & \sum_{i=B,A} (\langle S\mathbf{u}^i, \boldsymbol{\eta}^i \rangle_{\Sigma^i} + \langle N(\operatorname{div}[\mathbb{C}^i : \boldsymbol{\varepsilon}^{ip}]), \boldsymbol{\eta}^i \rangle_{\Sigma^i}) - \langle [\mathbb{C} : \boldsymbol{\varepsilon}^{ip}] \cdot \mathbf{n}, \boldsymbol{\eta}^i \rangle_{\Sigma^i} \\ & - \langle \mathbf{t}_{\varepsilon_C}, \boldsymbol{\eta}^A - \boldsymbol{\eta}^B \rangle_{\Gamma_C} = \sum_{i=B,A} \left( \langle N\hat{\mathbf{f}}^i, \boldsymbol{\eta}^i \rangle_{\Sigma^i} + \langle \hat{\mathbf{t}}^i, \boldsymbol{\eta}^i \rangle_{\Gamma_N^i} \right). \end{aligned} \quad (1.62)$$

$\forall \boldsymbol{\eta}^i \in H^{1/2}$  with  $\boldsymbol{\eta}^i = 0$  on  $\Gamma_D^i$ , where  $\boldsymbol{\varepsilon}^{ip}$  is determined by the corrector step (radial return) as described below.

We discretize the weak formulation (1.62) by defining partitions  $\mathcal{T}_h^i$  of the boundary  $\Gamma^i, i = B, A$  and choosing boundary element spaces

$$\begin{aligned} {}^h\boldsymbol{\nu}_D^i &:= \left\{ \boldsymbol{\eta}_h \in \mathbf{H}^{1/2}(\Gamma^i) \mid \forall \boldsymbol{\varepsilon} \in \mathcal{T}_h^i : \boldsymbol{\eta}_h|_{\boldsymbol{\varepsilon}} \in \mathcal{P}^1(\boldsymbol{\varepsilon}), \boldsymbol{\eta}_h|_{\boldsymbol{\varepsilon} \cap \Gamma_D^i} = \hat{\mathbf{u}}^i \right\}, \\ {}^h\boldsymbol{\nu}_0^i &:= \left\{ \boldsymbol{\eta}_h \in \mathbf{H}^{1/2}(\Gamma^i) \mid \forall \boldsymbol{\varepsilon} \in \mathcal{T}_h^i : \boldsymbol{\eta}_h|_{\boldsymbol{\varepsilon}} \in \mathcal{P}^1(\boldsymbol{\varepsilon}), \boldsymbol{\eta}_h|_{\boldsymbol{\varepsilon} \cap \Gamma_D^i} = 0 \right\}, \end{aligned}$$

With the product spaces

$${}^h\boldsymbol{\nu}_D := {}^h\boldsymbol{\nu}_D^B \times {}^h\boldsymbol{\nu}_D^A, \quad {}^h\boldsymbol{\nu}_0 := {}^h\boldsymbol{\nu}_0^B \times {}^h\boldsymbol{\nu}_0^A,$$

the discretized version of (1.62) is given by the Galerkin scheme:

Find  $\mathbf{u}_h = (\mathbf{u}_h^B, \mathbf{u}_h^A) \in {}^h\boldsymbol{\nu}_D$ , such that

$$\begin{aligned} & \sum_{i=B,A} \langle S\mathbf{u}_h^i, \boldsymbol{\eta}^i \rangle_{\Sigma^i} - \langle \mathbf{t}_{\varepsilon_C}, \boldsymbol{\eta}^A - \boldsymbol{\eta}^B \rangle_{\Gamma_C} = - \langle N(\operatorname{div}[\mathbb{C}^i : \boldsymbol{\varepsilon}^{ip}]), \boldsymbol{\eta}^i \rangle_{\Sigma^i} \\ & + \langle [\mathbb{C}^i : \boldsymbol{\varepsilon}^{ip}] \cdot \mathbf{n}, \boldsymbol{\eta} \rangle_{\Sigma^i} + \sum_{i=B,A} \langle N\hat{\mathbf{f}}^i, \boldsymbol{\eta}^i \rangle_{\Sigma^i} + \langle \hat{\mathbf{t}}^i, \boldsymbol{\eta}^i \rangle_{\Gamma_N^i}. \end{aligned} \quad (1.63)$$

for all  $\boldsymbol{\eta}^i \in {}^h\boldsymbol{\nu}_0^i := \{ \boldsymbol{\eta}_h \in \mathbf{H}^{1/2}(\Gamma^i) : \boldsymbol{\eta}_h|_e \text{ pw. lin.}, \boldsymbol{\eta}_h|_{e \cap \Gamma_D^i} = 0 \}$ . Note that in 1.63 we need the plastic strains  $\boldsymbol{\varepsilon}^{ip}$  which are computed by the evaluating the displacement  $\tilde{\mathbf{u}}^i$  in  $\Omega^i$  via the Somigliana representation formula for  $\mathbf{x} \in \Omega^i$ :

$$\tilde{\mathbf{u}}^i(\mathbf{x}) = \int_{\Gamma^i} \mathcal{G}(\mathbf{x}, \mathbf{y}) \cdot \mathcal{T}_{n_y}(\mathbf{u}_h^i) d\Gamma_y - \int_{\Gamma^i} \mathcal{T}_{n_y} \mathcal{G}(\mathbf{x}, \mathbf{y}) \mathbf{u}_h^B(\mathbf{y}) d\Gamma_y + \int_{\Omega^i} \sigma_{jki}^* \boldsymbol{\varepsilon}^p(\mathbf{u}^i), \quad (1.64)$$

with the traction operator  $\mathcal{T}_{n_y} := \boldsymbol{\sigma}(\mathbf{y}) \cdot \mathbf{n}(\mathbf{y})$ . Here  $\sigma_{jki}^*$  is given in [12, §6.6], see Section 3.1.1 for more details. Note that the relation (1.64) must be applied iteratively at each Newton step in the pseudo-time stepping procedure in (1.67).

Let us rewrite the formulation (1.63) as follows:

## 1.2 Discretization and solution procedure (incremental loading)

Find  $\mathbf{u}_h = (\mathbf{u}_h^B, \mathbf{u}_h^A) \in {}^h\mathcal{V}_D^B \times {}^h\mathcal{V}_D^A$ , such that

$$\overline{F}^{\text{int}}(\mathbf{u}_h, \boldsymbol{\eta}_h) = \overline{F}^{\text{ext}}(\boldsymbol{\eta}_h) - \overline{P}\tilde{\mathbf{u}}(\boldsymbol{\varepsilon}^p, \boldsymbol{\eta}_h) \quad \forall \boldsymbol{\eta}_h \in {}^h\mathcal{V}_0^B \times {}^h\mathcal{V}_0^A \quad (1.65)$$

with

$$\begin{aligned} \overline{F}^{\text{int}}(\mathbf{u}_h, \boldsymbol{\eta}_h) &:= \sum_{i=B,A} \langle S\mathbf{u}_h^i, \boldsymbol{\eta}_h^i \rangle_{\Sigma^i} - \langle \mathbf{t}_C^i, \boldsymbol{\eta}_h^i \rangle_{\Gamma_C}, \\ \overline{P}\tilde{\mathbf{u}}(\boldsymbol{\varepsilon}_h^p, \boldsymbol{\eta}_h) &:= \sum_{i=B,A} \langle N(\text{div}[\mathbb{C}^i : \boldsymbol{\varepsilon}_h^{ip}]), \boldsymbol{\eta}_h^i \rangle_{\Sigma^i} - \langle [\mathbb{C}^i : \boldsymbol{\varepsilon}_h^{ip}] \cdot \mathbf{n}^i, \boldsymbol{\eta}_h^i \rangle_{\Sigma^i}, \\ \overline{F}^{\text{ext}}(\boldsymbol{\eta}_h) &:= \sum_{i=B,A} \langle N\hat{\mathbf{f}}^i, \boldsymbol{\eta}_h^i \rangle_{\Sigma^i} + \langle \hat{\mathbf{t}}^i, \boldsymbol{\eta}_h^i \rangle_{\Gamma_N^i}. \end{aligned}$$

The contact term in the functional  $\overline{F}^{\text{int}}(\mathbf{u}_h, \boldsymbol{\eta}_h)$  is nonlinear due to the constitutive contact conditions. The functional  $\overline{P}\tilde{\mathbf{u}}(\boldsymbol{\varepsilon}_h^p, \boldsymbol{\eta}_h)$  is nonlinear when plastic deformations occur. The non-linear system (1.65) is solved by the following incremental loading technique (pseudo-time stepping) using the incremental data,  $j = 1, 2, \dots, N$ :

$$\begin{aligned} \hat{\mathbf{f}}_0^i &:= \hat{\mathbf{f}}^i(0) = \mathbf{0}, & \hat{\mathbf{f}}_j^i &:= \hat{\mathbf{f}}^i(t_j), & \text{in } \Omega^i, \\ \hat{\mathbf{t}}_0^i &:= \hat{\mathbf{t}}^i(0) = \mathbf{0}, & \hat{\mathbf{t}}_j^i &:= \hat{\mathbf{t}}^i(t_j), & \text{on } \Gamma_N^i, \\ \hat{\mathbf{u}}_0^i &:= \hat{\mathbf{u}}^i(0) = \mathbf{0}, & \hat{\mathbf{u}}_j^i &:= \hat{\mathbf{u}}^i(t_j), & \text{on } \Gamma_D^i. \end{aligned} \quad (1.66)$$

Pseudo-time stepping: For  $j = 1, 2, \dots, N$  find  $(\mathbf{u}_h)_j = ((\mathbf{u}_h^B)_j, (\mathbf{u}_h^A)_j) \in {}^h\mathcal{V}_{D_j}^B \times {}^h\mathcal{V}_{D_j}^A$ , such that

$$\overline{F}^{\text{int}}((\mathbf{u}_h)_j, \boldsymbol{\eta}_h) = \overline{P}\tilde{\mathbf{u}}((\boldsymbol{\varepsilon}_h^p)_j, \boldsymbol{\eta}_h) + \overline{F}_j^{\text{ext}}(\boldsymbol{\eta}_h) \quad \forall \boldsymbol{\eta}_h \in {}^h\mathcal{V}_0^B \times {}^h\mathcal{V}_0^A \quad (1.67)$$

Now we solve (1.67) by Newton's method using the linearization

$$\overline{F}^{\text{int}}((\mathbf{u}_h)_j^{(k)}, \boldsymbol{\eta}_h) = \overline{F}^{\text{int}}((\mathbf{u}_h)_j^{(k-1)}, \boldsymbol{\eta}_h) + \frac{\partial \overline{F}^{\text{int}}((\mathbf{u}_h)_j^{(k-1)}, \boldsymbol{\eta}_h)}{\partial (\mathbf{u}_h)_j^{(k-1)}} (\Delta \mathbf{u}_h)_j^{(k)} \quad (1.68)$$

and setting the iterates

$$(\mathbf{u}_h)_j^{(k)} := (\mathbf{u}_h)_j^{(k-1)} + (\Delta \mathbf{u}_h)_j^{(k)}, \quad k = 1, 2, \dots$$

With the initial values  $(\mathbf{u}_h)_j^{(0)} := (\mathbf{u}_h)_{j-1}$ ,  $(\boldsymbol{\varepsilon}^p)_j^{(0)} = (\boldsymbol{\varepsilon}^p)_{j-1}$ . Note that  $(\mathbf{u}_h)_0 := \mathbf{0}$ ,  $(\boldsymbol{\varepsilon}^p)_0 := \mathbf{0}$ . Here and in the following we use same letters for basis functions and coefficient vectors and write

Newton's method as: For  $k = 1, 2, \dots$ , and given  $(\mathbf{u}_h)_j^{(k-1)}$ ,  $(\boldsymbol{\varepsilon}^p)_j^{(k-1)}$  find  $\mathbf{x} := (\Delta \mathbf{u}_h)_j^k \in {}^h\mathcal{V}_D^B \times {}^h\mathcal{V}_D^A$  with

$$\mathfrak{A}\mathbf{x} = \mathbf{b}, \quad (1.69)$$

where

$$\mathfrak{A} := \frac{\partial \overline{F}^{\text{int}}((\mathbf{u}_h)_j^{(k-1)}, \boldsymbol{\eta}_h)}{\partial (\mathbf{u}_h)_j^{(k-1)}},$$

$$\mathfrak{b} := \overline{P}\tilde{\mathbf{u}}((\boldsymbol{\varepsilon}_h^p)_j^{(k-1)}, \boldsymbol{\eta}_h) + \overline{F}_j^{\text{ext}}(\boldsymbol{\eta}_h) - \overline{F}^{\text{int}}((\mathbf{u}_h)_j^{(k-1)}, \boldsymbol{\eta}_h).$$

we apply a backward Euler method for contact and a forward Euler method for plasticity. Note that at each Newton step we must compute  $\tilde{\mathbf{u}}$  with an extended Somigliana's representation formula (using  $(\mathbf{u}_h)_j^{(k)}$  and the corresponding boundary tractions) with additional suitable volume terms acting on  $(\boldsymbol{\varepsilon}^p)_j^{(k-1)}$ . Next we compute  $\boldsymbol{\varepsilon}_h(\tilde{\mathbf{u}}_h)^i := \frac{1}{2}(\nabla(\tilde{\mathbf{u}}_h)^i + (\tilde{\mathbf{u}}_h)^{iT})$  in  $\Omega^i$  and apply radial return mapping [43] to obtain  $(\boldsymbol{\varepsilon}_h^p)_j^{(k)}$  and go to the next Newton step.

Since we are interested in plasticity with isotropic and kinematic hardening [43] there are also internal variables  $\alpha$  and  $\overline{\boldsymbol{\eta}}^a$  which have to be initialized and updated at each Newton step; same for the tangential macro-displacement  $\mathbf{g}_T^p$ . Thus  $(\boldsymbol{\varepsilon}^p)_j^{(k+1)}$ ,  $\alpha_j^{(k+1)}$ ,  $\overline{\boldsymbol{\eta}}_j^{a(k+1)}$  and  $(\mathbf{g}_T^p)_j^{(k+1)}$  should satisfy the constitutive contact and plasticity conditions which are both enforced by the return-mapping procedure, for details see Section 1.3.

We use both boundaries  $\Gamma^A$  and  $\Gamma^B$  piecewise linear continuous functions for the displacement and piecewise constant discontinuous functions for the traction. We needed the discretization of the traction space for computing the discrete inverse of the single layer potential  $V^{-1}$ . We assume again, that both meshes do not fit each other on the contact boundary. We also assume, that there are no changes of boundary conditions type within one edge. The linear system  $\mathfrak{A}\mathfrak{x} = \mathfrak{b}$  has the following form

$$\begin{pmatrix} S_{\Gamma_N^B} & S_{\Gamma_C^B, \Gamma_N^B}^T & 0 & 0 \\ S_{\Gamma_C^B, \Gamma_N^B} & S_{\Gamma_C^B} + \mathcal{C}^{BB} & -\mathcal{C}^{BA} & 0 \\ 0 & -\mathcal{C}^{AB} & \mathcal{C}^{AA} + S_{\Gamma_C^A} & S_{\Gamma_C^A, \Gamma_N^A}^T \\ 0 & 0 & S_{\Gamma_C^A, \Gamma_N^A} & S_{\Gamma_M^A} \end{pmatrix} \begin{pmatrix} \mathfrak{x}_{\Gamma_N^B}^B \\ \mathfrak{x}_{\Gamma_C^B}^B \\ \mathfrak{x}_{\Gamma_C^A}^A \\ \mathfrak{x}_{\Gamma_N^A}^A \end{pmatrix} = \begin{pmatrix} 0 \\ \mathfrak{b}_{\Gamma_C^B}^B \\ -\mathfrak{b}_{\Gamma_C^A}^A \\ 0 \end{pmatrix} + \mathfrak{b}^{\text{ext}} - \mathfrak{b}^{\text{int}} + \mathfrak{b}_{\boldsymbol{\varepsilon}^p}.$$

Note that only the contact blocks  $\mathcal{C}^{BB}$ ,  $\mathcal{C}^{BA}$ ,  $\mathcal{C}^{AB}$ ,  $\mathcal{C}^{AA}$  of the matrix are updated, which corresponds to backward Euler scheme for contact and forward Euler scheme for plasticity. The details connected with linearization of the contact terms can be found below in section 1.3. With  $S_\Gamma$  the boundary element block for the Steklov operator is denoted. For implementation issues see the Appendix.

### 1.2.3 FEM/BEM

Based on the two previous sections, we can easily derive a FE-BE coupling method. In the following we discuss briefly the main points. Without loss of generality we use BEM discretization for the slave body and FEM discretization for the master body. With the discrete spaces

$${}^h\tilde{\mathbf{V}}_D := {}^h\mathbf{V}_D^B \times {}^h\mathbf{V}_D^A, \quad {}^h\tilde{\mathbf{V}}_0 := {}^h\mathbf{V}_0^B \times {}^h\mathbf{V}_0^A,$$

the coupling formulation now will be: Find  $\mathbf{u}_h = (\mathbf{u}_h^B, \mathbf{u}_h^A) \in {}^h\tilde{\mathbf{V}}_D$ :

$$\tilde{F}^{int}(\mathbf{u}_h, \boldsymbol{\eta}_h) - \tilde{P}_{\mathbf{u}_h}(\boldsymbol{\varepsilon}_h^p, \boldsymbol{\eta}_h) = \tilde{F}^{ext}(\boldsymbol{\eta}_h) \quad \forall \boldsymbol{\eta}_h \in {}^h\tilde{\mathbf{V}}_0, \quad (1.70)$$

where

$$\begin{aligned} \tilde{F}^{int}(\mathbf{u}_h, \boldsymbol{\eta}_h) &:= (\boldsymbol{\sigma}_h^i, \boldsymbol{\varepsilon}(\boldsymbol{\eta}_h^i))_{\Omega^A} + \langle S\mathbf{u}^i, \boldsymbol{\eta}^i \rangle_{\Sigma^B} - \sum_{i=B,A} \langle \mathbf{t}_{\varepsilon_C}^i, \boldsymbol{\eta}_h^i \rangle_{\Gamma_C}, \\ \tilde{P}_{\mathbf{u}_h}(\boldsymbol{\varepsilon}_h^p, \boldsymbol{\eta}_h) &:= \langle N(\operatorname{div}[\mathbb{C}^i : \boldsymbol{\varepsilon}_h^{ip}]), \boldsymbol{\eta}^i \rangle_{\Sigma^B} - \langle [\mathbb{C}^i : \boldsymbol{\varepsilon}_h^{ip}] \cdot \mathbf{n}, \boldsymbol{\eta}^i \rangle_{\Sigma^B} \\ \tilde{F}^{ext}(\boldsymbol{\eta}_h) &:= \langle N\hat{\mathbf{f}}^i, \boldsymbol{\eta}^i \rangle_{\Sigma^B} + (\hat{\mathbf{f}}^i, \boldsymbol{\eta}^i)_{\Omega^A} + \sum_{i=B,A} \langle \hat{\mathbf{t}}^i, \boldsymbol{\eta}_h^i \rangle_{\Gamma_N^i}, \\ \boldsymbol{\sigma}_h^i &:= \boldsymbol{\sigma}(\mathbf{u}_h^i), \quad \boldsymbol{\varepsilon}_h^{ip} := \boldsymbol{\varepsilon}^p(\mathbf{u}_h^i), \quad \mathbf{t}_{\varepsilon_C} := \mathbf{t}_{\varepsilon_C}(\mathbf{u}_h^i). \end{aligned}$$

We can use an incremental loading process analogously to above one together with Newton method. Then we end up with a linear system  $\mathfrak{A}\mathfrak{x} = \mathfrak{b}$  given by

$$\begin{pmatrix} S_{\Gamma_N^B} & S_{\Gamma_C^B, \Gamma_N^B}^T & 0 & 0 \\ S_{\Gamma_C^B, \Gamma_N^B} & S_{\Gamma_C^B} + \mathcal{C}^{BB} & -\mathcal{C}^{BA} & 0 \\ 0 & -\mathcal{C}^{AB} & \mathcal{C}^{AA} + C_{\Gamma_C^A}^{pl} & (B_{\Gamma_C^A}^{pl})^T \\ 0 & 0 & B_{\Gamma_C^A}^{pl} & A_{\Omega^A}^{pl} \end{pmatrix} \begin{pmatrix} \mathfrak{x}_{\Gamma_N^B}^B \\ \mathfrak{x}_{\Gamma_C^B}^B \\ \mathfrak{x}_{\Gamma_C^A}^A \\ \mathfrak{x}_{\Gamma_N^A}^A \end{pmatrix} = \begin{pmatrix} 0 \\ \mathfrak{b}_{\Gamma_C^B}^B \\ -\mathfrak{b}_{\Gamma_C^A}^A \\ 0 \end{pmatrix} + \begin{pmatrix} 0 \\ \mathfrak{b}_{\Gamma_C^B}^B \\ -\mathfrak{b}_{\Gamma_C^A}^A \\ 0 \end{pmatrix}.$$

The meaning of the particular terms is the same as in the above linear systems describing FEM/FEM and BEM/BEM approaches.

### 1.3 Linearizations of contact and elastoplasticity

In the linearization (1.68) we proceed with the non-linear contact terms as follows. With (1.44) we have for the contact term

$$\int_{\Gamma_C} \mathbf{t}_{\epsilon_C}(\mathbf{u}) \cdot \boldsymbol{\eta} = C_N(\mathbf{u}, \boldsymbol{\eta}) + C_T(\mathbf{u}, \boldsymbol{\eta})$$

with

$$C_N(\mathbf{u}, \boldsymbol{\eta}) := \frac{1}{\epsilon_N} \int_{\Gamma_C} (u_N^{BA} - g)^+ \eta_N^{BA} d\Gamma, \quad C_T(\mathbf{u}, \boldsymbol{\eta}) := \frac{1}{\epsilon_T} \int_{\Gamma_C} g_T^e(u_T) \eta_T^{BA} d\Gamma.$$

The segment-to-segment contact description is used.

The linearization gives

$$\begin{aligned} - \int_{\Gamma_C^B} (\mathbf{t}_{\epsilon_C})_n^{(k+1)} \cdot (\boldsymbol{\eta}^A - \boldsymbol{\eta}^B) d\Gamma &= - \int_{\Gamma_C^B} (\mathbf{t}_{\epsilon_C})_n^{(k)} \cdot (\boldsymbol{\eta}^A - \boldsymbol{\eta}^B) d\Gamma \\ &\quad - \int_{\Gamma_C^B} \Delta \mathbf{t}_{\epsilon_C} \cdot (\boldsymbol{\eta}^A - \boldsymbol{\eta}^B) d\Gamma = - \int_{\Gamma_C^B} (\mathbf{t}_{\epsilon_C})_n^{(k)} \cdot (\boldsymbol{\eta}^A - \boldsymbol{\eta}^B) d\Gamma \\ &\quad - \int_{\Gamma_C^B} [\Delta \sigma_N \mathbf{n}^A \cdot (\boldsymbol{\eta}^A - \boldsymbol{\eta}^B) + \Delta \boldsymbol{\sigma}_T \cdot (\boldsymbol{\eta}^A - \boldsymbol{\eta}^B)] d\Gamma. \end{aligned} \quad (1.71)$$

The values of  $\sigma_N$  and  $\boldsymbol{\sigma}_T$  are defined by (1.45) and (1.46). The first integrand is known from the previous  $k^{th}$  Newton iteration. It gives a contribution to the right hand side, second and third integrand contribute to the matrix. The increments of normal  $\sigma_N$  and tangential  $\boldsymbol{\sigma}_T$  parts of the traction  $\mathbf{t}_{\epsilon_C}$  on the contact boundary  $\Gamma_C$  are

$$\begin{aligned} \Delta \sigma_N &:= \frac{\partial C_N((\mathbf{u}_h)_j^{(k-1)}, \boldsymbol{\eta}_h)}{\partial (\mathbf{u}_h)_j^{(k-1)}} (\Delta \mathbf{u}_h)_j^{(k)}, \\ \Delta \boldsymbol{\sigma}_T &:= \frac{\partial C_T((\mathbf{u}_h)_j^{(k-1)}, \boldsymbol{\eta}_h)}{\partial (\mathbf{u}_h)_j^{(k-1)}} (\Delta \mathbf{u}_h)_j^{(k)}. \end{aligned}$$

For the normal component of the traction we obtain

$$\begin{aligned} \frac{\partial C_N((\mathbf{u}_h)_j^{(k-1)}, \boldsymbol{\eta}_h)}{\partial (\mathbf{u}_h)_j^{(k-1)}} (\Delta \mathbf{u}_h)_j^{(k)} &= \frac{d}{d\alpha} C_n((\mathbf{u}_h)_j^{(k-1)} + \alpha (\Delta \mathbf{u}_h)_j^{(k)}, \boldsymbol{\eta}_h) \Big|_{\alpha=0} \\ &= \frac{1}{\epsilon_N} \int_{\Gamma_C} \frac{d}{d\alpha} [( (\mathbf{u}_{h_n})_j^{(k-1)} + \alpha (\Delta \mathbf{u}_{h_n})_j^{(k)} ] - g \Big|_{\alpha=0} \eta_N^{BA} d\Gamma. \end{aligned}$$



with (note  $(\mathbf{u}_{h_n})$  denotes the normal component of  $\mathbf{u}_h$ )

$$\frac{d}{d\alpha} \left( [(\mathbf{u}_{h_n})_j^{(k-1)} + \alpha(\Delta \mathbf{u}_{h_n})_j^{(k)}] - g \right)^+ \Big|_{\alpha=0} = \begin{cases} [(\Delta \mathbf{u}_{h_n})_j^{(k)}], & \text{if } [(\mathbf{u}_{h_n})_j^{(k-1)}] - g > 0, \\ 0, & \text{if } [(\mathbf{u}_{h_n})_j^{(k-1)}] - g < 0. \end{cases}$$

For the tangential contact term we use the linearization

$$\begin{aligned} & \frac{d}{d\alpha} C_T((\mathbf{u}_h)_j^{(k-1)} + \alpha(\Delta \mathbf{u}_h)_j^{(k)}, \boldsymbol{\eta}_T) \Big|_{\alpha=0} \\ &= \begin{cases} \int_{\Gamma_C} \frac{1}{\epsilon_T} [(\Delta \mathbf{u}_{h_T})_j^{(k)}] [\boldsymbol{\eta}_{h_T}] d\Gamma, & \text{if } |g_T((\mathbf{u}_{h_T})_j^{(k-1)})| \leq \mu_f \frac{\epsilon_T}{\epsilon_N} g_N((\mathbf{u}_{h_N})_j^{(k-1)}) \text{ (stick),} \\ \int_{\Gamma_C} \frac{\mu_f}{\epsilon_N} \text{sign}(g_N((\mathbf{u}_{h_N})_j^{(k-1)})) g_T((\mathbf{u}_{h_T})_j^{(k-1)}) [(\Delta \mathbf{u}_{h_N})_j^{(k)}] [\boldsymbol{\eta}_{h_T}] d\Gamma, \\ \hspace{15em} \text{if } |g_T((\mathbf{u}_{h_T})_j^{(k-1)})| > \mu_f \frac{\epsilon_T}{\epsilon_N} g_N((\mathbf{u}_{h_N})_j^{(k-1)}) \text{ (slip).} \end{cases} \end{aligned}$$

This completes the linearization of the matrix terms in the Newton algorithm which converges if the load increments are chosen sufficiently small. This follows by application of the arguments of Blaheta in [5], where a pure finite element method is used.

Next, we consider the normal contact term in 1.71. Omitting indexes which represent iteration numbers we rewrite the normal contact term in (1.71) as

$$\begin{aligned} - \int_{\Gamma_C^B} \Delta \sigma_N \mathbf{n}^A \cdot (\boldsymbol{\eta}^A - \boldsymbol{\eta}^B) d\Gamma &= \frac{1}{\epsilon_N} \int_{\Gamma_C^B} \Delta g_N \mathbf{n}^A \cdot (\boldsymbol{\eta}^A - \boldsymbol{\eta}^B) d\Gamma \\ &= \frac{1}{\epsilon_N} \int_{\Gamma_C^B} ((\Delta \mathbf{u}^A - \Delta \mathbf{u}^B) \cdot \mathbf{n}^A) (\mathbf{n}^B \cdot (\boldsymbol{\eta}^A - \boldsymbol{\eta}^B)) d\Gamma \\ &= \frac{1}{\epsilon_N} \int_{\Gamma_C^B} (\Delta \mathbf{u}^A - \Delta \mathbf{u}^B) \cdot (\mathbf{n}^A \otimes \mathbf{n}^A) \cdot (\boldsymbol{\eta}^A - \boldsymbol{\eta}^B) d\Gamma \\ &= \frac{1}{\epsilon_N} \int_{\Gamma_C^B} \Delta \mathbf{u}^A \cdot (\mathbf{n}^A \otimes \mathbf{n}^A) \cdot \boldsymbol{\eta}^A d\Gamma \\ &\quad + \frac{1}{\epsilon_N} \int_{\Gamma_C^B} \Delta \mathbf{u}^B \cdot (\mathbf{n}^A \otimes \mathbf{n}^A) \cdot \boldsymbol{\eta}^B d\Gamma \\ &\quad - \frac{1}{\epsilon_N} \int_{\Gamma_C^B} \Delta \mathbf{u}^A \cdot (\mathbf{n}^A \otimes \mathbf{n}^A) \cdot \boldsymbol{\eta}^B d\Gamma \\ &\quad - \frac{1}{\epsilon_N} \int_{\Gamma_C^B} \Delta \mathbf{u}^B \cdot (\mathbf{n}^A \otimes \mathbf{n}^A) \cdot \boldsymbol{\eta}^A d\Gamma. \end{aligned}$$

All the integrals can be rewritten as a sum over all slave segments. For example, for the

fourth integral there holds

$$\begin{aligned} & \frac{1}{\epsilon_{\mathcal{N}}} \int_{\Gamma_C^B} \Delta \mathbf{u}^B \cdot (\mathbf{n}^A \otimes \mathbf{n}^A) \cdot \boldsymbol{\eta}^A d\Gamma \\ &= \sum_{I \subset \Gamma_C^B} \frac{1}{\epsilon_{\mathcal{N}}} \int_I \Delta \mathbf{u}^B \cdot (\mathbf{n}^A \otimes \mathbf{n}^A) \cdot \boldsymbol{\eta}^A d\Gamma \\ &= \sum_{I \subset \Gamma_C^B} \sum_{J \subset \Gamma_C^A} \frac{1}{\epsilon_{\mathcal{N}}} \int_{I(J)} \Delta \mathbf{u}^B \cdot (\mathbf{n}^A \otimes \mathbf{n}^A) \cdot \boldsymbol{\eta}^A ds, \end{aligned}$$

where  $I(J) = \{\mathbf{x}^B \in I : \mathbf{x}^A(\bar{\xi}) = \text{proj}(\mathbf{x}^B) \in J\}$  and  $i, j = B, A$ .

The functions  $\Delta \mathbf{u}^i$  on  $I$  and  $\boldsymbol{\eta}^j$  on  $J$  are approximated by linear splines, and therefore they can be represented as

$$\begin{aligned} \Delta \mathbf{u}^B &= \mathbf{u}_{I,1}^B \phi_{I,1}^B + \mathbf{u}_{I,2}^B \phi_{I,2}^B =: \mathbf{u}_I^B \phi_I^B, \\ \boldsymbol{\eta}^A &= \mathbf{v}_{J,1}^A \phi_{J,1}^A + \mathbf{v}_{J,2}^A \phi_{J,2}^A =: \mathbf{u}_J^A \phi_J^A. \end{aligned}$$

The components of the matrix  $\mathcal{C}^{BA}$ , corresponding to some segment  $I$  on the slave side and  $J$  on the master side, given by the integral

$$\frac{1}{\epsilon_{\mathcal{N}}} \int_{I(J)} \phi_I^B \cdot (\mathbf{n}^A \otimes \mathbf{n}^A) \cdot \phi_J^A d\Gamma.$$

This integral is computed via numerical quadrature as

$$\begin{aligned} & \frac{1}{\epsilon_{\mathcal{N}}} \sum_{x^B \in I(J)} \phi(x^B) \cdot (\mathbf{n}(x^A) \otimes \mathbf{n}(x^A)) \cdot \phi(x^A) \mathcal{J}_I w_{x^B}, \\ & \qquad \qquad \qquad x^A := \text{proj}(x^B), \end{aligned}$$

where  $\mathcal{J}_I$  is the Jacobian of transformation from the slave segment  $I$  to the reference segment  $[-1, 1]$ , and  $w_{x^B}$  is a weight of the Gauß point  $x^B$ . The components of other contact matrixes  $\mathcal{C}^{BB}, \mathcal{C}^{AB}, \mathcal{C}^{AA}$  are computed similarly. For  $\mathcal{C}^{ij}$  we have

$$\begin{aligned} \mathcal{C}^{ij} : & \frac{1}{\epsilon_{\mathcal{N}}} \sum_{x^B \in I(J)} \phi(x^i) \cdot (\mathbf{n}(x^A) \otimes \mathbf{n}(x^A)) \cdot \phi(x^j) \mathcal{J}_I w_{x^B}, \quad i, j = B, A \\ & \qquad \qquad \qquad x^A := \text{proj}(x^B). \end{aligned}$$

For computing of tangential contact integral in 1.71

$$- \int_{\Gamma_C^B} \Delta \boldsymbol{\sigma}_T \cdot (\boldsymbol{\eta}^A - \boldsymbol{\eta}^B) ds$$

we have to distinguish between stick state and slide state,

$$\Delta \boldsymbol{\sigma}_{\epsilon_T} = \begin{cases} -\frac{1}{\epsilon_T} \Delta \mathbf{g}_T^e & = -\frac{1}{\epsilon_T} ((\Delta \mathbf{u}^B - \Delta \mathbf{u}^A) \cdot \mathbf{e}^A) \mathbf{e}^A & \text{macro-stick,} \\ -\mu_f \frac{1}{\epsilon_N} \Delta g_N \frac{\mathbf{g}_T^e}{\|\mathbf{g}_T^e\|} & = -\mu_f \frac{1}{\epsilon_N} \text{sign}(\mathbf{g}_T^e \cdot \mathbf{e}^A) ((\Delta \mathbf{u}^B - \Delta \mathbf{u}^A) \cdot \mathbf{n}^A) \mathbf{e}^A & \text{macro-slip.} \end{cases}$$

Defining

$$\frac{1}{\epsilon_T^{sl}} = \mu_f \frac{1}{\epsilon_N} \text{sign}(\mathbf{g}_T^e \cdot \mathbf{e}^A),$$

analogously to the normal contact term, we obtain the following contributions to the contact matrices:

*macro-stick:*

$$\mathcal{C}^{ij} : \quad \frac{1}{\epsilon_T} \sum_{x^B \in I(J)} \boldsymbol{\phi}(x^i) \cdot (\mathbf{e}(x^A) \otimes \mathbf{e}(x^A)) \cdot \boldsymbol{\phi}(x^j) \mathcal{J}_I w_{x^B}, \quad i, j = B, A, \\ x^A := \text{proj}(x^B),$$

*macro-slip:*

$$\mathcal{C}^{ij} : \quad \frac{1}{\epsilon_T^{sl}} \sum_{x^B \in I(J)} \boldsymbol{\phi}(x^i) \cdot (\mathbf{n}(x^A) \otimes \mathbf{e}(x^A)) \cdot \boldsymbol{\phi}(x^j) \mathcal{J}_I w_{x^B}, \quad i, j = B, A, \\ x^A := \text{proj}(x^B).$$

Now, in (1.71) only one term is left - the contribution to the right hand side. We have

$$\begin{aligned} \int_{\Gamma_C^B} (\mathbf{t}_C)_n^{(k)} \cdot (\boldsymbol{\eta}^B - \boldsymbol{\eta}^A) d\Gamma &= \int_{\Gamma_C^B} (\mathbf{t}_C)_n^{(k)} \cdot \boldsymbol{\eta}^B ds - \int_{\Gamma_C^B} (\mathbf{t}_C)_n^{(k)} \cdot \boldsymbol{\eta}^A d\Gamma \\ &= \sum_{I \subset \Gamma_C^B} \int_I (\mathbf{t}_C)_n^{(k)} \cdot \boldsymbol{\eta}^B ds - \sum_{I \subset \Gamma_C^B} \sum_{J \subset \Gamma_C^A} \int_{I(J)} (\mathbf{t}_C)_n^{(k)} \cdot \boldsymbol{\eta}^A d\Gamma. \end{aligned}$$

That leads to the following elementary contributions to the vector of right hand side

$$\int_I (\mathbf{t}_C)_n^{(k)} \cdot \boldsymbol{\phi}_I^B ds, \quad \sum_{I \subset \Gamma_C^B} \int_{I(J)} (\mathbf{t}_C)_n^{(k)} \cdot \boldsymbol{\phi}_J^A d\Gamma.$$

Calculation of both terms can be done using numerical quadrature.

$$\begin{aligned} \hat{\mathbf{f}}^B : & \quad \sum_{I \subset \Gamma_C^B} \sum_{x^B \in I} (\mathbf{t}_C)_n^{(k)}(x^B) \cdot \boldsymbol{\phi}(x^B) \mathcal{J}_I w_{x^B}, \\ \hat{\mathbf{f}}^A : & \quad \sum_{I \subset \Gamma_C^B} \sum_{x^B \in I(J)} (\mathbf{t}_C)_n^{(k)}(x^B) \cdot \boldsymbol{\phi}(x^A) \mathcal{J}_I w_{x^B}, \\ & \quad x^A := \text{proj}(x^B). \end{aligned}$$

After every Newton iteration within the computation of the contact boundary tractions

the return mapping procedure is executed. It goes back to the fact that due to the Coulomb friction law in every point of the contact surfaces for the norm of tangential traction there holds

$$\|\boldsymbol{\sigma}_T\| \leq -\mu_f \sigma_N.$$

Sliding occurs when  $\|\boldsymbol{\sigma}_T\| = -\mu_f \sigma_N$  holds, i.e. the material point has non-zero macro-displacement  $\mathbf{g}^p \neq 0$ .

The *return mapping procedure* is performed in each Gauß point  $\mathbf{x}^B(\zeta^B)$  of the slave side. For the current iteration the parameter of the projection  $\bar{\zeta}_0^A(\zeta^B)$  of  $\mathbf{x}^B(\zeta^B)$  to the master side is known from the previous iteration. If such a projection does not exist or the point  $\mathbf{x}^B$  was not in contact with the master side, the tangential traction is set to zero. We detect the current projection  $\bar{\mathbf{x}}^A(\zeta^B) = \mathbf{x}^A(\bar{\zeta}^A(\zeta^B))$  of  $\mathbf{x}^B(\zeta^B)$ , by enforcing

$$[\mathbf{x}^A(\zeta^A) - \mathbf{x}^B(\zeta^B)] \cdot \mathbf{a}^A(\zeta^A) = 0,$$

where  $\mathbf{a}^A$  denotes the tangential vector of the corresponding master segment. We denote by  $\mathbf{n}^A$  its outward normal vector. The penetration function is computed by

$$g_N(\zeta^B) = [\bar{\mathbf{x}}^A(\zeta^B) - \mathbf{x}^B(\zeta^B)] \cdot \bar{\mathbf{n}}^A(\zeta^B)$$

If the point  $\mathbf{x}^B$  has no projection on the master side or the penetration function  $g_N$  is negative (i.e. the bodies are disjoint in  $\mathbf{x}^B$ ), then the return mapping procedure is not executed. The boundary tractions are set to zero, i.e.

$$\sigma_N = 0, \quad \boldsymbol{\sigma}_T = 0.$$

Otherwise, set the normal pressure

$$\sigma_N = -\frac{1}{\epsilon_N} g_N.$$

The value of the tangential traction is defined by the frictional yield function

$$\phi_C(\sigma_N, \boldsymbol{\sigma}_T) = \|\boldsymbol{\sigma}_T\| + \mu_f \sigma_N.$$

The total tangential displacement and the trial tangential tractions are computed as

$$\mathbf{g}_T = (\bar{\zeta}^A - \bar{\zeta}_0^A) \mathbf{a}^A, \quad \boldsymbol{\sigma}_T^{\text{trial}} = -\frac{1}{\epsilon_T} \mathbf{g}_T.$$

Now, the return mapping consists in constructing the physical solution by checking the

sign of the yield function:

$$\begin{aligned}\phi_C(\sigma_{\mathcal{N}}, \boldsymbol{\sigma}_{\mathcal{T}}^{\text{trial}}) \leq 0 &\implies \boldsymbol{\sigma}_{\mathcal{T}} = \boldsymbol{\sigma}_{\mathcal{T}}^{\text{trial}}, \\ \phi_C(\sigma_{\mathcal{N}}, \boldsymbol{\sigma}_{\mathcal{T}}^{\text{trial}}) > 0 &\implies \boldsymbol{\sigma}_{\mathcal{T}} = -\mu_f \sigma_{\mathcal{N}} \frac{\boldsymbol{\sigma}_{\mathcal{T}}^{\text{trial}}}{\|\boldsymbol{\sigma}_{\mathcal{T}}^{\text{trial}}\|}.\end{aligned}$$

If the yield condition is not satisfied, non-zero tangential macro-displacement  $\mathbf{g}_{\mathcal{T}}^p$  occurs, and the tangential traction is given by

$$\boldsymbol{\sigma}_{\mathcal{T}} = -\frac{1}{\epsilon_{\mathcal{T}}}(\mathbf{g}_{\mathcal{T}} - \mathbf{g}_{\mathcal{T}}^p), \quad \mathbf{g}_{\mathcal{T}}^p \neq 0.$$

Next we linearize the elastoplasticity term. Since we use the backward Euler method for the plasticity in case of FE discretization, the energy bilinear form is nonlinear. We restrict our attention to the case where one of the bodies has FE discretization and omit upper indexes "B" and "A" marking the master or the slave body.

Let us consider the linearization of the energy bilinear form closer. Using the Taylor expansion we get

$$(\boldsymbol{\sigma}(\mathbf{U}_n^{(k+1)}), \boldsymbol{\varepsilon}(\boldsymbol{\eta}_h)) = (\boldsymbol{\sigma}(\mathbf{U}_n^{(k)}), \boldsymbol{\varepsilon}(\boldsymbol{\eta}_h)) + \frac{\partial}{\partial \mathbf{U}_n^{(k)}}(\boldsymbol{\sigma}(\mathbf{U}_n^{(k)}), \boldsymbol{\varepsilon}(\boldsymbol{\eta}_h)) \Delta \mathbf{U}_n^{(k+1)}.$$

The first summand contribute to the right hand side and the second one contributes to the matrix of the linear system as explained in Section 1.2.1. Furthermore there holds

$$\frac{\partial \boldsymbol{\sigma}(\mathbf{U}_n^{(k)})}{\partial \mathbf{U}_n^{(k)}} \Delta \mathbf{U}_n^{(k+1)} = \frac{\partial}{\partial \mathbf{U}_n^{(k)}} \mathbb{C} : (\boldsymbol{\varepsilon}(\mathbf{U}_n^{(k)}) - \boldsymbol{\varepsilon}^p(\mathbf{U}_n^{(k)})) \Delta \mathbf{U}_n^{(k+1)} \quad (1.72)$$

$$= (\mathbb{C}^{ep})_n^{(k+1)} : \boldsymbol{\varepsilon}(\Delta \mathbf{U}_n^{(k+1)}). \quad (1.73)$$

We derive the explicit expression for  $(\mathbb{C}^{ep})_n^{(k+1)}$  below see Box 1.3.1 and 1.3.2.

Discretization of the yield condition, flow rule and hardening law (1.39) with  $\Delta\gamma := \gamma_{n+1} \Delta t$  provides

$$\begin{aligned}\boldsymbol{\eta}_n^{(k+1)} &:= \text{dev}[\boldsymbol{\sigma}_n^{(k+1)}] - \boldsymbol{\beta}_n^{(k+1)}, \quad \text{tr}[\boldsymbol{\beta}_n^{(k+1)}] := 0, \\ (\phi_{pl})_n^{(k+1)} &= \|\boldsymbol{\eta}_n^{(k+1)}\| - \sqrt{\frac{2}{3}} K(\alpha_n^{(k+1)}), \\ n_n^{(k+1)} &:= \frac{\eta_n^{(k+1)}}{\|\boldsymbol{\eta}_n^{(k+1)}\|} \\ (\boldsymbol{\varepsilon}^p)_n^{(k+1)} &= (\boldsymbol{\varepsilon}^p)_n^{(k)} + \Delta\gamma n_n^{(k+1)}, \\ \boldsymbol{\beta}_n^{(k+1)} &= \boldsymbol{\beta}_n^{(k)} + \sqrt{\frac{2}{3}} \Delta H_n^{(k+1)} n_n^{(k+1)},\end{aligned} \quad (1.74)$$

$$\alpha_n^{(k+1)} = \alpha_n^{(k)} + \Delta\gamma\sqrt{\frac{2}{3}},$$

where

$$\Delta H_n^{(k+1)} := H(\alpha_n^{(k+1)}) - H(\alpha_n^{(k)}).$$

Isotropic and kinematic hardening modules  $K(\alpha)$ ,  $H(\alpha)$  are defined by (1.40). The discrete version loading/unloading complementary Kuhn-Tucker conditions is

$$\Delta\gamma \geq 0, \quad (\phi_{pl})_n^{(k+1)} \leq 0, \quad \Delta\gamma(\phi_{pl})_n^{(k+1)} = 0. \quad (1.75)$$

In our numerical experiments we have implemented algorithms corresponding to the boxes below (see also [43]).

**Box 1.3.1.** *Consistency Condition. Determination of  $\Delta\gamma$  (see [43])*

1. *Initialize.*

$$\begin{aligned} \Delta\gamma^{(0)} &:= 0, \\ \alpha_{n+1}^{(0)} &:= 0. \end{aligned}$$

2. *Iterate.*

*DO UNTIL* :  $|g(\Delta\gamma^{(k)})| < TOL$ ,

$k \leftarrow k + 1$

2.1. *Compute iterate  $\Delta\gamma^{(k+1)}$  :*

$$\begin{aligned} g(\Delta\gamma^{(k)}) &:= -\sqrt{\frac{2}{3}}K(\alpha_{n+1}^{(k)}) + \|\xi_{n+1}^{trial}\| \\ &\quad - \left( 2\mu\Delta\gamma^{(k)} + \sqrt{\frac{2}{3}} \left( H(\alpha_{n+1}^{(k)}) - H(\alpha_n^{(k)}) \right) \right) \\ Dg(\Delta\gamma^{(k)}) &:= -2\mu \left( 1 + \frac{H'(\alpha_{n+1}^{(k)}) + K'(\alpha_{n+1}^{(k)})}{3\mu} \right) \\ \Delta\gamma^{(k+1)} &:= \Delta\gamma^{(k)} - \frac{g(\Delta\gamma^{(k)})}{Dg(\Delta\gamma^{(k)})} \end{aligned}$$

2.2. *Update equivalent plastic strain*

$$\alpha_{n+1}^{(k+1)} = \alpha_n + \sqrt{\frac{2}{3}}\Delta\gamma^{(k+1)}$$

**Box 1.3.2.** *Radial Return Algorithm.. Nonlinear Isotropic/Kinematic Hardening (see [43])*

1. Compute trial elastic stress.

$$\begin{aligned}\mathbf{e}_{n+1} &:= \boldsymbol{\varepsilon}_{n+1} - \frac{1}{3}(\text{tr}[\boldsymbol{\varepsilon}_{n+1}])\mathbf{1} \\ \mathbf{s}_{n+1}^{trial} &:= 2\mu(\mathbf{e}_{n+1} - \mathbf{e}_n^p) \\ \boldsymbol{\xi}_{n+1}^{trail} &:= \mathbf{s}_{n+1}^{trial} - \boldsymbol{\beta}_{n+1}\end{aligned}$$

2. Check yield condition

$$\phi_{n+1}^{trial} := \|\boldsymbol{\xi}_{n+1}^{trail}\| - \sqrt{\frac{2}{3}}K(\alpha_n)$$

IF  $\phi_{n+1}^{trial} < 0$  THEN:

Set  $(o)_{n+1} := (o)_{n+1}^{trial}$  & EXIT

ENDIF.

3. Compute  $\mathbf{n}_{n+1}$  and find  $\Delta\gamma$  from BOX 1.3.1. Set

$$\begin{aligned}\mathbf{n}_{n+1} &:= \frac{\boldsymbol{\xi}_{n+1}^{trail}}{\|\boldsymbol{\xi}_{n+1}^{trail}\|}, \\ \alpha_{n+1} &:= \alpha_n + \sqrt{\frac{2}{3}}\Delta\gamma\end{aligned}$$

4. Update back stress, plastic strain and stress

$$\begin{aligned}\boldsymbol{\beta}_{n+1} &:= \boldsymbol{\beta}_n + \sqrt{\frac{2}{3}}[H(\alpha_{n+1}) - H(\alpha_n)]\mathbf{n}_{n+1}, \\ \mathbf{e}_{n+1}^p &:= \mathbf{e}_n^p + \Delta\gamma\mathbf{n}_{n+1}, \\ \boldsymbol{\sigma}_{n+1} &:= k \text{tr}[\boldsymbol{\varepsilon}_{n+1}]\mathbf{1} + \mathbf{s}_{n+1}^{trial} - 2\mu\Delta\gamma\mathbf{n}_{n+1}.\end{aligned}$$

5. Compute consistent elastoplastic tangent moduli

$$\begin{aligned}\mathbf{C}_{n+1} &:= k\mathbf{1} \otimes \mathbf{1} + 2\mu\vartheta_{n+1}[\mathbf{I} - \frac{1}{3}\mathbf{1} \otimes \mathbf{1}] - 2\mu\bar{\vartheta}_{n+1}\mathbf{n}_{n+1} \otimes \mathbf{n}_{n+1}, \\ \vartheta_{n+1} &:= 1 - \frac{2\mu\Delta\gamma}{\|\boldsymbol{\xi}_{n+1}^{trail}\|}, \\ \bar{\vartheta}_{n+1} &:= \frac{1}{1 + \frac{[K'+H']_{n+1}}{3\mu}} - (1 - \bar{\vartheta}_{n+1}).\end{aligned}$$

This representation used in (1.72) generates the linear system matrix contribution corresponding to the plastic behavior.

## 1.4 Contact functional investigation

Recall the definition of the yield contact function ( $\mathbf{t} := (\sigma_N, \boldsymbol{\sigma}_T)$ )

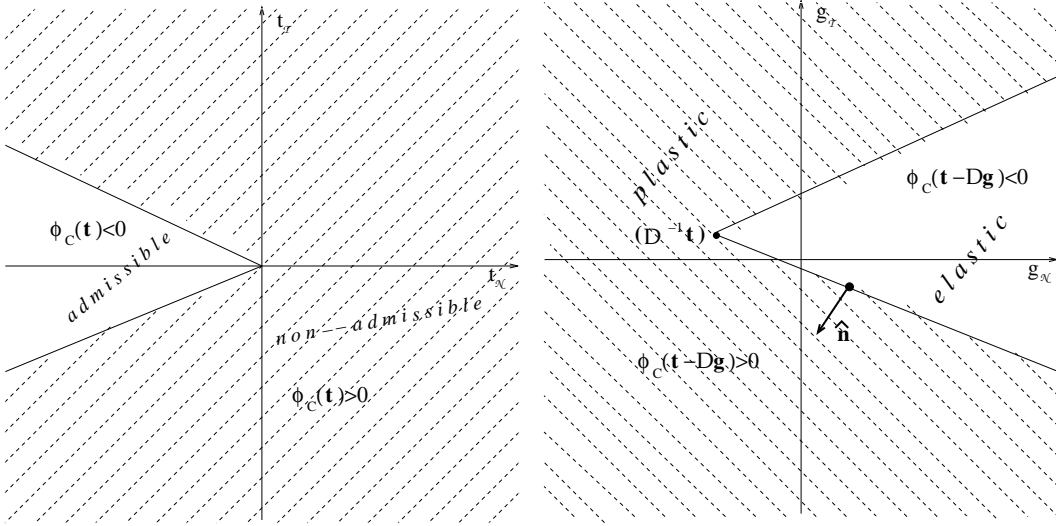


Figure 1.1: Admissible region of traction  
Figure 1.2: Elastic and plastic regions of penetration

$$\phi_C(\mathbf{t}) = \|\boldsymbol{\sigma}_T\| + \mu_f \sigma_N, \quad \phi_C : \mathbf{t} \mapsto \mathbb{R}. \quad (1.76)$$

We will use an equivalent and more convenient representation of a traction  $\mathbf{t}$  and a gap  $\mathbf{g}$  in case of two dimensions. The normal part of both vectors in 2D and 3D is represented by a scalar, whereas in 2D a tangential part one can also define by a scalar. Let  $\boldsymbol{\tau}$  be a unit tangent vector to the boundary  $\Gamma^A$ , then we define  $\sigma_T := \boldsymbol{\sigma}_T \cdot \boldsymbol{\tau}$  and  $g_T := \mathbf{g}_T \cdot \boldsymbol{\tau}$ .

The admissible set of tractions  $\mathbf{t}$  is defined as (see Fig. 1.1)

$$S_C := \{\mathbf{t} \in \mathbb{R}^2 \mid \phi_C(\mathbf{t}) \leq 0\}. \quad (1.77)$$

$$S_C(\Gamma) := \left\{ \mathbf{t} \in H^1(0, T; (H^{1/2}(\Gamma))^2) \mid \phi_C(\mathbf{t}(t, \mathbf{x})) \leq 0, \text{ for a.a. } (t, \mathbf{x}) \in [0, T] \times \Gamma \right\}. \quad (1.78)$$



In addition we define following sets:

$$S_C^e := \{\mathbf{t} \in \mathbb{R}^2 \mid \phi_C(\mathbf{t}) < 0\}, \quad (1.79)$$

$$S_C^p := \{\mathbf{t} \in \mathbb{R}^2 \mid \phi_C(\mathbf{t}) > 0\}, \quad (1.80)$$

$$S_C^{ep} := S_C^e \cup S_C^p, \quad (1.81)$$

$$S_C^i := \{\mathbf{t} \in \mathbb{R}^2 \mid \phi_C(\mathbf{t}) = 0 \text{ or } (\|\boldsymbol{\sigma}_T\| = 0, \phi_C(\mathbf{t}) > 0)\}, \quad (1.82)$$

$$S_C^e(\Gamma) := \left\{ \mathbf{t} \in H^1(0, T; (H^{1/2}(\Gamma))^2) \mid \phi_C(\mathbf{t}(t, \mathbf{x})) < 0, \text{ for a.a. } (t, \mathbf{x}) \in [0, T] \times \Gamma \right\},$$

$$S_C^p(\Gamma) := \left\{ \mathbf{t} \in H^1(0, T; (H^{1/2}(\Gamma))^2) \mid \phi_C(\mathbf{t}(t, \mathbf{x})) > 0, \text{ for a.a. } (t, \mathbf{x}) \in [0, T] \times \Gamma \right\},$$

$$S_C^i(\Gamma) := \left\{ \mathbf{t} \in H^1(0, T; (H^{1/2}(\Gamma))^2) \mid \text{for a.a.: } (t, \mathbf{x}) \in [0, T] \times \Gamma \left[ \begin{array}{l} \phi_C(\mathbf{t}(t, \mathbf{x})) = 0 \\ (\|\boldsymbol{\sigma}_T\| = 0, \phi_C(\mathbf{t}) > 0) \end{array} \right] \right\}.$$

This means that a norm of a tangential part of a traction is bounded from above by a nonnegative normal part multiplied with a friction coefficient  $\mu_f$ .

*Gap/Penetration*

$$\mathbf{g}(t, \zeta^B) := \bar{\mathbf{X}}^A(\zeta^B) - \mathbf{X}^B(\zeta^B) + \mathbf{u}^A(\bar{\mathbf{X}}^A(\zeta^B), t) - \mathbf{u}^B(t, \zeta^B). \quad (1.83)$$

*Normal gap/penetration*

$$g_N(t, \zeta^B) := \mathbf{g}(t, \zeta^B) \cdot \bar{\mathbf{n}}^A. \quad (1.84)$$

*Tangential gap/penetration*

$$\mathbf{g}_T(t, \zeta^B) := \mathbf{g}(t, \zeta^B) - g_N(t, \zeta^B) \bar{\mathbf{n}}^A. \quad (1.85)$$

If  $g_N \geq 0$  then we use term *gap* in equations (1.83)-(1.85), in other case we are talking about *penetration*.

**Signorini contact with Coulomb friction** (see Laursen [35])

$$\left. \begin{array}{l} g_N \leq 0, \\ \text{if } g_N = 0, \text{ then } \sigma_N < 0 \text{ else } \sigma_N = 0, \\ \text{if } \phi_C(\mathbf{t}) < 0, \text{ then } \mathbf{g}_T = 0, \\ \text{if } \phi_C(\mathbf{t}) = 0, \text{ then } \exists \lambda \geq 0 : \mathbf{g}_T = -\lambda \boldsymbol{\sigma}_T \end{array} \right\} \text{ on } \Gamma_C. \quad (1.86)$$

**Regularization of contact conditions**

1 Elastoplastic contact problems. Small deformations

Normal traction. Using penalty parameter  $\epsilon_{\mathcal{N}} > 0$

$$\sigma_{\mathcal{N}}(t, \zeta^B) := -\frac{1}{\epsilon_{\mathcal{N}}} \mathfrak{g}_{\mathcal{N}}^+(t, \zeta^B), \quad (1.87)$$

where

$$\mathfrak{g}_{\mathcal{N}}^+(t, \zeta^B) := \begin{cases} \mathfrak{g}_{\mathcal{N}}(t, \zeta^B), & \text{if } \mathfrak{g}_{\mathcal{N}}(t, \zeta^B) \geq 0, \\ 0, & \text{if } \mathfrak{g}_{\mathcal{N}}(t, \zeta^B) < 0, \end{cases} \quad (1.88)$$

$$\mathfrak{g}_{\mathcal{N}}^p(t, \zeta^B) := -\mathfrak{g}_{\mathcal{N}}^+(t, \zeta^B) + \mathfrak{g}_{\mathcal{N}}(t, \zeta^B), \quad (1.89)$$

$$\mathfrak{g}_{\mathcal{N}}^e(t, \zeta^B) := \mathfrak{g}_{\mathcal{N}}^+(t, \zeta^B). \quad (1.90)$$

Flow rule for normal term

$$\dot{\mathfrak{g}}_{\mathcal{N}}^p = \dot{\gamma}(t, \zeta^B) \frac{\partial \phi_C(\mathbf{t})}{\partial \sigma_{\mathcal{N}}}. \quad (1.91)$$

Tangential traction. Using penalty parameter  $\epsilon_{\mathcal{T}} > 0$

$$\dot{\boldsymbol{\sigma}}_{\mathcal{T}}(t, \zeta^B) := -\frac{1}{\epsilon_{\mathcal{T}}} \left( \dot{\mathfrak{g}}_{\mathcal{T}}(t, \zeta^B) - \dot{\gamma}(t, \zeta^B) \frac{\boldsymbol{\sigma}_{\mathcal{T}}(t, \zeta^B)}{\|\boldsymbol{\sigma}_{\mathcal{T}}(t, \zeta^B)\|} \right), \quad (1.92)$$

such that

$$\left. \begin{aligned} \phi_C(\mathbf{t}) &\leq 0, \\ \dot{\gamma}(t, \zeta^B) &\geq 0, \\ \dot{\gamma}(t, \zeta^B) \phi_C(\mathbf{t}) &= 0. \end{aligned} \right\} \quad (1.93)$$

Definition of plastic tangential gap

$$\dot{\mathfrak{g}}_{\mathcal{T}}^p(t, \zeta^B) := \dot{\gamma}(t, \zeta^B) \frac{\boldsymbol{\sigma}_{\mathcal{T}}(t, \zeta^B)}{\|\boldsymbol{\sigma}_{\mathcal{T}}(t, \zeta^B)\|}, \quad (1.94)$$

$$\mathfrak{g}_{\mathcal{T}}^e(t, \zeta^B) := \mathfrak{g}_{\mathcal{T}}(t, \zeta^B) - \mathfrak{g}_{\mathcal{T}}^p(t, \zeta^B). \quad (1.95)$$

If we now consider  $\mathbf{g} := (\mathfrak{g}_{\mathcal{N}}, \mathfrak{g}_{\mathcal{T}})$  and  $\mathbf{t} := (\sigma_{\mathcal{N}}, \boldsymbol{\sigma}_{\mathcal{T}})$ , then we can think about  $\mathbf{g}$  as strain and about  $\mathbf{t}$  as stress in the associative von Mises elastoplasticity theory with the yield function  $\phi_C(\mathbf{t})$ . The constitutive law for this model is gathered by following conditions

(1.96)-(1.99)

*decomposition of stain*

$$\mathbf{g} = \mathbf{g}^e + \mathbf{g}^p, \quad (1.96)$$

*stress-strain relationship*

$$\mathbf{t} = -\mathbb{D}\mathbf{g}^e, \quad \text{where } \mathbb{D}\mathbf{g}^e := \left( \frac{1}{\epsilon_{\mathcal{N}}}\mathbf{g}_{\mathcal{N}}^e, \frac{1}{\epsilon_{\mathcal{T}}}\mathbf{g}_{\mathcal{T}}^e \right)^T, \quad (1.97)$$

*yield condition*

$$\phi_C(\mathbf{t}) \leq 0, \quad (1.98)$$

*flow rule for plastic strain rate*

$$\dot{\mathbf{g}}^p = \dot{\gamma}(t, \zeta^B) \frac{\partial \phi_C(\mathbf{t})}{\partial \mathbf{t}}. \quad (1.99)$$

where  $\mathbb{D}$  is the analog of the Hooke's tensor in the theory of linear elasticity and has the same major properties: positive definiteness and symmetry, while

$$\mathbb{D} = \begin{pmatrix} \frac{1}{\epsilon_{\mathcal{N}}} & 0 \\ 0 & \frac{1}{\epsilon_{\mathcal{T}}} \end{pmatrix}. \quad (1.100)$$

The contact return mapping projection, for given traction  $\mathbf{t}(t, \zeta^B)$  maps the increment of the interpenetration  $\Delta \mathbf{g}(t, \Delta t, \zeta^B) := \mathbf{g}(t + \Delta t, \zeta^B) - \mathbf{g}(t, \zeta^B)$  to the increment of the contact traction  $\Delta \mathbf{t}(t, \Delta t, \zeta^B) := \mathbf{t}(t + \Delta t, \zeta^B) - \mathbf{t}(t, \zeta^B)$ . For a fixed traction vector  $\mathbf{t}(t, \zeta^B)$  we consider the return mapping operator  $\mathbf{T}_C : \Delta \mathbf{g} \mapsto \Delta \mathbf{t}$  defined by

$$\mathbf{T}_C(\Delta \mathbf{g}(t, \Delta t, \zeta^B)) := \begin{cases} -\mathbb{D}\Delta \mathbf{g}(t, \Delta t, \zeta^B), & \text{if } \phi_C(\mathbf{t}(t, \zeta^B) - \mathbb{D}\Delta \mathbf{g}(t, \Delta t, \zeta^B)) \leq 0, \\ -\mathbb{D}\Delta \mathbf{g}(t, \Delta t, \zeta^B) + \gamma_R(t, \Delta t, \zeta^B) \hat{\mathbf{n}}(t, \zeta^B), & \text{if } \phi_C(\mathbf{t}(t, \zeta^B) - \mathbb{D}\Delta \mathbf{g}(t, \Delta t, \zeta^B)) > 0, \end{cases} \quad (1.101)$$

where

$$\hat{\mathbf{n}}(t, \Delta t, \zeta^B) := -\frac{\mathbb{D} \frac{\partial \phi_C}{\partial \mathbf{t}}}{\|\mathbb{D} \frac{\partial \phi_C}{\partial \mathbf{t}}\|} = -\frac{\left( \mu_f \frac{1}{\epsilon_{\mathcal{N}}}, \frac{1}{\epsilon_{\mathcal{T}}} \text{sign}(\sigma_{\mathcal{T}}(t, \zeta^B) - \frac{1}{\epsilon_{\mathcal{T}}} \Delta g_{\mathcal{T}}(t, \Delta t, \zeta^B)) \right)}{\sqrt{\mu_f^2 \frac{1}{\epsilon_{\mathcal{N}}^2} + \frac{1}{\epsilon_{\mathcal{T}}^2}}}. \quad (1.102)$$

The vector  $\hat{\mathbf{n}}$  is a normal vector to the yield surface  $\phi_C(\mathbf{g}) := \phi_C(\mathbf{t} - \mathbb{D}\mathbf{g}) = 0$  at a boundary point  $\mathbf{t} - \mathbb{D}\mathbf{g}$  (see Fig. 1.2).

*Remark 1.4.1.* For convenience we do not explicitly stress the dependence of the return mapping operator  $\mathbf{T}_C$  on the value of the boundary traction  $\mathbf{t}$ , since the investigation below is carried out for a fixed  $\mathbf{t}$ . But for the investigation of the solution procedure or for the numerical implementation one has to take this relation into account.

**Theorem 1.4.1.** *For given fixed  $\mathbf{t} \in S_C$  and  $\forall \mathbf{g} \in \mathbb{R}^2$  there holds*

1) if  $\mathbf{t} - \mathbb{D}\mathbf{g} \in S_C^{ep}$ , then

$\mathbf{T}_C$  has the Frechet derivative  $\mathbf{T}'_C(\mathbf{g})\boldsymbol{\eta} := \lim_{\theta \rightarrow 0} \frac{\mathbf{T}_C(\mathbf{g} + \theta\boldsymbol{\eta}) - \mathbf{T}_C(\mathbf{g})}{\theta}$

$$\mathbf{T}'_C(\mathbf{g})\boldsymbol{\eta} = \begin{cases} -\mathbb{D}\boldsymbol{\eta}, & \mathbf{t} - \mathbb{D}\mathbf{g} \in S_C^e, \\ -\mathbb{D}\boldsymbol{\eta} + \frac{\hat{\mathbf{n}}\boldsymbol{\eta}(\frac{1}{\epsilon_T^2} + \frac{1}{\epsilon_N^2}\mu_f^2)}{\frac{1}{\epsilon_T} + \frac{1}{\epsilon_N}\mu_f^2}\hat{\mathbf{n}}, & \mathbf{t} - \mathbb{D}\mathbf{g} \in S_C^p. \end{cases} \quad (1.103)$$

2) if  $\mathbf{t} - \mathbb{D}\mathbf{g} \in S_C^i(t, \zeta^B) \cup \{\mathbf{t} \mid \|\boldsymbol{\sigma}_T\| \neq 0\}$  there exists only one side derivative

$$\mathbf{T}'_C(\mathbf{g}_+)\boldsymbol{\eta} := \lim_{\theta \rightarrow 0} \frac{\mathbf{T}_C(\mathbf{g} + \theta\boldsymbol{\eta}) - \mathbf{T}_C(\mathbf{g})}{\theta}, \quad (1.104)$$

$$\mathbf{T}'_C(\mathbf{g}_+)\boldsymbol{\eta} = \begin{cases} -\mathbb{D}\boldsymbol{\eta} + \frac{\hat{\mathbf{n}}\boldsymbol{\eta}(\frac{1}{\epsilon_T^2} + \frac{1}{\epsilon_N^2}\mu_f^2)}{\frac{1}{\epsilon_T} + \frac{1}{\epsilon_N}\mu_f^2}\hat{\mathbf{n}}, & \phi_C(\mathbf{t}(t, \zeta^B) - \mathbb{D}\mathbf{g}) = 0, \|\boldsymbol{\sigma}_T - \frac{1}{\epsilon_T}\mathbf{g}_T\| \neq 0, \\ & \boldsymbol{\eta}\hat{\mathbf{n}} \geq 0, \\ -\mathbb{D}\boldsymbol{\eta}, & \phi_C(\mathbf{t}(t, \zeta^B) - \mathbb{D}\mathbf{g}) = 0, \|\boldsymbol{\sigma}_T - \frac{1}{\epsilon_T}\mathbf{g}_T\| \neq 0, \\ & \boldsymbol{\eta}\hat{\mathbf{n}} < 0. \end{cases}$$

**Proof.** We start with proving the first statement of the theorem. That will be done in two steps (1.e) and (1.p), that refers to the pure elastic and the pure plastic increment  $\mathbf{g}$  respectively. In (1.e) we prove the first statement in (1.103) and in (1.p) the second.

1.e) Let  $\mathbf{t} - \mathbb{D}\mathbf{g} \in S_C^e$ , i.e. we have a pure elastic reversible increment  $\mathbf{g}$ . Then for sufficiently small  $\theta \in \mathbb{R}$  and for each arbitrary but fix  $\boldsymbol{\eta} \in \mathbb{R}^2$ , we have  $\mathbf{t} - \mathbb{D}(\mathbf{g} + \theta\boldsymbol{\eta}) \in S_C^e$ . Using the definition (1.101) of  $\mathbf{T}_C$  we calculate the Frechet derivative of  $\mathbf{T}_C$  at  $\mathbf{g}$  in the direction  $\boldsymbol{\eta}$  as follows

$$\begin{aligned} \mathbf{T}'_C(\mathbf{g})\boldsymbol{\eta} &:= \lim_{\theta \rightarrow 0} \frac{\mathbf{T}_C(\mathbf{g} + \theta\boldsymbol{\eta}) - \mathbf{T}_C(\mathbf{g})}{\theta} \mathbb{D}\boldsymbol{\eta} = \lim_{\theta \rightarrow 0} \frac{-\mathbb{D}(\mathbf{g} + \theta\boldsymbol{\eta}) + \mathbb{D}(\mathbf{g})}{\theta} \\ &= \lim_{\theta \rightarrow 0} \frac{-\theta\mathbb{D}\boldsymbol{\eta}}{\theta} = -\mathbb{D}\boldsymbol{\eta}. \end{aligned} \quad (1.105)$$

That proves the first assertion in (1.103).

In order to prove the second statemet in (1.103) we consider now the case of a pure plastic increment  $\mathbb{D}\mathbf{g}$ :

1.p)  $\mathbf{t} - \mathbb{D}\mathbf{g} \in S_C^p$ , then from (1.101) we conclude

$$\mathbf{T}_C(\mathbf{g}) = -\mathbb{D}\mathbf{g} + \gamma_R \hat{\mathbf{n}},$$

where

$$\hat{\mathbf{n}} := -\frac{\mathbb{D}\frac{\partial\phi_C}{\partial\mathbf{t}}}{\|\mathbb{D}\frac{\partial\phi_C}{\partial\mathbf{t}}\|} = -\frac{\left(\mu_f \frac{1}{\epsilon_N}, \frac{1}{\epsilon_T} \text{sign}(\sigma_T(t, \zeta^B) - \frac{1}{\epsilon_T} \mathbf{g}_T)\right)}{\sqrt{\mu_f^2 \frac{1}{\epsilon_N^2} + \frac{1}{\epsilon_T^2}}}. \quad (1.106)$$

Recall that  $\mu_f, \epsilon_N, \epsilon_T$  - are positive constants,  $\sigma_T(t, \zeta^B) - \frac{1}{\epsilon_T} \mathbf{g}_T$  - does not change the sign for the fixed value  $\sigma_T(t, \zeta^B)$  and sufficiently small  $\mathbf{g}_T$ , moreover, it has the same sign as  $\sigma_T(t, \zeta^B)$ . The  $\gamma_R(\mathbf{g})$  has to be found from

$$\phi_C(\mathbf{t} - \mathbb{D}\mathbf{g} + \gamma_R \hat{\mathbf{n}}) = 0, \quad (1.107)$$

which corresponds to  $\phi_C(\mathbf{t} - \mathbb{D}\mathbf{g})$ . We are looking for the derivative of  $\gamma_R$  with respect to  $\mathbf{g}$ . Since we do not have an explicit formula for  $\gamma_R$  we use the implicit definition (1.107) of this function. For sufficiently small  $\theta \in \mathbb{R}$  the equation 1.107 implies for all  $\boldsymbol{\eta} \in \mathbb{R}^2$ :

$$\phi_C(\mathbf{t} - \mathbb{D}(\mathbf{g} + \theta\boldsymbol{\eta}) + \gamma_R(\mathbf{g} + \theta\boldsymbol{\eta})\hat{\mathbf{n}}) = 0, \quad (1.108)$$

$$\left. \frac{d\phi_C}{d\theta} \right|_{\theta=0} = \lim_{\theta \rightarrow 0} \frac{\phi_C(\mathbf{t} - \mathbb{D}(\mathbf{g} + \theta\boldsymbol{\eta}) + \gamma_R(\mathbf{g} + \theta\boldsymbol{\eta})\hat{\mathbf{n}}) - \phi_C(\mathbf{t} - \mathbb{D}\mathbf{g} + \gamma_R(\mathbf{g})\hat{\mathbf{n}})}{\theta}. \quad (1.109)$$

From (1.107), (1.108) and (1.108) we get

$$\left. \frac{d\phi_C}{d\theta} \right|_{\theta=0} = 0 \quad (1.110)$$

or by the direct evaluation of the Frechet derivative in (1.109)

$$\begin{aligned} \left. \frac{d\phi_C}{d\theta} \right|_{\theta=0} &= \lim_{\theta \rightarrow 0} \frac{1}{\theta} \left\{ \left| \sigma_T - \frac{1}{\epsilon_T} (\mathbf{g}_T + \theta\boldsymbol{\eta}_T) + \gamma_R(\mathbf{g} + \theta\boldsymbol{\eta})\hat{\mathbf{n}}_T \right| \right. \\ &\quad \left. + \mu_f \left( \sigma_N - \frac{1}{\epsilon_N} (\mathbf{g}_N + \theta\boldsymbol{\eta}_N) + \gamma_R(\mathbf{g} + \theta\boldsymbol{\eta})\hat{\mathbf{n}}_N \right) \right\} \end{aligned}$$

$$\begin{aligned}
& - \left| \sigma_T - \frac{1}{\epsilon_T} \mathbf{g}_T + \gamma_R(\mathbf{g}) \hat{n}_T \right| - \mu_f \left( \sigma_N - \frac{1}{\epsilon_N} \mathbf{g}_N + \gamma_R(\mathbf{g}) \hat{n}_N \right) \Big\} \\
& = \lim_{\theta \rightarrow 0} \frac{1}{\theta} \left\{ \text{sign} \left( \sigma_T - \frac{1}{\epsilon_T} \mathbf{g}_T \right) \left( -\theta \frac{1}{\epsilon_T} \eta_T + \gamma_R(\mathbf{g} + \theta \boldsymbol{\eta}) \hat{n}_T - \gamma_R(\mathbf{g}) \hat{n}_T \right) \right. \\
& + \left. \mu_f \left( -\theta \frac{1}{\epsilon_N} \eta_N + \gamma_R(\mathbf{g} + \theta \boldsymbol{\eta}) \hat{n}_N - \gamma_R(\mathbf{g}) \hat{n}_N \right) \right\} \\
& = \text{sign} \left( \sigma_T - \frac{1}{\epsilon_T} \mathbf{g}_T \right) \left( -\frac{1}{\epsilon_T} \eta_T + \gamma'_R \hat{n}_T \right) - \mu_f \left( \frac{1}{\epsilon_N} \eta_N - \gamma'_R \hat{n}_N \right) = 0 \quad (1.111)
\end{aligned}$$

since

$$\begin{aligned}
\text{sign} \left( \sigma_T - \frac{1}{\epsilon_T} (\mathbf{g}_T + \theta \eta_T) + \gamma_R(\mathbf{g} + \theta \boldsymbol{\eta}) \hat{n}_T \right) & = \text{sign} \left( \sigma_T - \frac{1}{\epsilon_T} \mathbf{g}_T + \gamma_R(\mathbf{g}) \hat{n}_T \right) \\
& = \text{sign} \left( \sigma_T - \frac{1}{\epsilon_T} \mathbf{g}_T \right).
\end{aligned}$$

In (1.111) the derivative  $\gamma'_R$  depends on  $\mathbf{g}$  and acts on  $\boldsymbol{\eta}$ , i.e.  $\gamma'_R = \gamma'_R(\mathbf{g})(\boldsymbol{\eta})$ . Inserting the definition of  $\hat{\mathbf{n}}$  (1.106) into (1.111) and solving for  $\gamma'_R(\mathbf{g})(\boldsymbol{\eta})$  we obtain

$$\begin{aligned}
\gamma'_R & = \frac{\left( -\frac{\mu_f}{\epsilon_N} \right) \eta_N + \left( -\text{sign} \left( \sigma_T - \frac{1}{\epsilon_T} \mathbf{g}_T \right) \frac{1}{\epsilon_T} \right) \eta_T \sqrt{\frac{\mu_f^2}{\epsilon_N^2} + \frac{1}{\epsilon_T^2}}}{\frac{1}{\epsilon_T} + \frac{\mu_f^2}{\epsilon_N}} \\
& = \frac{\sqrt{\frac{\mu_f^2}{\epsilon_N^2} + \frac{1}{\epsilon_T^2}} \hat{n}_N \eta_N + \sqrt{\frac{\mu_f^2}{\epsilon_N^2} + \frac{1}{\epsilon_T^2}} \hat{n}_T \eta_T}{\frac{1}{\epsilon_T} + \frac{\mu_f^2}{\epsilon_N}} \sqrt{\frac{\mu_f^2}{\epsilon_N^2} + \frac{1}{\epsilon_T^2}} \\
& = \frac{\hat{\mathbf{n}} \cdot \boldsymbol{\eta}}{\frac{1}{\epsilon_T} + \frac{\mu_f^2}{\epsilon_N}} \left( \frac{\mu_f^2}{\epsilon_N^2} + \frac{1}{\epsilon_T^2} \right). \quad (1.112)
\end{aligned}$$

Hence,

$$\mathbf{T}'_C(\mathbf{g})(\boldsymbol{\eta}) = -\mathbb{D}\boldsymbol{\eta} + \gamma'_R(\mathbf{g})(\boldsymbol{\eta}) \hat{\mathbf{n}} = -\mathbb{D}\boldsymbol{\eta} + \frac{\hat{\mathbf{n}} \cdot \boldsymbol{\eta} \left( \frac{1}{\epsilon_N} \mu_f^2 + \frac{1}{\epsilon_T} \right)}{\frac{1}{\epsilon_N} \mu_f^2 + \frac{1}{\epsilon_T}} \hat{\mathbf{n}}, \quad (1.113)$$

that proves the second assertion in (1.103). Thus, the first statement of the theorem is totally proved. Let us proceed to the second one.

2) Let  $\mathbf{t} - \mathbb{D}\mathbf{g} \in S_C^i$

2.1) If  $\phi_C(\mathbf{t} - \mathbb{D}\mathbf{g}) = 0$ ,  $\|\boldsymbol{\sigma}_T - \frac{1}{\epsilon_N} \mathbf{g}_T\| \neq 0$  then we distinguish two cases:

- If  $\boldsymbol{\eta} \hat{\mathbf{n}} < 0$ , then

there exists  $\theta_0$  such that  $\forall \theta : 0 < \theta < \theta_0$  there holds  $\mathbf{g} + \theta \boldsymbol{\eta} \in S_C^e \Rightarrow$

$$\mathbf{T}'_C(\mathbf{g}_+)(\boldsymbol{\eta}) = \lim_{\theta \rightarrow 0} \frac{\mathbf{T}_C(\mathbf{g} + \theta \boldsymbol{\eta}) - \mathbf{T}_C(\mathbf{g})}{\theta} = -\mathbb{D}\boldsymbol{\eta}. \quad (1.114)$$

- If  $\boldsymbol{\eta} \hat{\mathbf{n}} \geq 0$ , then

there exists  $\theta_0$  such that  $\forall \theta: 0 < \theta < \theta_0$  there holds  $\mathbf{g} + \theta \boldsymbol{\eta} \in S_C^p \Rightarrow$ .

$$\mathbf{T}'_C(\mathbf{g}_+)(\boldsymbol{\eta}) = -\mathbb{D}\boldsymbol{\eta} + \gamma'_R \hat{\mathbf{n}} = -\mathbb{D}\boldsymbol{\eta} + \frac{\hat{\mathbf{n}} \boldsymbol{\eta} \left( \frac{1}{\epsilon_T^2} + \frac{1}{\epsilon_N^2} \mu_f^2 \right)}{\frac{1}{\epsilon_T} + \frac{1}{\epsilon_N} \mu_f^2} \hat{\mathbf{n}} \quad (1.115)$$

□

**Theorem 1.4.2.** For fixed  $\mathbf{t} \in S_C^e$ , the derivative  $\mathbf{T}'_C(\mathbf{g})$ ,  $\mathbf{t} - \mathbb{D}\mathbf{g} \in S_C^e$ , is symmetric and negative semi-definite (non-positive).

**Proof.** The symmetricity of the derivative follows from the fact that it can be represented as a symmetric matrix. By (1.103) at  $\mathbf{g} \in S_C^e$  we have  $\mathbf{T}'_C(\mathbf{g}) = -\mathbb{D}$ , where  $\mathbb{D}$  is a symmetric matrix by the definition (1.100). At  $\mathbf{g} \in S_C^p$  by (1.103) we have

$$\mathbf{T}'_C(\mathbf{g}) = -\mathbb{D} + \frac{\left( \frac{1}{\epsilon_T^2} + \frac{1}{\epsilon_N^2} \mu_f^2 \right)}{\frac{1}{\epsilon_T} + \frac{1}{\epsilon_N} \mu_f^2} \hat{\mathbf{n}} \otimes \hat{\mathbf{n}}. \quad (1.116)$$

In order to prove that the derivative is negative semi-definite we distinguish two cases:

- $\mathbf{t} - \mathbb{D}\mathbf{g} \in S_C^e$ :

$$\langle \mathbf{T}'_C(\mathbf{g})(\boldsymbol{\eta}), \boldsymbol{\eta} \rangle = \langle -\mathbb{D}\boldsymbol{\eta}, \boldsymbol{\eta} \rangle = -\frac{1}{\epsilon_N} \eta_N^2 - \frac{1}{\epsilon_T} \eta_T^2 \leq 0. \quad (1.117)$$

- $\mathbf{t} - \mathbb{D}\mathbf{g} \in S_C^p$ :

$$\begin{aligned} \langle \mathbf{T}'_C(\mathbf{g})(\boldsymbol{\eta}), \boldsymbol{\eta} \rangle &= \left\langle -\mathbb{D}\boldsymbol{\eta} + \frac{\hat{\mathbf{n}} \boldsymbol{\eta} \left( \frac{1}{\epsilon_T^2} + \frac{1}{\epsilon_N^2} \mu_f^2 \right)}{\frac{1}{\epsilon_T} + \frac{1}{\epsilon_N} \mu_f^2} \hat{\mathbf{n}}, \boldsymbol{\eta} \right\rangle \\ &= -\frac{\left( \frac{1}{\epsilon_T} \eta_N^2 + \frac{1}{\epsilon_T} \eta_T^2 \right) \left( \frac{1}{\epsilon_T} + \frac{1}{\epsilon_N} \mu_f^2 \right)}{\frac{1}{\epsilon_T} + \frac{1}{\epsilon_N} \mu_f^2} + \frac{\left( \frac{1}{\epsilon_T} \eta_T \operatorname{sign}(\sigma_T - \frac{1}{\epsilon_T} g_N) - \mu_f \frac{1}{\epsilon_N} \eta_N \right)^2}{\frac{1}{\epsilon_T} + \frac{1}{\epsilon_N} \mu_f^2} \\ &= -\frac{\frac{1}{\epsilon_N} \frac{1}{\epsilon_T}}{\mu_f^2 \frac{1}{\epsilon_N} + \frac{1}{\epsilon_T}} \left( \eta_N^2 + \mu_f^2 \eta_T^2 + 2\mu_f \eta_T \eta_N \operatorname{sign}(\sigma_T - \frac{1}{\epsilon_T} g_T) \right) \\ &= -\frac{\frac{1}{\epsilon_N} \frac{1}{\epsilon_T}}{\mu_f^2 \frac{1}{\epsilon_N} + \frac{1}{\epsilon_T}} \left( \eta_N \operatorname{sign}(\sigma_T - \frac{1}{\epsilon_T} g_T) + \mu_f \eta_T \right)^2 \leq 0 \end{aligned} \quad (1.118)$$

□

**Theorem 1.4.3.** *For given fixed  $\mathbf{t} \in S_C$  and for all  $\mathbf{g}$  with  $\mathbf{t} - \mathbb{D}\mathbf{g} \in S_C^{ep}$  the derivative  $\mathbf{T}'_C(\mathbf{g})$ , is Lipschitz continuous.*

**Proof.** In order to prove that the derivative is Lipschitz continuous we distinguish two cases:

- $\mathbf{t} - \mathbb{D}\mathbf{g} \in S_C^e$ , then by (1.103) we have  $\forall \mathbf{g}_1 : \mathbf{t} - \mathbb{D}\mathbf{g}_1 \in S_C^e$ :

$$\begin{aligned} \|\mathbf{T}'_C(\mathbf{g}) - \mathbf{T}'_C(\mathbf{g}_1)\| &= \sup_{\mathbb{R}^2 \ni \boldsymbol{\eta} \neq 0} \frac{\langle (\mathbf{T}'_C(\mathbf{g}) - \mathbf{T}'_C(\mathbf{g}_1)) \boldsymbol{\eta}, \boldsymbol{\eta} \rangle}{\|\boldsymbol{\eta}\|^2} \\ &= \sup_{\mathbb{R}^2 \ni \boldsymbol{\eta} \neq 0} \frac{\langle \mathbf{T}'_C(\mathbf{g})\boldsymbol{\eta} - \mathbf{T}'_C(\mathbf{g}_1)\boldsymbol{\eta}, \boldsymbol{\eta} \rangle}{\|\boldsymbol{\eta}\|^2} \\ &= \sup_{\mathbb{R}^2 \ni \boldsymbol{\eta} \neq 0} \frac{\langle -\mathbb{D}\boldsymbol{\eta} + \mathbb{D}\boldsymbol{\eta}, \boldsymbol{\eta} \rangle}{\|\boldsymbol{\eta}\|^2} = 0. \end{aligned} \quad (1.119)$$

Hence,  $\mathbf{T}'_C(\mathbf{g})$  is constant and consequently Lipschitz continuous  $\forall \mathbf{g} : \mathbf{t} - \mathbb{D}\mathbf{g} \in S_C^e$ .

- $\mathbf{t} - \mathbb{D}\mathbf{g} \in S_C^p$ , then by (1.103) we have  $\forall \mathbf{g}_1 : \mathbf{t} - \mathbb{D}\mathbf{g}_1 \in S_C^p$ :

$$\begin{aligned} \|\mathbf{T}'_C(\mathbf{g}) - \mathbf{T}'_C(\mathbf{g}_1)\| &= \sup_{\mathbb{R}^2 \ni \boldsymbol{\eta} \neq 0} \frac{\langle (\mathbf{T}'_C(\mathbf{g}) - \mathbf{T}'_C(\mathbf{g}_1)) \boldsymbol{\eta}, \boldsymbol{\eta} \rangle}{\|\boldsymbol{\eta}\|^2} \\ &= \sup_{\mathbb{R}^2 \ni \boldsymbol{\eta} \neq 0} \frac{\langle \mathbf{T}'_C(\mathbf{g})\boldsymbol{\eta} - \mathbf{T}'_C(\mathbf{g}_1)\boldsymbol{\eta}, \boldsymbol{\eta} \rangle}{\|\boldsymbol{\eta}\|^2} \\ &= \sup_{\mathbb{R}^2 \ni \boldsymbol{\eta} \neq 0} \frac{\left\langle -\mathbb{D}\boldsymbol{\eta} + \frac{\hat{\mathbf{n}}\boldsymbol{\eta}(\frac{1}{\epsilon_T^2} + \frac{1}{\epsilon_N^2}\mu_f^2)}{\frac{1}{\epsilon_T} + \frac{1}{\epsilon_N}\mu_f^2} \hat{\mathbf{n}} + \mathbb{D}\boldsymbol{\eta} - \frac{\hat{\mathbf{n}}\boldsymbol{\eta}(\frac{1}{\epsilon_T^2} + \frac{1}{\epsilon_N^2}\mu_f^2)}{\frac{1}{\epsilon_T} + \frac{1}{\epsilon_N}\mu_f^2} \hat{\mathbf{n}}, \boldsymbol{\eta} \right\rangle}{\|\boldsymbol{\eta}\|^2} \\ &= 0. \end{aligned} \quad (1.120)$$

Hence,  $\mathbf{T}'_C(\mathbf{g})$  is constant and consequently Lipschitz continuous  $\forall \mathbf{g} : \mathbf{t} - \mathbb{D}\mathbf{g} \in S_C^p$ .

□

The return mapping algorithm presented above corresponds to the implicit time discretization of the constitutive law (1.96)-(1.99). The explicit integration of the model (1.96)-(1.99) can be done in the same way as for the elastoplasticity [2, 6, 34]. For that reason we use the incremental constitutive relation

$$\dot{\mathbf{t}} = \mathbb{D}_{ep}(\mathbf{t}, \dot{\mathbf{g}})\dot{\mathbf{g}}, \quad (1.121)$$

where

$$\mathbb{D}_{ep}(\mathbf{t}, \dot{\mathbf{g}}) := \mathbb{D} - \rho_C(\mathbf{t}, \dot{\mathbf{g}})\mathbb{D}_p(\mathbf{t}), \quad (1.122)$$



with  $\rho_C(\mathbf{t}, \dot{\mathbf{g}})$ :

$$\rho_C(\mathbf{t}, \dot{\mathbf{g}}) := \begin{cases} 0, & \text{if } \left(\frac{\partial \phi_C}{\partial \mathbf{t}}\right)^T \mathbb{D} \dot{\mathbf{g}} \leq 0, \\ 1, & \text{if } \left(\frac{\partial \phi_C}{\partial \mathbf{t}}\right)^T \mathbb{D} \dot{\mathbf{g}} > 0, \end{cases} \quad (1.123)$$

$$\mathbb{D}_p(\mathbf{t}) := \frac{\mathbb{D} \frac{\partial \phi_C}{\partial \mathbf{t}} \left(\frac{\partial \phi_C}{\partial \mathbf{t}}\right)^T \mathbb{D}}{\left(\frac{\partial \phi_C}{\partial \mathbf{t}}\right)^T \mathbb{D} \frac{\partial \phi_C}{\partial \mathbf{t}}}. \quad (1.124)$$

The explicit time discretization of (1.121) leads to

$$\Delta \mathbf{t} = \mathbb{D}_{ep}(\mathbf{t}, \Delta \mathbf{g}) \Delta \mathbf{g}, \quad (1.125)$$

where

$$\mathbb{D}_{ep}(\mathbf{t}, \Delta \mathbf{g}) := \mathbb{D} - \rho_C(\mathbf{t}, \Delta \mathbf{g}) \mathbb{D}_p(\mathbf{t}), \quad (1.126)$$

with  $\rho_C(\mathbf{t}, \Delta \mathbf{g})$ :

$$\rho_C(\mathbf{t}, \Delta \mathbf{g}) := \begin{cases} 0, & \text{if } \phi_C(\mathbf{t} - \mathbb{D} \Delta \mathbf{g}) \leq 0, \\ 1, & \text{if } \phi_C(\mathbf{t} - \mathbb{D} \Delta \mathbf{g}) > 0. \end{cases} \quad (1.127)$$

The operator  $\mathbb{D}_{ep}$  (1.126) is not continuous due to the jump function  $\rho_C(\mathbf{t}, \Delta \mathbf{g})$  (1.127). Employing the regularization procedure used in [34, 6], we smooth the function  $\rho_C(\mathbf{t}, \Delta \mathbf{g})$  introducing its approximation  $\rho_{C,\delta}(\mathbf{t}, \Delta \mathbf{g})$  for  $\delta > 0$ :

$$\rho_{C,\delta}(\mathbf{t}, \Delta \mathbf{g}) := \begin{cases} 0, & \text{if } \phi_C(\mathbf{t} - \mathbb{D} \Delta \mathbf{g}) \leq -\delta, \\ 1 + \frac{\phi_C(\mathbf{t} - \mathbb{D} \Delta \mathbf{g})}{\delta}, & \text{if } -\delta < \phi_C(\mathbf{t} - \mathbb{D} \Delta \mathbf{g}) \leq 0, \\ 1, & \text{if } \phi_C(\mathbf{t} - \mathbb{D} \Delta \mathbf{g}) > 0. \end{cases} \quad (1.128)$$

Thus, the  $\delta$ -regularization of (1.125) is carried out for  $\delta > 0$ :

$$\Delta \mathbf{t} = \mathbb{D}_{ep,\delta}(\mathbf{t}, \Delta \mathbf{g}) \Delta \mathbf{g}, \quad (1.129)$$

where

$$\mathbb{D}_{ep,\delta}(\mathbf{t}, \Delta \mathbf{g}) := \mathbb{D} - \rho_{C,\delta}(\mathbf{t}, \Delta \mathbf{g}) \mathbb{D}_p(\mathbf{t}). \quad (1.130)$$

## 1.5 A Newton-type method for two-body elastoplastic contact with friction

We extend a Newton-type algorithm for elastoplasticity with hardening investigated in [5, 2] onto two-body elastoplastic problem with regularized contact with friction.

The contact regularization is done as in Section 1.4. Our approach is based on the implicit computation of the increment of the stress (contact traction) using the increment of the strain (relative contact gap). In the literature this method is referred to as Return Mapping Algorithm. Consider a discrete problem (1.58) defined in Section 1.2.1. Subtracting the equation at time step  $n - 1$  from the the equation at time step  $n$  we obtain

$$F_{\mathbf{u}_h}^{int}(\Delta(\boldsymbol{\sigma}^i)_n, \Delta(\mathbf{t}_{\epsilon_C})_n, \boldsymbol{\eta}_h) = \Delta F_n^{ext}(\boldsymbol{\eta}_h) \quad \forall \boldsymbol{\eta}_h \in {}^h\mathbf{V}_0, \quad (1.131)$$

where the contact and the elastoplastic constitutive conditions from Section 1.4 and Section 1.2 are given via

$$\Delta(\boldsymbol{\sigma}^i)_n = \mathbf{T}_{pl}^i((\boldsymbol{\sigma}^i)_{n-1}, (\boldsymbol{\xi}^i)_{n-1}, \Delta(\boldsymbol{\varepsilon}^i)_n), \quad (1.132)$$

$$\Delta(\boldsymbol{\xi}^i)_n = \mathbf{G}_{pl}^i((\boldsymbol{\sigma}^i)_{n-1}, (\boldsymbol{\xi}^i)_{n-1}, \Delta(\boldsymbol{\varepsilon}^i)_n), \quad (1.133)$$

$$\Delta(\boldsymbol{\varepsilon}^i)_n = \boldsymbol{\varepsilon}(\Delta(\mathbf{u}^i)_n),$$

$$\Delta(\mathbf{t}_{\epsilon_C})_n = \mathbf{T}_C((\mathbf{t}_{\epsilon_C})_{n-1}, \Delta(\mathbf{u}^A - \mathbf{u}^B)_n), \quad (1.134)$$

where  $\Delta(\bullet)_n := (\bullet)_n - (\bullet)_{n-1}$ ,  $\boldsymbol{\xi}$  in our case is  $\boldsymbol{\xi} := (\alpha, \beta)$ . A return mapping algorithm for plasticity (Section 1.2) maps  $(\mathbf{u}^i)_n, (\mathbf{u}^i)_{n-1}, (\boldsymbol{\xi}^i)_{n-1}, (\boldsymbol{\varepsilon}^{ip})_{n-1} := \boldsymbol{\varepsilon}((\mathbf{u}^i)_{n-1}) - (\mathbb{C}^i)^{-1} : (\boldsymbol{\sigma}^i)_{n-1}$  onto  $(\boldsymbol{\xi}^i)_n$  and  $(\boldsymbol{\varepsilon}^{ip})_n := \boldsymbol{\varepsilon}((\mathbf{u}^i)_n) - (\mathbb{C}^i)^{-1} : (\boldsymbol{\sigma}^i)_n$  (or  $(\boldsymbol{\xi}^i)_n$  and  $(\boldsymbol{\sigma}^i)_n$ ); exactly this is written in functional form in (1.132), (1.133). A return mapping algorithm for contact (1.101) in Section 1.4 maps  $\Delta \mathbf{g} := ((\mathbf{u}^A)_n - (\mathbf{u}^B)_n)$  and  $(\mathbf{t}_{\epsilon_C})_{n-1}$  onto  $\Delta(\mathbf{t}_{\epsilon_C})_n$ ; exactly this is written in functional form in (1.134).

Defining

$$(\mathbf{T}_{pl}^i)_{n-1}(\Delta(\boldsymbol{\varepsilon}^i)_n) := \mathbf{T}_{pl}^i((\boldsymbol{\sigma}^i)_{n-1}, (\boldsymbol{\xi}^i)_{n-1}, \Delta(\boldsymbol{\varepsilon}^i)_n), \quad (1.135)$$

$$(\mathbf{G}_{pl}^i)_{n-1}(\Delta(\boldsymbol{\varepsilon}^i)_n) := \mathbf{G}_{pl}^i((\boldsymbol{\sigma}^i)_{n-1}, (\boldsymbol{\xi}^i)_{n-1}, \Delta(\boldsymbol{\varepsilon}^i)_n), \quad (1.136)$$

$$(\mathbf{T}_C)_{n-1}(\Delta(\mathbf{u}^A - \mathbf{u}^B)_n) := \mathbf{T}_C((\mathbf{t}_{\epsilon_C})_{n-1}, \Delta(\mathbf{u}^A - \mathbf{u}^B)_n), \quad (1.137)$$

we have for  $F_{\mathbf{u}_h}^{int}$  defined in Section 1.2.1

$$F_{\mathbf{u}_h}^{int}(\Delta \boldsymbol{\sigma}^i, \Delta \mathbf{t}_C, \boldsymbol{\eta}_h) = \sum_{i=B,A} ((\mathbf{T}_{pl})_{n-1}(\Delta(\boldsymbol{\varepsilon}^i)_n), \boldsymbol{\varepsilon}(\boldsymbol{\eta}_h^i))_{\Omega^i} - \langle (\mathbf{T}_C)_{n-1}(\Delta(\mathbf{u}^A - \mathbf{u}^B)_n), \boldsymbol{\eta}_h^i \rangle_{\Gamma_C}. \quad (1.138)$$

The convergence of a Newton-type Method introduced below depends on the properties of the functionals

$$\mathcal{F}_{pl,n-1}(\Delta(\mathbf{u}^i)_n, \boldsymbol{\eta}_h) := \sum_{i=B,A} ((\mathbf{T}_{pl})_{n-1}(\Delta(\boldsymbol{\varepsilon}^i)_n), \boldsymbol{\varepsilon}(\boldsymbol{\eta}_h^i))_{\Omega^i} \quad (1.139)$$

and

$$\mathcal{F}_{C,n-1}(\Delta(\mathbf{u}^i)_n, \boldsymbol{\eta}_h) := - \langle (\mathbf{T}_C)_{n-1}(\Delta(\mathbf{u}^A - \mathbf{u}^B)_n), \boldsymbol{\eta}_h^i \rangle_{\Gamma_C}. \quad (1.140)$$

## 1.5 A Newton-type method for two-body elastoplastic contact with friction

The functional  $\mathcal{F}_{pl,n-1}$  was investigated in [5] and has the following properties that we formulate as a sequence of lemmas. For convenience using the isomorphism  $\mathbb{R}^N \leftrightarrow {}^h\mathbf{V}$  we consider operators acting on  $\mathbb{R}^N$  instead of  ${}^h\mathbf{V}$ . We write  $\mathbf{U}$  for the coefficients of the expansion of  $\mathbf{u}_h$  in the basis in the discrete space  ${}^h\mathbf{V}_D$ , i.e.  $\mathbf{u}_h = \sum_{j=1}^{n_{el}} U^j \psi^j$ . The next three lemmas state the necessary properties of the functional  $\mathcal{F}_{pl,n-1}$ , i.e. Lemma 1.5.1 gives the differentiability conditions, Lemma 1.5.2 gives the symmetry and positive definiteness, and Lemma 1.5.3 gives the Lipschitz continuity of the Fréchet derivative.

**Lemma 1.5.1** ([5] Lemma 5.1). *The operator  $\mathcal{F}_{pl,n-1} : \mathbb{R}^N \rightarrow \mathbb{R}^N$  is differentiable in  $\mathbb{R}_{pl,ep}^N \subset \mathbb{R}^N$ . For  $\mathbf{U} \in \mathbb{R}_{pl,ep}^N$ , there exists the Fréchet derivative of  $\mathcal{F}_{pl,n-1}$  given by*

$$\langle \mathcal{F}'_{pl,n-1}(\mathbf{U})\mathbf{V}, \mathbf{W} \rangle := \sum_{i=A,B} \int_{\Omega^i} (\mathbf{T}'_{pl})_{n-1}(\boldsymbol{\varepsilon}(\mathbf{u}_h^i)) \boldsymbol{\varepsilon}(\mathbf{v}_h^i) \cdot \boldsymbol{\varepsilon}(\mathbf{w}_h^i) d\Omega, \quad (1.141)$$

for all  $\mathbf{V}, \mathbf{W} \in \mathbb{R}^N$ , where  $\mathbf{u}_h := \sum_{j=1}^{n_{el}} U^j \psi^j$ ,  $\mathbf{v}_h := \sum_{j=1}^{n_{el}} V^j \psi^j$ ,  $\mathbf{w}_h := \sum_{j=1}^{n_{el}} W^j \psi^j$ .

Here we have used a notation  $\mathbb{R}_{pl,ep}^N := \{ \mathbf{U} \in \mathbb{R}^N \mid \boldsymbol{\varepsilon}(\mathbf{u}_h(x)) \notin S_{pl,n-1}^i(x) \text{ for all } x \in \Omega \}$ , where

$$S_{pl,n-1}^i(x) := \{ \boldsymbol{\varepsilon} \in S \mid \phi_{pl}(\boldsymbol{\sigma}_{hn-1}(x) + \mathbb{C}\boldsymbol{\varepsilon}, \boldsymbol{\xi}_{hn-1}(x)) = 0 \}.$$

**Lemma 1.5.2** ([5] Lemma 5.2, Conclusion 5.1). *Let us consider  $\mathbf{U} \in \mathbb{R}_{pl,ep}^N$ , then the derivative  $\mathcal{F}'_{pl,n-1}(\mathbf{U})$  is symmetric and positive definite. Moreover, the positive definiteness is locally uniform, i.e. for any  $c > 0$  there is  $m_{pl}(c) > 0$ , such that*

$$m_{pl}(c) \|\mathbf{V}\|^2 \leq \langle \mathcal{F}'_{pl,n-1}(\mathbf{U})\mathbf{V}, \mathbf{V} \rangle, \quad (1.142)$$

for all  $\mathbf{V} \in \mathbb{R}^N$  and  $\mathbf{V} \in \mathbb{R}_{pl,ep}^N$  such that  $\|\mathbf{U}\| \leq c$ , moreover, for any  $c$  there exists a constant  $M_{pl}(c)$  such that for all  $\mathbf{U} \in \mathbb{R}_{pl,ep}^N$ ,  $\|\mathbf{U}\| \leq c$  there exists  $(\mathcal{F}'_{pl,n-1}(\mathbf{U}))^{-1}$  satisfying

$$\|(\mathcal{F}'_{pl,n-1}(\mathbf{U}))^{-1}\| \leq M_{pl}(c). \quad (1.143)$$

**Proof.** see [5] Lemma 5.2 and Conclusion 5.1. □

Here and below we use a standard Euclidian norm in discrete space  $\mathbb{R}^N$ :

$$\|\mathbf{V}\| := \sqrt{\langle \mathbf{V}, \mathbf{V} \rangle}. \quad (1.144)$$

Note, that in [5] all estimates are obtained in energy norm

$$\|\mathbf{V}\|_{\mathbb{C}} := \sqrt{\langle \mathbb{C}\mathbf{V}, \mathbf{V} \rangle}. \quad (1.145)$$

since in finite dementional spaces all norms are equivalent we may replace the energy norm with the Euclidian one.

**Lemma 1.5.3** ([5] Lemma 5.3). *The derivative  $\mathcal{F}'_{pl,n-1}(\mathbf{U})$  is Lipschitz continuous in  $\mathbb{R}_{pl,ep}^N$  or more exactly there exists a constant  $C_{pl,L}$ , such that*

$$\|\mathcal{F}'_{pl,n-1}(\mathbf{U} + \Theta) - \mathcal{F}'_{pl,n-1}(\mathbf{U})\| \leq C_{pl,L} \|\Theta\|, \quad (1.146)$$

for all  $\mathbf{U}, \Theta \in \mathbb{R}_{pl,ep}^N$ , such that  $\mathbf{U} + \theta\Theta \in \mathbb{R}_{pl,ep}^N$  for all  $\theta \in [0, 1]$ .

The next three lemmas correspond to the properties of the functional  $\mathcal{F}_{C,n-1}(\mathbf{U})$  and its Fréchet derivative. Instead of positive definiteness as it was obtained for  $\mathcal{F}'_{pl,n-1}(\mathbf{U})$ , the Fréchet derivative  $\mathcal{F}'_{C,n-1}(\mathbf{U})$  is only positive semi-definite, whereas the sum  $\mathcal{F}_{C,n-1}(\mathbf{U}) + \mathcal{F}_{pl,n-1}(\mathbf{U})$  is positive definite on appropriate space.

**Lemma 1.5.4** (Analog of Lemma 1.5.1). *The operator  $\mathcal{F}_{C,n-1} : \mathbb{R}^N \rightarrow \mathbb{R}^N$  is differentiable in  $\mathbb{R}_{pl,ep}^N \subset \mathbb{R}^N$ . For  $\mathbf{U} \in \mathbb{R}_{pl,ep}^N$ , there exists the Fréchet derivative of  $\mathcal{F}_{C,n-1}$  given by*

$$\langle \mathcal{F}'_{C,n-1}(\mathbf{U})\mathbf{V}, \mathbf{W} \rangle := - \int_{\Gamma_C} (\mathbf{T}'_C)_{n-1}(\mathbf{u}_h^i) \mathbf{v}_h^i \cdot \mathbf{w}_h^i d\Gamma, \quad (1.147)$$

for all  $\mathbf{V}, \mathbf{W} \in \mathbb{R}^N$ .

**Proof.** The assertion of Lemma follows straightforward from Theorem 1.4.1. □

**Lemma 1.5.5** (Analog of Lemma 1.5.2). *Let us consider  $\mathbf{U} \in \mathbb{R}_{pl,ep}^N$ , then the derivative  $\mathcal{F}'_{pl,n-1}(\mathbf{U})$  is symmetric and positive semi-definite:*

$$0 \leq \langle \mathcal{F}'_{pl,n-1}(\mathbf{U})\mathbf{V}, \mathbf{V} \rangle, \quad (1.148)$$

for all  $\mathbf{V} \in \mathbb{R}^N$ .

**Proof.** The assertions of Lemma follow straightforward from Theorem 1.4.2. □

**Lemma 1.5.6** (Analog of Lemma 1.5.3). *The derivative  $\mathcal{F}'_{C,n-1}(\mathbf{U})$  is Lipschitz continuous in  $\mathbb{R}_{C,ep}^N$  or more exactly there exists a constant  $C_{C,L}$ , such that*

$$\|\mathcal{F}'_{C,n-1}(\mathbf{U} + \Theta) - \mathcal{F}'_{C,n-1}(\mathbf{U})\| \leq C_{C,L} \|\Theta\|, \quad (1.149)$$

for all  $\mathbf{U}, \Theta \in \mathbb{R}_{C,ep}^N$ , such that  $\mathbf{U} + \theta\Theta \in \mathbb{R}_{C,ep}^N$  for all  $\theta \in [0, 1]$ . Here we have used a notation  $\mathbb{R}_{C,ep}^N := \{\mathbf{U} \in \mathbb{R}^N \mid \mathbf{u}_h(x) \notin S_{C,n-1}^i(x) \text{ for all } x \in \Omega\}$ , where

$$S_{C,n-1}^i(x) := \{\mathbf{g} \in \mathbb{R}^2 \mid \phi_C(\mathbf{t}_{hn-1}(x) - \mathbb{D}\mathbf{g}) = 0\}.$$

**Proof.**

$$\begin{aligned}
 \left\| \mathcal{F}'_{C,n-1}(\tilde{\mathbf{U}}) - \mathcal{F}'_{C,n-1}(\mathbf{U}) \right\| &:= \sup_{\mathbf{V} \neq 0} \sup_{\mathbf{W} \neq 0} \frac{\langle [\mathcal{F}'_{C,n-1}(\tilde{\mathbf{U}}) - \mathcal{F}'_{C,n-1}(\mathbf{U})] \mathbf{V}, \mathbf{W} \rangle}{\|\mathbf{V}\| \|\mathbf{W}\|} \\
 &\leq \sup_{\mathbf{x} \in \Gamma_C} \|\mathbf{T}'_{C,n-1}(\tilde{\mathbf{u}}_h(\mathbf{x})) - \mathbf{T}'_{C,n-1}(\mathbf{u}_h(\mathbf{x}))\| \sup_{\mathbf{V} \neq 0} \sup_{\mathbf{W} \neq 0} \frac{\langle \mathbf{V}, \mathbf{W} \rangle}{\|\mathbf{V}\| \|\mathbf{W}\|} \\
 &\leq C_1 \|\tilde{\mathbf{u}}_h - \mathbf{u}_h\|_{H^{1/2}(\Gamma_C)} \sup_{\mathbf{V} \neq 0} \sup_{\mathbf{W} \neq 0} \frac{\langle \mathbf{V}, \mathbf{W} \rangle}{\|\mathbf{V}\| \|\mathbf{W}\|} \\
 &\leq C_1 \|\tilde{\mathbf{u}}_h - \mathbf{u}_h\|_{H^{1/2}(\Gamma_C)} \sup_{\mathbf{v}_h \neq 0, \mathbf{w}_h \neq 0} \frac{\|\mathbf{v}_h\|_{H^{1/2}(\Gamma_C)} \|\mathbf{w}_h\|_{H^{1/2}(\Gamma_C)}}{\|\mathbf{v}_h\|_{H^1(\Omega)} \|\mathbf{w}_h\|_{H^1(\Omega)}} \\
 &\leq C_1 C_{\Gamma_C}^3 \|\tilde{\mathbf{u}}_h - \mathbf{u}_h\|_{H^1(\Omega)} \\
 &\leq C_1 C_{\Gamma_C}^3 \|\tilde{\mathbf{U}} - \mathbf{U}\|
 \end{aligned} \tag{1.150}$$

where we have used the Lipschitz continuity of  $\mathbf{T}'$  Theorem 1.4.3 and the fact that  $\|\mathbf{v}_h\|_{H^{1/2}(\Gamma_C)} \leq C_{\Gamma_C} \|\mathbf{v}_h\|_{H^1(\Omega)}$ . Setting  $\tilde{\mathbf{U}} := \mathbf{U} + \Theta$  we obtain the assertion of the Theorem with  $C_{C,L} := C_1 C_{\Gamma_C}^3$ .  $\square$

The use of the lemma 1.5.1 and the lemma 1.5.4 gives the following result

**Lemma 1.5.7.** *The operator  $\mathcal{F}_{n-1} := \mathcal{F}_{pl,n-1} + \mathcal{F}_{C,n-1} : \mathbb{R}^N \rightarrow \mathbb{R}^N$  is differentiable in  $\mathbb{R}_{ep}^N := \mathbb{R}_{pl,ep}^N \cap \mathbb{R}_{C,ep}^N \subset \mathbb{R}^N$ . For  $\mathbf{U} \in \mathbb{R}_{ep}^N$ , there exists the Fréchet derivative of  $\mathcal{F}_{n-1}$  given by*

$$\langle \mathcal{F}'_{n-1}(\mathbf{U}) \mathbf{V}, \mathbf{W} \rangle := \langle \mathcal{F}'_{C,n-1}(\mathbf{U}) \mathbf{V}, \mathbf{W} \rangle + \langle \mathcal{F}'_{pl,n-1}(\mathbf{U}) \mathbf{V}, \mathbf{W} \rangle, \tag{1.151}$$

for all  $\mathbf{V}, \mathbf{W} \in \mathbb{R}^N$ .

The use of the lemma 1.5.2 and the lemma 1.5.5 gives the following result

**Lemma 1.5.8.** *Let us consider  $\mathbf{U} \in \mathbb{R}_{ep}^N$ , then the derivative  $\mathcal{F}'_{n-1}(\mathbf{U})$  is symmetric and positive definite. Moreover, the positive definiteness is locally uniform, i.e. for any  $c > 0$  there is  $m(c) > 0$  (the same constants as in Lemma 1.5.2  $m(c) = m_{pl}(c)$ ) such that*

$$m(c) \|\mathbf{V}\|^2 \leq \langle \mathcal{F}'_{n-1}(\mathbf{U}) \mathbf{V}, \mathbf{V} \rangle, \tag{1.152}$$

for all  $\mathbf{V} \in \mathbb{R}^N$  and  $\mathbf{U} \in \mathbb{R}_{ep}^N$  such that  $\|\mathbf{U}\| \leq c$ , moreover, for any  $c$  there exists a constant  $M(c)$  (the same constants as in Lemma 1.5.2  $M(c) = M_{pl}(c)$ ) such that for all  $\mathbf{U} \in \mathbb{R}_{ep}^N$ ,  $\|\mathbf{U}\| \leq c$  there exists  $(\mathcal{F}'_{n-1}(\mathbf{U}))^{-1}$  satisfying

$$\left\| (\mathcal{F}'_{n-1}(\mathbf{U}))^{-1} \right\| \leq M(c). \tag{1.153}$$

The use of the lemma 1.5.3 and the lemma 1.5.6 gives the following result

**Lemma 1.5.9.** *The derivative  $\mathcal{F}'_{n-1}(\mathbf{U})$  is Lipschitz continuous in  $\mathbb{R}_{ep}^N$  or more exactly there exists a constant  $C_L$  ( $C_L = \max\{C_{pl,L}, C_{C,L}\}$ ), such that*

$$\|\mathcal{F}'_{n-1}(\mathbf{U} + \Theta) - \mathcal{F}'_{n-1}(\mathbf{U})\| \leq C_L \|\Theta\|, \quad (1.154)$$

for all  $\mathbf{U}, \Theta \in \mathbb{R}_{ep}^N$ , such that  $\mathbf{U} + \theta\Theta \in \mathbb{R}_{ep}^N$  for all  $\theta \in [0, 1]$ .

In order to solve (1.131) we apply a Newton-type Method like in [5] Section 7. Define

$$F_*^{int}(\mathbf{U}, \boldsymbol{\eta}_h) := F^{int}(\mathbf{u}_h, \boldsymbol{\eta}_h).$$

Therefore (1.131) becomes

$$F_*^{int}(\Delta\mathbf{U}_n, \boldsymbol{\eta}_h) = \Delta F_n^{ext}(\boldsymbol{\eta}_h) \quad \forall \boldsymbol{\eta}_h \in {}^h\mathbf{V}_0. \quad (1.155)$$

The system of equations (1.155) can be written in a vector form

$$\mathcal{F}(\Delta\mathbf{U}_n) = \Delta f_n. \quad (1.156)$$

Then the Newton-type Method for (1.156) reads as follows.

Start with an initial guess  $\Delta\mathbf{U}_n^{(0)}$ ,

for  $i = 1, 2 \dots$  iterate

1. find Newton increment  $\boldsymbol{\delta}^{(i)}$  satisfying

$$\mathcal{F}'(\Delta\mathbf{U}_n^{(i-1)}) \cdot \boldsymbol{\delta}^{(i)} = r^{(i-1)} := \Delta f_n - \mathcal{F}(\Delta\mathbf{U}_n^{(i-1)}). \quad (1.157)$$

2. Update

$$\Delta\mathbf{U}_n^{(i)} := \Delta\mathbf{U}_n^{(i-1)} + \boldsymbol{\delta}^{(i)}. \quad (1.158)$$

continue

For fixed time step  $n$  we have the following theorem that provides convergence of Newton Method suggested above in this section. For convenience we will omit subscript  $n$ .

**Theorem 1.5.1.** *Assume that*

1. the system (1.156) has a solution  $\Delta\mathbf{U} \in \mathbb{R}^N$ ,
2.  $\Delta\mathbf{U}^{(0)}$  be a sufficiently good initial guess of  $\Delta\mathbf{U}$ ,

1.5 A Newton-type method for two-body elastoplastic contact with friction

3. the Newton Iterations (1.157), (1.158) are well defined, i.e.  $\Delta \mathbf{U}^{(i)} \in \mathbb{R}_{ep}^N$  for  $i = 1, 2, \dots$

Then, the Newton Iterations  $\Delta \mathbf{U}^{(i)}$  converge quadratically to the solution  $\Delta \mathbf{U}$  of (1.156), that exists by the first assumption.

*Remark 1.5.1.*  $\mathbb{R}_{ep}^N$  in Theorem 1.5.1 is an intersection of elastoplastic region (see [5]) and *elastoplastic* contact region ( cf.  $S_C^{ep}(\Gamma)$  in Section 1.4 )

**Proof.** We are on the position to give a proof of Theorem 1.5.1.

Assume that  $\Delta \mathbf{U}^{(0)}$  is close to  $\Delta \mathbf{U}$ , such that

$$\frac{1}{2} C_L M \|\Delta \mathbf{U}^{(0)} - \Delta \mathbf{U}\| = \varrho < 1 \quad (1.159)$$

$C_L : \max\{C_{C,L}, C_{pl,L}\}$ , where  $C_{C,L}$  is taken from the Lemma 1.5.6 and  $C_{pl,L}$  from the Lemma 1.5.3.  $M := M(c)$  where  $M(c)$  is taken from the Lemma 1.5.8 with  $c := \|\Delta \mathbf{U}\| + \|\mathbf{U}^{(0)} - \Delta \mathbf{U}\| \geq \|\Delta \mathbf{U}^{(0)}\|$ . Assume that  $\|\Delta \mathbf{U}^{(0)} - \Delta \mathbf{U}\|$  is small enough, such that

$$\Delta \mathbf{U}^{(0)} + \theta(\Delta \mathbf{U} - \Delta \mathbf{U}^{(0)}) \in \mathbb{R}_{ep}^N, \quad \forall \theta \in [0, 1) \quad (1.160)$$

Hence, for the solution  $\Delta \mathbf{U}$  of (1.156) and the first Newton iteration  $\Delta \mathbf{U}^{(0)} \mapsto \Delta \mathbf{U}^{(1)}$  we have from (1.156) and (1.157) ( $i = 1$ )

$$\begin{aligned} 0 &= \Delta f_n - \mathcal{F}(\Delta \mathbf{U}) = r^{(0)} + \mathcal{F}(\Delta \mathbf{U}^{(0)}) - \mathcal{F}(\Delta \mathbf{U}) \\ &= \mathcal{F}'(\Delta \mathbf{U}^{(0)})(\Delta \mathbf{U}^{(1)} - \Delta \mathbf{U}^{(0)}) - \int_{\Delta \mathbf{U}^{(0)}}^{\Delta \mathbf{U}} \mathcal{F}'(\mathbf{V}) d\mathbf{V} \quad (\text{setting } \mathbf{V} := \Delta \mathbf{U}^{(0)} + \theta(\Delta \mathbf{U} - \Delta \mathbf{U}^{(0)})) \\ &= \mathcal{F}'(\Delta \mathbf{U}^{(0)})(\Delta \mathbf{U}^{(1)} - \Delta \mathbf{U}^{(0)}) - \int_0^1 \mathcal{F}'(\Delta \mathbf{U}^{(0)} + \theta(\Delta \mathbf{U} - \Delta \mathbf{U}^{(0)}))(\Delta \mathbf{U} - \Delta \mathbf{U}^{(0)}) d\theta \\ &= \mathcal{F}'(\Delta \mathbf{U}^{(0)})(\Delta \mathbf{U}^{(1)} - \Delta \mathbf{U}^{(0)}) - \mathcal{F}'(\Delta \mathbf{U}^{(0)})(\Delta \mathbf{U} - \Delta \mathbf{U}^{(0)}) \\ &\quad - \int_0^1 [\mathcal{F}'(\Delta \mathbf{U}^{(0)} + \theta(\Delta \mathbf{U} - \Delta \mathbf{U}^{(0)})) - \mathcal{F}'(\Delta \mathbf{U}^{(0)})](\Delta \mathbf{U} - \Delta \mathbf{U}^{(0)}) d\theta \\ &= \mathcal{F}'(\Delta \mathbf{U}^{(0)})(\Delta \mathbf{U}^{(1)} - \Delta \mathbf{U}) \\ &\quad - \int_0^1 [\mathcal{F}'(\Delta \mathbf{U}^{(0)} + \theta(\Delta \mathbf{U} - \Delta \mathbf{U}^{(0)})) - \mathcal{F}'(\Delta \mathbf{U}^{(0)})](\Delta \mathbf{U} - \Delta \mathbf{U}^{(0)}) d\theta. \end{aligned}$$

Thus,

$$\mathcal{F}'(\Delta \mathbf{U}^{(0)})(\Delta \mathbf{U}^{(1)} - \Delta \mathbf{U}) = \int_0^1 [\mathcal{F}'(\Delta \mathbf{U}^{(0)} + \theta(\Delta \mathbf{U} - \Delta \mathbf{U}^{(0)})) - \mathcal{F}'(\Delta \mathbf{U}^{(0)})](\Delta \mathbf{U} - \Delta \mathbf{U}^{(0)}) d\theta. \quad (1.161)$$

Employing results of Lemmas 1.5.8 and 1.5.9 under the assumption (1.159) we will investigate the equation (1.161) as follows:

using the Lemma 1.5.9 we estimate the integral in the right hand side of (1.161):

$$\begin{aligned} & \left\| \int_0^1 [\mathcal{F}'(\Delta \mathbf{U}^{(0)} + \theta(\Delta \mathbf{U} - \Delta \mathbf{U}^{(0)})) - \mathcal{F}'(\Delta \mathbf{U}^{(0)})](\Delta \mathbf{U} - \Delta \mathbf{U}^{(0)}) d\theta \right\| \\ & \leq \int_0^1 \|\mathcal{F}'(\Delta \mathbf{U}^{(0)} + \theta(\Delta \mathbf{U} - \Delta \mathbf{U}^{(0)})) - \mathcal{F}'(\Delta \mathbf{U}^{(0)})\| \|\Delta \mathbf{U} - \Delta \mathbf{U}^{(0)}\| d\theta \\ & \leq C_L \|\Delta \mathbf{U} - \Delta \mathbf{U}^{(0)}\| \|\Delta \mathbf{U} - \Delta \mathbf{U}^{(0)}\| \int_0^1 \theta d\theta \\ & = \frac{1}{2} C_L \|\Delta \mathbf{U} - \Delta \mathbf{U}^{(0)}\|^2. \end{aligned} \quad (1.162)$$

using the above estimate and the Lemma 1.5.8 we estimate the norm of the difference  $\Delta \mathbf{U}^{(1)} - \Delta \mathbf{U}$ :

$$\begin{aligned} & \|\Delta \mathbf{U}^{(1)} - \Delta \mathbf{U}\| = \\ & \left\| \mathcal{F}'^{-1}(\Delta \mathbf{U}^{(0)}) \int_0^1 [\mathcal{F}'(\Delta \mathbf{U}^{(0)} + \theta(\Delta \mathbf{U} - \Delta \mathbf{U}^{(0)})) - \mathcal{F}'(\Delta \mathbf{U}^{(0)})](\Delta \mathbf{U} - \Delta \mathbf{U}^{(0)}) d\theta \right\| \leq \\ & \|\mathcal{F}'^{-1}(\Delta \mathbf{U}^{(0)})\| \left\| \int_0^1 [\mathcal{F}'(\Delta \mathbf{U}^{(0)} + \theta(\Delta \mathbf{U} - \Delta \mathbf{U}^{(0)})) - \mathcal{F}'(\Delta \mathbf{U}^{(0)})](\Delta \mathbf{U} - \Delta \mathbf{U}^{(0)}) d\theta \right\| \leq \\ & \leq \|\mathcal{F}'^{-1}(\Delta \mathbf{U}^{(0)})\| \frac{1}{2} C_L \|\Delta \mathbf{U} - \Delta \mathbf{U}^{(0)}\|^2 = \frac{1}{2} C_L M \|\Delta \mathbf{U} - \Delta \mathbf{U}^{(0)}\|^2. \end{aligned} \quad (1.163)$$

Hence, (1.163) together with the assumption (1.159) gives the estimates

$$\frac{1}{2} C_L M \|\Delta \mathbf{U}^{(1)} - \Delta \mathbf{U}\| \leq \left( \frac{1}{2} C_L M \|\Delta \mathbf{U} - \Delta \mathbf{U}^{(0)}\| \right)^2 \leq \varrho^2 < 1. \quad (1.164)$$

$$\|\Delta \mathbf{U}^{(1)} - \Delta \mathbf{U}\| \leq \|\Delta \mathbf{U}^{(0)} - \Delta \mathbf{U}\|. \quad (1.165)$$

The triangle inequality and (1.165) give the estimate of  $\|\Delta \mathbf{U}^{(1)}\|$

$$\|\Delta \mathbf{U}^{(1)}\| \leq \|\Delta \mathbf{U}\| + \|\Delta \mathbf{U}^{(1)} - \Delta \mathbf{U}\| \leq c, \quad (1.166)$$



where the constant  $c$  is defined above and is equal  $\|\Delta\mathbf{U}\| + \|\Delta\mathbf{U}^{(0)} - \Delta\mathbf{U}\|$ .

Applying the arguments above with  $i = 2, \dots$  we get

$$\|\Delta\mathbf{U}^{(i)} - \Delta\mathbf{U}\| \leq \frac{1}{2}C_L M \|\Delta\mathbf{U}^{(i-1)} - \Delta\mathbf{U}\|^2 \quad (1.167)$$

$$\frac{1}{2}C_L M \|\Delta\mathbf{U}^{(i)} - \Delta\mathbf{U}\| \leq \varrho^{2^i}. \quad (1.168)$$

From (1.168) we conclude the convergence of  $\Delta\mathbf{U}^{(i)}$  to  $\Delta\mathbf{U}$ , whereas (1.167) shows that the Newton Iterations converge quadratically to  $\mathbf{U}$ , which ends the proof of the theorem.  $\square$

*Remark 1.5.2.* In order to perform the Newton algorithm we need the Fréchet derivative of the non-linear functional  $\mathcal{F}$ , that exists only on the subspace of  $\mathbb{R}^N$ . If during Newton iterations the increment of  $\mathbf{U}^k$  changes the elastoplastic zone, i.e. we are on the boundary between elastic and plastic zones, then the the Fréchet derivative at  $\mathbf{U}^k$  do not exists. In that case we can choose an arbitrary directional derivative of  $\mathcal{F}$ , or a pure elastic stiffness matrix.

## 1.6 Newton-like iterations for two-body elastoplastic contact with friction

We extend a Newton-like iterations for elastoplasticity with hardening investigated in [2, 6] onto two-boy elastoplastic problem with regularized contact with friction. The  $\dot{\boldsymbol{\sigma}} - \dot{\boldsymbol{\varepsilon}}$  relation is regularized as in [34, 2, 6], whereas the regularization for contact done as in Section 1.4. Our approach is based on the explicit computation of the increment of the stress (contact traction) using the increment of the strain (relative contact gap). In the literature this method is referred as Prandtl-Reuss stress computation. Consider a discrete problem (1.131) defined in Section 1.5.

$$F_{\mathbf{u}_n}^{int}(\Delta(\boldsymbol{\sigma}^i)_n, \Delta(\mathbf{t}_{\epsilon_C})_n, \boldsymbol{\eta}_h) = \Delta F_n^{ext}(\boldsymbol{\eta}_h) \quad \forall \boldsymbol{\eta}_h \in {}^h\mathbf{V}_0, \quad (1.169)$$

where the contact and the elastoplastic constitutive conditions from Section 1.4 and Section 1.2 are given via

$$\Delta(\boldsymbol{\sigma}^i)_n = \tilde{\mathbf{T}}_{pl}^i((\boldsymbol{\sigma}^i)_{n-1}, (\boldsymbol{\xi}^i)_{n-1}, \Delta(\boldsymbol{\varepsilon}^i)_n) \Delta(\boldsymbol{\varepsilon}^i)_n, \quad (1.170)$$

$$\Delta(\boldsymbol{\xi}^i)_n = \tilde{\mathbf{G}}_{pl}^i((\boldsymbol{\sigma}^i)_{n-1}, (\boldsymbol{\xi}^i)_{n-1}, \Delta(\boldsymbol{\varepsilon}^i)_n) \Delta(\boldsymbol{\varepsilon}^i)_n, \quad (1.171)$$

$$\Delta(\boldsymbol{\varepsilon}^i)_n = \boldsymbol{\varepsilon}(\Delta(\mathbf{u}^i)_n),$$

$$\Delta(\mathbf{t}_{\epsilon_C})_n = \tilde{\mathbf{T}}_C((\mathbf{t}_{\epsilon_C})_{n-1}, \Delta(\mathbf{u}^A - \mathbf{u}^B)_n) (\Delta(\mathbf{u}^A - \mathbf{u}^B)_n), \quad (1.172)$$

where  $\Delta(\bullet)_n := (\bullet)_n - (\bullet)_{n-1}$ ,  $\boldsymbol{\xi}$  in our case is  $\boldsymbol{\xi} := (\alpha, \beta)$ . A Prandtl-Reuss stress computation algorithm for plasticity ([2] Section 3) maps  $(\mathbf{u}^i)_n, (\mathbf{u}^i)_{n-1}, (\boldsymbol{\xi}^i)_{n-1}, (\boldsymbol{\varepsilon}^{ip})_{n-1} := \boldsymbol{\varepsilon}((\mathbf{u}^i)_{n-1}) - (\mathbb{C}^i)^{-1} : (\boldsymbol{\sigma}^i)_{n-1}$  onto  $(\boldsymbol{\xi}^i)_n$  and  $(\boldsymbol{\varepsilon}^{ip})_n := \boldsymbol{\varepsilon}((\mathbf{u}^i)_n) - (\mathbb{C}^i)^{-1} : (\boldsymbol{\sigma}^i)_n$  (or  $(\boldsymbol{\xi}^i)_n$  and  $(\boldsymbol{\sigma}^i)_n$ ); exactly this is written in functional form in (1.170), (1.171). A regularized Prandtl-Reuss traction computation algorithm for contact (1.129) in Section 1.4 maps  $\Delta \mathbf{g} := ((\mathbf{u}^A)_n - (\mathbf{u}^B)_n)$  and  $(\mathbf{t}_{\varepsilon C})_{n-1}$  onto  $\Delta(\mathbf{t}_{\varepsilon C})_n$ ; exactly this is written in functional form in (1.172).

Defining

$$(\tilde{\mathbf{T}}_{pl}^i)_{n-1}(\Delta(\boldsymbol{\varepsilon}^i)_n) := \tilde{\mathbf{T}}_{pl}^i((\boldsymbol{\sigma}^i)_{n-1}, (\boldsymbol{\xi}^i)_{n-1}, \Delta(\boldsymbol{\varepsilon}^i)_n), \quad (1.173)$$

$$(\tilde{\mathbf{G}}_{pl}^i)_{n-1}(\Delta(\boldsymbol{\varepsilon}^i)_n) := \tilde{\mathbf{G}}_{pl}^i((\boldsymbol{\sigma}^i)_{n-1}, (\boldsymbol{\xi}^i)_{n-1}, \Delta(\boldsymbol{\varepsilon}^i)_n), \quad (1.174)$$

$$(\tilde{\mathbf{T}}_C)_{n-1}(\Delta(\mathbf{u}^A - \mathbf{u}^B)_n) := \tilde{\mathbf{T}}_C((\mathbf{t}_{\varepsilon C})_{n-1}, \Delta(\mathbf{u}^A - \mathbf{u}^B)_n), \quad (1.175)$$

we have for  $F_{\mathbf{u}_h}^{int}$  defined in Section 1.2.1

$$F_{\mathbf{u}_h}^{int}(\Delta \boldsymbol{\sigma}^i, \Delta \mathbf{t}_C, \boldsymbol{\eta}_h) = \sum_{i=B,A} ((\tilde{\mathbf{T}}_{pl})_{n-1}(\Delta(\boldsymbol{\varepsilon}^i)_n), \boldsymbol{\varepsilon}(\boldsymbol{\eta}_h^i))_{\Omega^i} - \left\langle (\tilde{\mathbf{T}}_C)_{n-1}(\Delta(\mathbf{u}^A - \mathbf{u}^B)_n), \boldsymbol{\eta}_h^i \right\rangle_{\Gamma_C}. \quad (1.176)$$

The convergence of Newton-like iterations introduced below depends on the properties of the functionals

$$\mathcal{F}_{pl,n-1}(\Delta(\mathbf{u}^i)_n, \boldsymbol{\eta}_h) := \sum_{i=B,A} ((\tilde{\mathbf{T}}_C)_{n-1}(\Delta(\boldsymbol{\varepsilon}^i)_n) \Delta(\boldsymbol{\varepsilon}^i)_n, \boldsymbol{\varepsilon}(\boldsymbol{\eta}_h^i))_{\Omega^i} \quad (1.177)$$

and

$$\mathcal{F}_{C,n-1}(\Delta(\mathbf{u}^i)_n, \boldsymbol{\eta}_h) := - \left\langle (\tilde{\mathbf{T}}_C)_{n-1}(\Delta(\mathbf{u}^A - \mathbf{u}^B)_n) (\Delta(\mathbf{u}^A - \mathbf{u}^B)_n), \boldsymbol{\eta}_h^i \right\rangle_{\Gamma_C}. \quad (1.178)$$

**Definition 1.6.1.** For  $\mathbf{u}, \mathbf{v} \in {}^h\mathbf{V}$ :

$$\langle \mathcal{A}_e \mathbf{u}, \mathbf{v} \rangle := \int_{\Omega} \boldsymbol{\varepsilon}(\mathbf{u}) : \mathbb{C} : \boldsymbol{\varepsilon}(\mathbf{v}) \, d\Omega, \quad (1.179)$$

$$\langle \Delta \mathbf{f}_n, \mathbf{v} \rangle := \int_{\Omega} \Delta \mathbf{f}_n \cdot \boldsymbol{\varepsilon}(\mathbf{v}) \, d\Omega, \quad (1.180)$$

$$\|\mathbf{u}\|_E := \sqrt{\langle \mathcal{A}_e \mathbf{u}, \mathbf{u} \rangle}, \quad (1.181)$$

$$\|\mathbf{u}\|_{-E} := \sqrt{\langle \mathcal{A}_e^{-1} \mathbf{u}, \mathbf{u} \rangle}. \quad (1.182)$$

The functional  $\mathcal{F}_{pl,n-1}$  was investigated in [6] and has the following properties that we

formulate as a sequence of lemmas. For convenience using the isomorphism  $\mathbb{R}^N \leftrightarrow {}^h\mathbf{V}$  we consider operators acting on  $\mathbb{R}^N$  instead of  ${}^h\mathbf{V}$ . We write  $\mathbf{U}$  for the coefficients of the expansion of  $\mathbf{u}_h$  in the basis in the discrete space  ${}^h\mathbf{V}_D$ , i.e.  $\mathbf{u}_h = \sum_{j=1}^{n_{el}} U^j \psi^j$ . The next three lemmas a theorem state the necessary properties of the functional  $\mathcal{F}_{pl,n-1}$ , i.e. Lemma 1.6.1 gives the continuity estimates for regularized  $\rho_{pl,\delta}$ , Lemma 1.6.2 gives the upper bound estimate for the seminorm induced by  $\mathbb{C}_p$ , Theorem 1.6.1 gives the upper bound estimate for the seminorm in  $\mathbf{H}^1(\Omega)$  induced by  $\mathbb{C}_p$ .

**Lemma 1.6.1** ([6] Lemma 1). *For  $\mathbf{x} \in \Omega$  we define a norm in  $S$  by*

$$\|\mathbf{s}\|_{\mathbb{C}} := \|\mathbf{s}\|_{\mathbb{C}(\mathbf{x})} := \sqrt{\mathbf{s} : \mathbb{C}(\mathbf{x}) : \mathbf{s}}. \quad (1.183)$$

If  $\frac{\partial \phi_{pl}}{\partial \boldsymbol{\sigma}}$  is uniformly bounded with respect to  $\boldsymbol{\sigma}$ , i.e.

$$\left\| \frac{\partial \phi_{pl}}{\partial \boldsymbol{\sigma}} \right\|_{\mathbb{C}} \leq C_{pl}, \quad (1.184)$$

then

$$|\rho_{pl,\delta}(\mathbf{x}, \mathbf{u}) - \rho_{pl,\delta}(\mathbf{x}, \mathbf{v})| \leq \frac{C_{pl}}{\delta} \|\boldsymbol{\varepsilon}(\mathbf{u}(\mathbf{x})) - \boldsymbol{\varepsilon}(\mathbf{v}(\mathbf{x}))\|_{\mathbb{C}}. \quad (1.185)$$

Moreover, there exists a constant  $K$  such that

$$\operatorname{esssup}_{\mathbf{x} \in \Omega} |\rho_{pl,\delta}(\mathbf{x}, \mathbf{u}) - \rho_{pl,\delta}(\mathbf{x}, \mathbf{v})| \leq K \|\mathbf{u} - \mathbf{v}\|_E. \quad (1.186)$$

**Lemma 1.6.2** ([6] Lemma 2). *Let  $0 < \nu_0 < 1$  be a constant from [6] Eqn. (3),  $\mathbf{x} \in \Omega$  and let*

$$|\mathbf{s}|_{\mathbb{C}_p} := |\mathbf{s}|_{\mathbb{C}_p(\mathbf{x})} := \sqrt{\mathbf{s} : \mathbb{C}_p : \mathbf{s}}, \quad (1.187)$$

be a seminorm in  $S$ . Then

$$|\mathbf{s}|_{\mathbb{C}_p(\mathbf{x})} \leq \sqrt{\nu_0} \|\mathbf{s}\|_{\mathbb{C}(\mathbf{x})}, \quad \mathbf{s} \in S. \quad (1.188)$$

**Lemma 1.6.3** ([6] Lemma 3). *For all  $\mathbf{v}, \mathbf{w} \in {}^h\mathbf{V}_0$  we have*

$$\int_{\Omega} |\boldsymbol{\varepsilon}(\mathbf{v}) : \mathbb{C}_p : \boldsymbol{\varepsilon}(\mathbf{w})| d\Omega \leq \nu_0 \|\mathbf{v}\|_E \|\mathbf{w}\|_E. \quad (1.189)$$

**Theorem 1.6.1** ([6] Theorem 1). *Let  $\alpha$  be such that  $\vartheta := \nu_0 + \nu_0 K \alpha < 1$  for  $\nu_0$  defined in [6] Eqn. (3) and  $K$  defined in (1.186). Denote  $m = 1 - \vartheta$ ,  $M = 1 + \vartheta$ . Moreover, let  $\omega \in (0, \frac{2m}{M^2})$  which gives that*

$$c := \sqrt{1 - 2m\omega + M^2\omega^2} < 1.$$

1 Elastoplastic contact problems. Small deformations

Further, let the load increment  $\Delta \mathbf{f}_n$  be sufficiently small, e.g.

$$\|\Delta \mathbf{f}_n\|_{-E} \leq \frac{1-c}{\omega} \alpha.$$

Then the iterations  $k = 1, 2, \dots$

$$\Delta \mathbf{u}_n^{(k)} := \Delta \mathbf{u}_n^{(k-1)} + \omega A_e^{-1}(\Delta \mathbf{f}_n - \mathcal{F}_{pl,\delta}(\Delta \mathbf{u}_n^{(k-1)})), \quad \Delta \mathbf{u}_n^{(0)} := 0. \quad (1.190)$$

converge to the unique solution of the equation  $\mathcal{F}_{pl,\delta}(\Delta \mathbf{u}_n) = \Delta \mathbf{f}_n$ .

Next, let us consider the nonlinear mapping  $\mathcal{F}_\delta := \mathcal{F}_{pl,\delta} + \mathcal{F}_{C,\delta}$ . For  $\mathbf{u} = (\mathbf{u}^A, \mathbf{u}^B)$ ,  $\mathbf{v} = (\mathbf{v}^A, \mathbf{v}^B)$ ,  $\mathbf{w} = (\mathbf{w}^A, \mathbf{w}^B) \in {}^h\mathbf{V}_0$ ,  $(\Omega := \Omega^A \times \Omega^B, [\mathbf{u}] := \mathbf{u}^A - \mathbf{u}^B)$  we obtain

$$\begin{aligned} \langle \mathcal{F}_\delta(\mathbf{u}) - \mathcal{F}_\delta(\mathbf{v}), \mathbf{w} \rangle &= \int_{\Omega} \boldsymbol{\varepsilon}(\mathbf{u} - \mathbf{v}) : \mathbb{C} : \boldsymbol{\varepsilon}(\mathbf{w}) d\Omega + \int_{\Gamma_C} [\mathbf{u} - \mathbf{v}] : \mathbb{D} : [\mathbf{w}] d\Gamma \\ &- \int_{\Omega} (\rho_{pl,\delta}(\mathbf{x}, \mathbf{u}) \mathbb{C}_p \boldsymbol{\varepsilon}(\mathbf{u}) - \rho_{pl,\delta}(\mathbf{x}, \mathbf{v}) \mathbb{C}_p \boldsymbol{\varepsilon}(\mathbf{v})) : \boldsymbol{\varepsilon}(\mathbf{w}) d\Omega \\ &- \int_{\Gamma_C} (\rho_{C,\delta}(\mathbf{x}, \mathbf{u}) \mathbb{D}_p [\mathbf{u}] - \rho_{C,\delta}(\mathbf{x}, \mathbf{v}) \mathbb{D}_p [\mathbf{v}]) : [\mathbf{w}] d\Gamma \\ &= \langle \mathcal{A}_e(\mathbf{u} - \mathbf{v}), \mathbf{w} \rangle + \int_{\Gamma_C} [\mathbf{u} - \mathbf{v}] : \mathbb{D} : [\mathbf{w}] d\Gamma - I_1 - I_2, \end{aligned} \quad (1.191)$$

where

$$I_1 := I_{pl,1} + I_{C,1},$$

$$I_2 := I_{pl,2} + I_{C,2},$$

$$I_{pl,1} := \int_{\Omega} (\rho_{pl,\delta}(\mathbf{x}, \mathbf{u}) \mathbb{C}_p \boldsymbol{\varepsilon}(\mathbf{u} - \mathbf{v})) \mathbf{w} d\Omega,$$

$$I_{pl,2} := \int_{\Omega} (\rho_{pl,\delta}(\mathbf{x}, \mathbf{u}) - \rho_{pl,\delta}(\mathbf{x}, \mathbf{v})) \mathbb{C}_p \boldsymbol{\varepsilon}(\mathbf{v}) \boldsymbol{\varepsilon}(\mathbf{w}) d\Omega,$$

$$I_{C,1} := \int_{\Gamma_C} (\rho_{C,\delta}(\mathbf{x}, \mathbf{u}) \mathbb{D}_p [\mathbf{u} - \mathbf{v}]) [\mathbf{w}] d\Omega,$$

$$I_{C,2} := \int_{\Gamma_C} (\rho_{C,\delta}(\mathbf{x}, \mathbf{u}) - \rho_{C,\delta}(\mathbf{x}, \mathbf{v})) \mathbb{D}_p[\mathbf{v}][\mathbf{w}] d\Omega. \quad (1.192)$$

We have the following estimates for  $I_{pl,1}$ ,  $I_{pl,2}$ ,  $I_{C,1}$ ,  $I_{C,2}$  in the right hand side of (1.191): Lemmas 1.6.1, 1.6.3 yield

$$\begin{aligned} |I_{pl,2}| &\leq \nu_0 K \|\mathbf{v}\|_E \|\mathbf{u} - \mathbf{v}\|_E \|\mathbf{w}\|_E, \\ |I_{pl,1}| &\leq \nu_0 \|\mathbf{u} - \mathbf{v}\|_E \|\mathbf{w}\|_E, \end{aligned} \quad (1.193)$$

Employing the trace theorem we obtain

$$\begin{aligned} |I_{C,2}| &\leq C_1^3 \|\mathbf{v}\|_E \|\mathbf{u} - \mathbf{v}\|_E \|\mathbf{w}\|_E, \\ |I_{C,1}| &\leq C_1^2 \|\mathbf{u} - \mathbf{v}\|_E \|\mathbf{w}\|_E, \\ \left| \int_{\Gamma_C} [\mathbf{u} - \mathbf{v}] : \mathbb{D} : [\mathbf{w}] d\Gamma \right| &\leq C_1^2 \|\mathbf{u} - \mathbf{v}\|_E \|\mathbf{w}\|_E. \end{aligned}$$

*Remark 1.6.1.* The above estimates imply that  $\mathcal{F}_\delta$  is Lipschitz continuous and strongly monotone in any ball  $B_\alpha = \{\mathbf{v} \in {}^h\mathbf{V}_0 \mid \|\mathbf{v}\|_E \leq \alpha\}$  if  $\vartheta := \nu_0 + \alpha(\nu_0 K + C_1^3) < 1$ .

**Theorem 1.6.2.** *Let  $\alpha$  be such that  $\vartheta := \nu_0 + \alpha(\nu_0 K + C_1^3) < 1$  for  $\nu_0$  defined in [6] Eqn. (3) and  $K$  defined in (1.186). Denote  $m = 1 - \vartheta$ ,  $M = 1 + \vartheta$ . Moreover, let  $\omega \in (0, \frac{2m}{M^2})$  which gives that*

$$c := \sqrt{1 - 2m\omega + M^2\omega^2} < 1.$$

Further, let the load increment  $\Delta \mathbf{f}_n$  be sufficiently small, e.g.

$$\|\Delta \mathbf{f}_n\|_{-E} \leq \frac{1-c}{\omega} \alpha.$$

Then the iterations  $k = 1, 2, \dots$

$$\Delta \mathbf{u}_n^{(k)} := \Delta \mathbf{u}_n^{(k-1)} + \omega A_e^{-1} (\Delta \mathbf{f}_n - \mathcal{F}_\delta(\Delta \mathbf{u}_n^{(k-1)})), \quad \Delta \mathbf{u}_n^{(0)} := 0. \quad (1.194)$$

converge to the unique solution of the equation  $\mathcal{F}_\delta(\Delta \mathbf{u}_n) = \Delta \mathbf{f}_n$ .

**Proof.** Let  $\Delta \mathbf{u}^{(k-2)} \in B_\alpha$ , then using (1.194) we get

$$\Delta \mathbf{u}_n^{(k)} - \Delta \mathbf{u}_n^{(k-1)} = \Delta \mathbf{u}_n^{(k-1)} - \Delta \mathbf{u}_n^{(k-2)} + \omega A_e^{-1} (\mathcal{F}_\delta(\Delta \mathbf{u}_n^{(k-2)}) - \mathcal{F}_\delta(\Delta \mathbf{u}_n^{(k-1)})), \quad (1.195)$$

consequently

$$\begin{aligned}
\|\Delta \mathbf{u}_n^{(k)} - \Delta \mathbf{u}_n^{(k-1)}\|_E^2 &= \|\Delta \mathbf{u}_n^{(k-1)} - \Delta \mathbf{u}_n^{(k-2)}\|_E^2 \\
&\quad - 2\omega \langle \Delta \mathbf{u}_n^{(k-1)} - \Delta \mathbf{u}_n^{(k-2)}, \mathcal{F}_\delta(\Delta \mathbf{u}_n^{(k-1)}) - \mathcal{F}_\delta(\Delta \mathbf{u}_n^{(k-2)}) \rangle \\
&\quad + \omega^2 \|\mathcal{A}_e^{-1} (\mathcal{F}_\delta(\Delta \mathbf{u}_n^{(k-1)}) - \mathcal{F}_\delta(\Delta \mathbf{u}_n^{(k-2)}))\| \\
(*) &\leq \|\Delta \mathbf{u}_n^{(k-1)} - \Delta \mathbf{u}_n^{(k-2)}\|_E^2 \\
&\quad - 2\omega m \|\Delta \mathbf{u}_n^{(k-1)} - \Delta \mathbf{u}_n^{(k-2)}\| \\
&\quad + \omega^2 \|\mathcal{A}_e^{-1} (\mathcal{F}_\delta(\Delta \mathbf{u}_n^{(k-1)}) - \mathcal{F}_\delta(\Delta \mathbf{u}_n^{(k-2)}))\| \\
(**) &\leq \|\Delta \mathbf{u}_n^{(k-1)} - \Delta \mathbf{u}_n^{(k-2)}\|_E^2 \\
&\quad - 2\omega m \|\Delta \mathbf{u}_n^{(k-1)} - \Delta \mathbf{u}_n^{(k-2)}\|_E^2 \\
&\quad + \omega^2 M \|\Delta \mathbf{u}_n^{(k-1)} - \Delta \mathbf{u}_n^{(k-2)}\|_E^2 \\
&\leq c^2 \|\Delta \mathbf{u}_n^{(k-1)} - \Delta \mathbf{u}_n^{(k-2)}\|_E^2. \tag{1.196}
\end{aligned}$$

Using the local strong monotonicity of  $\mathcal{F}_\delta$ , i.e

$$\langle \mathcal{F}_\delta(\Delta \mathbf{u}_n^{(k-1)}) - \mathcal{F}_\delta(\Delta \mathbf{u}_n^{(k-2)}), \Delta \mathbf{u}_n^{(k-1)} - \Delta \mathbf{u}_n^{(k-2)} \rangle \geq m \|\Delta \mathbf{u}_n^{(k-1)} - \Delta \mathbf{u}_n^{(k-2)}\|_E$$

we obtained the inequality (\*) in (1.196). Employing the Lipschitz continuity of  $\mathcal{F}_\delta$  we obtain the estimate

$$\begin{aligned}
&\|\mathcal{A}_e^{-1} (\mathcal{F}_\delta(\Delta \mathbf{u}_n^{(k-1)}) - \mathcal{F}_\delta(\Delta \mathbf{u}_n^{(k-2)}))\|_E \\
&= \sup_{\mathbf{w} \neq 0} \frac{\langle \mathcal{A}_e \mathcal{A}_e^{-1} (\mathcal{F}_\delta(\Delta \mathbf{u}_n^{(k-1)}) - \mathcal{F}_\delta(\Delta \mathbf{u}_n^{(k-2)})), \mathbf{w} \rangle}{\|\mathbf{w}\|_E} \\
&= \sup_{\mathbf{w} \neq 0} \frac{\langle (\mathcal{F}_\delta(\Delta \mathbf{u}_n^{(k-1)}) - \mathcal{F}_\delta(\Delta \mathbf{u}_n^{(k-2)})), \mathbf{w} \rangle}{\|\mathbf{w}\|_E} \\
&\leq M \|\Delta \mathbf{u}_n^{(k-1)} - \Delta \mathbf{u}_n^{(k-2)}\|_E,
\end{aligned}$$

that is used in order to get the inequality (\*\*) in (1.196). We prove that the iterations  $\Delta \mathbf{u}_n^{(k)}$  belong to  $B_\alpha$  for all  $k \geq 0$  by induction.

- $i = 0$ ,  $\Delta \mathbf{u}_n^{(0)} = 0$ , i.e.  $\Delta \mathbf{u}_n^{(0)} \in B_\alpha$ .
- $i = 1$ ,  $\|\Delta \mathbf{u}_n^{(1)}\|_E = \|\omega \mathcal{A}_e^{-1} \Delta \mathbf{f}_n\|_{-E} \leq \alpha$ , i.e.  $\Delta \mathbf{u}_n^{(1)} \in B_\alpha$ .

- For  $i > 1$ , let  $\Delta \mathbf{u}_n^{(k)} \in B_\alpha$ , for all  $k < i$ .  $\Delta \mathbf{u}_n^{(i)} \in B_\alpha$  follows from the estimate:

$$\begin{aligned}
 \|\Delta \mathbf{u}_n^{(i)}\|_E &= \|\Delta \mathbf{u}_n^{(i)} - \Delta \mathbf{u}_n^{(i-1)} + \dots + \Delta \mathbf{u}_n^{(1)} - \Delta \mathbf{u}_n^{(0)}\|_E \\
 &\leq \|\Delta \mathbf{u}_n^{(i)} - \Delta \mathbf{u}_n^{(i-1)}\|_E + \dots + \|\Delta \mathbf{u}_n^{(1)} - \Delta \mathbf{u}_n^{(0)}\|_E \\
 &\leq (c^{i-1} + c^{i-2} + \dots + 1) \|\Delta \mathbf{u}_n^{(1)} - \Delta \mathbf{u}_n^{(0)}\|_E \\
 &\leq \frac{1}{1-c} \omega \|\Delta \mathbf{f}_n\|_{-E} \leq \alpha,
 \end{aligned} \tag{1.197}$$

where we have used the consequence of (1.196), i.e. the fact that

$$\|\Delta \mathbf{u}_n^{(k)} - \Delta \mathbf{u}_n^{(k-1)}\|_E \leq c^{k-1} \|\Delta \mathbf{u}_n^{(1)} - \Delta \mathbf{u}_n^{(0)}\|_E. \tag{1.198}$$

The estimate

$$\begin{aligned}
 \|\Delta \mathbf{u}_n^{(i+k)} - \Delta \mathbf{u}_n^{(i)}\|_E &\leq \|\Delta \mathbf{u}_n^{(i+k)} - \Delta \mathbf{u}_n^{(i+k-1)}\|_E + \dots + \|\Delta \mathbf{u}_n^{(i+1)} - \Delta \mathbf{u}_n^{(i)}\|_E \\
 &\leq (c^{i+k-1} + \dots + c^i) \|\Delta \mathbf{u}_n^{(1)} - \Delta \mathbf{u}_n^{(0)}\|_E \\
 &= c^i (c^{k-1} + \dots + 1) \|\Delta \mathbf{u}_n^{(1)} - \Delta \mathbf{u}_n^{(0)}\|_E \\
 &\leq c^i \frac{1}{1-c} \omega \|\Delta \mathbf{f}_n\|_{-E} \leq c^i \alpha
 \end{aligned} \tag{1.199}$$

shows that the sequence  $\{\Delta \mathbf{u}_n^{(i)}\}$  satisfies the Cauchy condition. (1.199) together with (1.197) yields that the sequence  $\{\Delta \mathbf{u}_n^{(i)}\}$  has a unique limit  $\Delta \mathbf{u}_n$  in  $B_\alpha$ . On the other hand this limit is a solution of the nonlinear equation  $\mathcal{F}_\delta(\Delta \mathbf{u}_n) = \Delta \mathbf{f}_n$ . The proof of the uniqueness is standard. Let  $\Delta \mathbf{u}_n^1, \Delta \mathbf{u}_n^2 \in B_\alpha$  solve  $\mathcal{F}_\delta(\Delta \mathbf{u}_n) = \Delta \mathbf{f}_n$ . Then

$$\mathcal{F}_\delta(\Delta \mathbf{u}_n^1) = \mathcal{F}_\delta(\Delta \mathbf{u}_n^2).$$

Due to the local monotonicity of  $\mathcal{F}_\delta$  in  $B_\alpha$  we obtain

$$0 = \langle \mathcal{F}_\delta(\Delta \mathbf{u}_n^1) - \mathcal{F}_\delta(\Delta \mathbf{u}_n^2), \Delta \mathbf{u}_n^1 - \Delta \mathbf{u}_n^2 \rangle_m \|\Delta \mathbf{u}_n^1 - \Delta \mathbf{u}_n^2\|_E^2. \tag{1.200}$$

Thus  $\Delta \mathbf{u}_n^1 = \Delta \mathbf{u}_n^2$ . □

In order to solve (1.169) we apply Newton-like iterations like in [6] Section 7. Define

$$F_*^{int}(\mathbf{U}, \boldsymbol{\eta}_h) := F^{int}(\mathbf{u}_h, \boldsymbol{\eta}_h).$$

Therefore (1.169) becomes

$$F_*^{int}(\Delta \mathbf{U}_n, \boldsymbol{\eta}_h) = \Delta F_n^{ext}(\boldsymbol{\eta}_h) \quad \forall \boldsymbol{\eta}_h \in {}^h \mathbf{V}_0. \tag{1.201}$$

The system of equations (1.201) can be written in a vector form

$$\mathcal{F}_\delta(\Delta \mathbf{U}_n) = \Delta \mathbf{f}_n. \quad (1.202)$$

Then the Newton-like iterations for (1.202) read as follows.

Start with an initial guess  $\Delta \mathbf{U}_n^{(0)}$ ,

for  $i = 1, 2 \dots$  iterate

1. find Newton increment  $\mathbf{d}^{(i)}$  satisfying

$$\mathcal{A}_e \mathbf{d}^{(i)} = \mathbf{r}^{(i-1)} := \Delta \mathbf{f}_n - \mathcal{F}_\delta(\Delta \mathbf{U}_n^{(i-1)}) \quad (1.203)$$

2. Update

$$\Delta \mathbf{U}_n^{(i)} := \Delta \mathbf{U}_n^{(i-1)} + \omega \mathbf{d}^{(i)}. \quad (1.204)$$

continue

*Remark 1.6.2.* The convergence of Newton-like iterations is provided by the Theorem 1.6.2.

*Remark 1.6.3.* The inexact version of this algorithm will be obtained by assuming that the iteration solver solves the linear system (1.203) with the tolerance  $\eta$ , i.e.

$$\|\mathcal{A}_e \mathbf{d}^{(i)} - \mathbf{r}^{(i-1)}\|_{-E} \leq \eta \|\mathbf{r}^{(i-1)}\|. \quad (1.205)$$

## 1.7 Numerical simulations

### Example 1

The model problem can be interpreted as an idealized isothermic metal forming process. The elastic stamp comes in contact with the plastic work piece and leaves some plastic deformations in it. Then the stamp changes its location, comes into contact with the work piece in the neighbors place and initiates some plastic deformations again. Without loss of generality we choose the stamp as a slave body, the work piece as a master body. The coordinates of the stamp in the moment of the first touch are  $\Omega_1^B := [0.2, 1.2] \times [-1, 1]$ , in the moment of the second touch are  $\Omega_2^B := [-1.8, -0.8] \times [-1, 1]$ . The work piece is given by  $\Omega^A := [-2, 2] \times [-3, -1]$ . Both touches are performed by setting prescribed total displacements on the Dirichlet boundary of the work piece  $\Gamma_D^A := [-2, 2] \times \{-3\}$  by  $\mathbf{u}_D^A := 4, 3 \cdot 10^{-3}$ . This total displacement is applied in the incremental form. The homogeneous displacements  $\mathbf{u}_D^B = 0$  are prescribed on the Dirichlet boundary



$\Gamma_{D,1}^B := [0.2, 1.2] \times \{1\}$ ,  $\Gamma_{D,2}^B := [-1.8, -0.8] \times \{1\}$  of the stamp in the first and second touch respectively. The linear system within each Newton step is solved using the Conjugate Gradient method with the diagonal preconditioner. In average the Newton method converges after 10 iterations.

Variable	mathematical notation	Slave	Master	dimension
Young	$E$	266926.0	26692.60	-
Poisson	$\nu$	0.29	0.29	-
Yield stress	$\sigma_Y$	-	45.0	-
Isotropic hardening	$h$	-	450.0	-

Table 1.1: Material data

Parameter	mathematical notation	value	dimension
Normal Penalty parameter	$\epsilon_N$	$10^{-6}$	-
Tangential Penalty parameter	$\epsilon_T$	$10^{-4}$	-
Friction coefficient	$\mu$	0.2	-

Table 1.2: Contact parameters

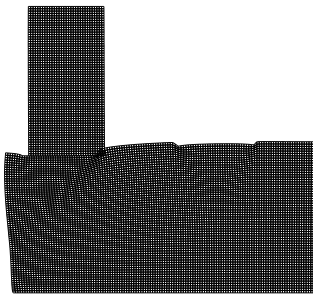


Figure 1.3: FE/FE: deformed mesh

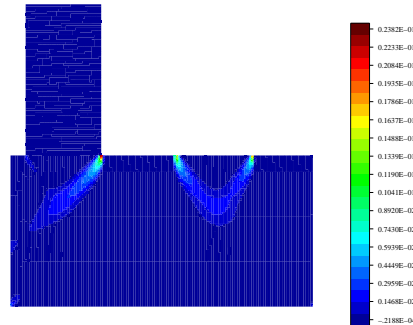


Figure 1.4: FE/FE:  $\|\epsilon^p\|$

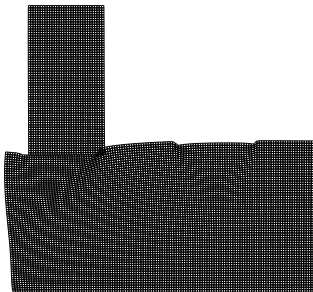


Figure 1.5: FE/BE: deformed mesh

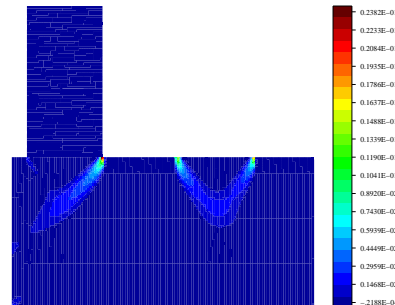


Figure 1.6: FE/BE:  $\|\epsilon^p\|$

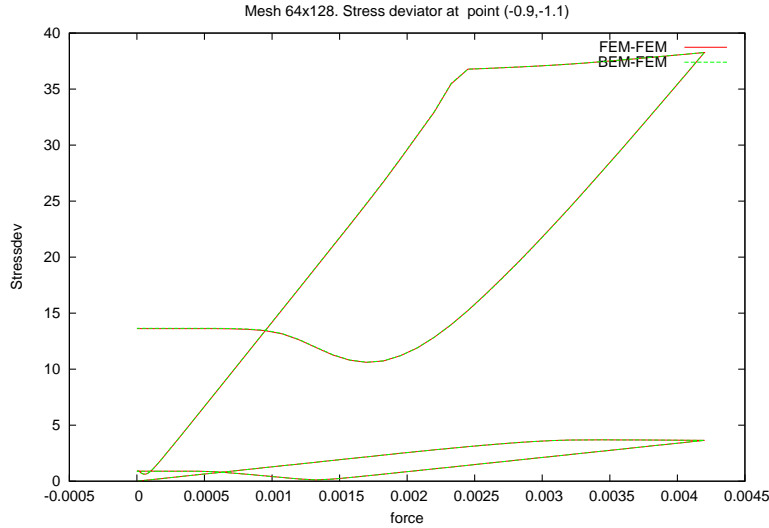


Figure 1.7: FE/FE, FE/BE:  $\|\boldsymbol{\varepsilon}^p\|$

On Fig. 1.3 - 1.6 we present the deformed mesh and the norm of the plastic strain tensor  $\|\boldsymbol{\varepsilon}^p\| := \sqrt{\boldsymbol{\varepsilon}^p : \boldsymbol{\varepsilon}^p}$  in both bodies for both approaches. One can clearly observe the similar plastic deformations in the work piece for FEM and BEM modeling of the stamp. To make more feeling of deformation inside the stamp modelled with BEM, we interpolate the FE mesh, compute displacements inside the body using the representation formula and compute corresponding deformed state. The displacements are multiplied with the factor 100 to make them visible. The evolution of the stress deviator norm in dependence of the applied force in the characteristic point  $X = (-0.9; -1, 1)$  in the work piece is shown on Fig. 1.7. The curves for FE/FE and FE/BE simulations are very close.

## Example 2

We make now a single touch in the middle of the work piece. The coordinates of the stamp in the moment of the touch are  $\Omega^B := [-1, 1] \times [-1, 0]$ . The work piece is given again by  $\Omega^A := [-2, 2] \times [-3, -1]$ . The Dirichlet boundary of the stamp  $\Gamma_D^B := [-1, 1] \times \{0\}$  is assumed to be fixed, i.e.  $\hat{\boldsymbol{u}}^B = 0$ . The Dirichlet boundary of the work piece  $\Gamma_D^A := [-2, 2] \times \{-3\}$  is subjected to the total displacement  $\hat{\boldsymbol{u}}^A := 4.2 \cdot 10^{-3}$  applied incrementally as shown on Fig. 1.10 with a time increment  $\Delta t = 0.625 \cdot 10^{-5}$ . The linear system within each Newton step is solved using the Conjugate Gradient method with the diagonal preconditioner. In average the Newton method converges after 10 iterations.

On Fig. 1.11 - 1.16 we present deformed meshes and the plastic strain norms. They reflect qualitatively the same behavior. On Fig. 1.17 we show the evolution of the norm of stress deviator for all three methods in the characteristic point  $X = (1; -1, 1)$ . One observes that both curves with the FEM modeling are pretty close. The curve for BEM in the work piece shows qualitatively similar behavior.

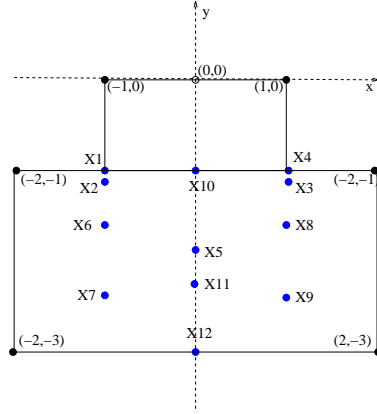


Figure 1.8: Characteristic points

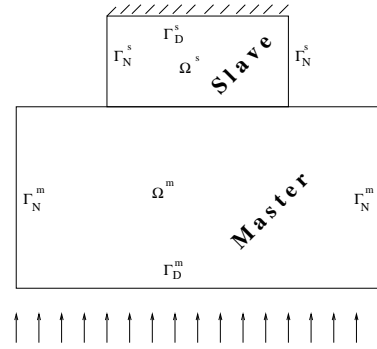


Figure 1.9: Geometry

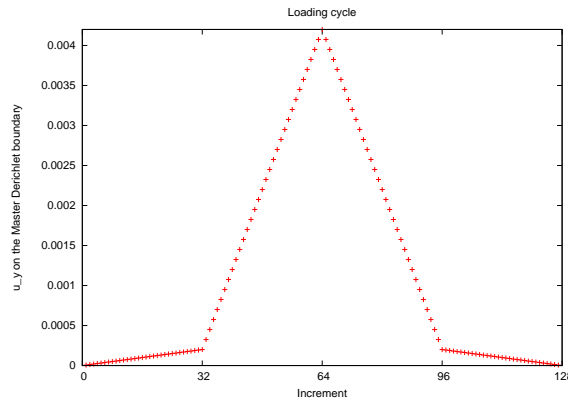


Figure 1.10: incremental loading of  $u_y$  at segment  $\overline{(-2, -3), (2, -3)}$

The performed loading process is depicted in Fig. 1.10, whereas material parameters and contact parameters are given in Tables 1.1, 1.2 respectively. We performed further numerical experiments and plotted at various points (see Fig. 1.8) in the elastoplastic work piece the norm of the stress deviator and the displacements depending on the loading (Fig. 1.20-1.31 and Fig. 1.32 - 1.43). The numerical experiments show expected behavior: the displacement is symmetric and the hysteresis is smaller in the elastic region. On Fig 1.18 you find the same diagram for the FEM/BEM coupling for different mesh sizes. One observes that the diagrams for the three finest mesh sizes lie closer to each other as for the coarser meshes, i.e. it starts to converge. On Fig. 1.19 we plot the absolute error for the norm of the stress deviator evaluated at difference points using Aitken extrapolant as an exact value. Aitken extrapolant is an approximation of the of series limit by three terms, i.e. for series  $\{x_k\}$  we have the approximation of the limit

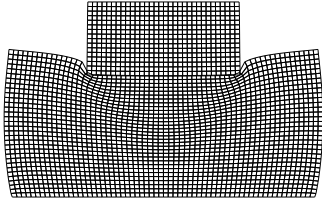


Figure 1.11: FE/FE: deformed mesh

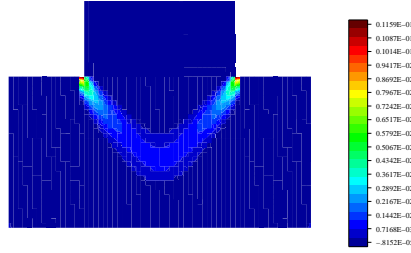


Figure 1.12: FE/FE:  $\|\epsilon^p\|$

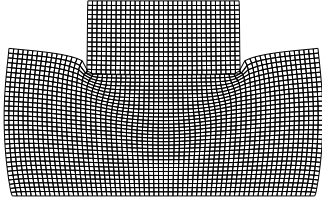


Figure 1.13: FE/BE: deformed mesh

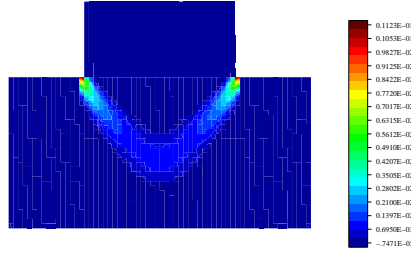


Figure 1.14: FE/BE:  $\|\epsilon^p\|$

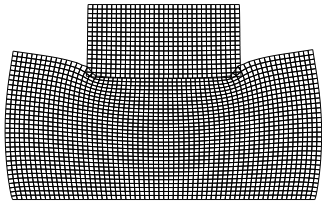


Figure 1.15: BE/BE: deformed mesh

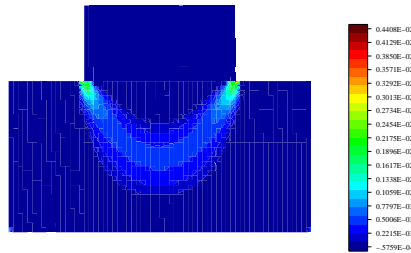


Figure 1.16: BE/BE:  $\|\epsilon^p\|$

$x := \lim_{k \rightarrow \infty} x_k$  by  $x_k, x_{k-1}$  and  $x_{k-2}$

$$x_{aitken} = x_k - \frac{(x_k - x_{k-1})}{(x_k - 2 * x_{k-1} + x_{k-2})}(x_k - x_{k-1}). \quad (1.206)$$

On Fig. 1.19 (a) we observe that for a fixed number of degrees of freedom the error does not depend on the ratio  $\epsilon/h$ , i.e. as the ratio  $\epsilon/h$  decreases the error of  $\|\text{dev } \sigma\|$  tends to a constant value that depends on the number of degrees of freedom. Fig. 1.19 (b) shows the convergence of  $\|\text{dev } \sigma\|$  of the order 0.7, i.e.  $\| \|\text{dev } \sigma_h\| - \|\text{dev } \sigma\| \| = O(\frac{1}{DOF^{0.7}})$ . On Fig. 1.19 (c) the error is plotted at different points for a fixed ratio  $\epsilon/h = 0.00000025$ . On Fig. 1.19 (d) the error is plotted at different points for a fixed penalty parameter  $\epsilon = 10^{-6}$ . Comparing Fig. 1.19 (c) and Fig. 1.19 (d) one observes that a convergence rate is better in case when the penalty parameter is proportional to the mesh size, i.e. the penalty parameter is smaller for finer meshes.

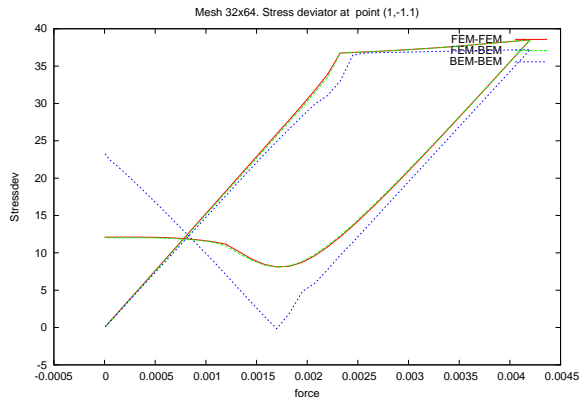


Figure 1.17: FE/FE, FE/BE, BE/BE:  $\|\text{dev } \sigma\|$

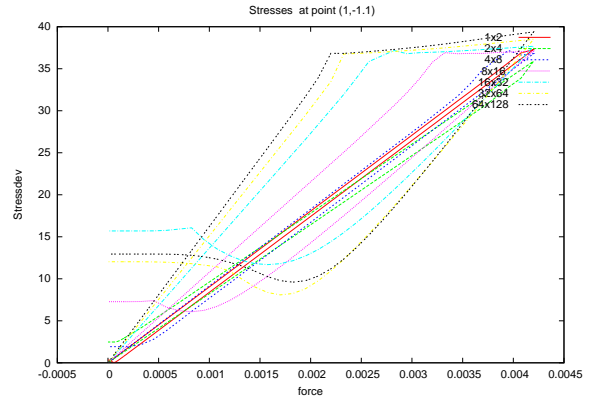
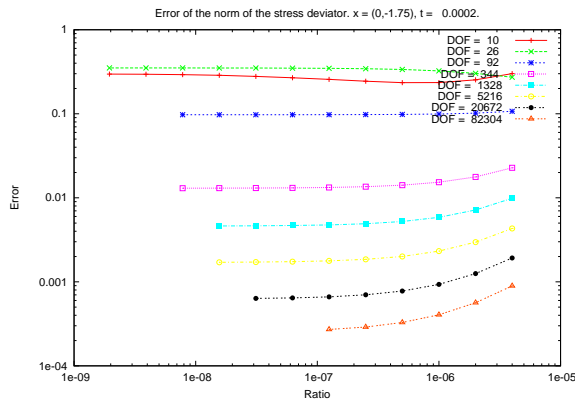
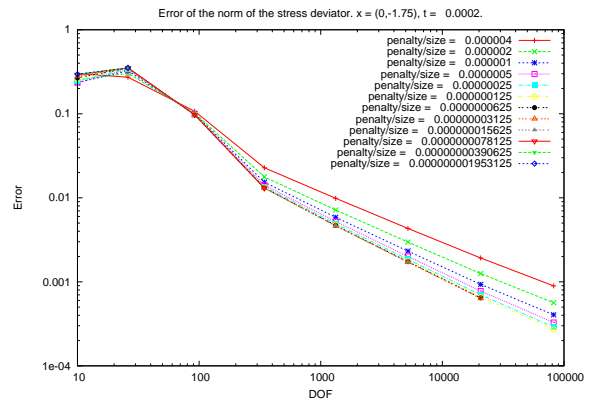


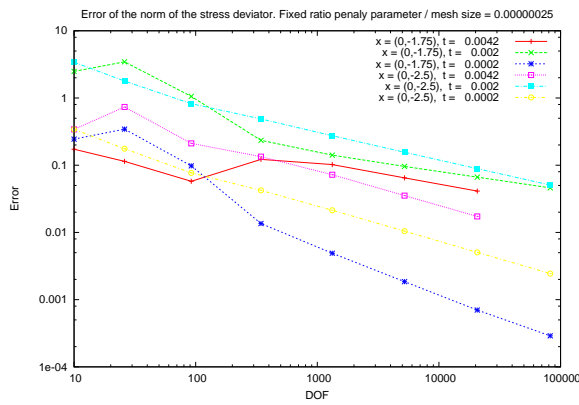
Figure 1.18: FE/BE:  $\|\text{dev } \sigma\|$  for different mesh sizes



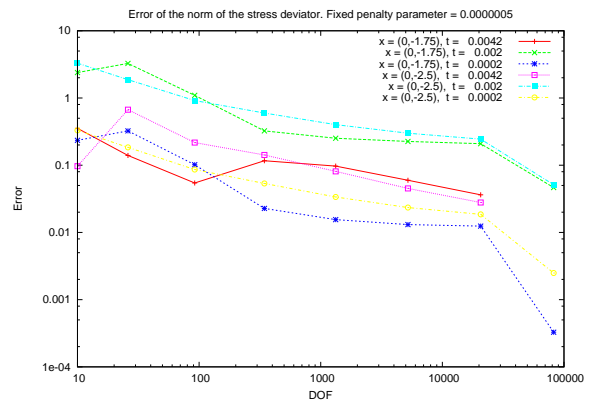
(a)



(b)



(c)



(d)

Figure 1.19: Error of  $\|\text{dev } \sigma\|$

1 Elastoplastic contact problems. Small deformations

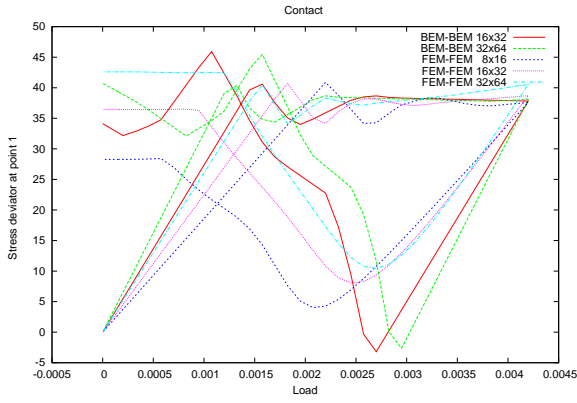


Figure 1.20:  $\|\text{dev}[\sigma]\|$  at  $X_1 = (-1, -1)$

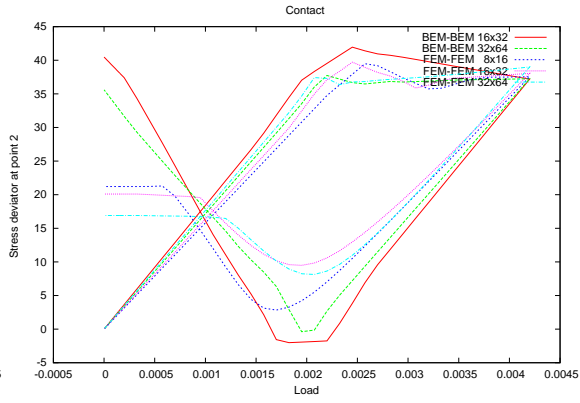


Figure 1.21:  $\|\text{dev}[\sigma]\|$  at  $X_2 = (-1, -1.1)$

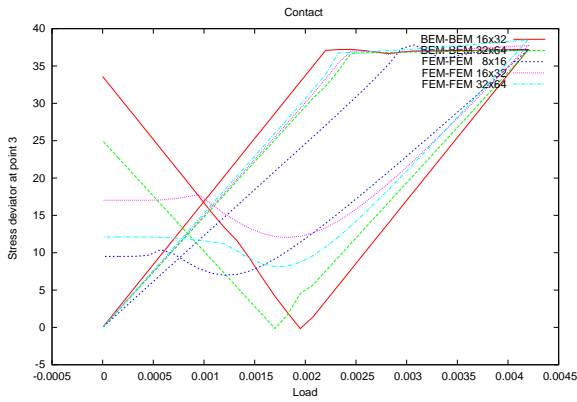


Figure 1.22:  $\|\text{dev}[\sigma]\|$  at  $X_3 = (1, -1.1)$

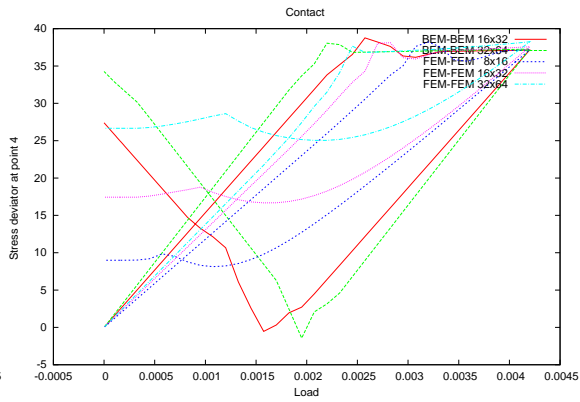


Figure 1.23:  $\|\text{dev}[\sigma]\|$  at  $X_4 = (1, -1)$

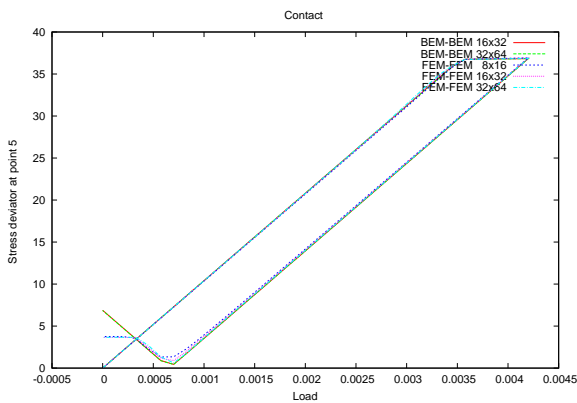


Figure 1.24:  $\|\text{dev}[\sigma]\|$  at  $X_5 = (0, -1.75)$

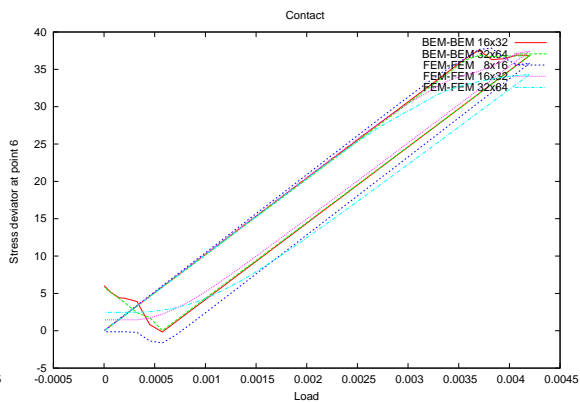


Figure 1.25:  $\|\text{dev}[\sigma]\|$  at  $X_6 = (-1, -1.5)$

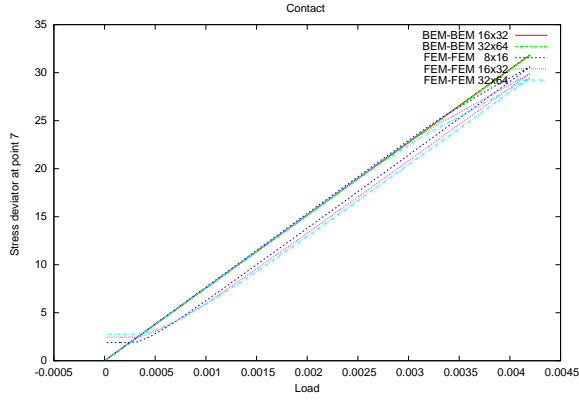


Figure 1.26:  $\|\text{dev}[\sigma]\|$  at  $X_7 = (-1, -2.5)$

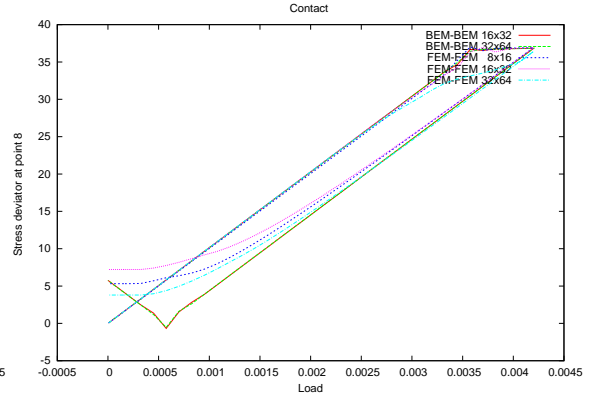


Figure 1.27:  $\|\text{dev}[\sigma]\|$  at  $X_8 = (1, -1.5)$

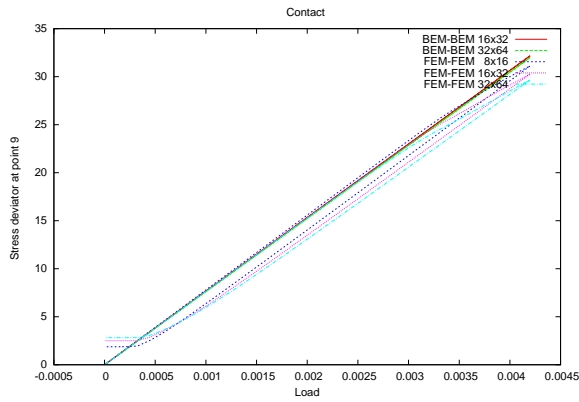


Figure 1.28:  $\|\text{dev}[\sigma]\|$  at  $X_9 = (1, -2.5)$

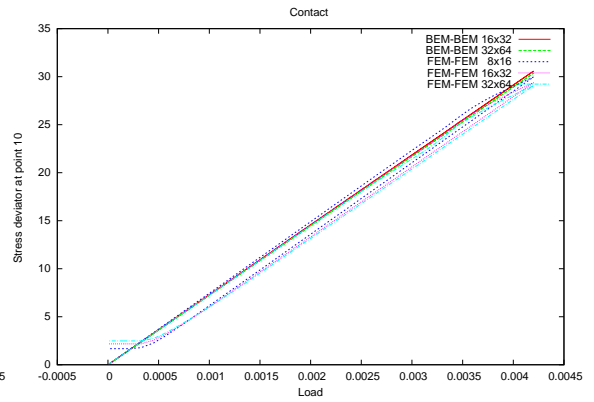


Figure 1.29:  $\|\text{dev}[\sigma]\|$  at  $X_{10} = (0, -1)$

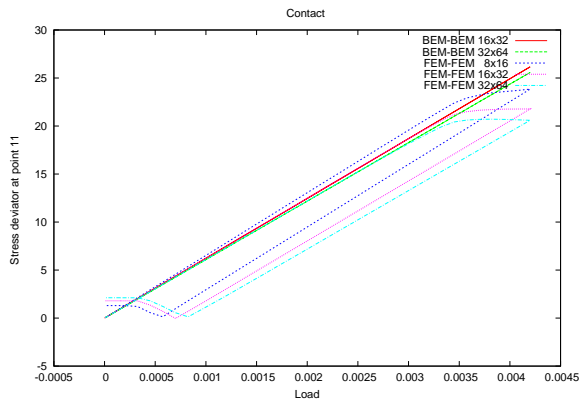


Figure 1.30:  $\|\text{dev}[\sigma]\|$  at  $X_{11} = (0, -2)$

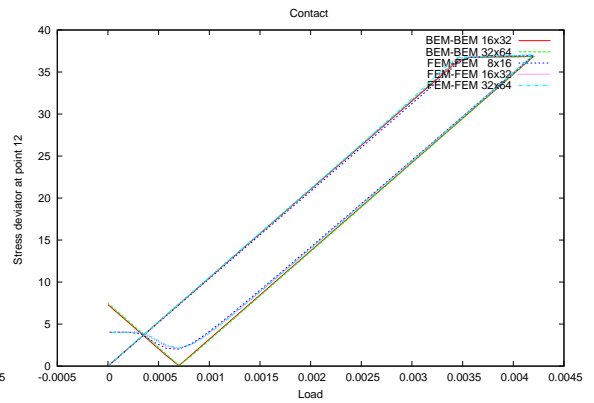


Figure 1.31:  $\|\text{dev}[\sigma]\|$  at  $X_{12} = (0, -3)$

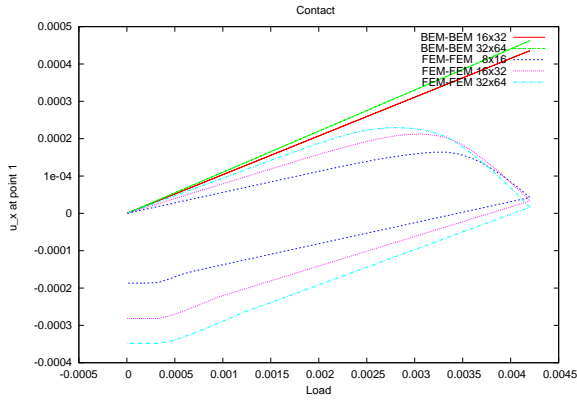


Figure 1.32:  $u_x$  at  $X_1 = (-1, -1)$

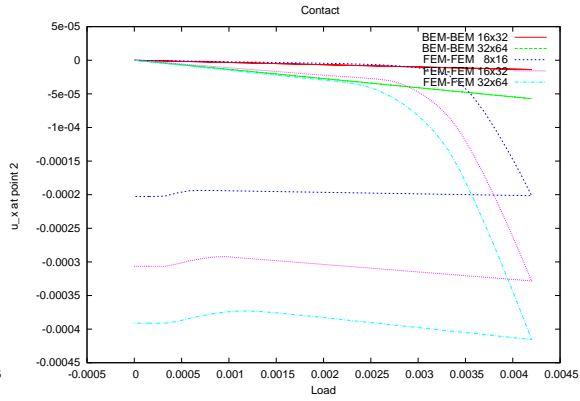


Figure 1.33:  $u_x$  at  $X_2 = (-1, -1.1)$

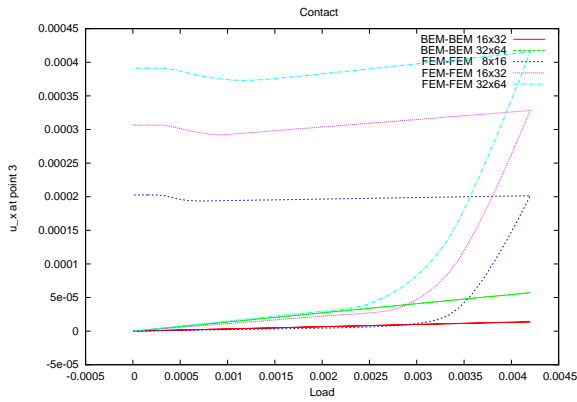


Figure 1.34:  $u_x$  at  $X_3 = (1, -1.1)$

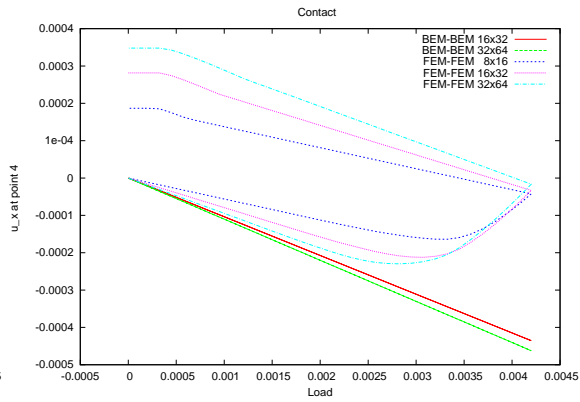


Figure 1.35:  $u_x$  at  $X_4 = (1, -1)$

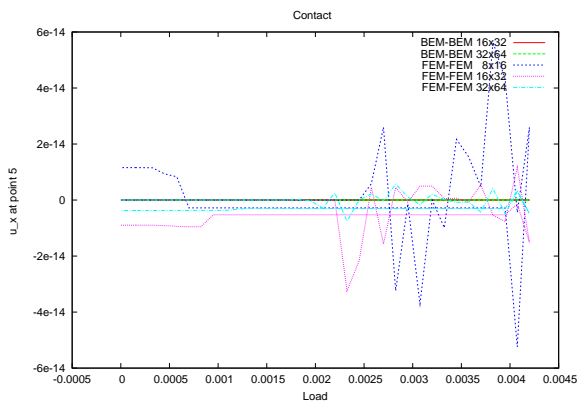


Figure 1.36:  $u_x$  at  $X_5 = (0, -1.75)$

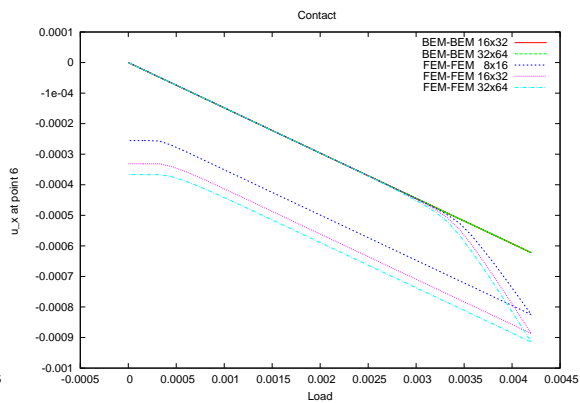


Figure 1.37:  $u_x$  at  $X_6 = (-1, -1.5)$



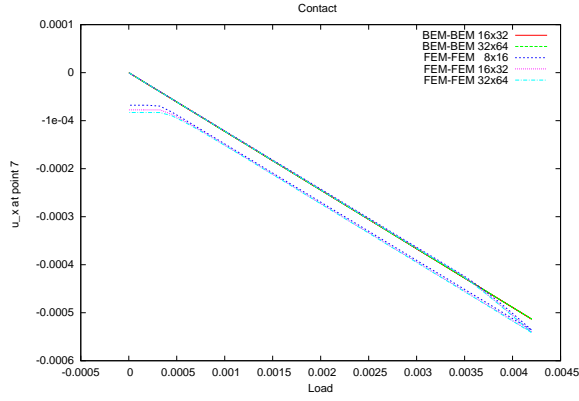


Figure 1.38:  $u_x$  at  $X_7 = (-1, -2.5)$

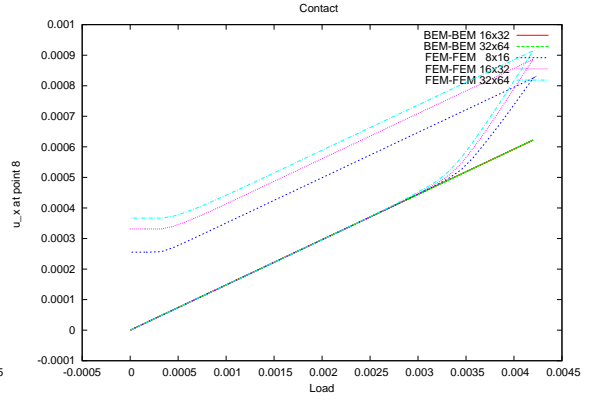


Figure 1.39:  $u_x$  at  $X_8 = (1, -1.5)$

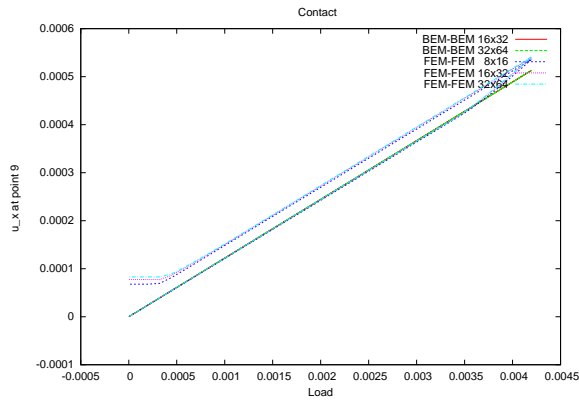


Figure 1.40:  $u_x$  at  $X_9 = (1, -2.5)$

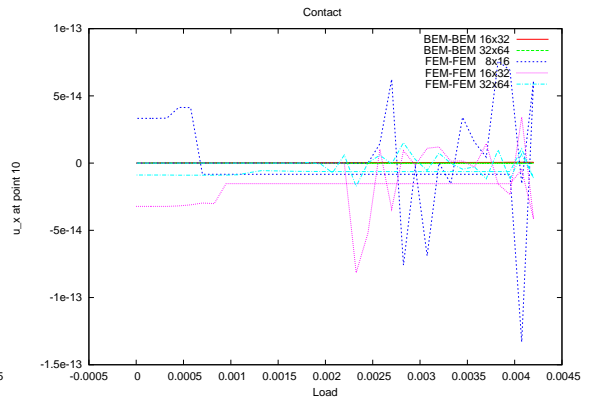


Figure 1.41:  $u_x$  at  $X_{10} = (0, -1)$

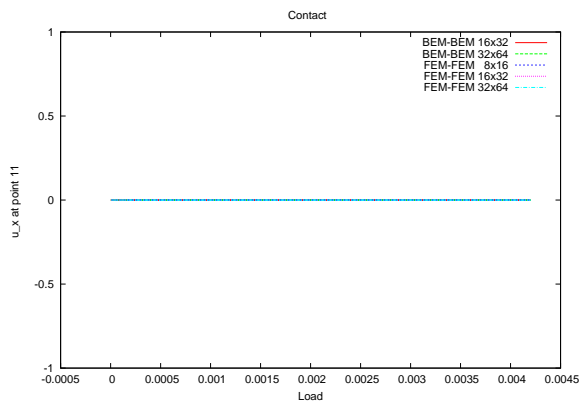


Figure 1.42:  $u_x$  at  $X_{11} = (0, -2)$

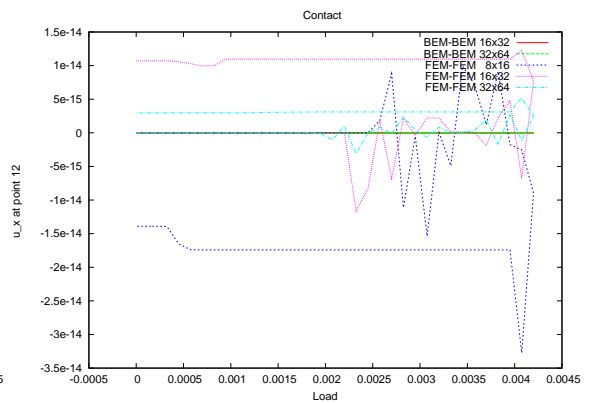


Figure 1.43:  $u_x$  at  $X_{12} = (0, -3)$

## 1.8 FEM/BEM domain decomposition for frictional contact

In this section we analyse a saddle point formulation with Lagrangian multipliers for the two body contact problem with friction and elastoplastic material. We decompose the work piece into plastic and elastic parts and apply boundary elements and finite elements respectively. The contact is modeled by a penalty approach described in Sections 1.2, 1.3. We use finite elements in the linear elastic work tool. We perform an incremental loading procedure and use backward Euler time discretization for contact and forward Euler time discretization for plasticity. At each loading step the Newton algorithm is applied to solve the nonlinear discrete system. In subsection 1.8.4 we present a numerical benchmark.

The geometry for our model problem is shown in the Fig. 1.44. Let  $\Omega^1$  be the domain occupied by the elastic stamp,  $\Omega^2$  be the part of the work piece directly below the contact zone where plastic deformations occur and  $\Omega^3$  be the elastic part of the work piece. Note that the work piece occupies  $\Omega^2 \cup \Omega^3$ . Denote  $\Gamma^i := \partial\Omega^i, i = 1, 2, 3$ . Let  $\Gamma_I := \Omega^2 \cap \Omega^3$  be the interface boundary in the work piece.

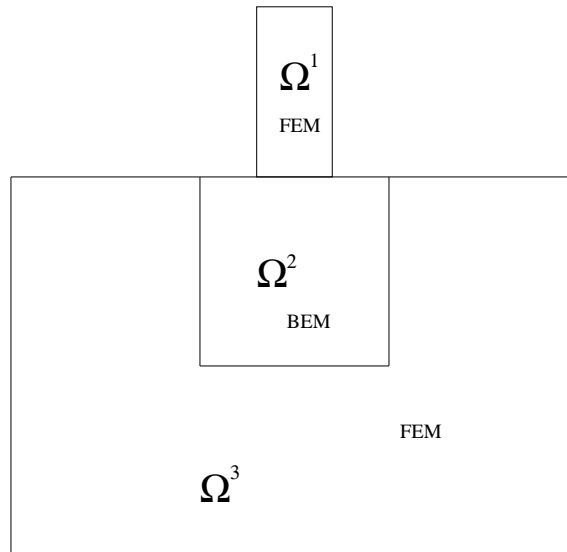


Figure 1.44: The model geometry

Assume for simplicity that the boundary of the plastic domain consists of the interface boundary and the contact boundary, i.e.  $\Gamma^2 := \Gamma_C^2 \cup \Gamma_I^2$ . Furthermore, let the boundary of the elastic part of the work piece consist of interface, Dirichlet (prescribed displacements) and Neumann (prescribed surface tractions) parts, i.e.  $\Gamma^3 := \Gamma_I^3 \cup \Gamma_D^3 \cup \Gamma_N^3$ . Finally, let the stamp boundary be decomposed into Dirichlet, Neumann and contact parts,  $\Gamma^1 := \Gamma_D^1 \cup \Gamma_N^1 \cup \Gamma_C^1$ . Let  $\mathbf{n}, \mathbf{e}$  denote the normal and tangential vector respectively.

The classical formulation of our model problem is

$$\begin{aligned}
 & \operatorname{div} \boldsymbol{\sigma}^i = \hat{\mathbf{f}}^i \\
 & \boldsymbol{\sigma}^j = \mathbb{C}^j : \boldsymbol{\varepsilon}^j && \text{in } \Omega^i, \\
 & \boldsymbol{\sigma}^2 = \mathbb{C}^2 : (\boldsymbol{\varepsilon}^2 - \boldsymbol{\varepsilon}^{2p}) \\
 & \mathbf{u}^j = \hat{\mathbf{u}}^j && \text{on } \Gamma_D^j, \\
 & \mathbf{t}^j = \hat{\mathbf{t}}^j && \text{on } \Gamma_N^j, \\
 & i = 1, 2, 3, \\
 & j = 1, 3, \\
 & k = 1, 2, \\
 & \mathbf{u}^2 = \mathbf{u}^3 && \text{on } \Gamma_I, \\
 & \mathbf{t}^2 = -\mathbf{t}^3 \\
 & \left. \begin{aligned}
 & \mathbf{n}^2 \cdot \boldsymbol{\sigma}^2 \cdot \mathbf{n}^2 = \mathbf{n}^1 \cdot \boldsymbol{\sigma}^1 \cdot \mathbf{n}^1 =: \sigma_N, \\
 & \text{if } u_N^{21} = g, \text{ then } \sigma_N \leq 0, \\
 & \sigma^2 \cdot \mathbf{n}^2 - \sigma_N \mathbf{n}^2 = -(\boldsymbol{\sigma}^1 \cdot \mathbf{n}^1 - \sigma_N \mathbf{n}^1) =: \boldsymbol{\sigma}_T \quad \sigma_T := \boldsymbol{\sigma}_T \cdot \mathbf{e}^2, \\
 & \text{if } |\sigma_T| < \mu_f |\sigma_N|, \text{ then } u_T = 0, \\
 & \text{if } |\sigma_T| = \mu_f |\sigma_N|, \text{ then } \exists \lambda \geq 0 : [u_T] = -\lambda \sigma_T
 \end{aligned} \right\} && \text{on } \Gamma_C^k,
 \end{aligned} \tag{1.207}$$

where  $[u_l] = u_l^1 - u_l^2$ ,  $l = \mathcal{N}, \mathcal{T}$ , the symmetric gradient  $\boldsymbol{\varepsilon}^i(\mathbf{u}^i) = 1/2(\nabla \mathbf{u}^i + (\nabla \mathbf{u}^i)^T)$ ,  $\mathbb{C}$  is the fourth order elastic Hooke's tensor, and the plastic deformation tensor  $\boldsymbol{\varepsilon}^p$  is subjected to constitutive equations for plasticity described above.  $\mathbf{n}^a$  and  $\mathbf{e}^a$  are the outer normal and adjoint unit tangent vectors on the contact boundary of  $\Omega^a$  respectively ( $a = 1, 2, 3$ ).  $\mathbf{t}^a := \boldsymbol{\sigma}^a \cdot \mathbf{n}^a$ .  $\mathbb{C}^2 \equiv \mathbb{C}^3$  since  $\Omega^2$  and  $\Omega^3$  are nothing more than two parts of the same body. We write in the sequel

$$\mathbf{t}_C := \sigma_N \mathbf{n}^2 + \sigma_T \mathbf{e}^2 \tag{1.208}$$

for the boundary traction,  $\mathbf{t}_I := \mathbf{t}^2|_{\Gamma_I} = -\mathbf{t}^3|_{\Gamma_I}$  for interface traction and use the following notation for scalar products in the domain and on the boundary

$$\begin{aligned}
 (\boldsymbol{\sigma}, \boldsymbol{\varepsilon})_\Omega &= \int_\Omega \boldsymbol{\sigma} : \boldsymbol{\varepsilon} \, d\Omega, \\
 (\mathbf{u}, \mathbf{v})_\Omega &= \int_\Omega \mathbf{u} \cdot \mathbf{v} \, d\Omega, \\
 \langle \mathbf{u}, \mathbf{v} \rangle_\Gamma &= \int_\Gamma \mathbf{u} \cdot \mathbf{v} \, d\Gamma.
 \end{aligned}$$

### 1.8.1 Weak formulations

In the following we derive a weak formulation with FE in the plastic domain. Therefore, we give first the weak formulation for the work piece and then as a generalization, we obtain the weak formulation of the total problem. Let us assume for a moment that the stamp does not come into contact with the work piece and the exact contact pressure

$\mathbf{t}_C$  is known in advance. Assume that the exact interface traction  $\mathbf{t}_I$  in the work piece is known as well. This means that  $\mathbf{t}_C$  and  $\mathbf{t}_I$  can be treated as given Neumann data. Testing the equilibrium equations for both parts in the work piece with some suitable test functions  $(\boldsymbol{\eta}^2, \boldsymbol{\eta}^3) \in \mathbf{V}_0^{2,3} := \mathbf{H}^1(\Omega^2) \times \mathbf{H}_0^1(\Omega^3)$  and integration by parts gives

$$\begin{aligned} (\boldsymbol{\sigma}^2, \boldsymbol{\varepsilon}(\boldsymbol{\eta}^2))_{\Omega^2} - \langle \mathbf{t}_I, \boldsymbol{\eta}^2 \rangle_{\Gamma_I} &= (\hat{\mathbf{f}}^2, \boldsymbol{\eta}^2)_{\Omega^2} + \langle \mathbf{t}_C, \boldsymbol{\eta}^2 \rangle_{\Gamma_C}, \\ (\boldsymbol{\sigma}^3, \boldsymbol{\varepsilon}(\boldsymbol{\eta}^3))_{\Omega^3} + \langle \mathbf{t}_I, \boldsymbol{\eta}^3 \rangle_{\Gamma_I} &= (\hat{\mathbf{f}}^3, \boldsymbol{\eta}^3)_{\Omega^3} + \left\langle \hat{\mathbf{t}}^3, \boldsymbol{\eta}^3 \right\rangle_{\Gamma_N^3}. \end{aligned}$$

That is equivalent to the corresponding minimization problem of finding  $(\mathbf{u}^2, \mathbf{u}^3) \in \mathbf{V}_D^{2,3} := \mathbf{H}^1(\Omega^2) \times \mathbf{H}_D^1(\Omega^3)$ , such that

$$\begin{aligned} \Pi^2(\mathbf{u}^2) &:= (\boldsymbol{\sigma}^2, \boldsymbol{\varepsilon}(\mathbf{u}^2))_{\Omega^2} - \langle \mathbf{t}_I, \mathbf{u}^2 \rangle_{\Gamma_I} - (\hat{\mathbf{f}}^2, \mathbf{u}^2)_{\Omega^2} - \langle \mathbf{t}_C, \boldsymbol{\eta}^2 \rangle_{\Gamma_C} \rightarrow \min, \\ \Pi^3(\mathbf{u}^3) &:= (\boldsymbol{\sigma}^3, \boldsymbol{\varepsilon}(\mathbf{u}^3))_{\Omega^3} + \langle \mathbf{t}_I, \mathbf{u}^3 \rangle_{\Gamma_I} - (\hat{\mathbf{f}}^3, \mathbf{u}^3)_{\Omega^3} - \left\langle \hat{\mathbf{t}}^3, \mathbf{u}^3 \right\rangle_{\Gamma_N^3} \rightarrow \min, \end{aligned}$$

where  $\mathbf{H}^1(\Omega^2) := [H^1(\Omega^2)]^2$ ,  $\mathbf{H}_D^1(\Omega^3) := \{\mathbf{v} \in [H_D^1(\Omega^3)]^2 \mid \mathbf{v}|_{\Gamma_D} = \hat{\mathbf{u}}\}$ . Therefore the problem for the work piece for some fixed interface traction is: Find  $(\mathbf{u}^2, \mathbf{u}^3) \in \mathbf{V}_D^{2,3}$  such that

$$\begin{aligned} \Pi(\mathbf{u}^2, \mathbf{u}^3) &:= \sum_{l=2,3} \left\{ (\boldsymbol{\sigma}^l, \boldsymbol{\varepsilon}(\mathbf{u}^l))_{\Omega^l} - (\hat{\mathbf{f}}^l, \mathbf{u}^l)_{\Omega^l} \right\} \\ &\quad - \langle \mathbf{t}_I, \mathbf{u}^2 - \mathbf{u}^3 \rangle_{\Gamma_I} - \langle \mathbf{t}_C, \boldsymbol{\eta}^2 \rangle_{\Gamma_C} - \left\langle \hat{\mathbf{t}}^3, \mathbf{u}^3 \right\rangle_{\Gamma_N^3} \rightarrow \min. \end{aligned}$$

or : Find  $(\mathbf{u}^2, \mathbf{u}^3) \in \mathbf{V}_{DI}^{2,3} := \{(\mathbf{u}^2, \mathbf{u}^3) \in \mathbf{V}_D^{2,3} : \mathbf{u}^2|_{\Gamma_I} = \mathbf{u}^3|_{\Gamma_I}\}$

$$\begin{aligned} \Pi(\mathbf{u}^2, \mathbf{u}^3) &:= \sum_{l=2,3} \left\{ (\boldsymbol{\sigma}^l, \boldsymbol{\varepsilon}(\mathbf{u}^l))_{\Omega^l} - (\hat{\mathbf{f}}^l, \mathbf{u}^l)_{\Omega^l} \right\} \\ &\quad - \langle \mathbf{t}_C, \boldsymbol{\eta}^2 \rangle_{\Gamma_C} - \left\langle \hat{\mathbf{t}}^3, \mathbf{u}^3 \right\rangle_{\Gamma_N^3} \rightarrow \min. \end{aligned} \tag{1.209}$$

Furthermore, using a Lagrangian approach, problem (1.209) can be reformulated over the unconstrained displacement space as: Find  $(\mathbf{u}^2, \mathbf{u}^3) \in \mathbf{V}_D^{2,3}$ ,  $\boldsymbol{\lambda} \in \mathcal{M} := \{\boldsymbol{\mu} \mid \boldsymbol{\mu} \in \mathbf{H}^{-1/2}(\Gamma_I)\}$ :

$$\delta L(\mathbf{u}^2, \mathbf{u}^3, \boldsymbol{\lambda}) = 0, \tag{1.210}$$

where

$$L(\mathbf{u}^2, \mathbf{u}^3, \boldsymbol{\lambda}) = \Pi(\mathbf{u}^2, \mathbf{u}^3) - \langle \boldsymbol{\lambda}, \mathbf{u}^2 - \mathbf{u}^3 \rangle_{\Gamma_I}.$$

The variation of the Lagrangian has the form

$$\delta L(\mathbf{u}^2, \mathbf{u}^3, \boldsymbol{\lambda}) = \frac{\partial L}{\partial \mathbf{u}^2}(\mathbf{u}^2, \mathbf{u}^3, \boldsymbol{\lambda}) \delta \mathbf{u}^2 + \frac{\partial L}{\partial \mathbf{u}^3}(\mathbf{u}^2, \mathbf{u}^3, \boldsymbol{\lambda}) \delta \mathbf{u}^3 + \frac{\partial L}{\partial \boldsymbol{\lambda}}(\mathbf{u}^2, \mathbf{u}^3, \boldsymbol{\lambda}) \delta \boldsymbol{\lambda}.$$

As  $\delta \mathbf{u}^2, \delta \mathbf{u}^3$  are independent of  $\delta \boldsymbol{\lambda}$  problem (1.210) is equivalent to

$$\frac{\partial L}{\partial \mathbf{u}^2}(\mathbf{u}^2, \mathbf{u}^3, \boldsymbol{\lambda}) \delta \mathbf{u}^2 + \frac{\partial L}{\partial \mathbf{u}^3}(\mathbf{u}^2, \mathbf{u}^3, \boldsymbol{\lambda}) \delta \mathbf{u}^3 = 0, \quad \frac{\partial L}{\partial \boldsymbol{\lambda}}(\mathbf{u}^2, \mathbf{u}^3, \boldsymbol{\lambda}) \delta \boldsymbol{\lambda} = 0,$$

or to the variational saddle point formulation: Find  $(\mathbf{u}^2, \mathbf{u}^3) \in \mathbf{V}^{2,3}, \boldsymbol{\lambda} \in \mathcal{M}$ :

$$\begin{aligned} \sum_{l=2,3} (\boldsymbol{\sigma}^l, \boldsymbol{\varepsilon}(\boldsymbol{\eta}^l))_{\Omega^l} - \langle \boldsymbol{\lambda}, \boldsymbol{\eta}^2 - \boldsymbol{\eta}^3 \rangle_{\Gamma_I} &= \tilde{L}(\boldsymbol{\eta}^2, \boldsymbol{\eta}^3) \quad \forall (\boldsymbol{\eta}^2, \boldsymbol{\eta}^3) \in \mathbf{V}_0^{2,3}, \\ \langle \boldsymbol{\mu}, \mathbf{u}^2 - \mathbf{u}^3 \rangle_{\Gamma_I} &= 0 \quad \forall \boldsymbol{\mu} \in \mathcal{M}, \end{aligned} \quad (1.211)$$

where the right hand side is

$$\tilde{L}(\boldsymbol{\eta}^2, \boldsymbol{\eta}^3) := \sum_{l=2,3} (\hat{\mathbf{f}}^l, \boldsymbol{\eta}^l)_{\Omega^l} + \langle \mathbf{t}_C, \boldsymbol{\eta}^2 \rangle_{\Gamma_C} + \langle \hat{\mathbf{t}}^3, \boldsymbol{\eta}^3 \rangle_{\Gamma_N^3},$$

and  $\boldsymbol{\eta}^2, \boldsymbol{\eta}^3, \boldsymbol{\mu}$  stand for the variations

$$\boldsymbol{\eta}^2 := \delta \mathbf{u}^2, \quad \boldsymbol{\eta}^3 := \delta \mathbf{u}^3, \quad \boldsymbol{\mu} := \delta \boldsymbol{\lambda}.$$

To secure existence and uniqueness of the solution of (1.211) the following *Babuška-Brezzi* condition should be specified on the discrete spaces [8]:  $\exists C_{BB} > 0$ :

$$\inf_{\boldsymbol{\mu} \in \mathcal{M}} \sup_{(\boldsymbol{\eta}^2, \boldsymbol{\eta}^3) \in \mathbf{V}_0^{2,3}} \frac{\langle \boldsymbol{\mu}, \boldsymbol{\eta}^2 - \boldsymbol{\eta}^3 \rangle_{\Gamma_I}}{\|\boldsymbol{\mu}\|_{\mathcal{M}} (\|\boldsymbol{\eta}^2\|_{\mathbf{H}^1(\Omega^2)}^2 + \|\boldsymbol{\eta}^3\|_{\mathbf{H}_0^1(\Omega^3)}^2)^{1/2}} \geq C_{BB}.$$

Following [3] one can show that constrained problem (1.209) and the saddle point formulation (1.211) are equivalent .

On the other hand for the stamp the following weak formulation holds:

Find  $\mathbf{u} \in \mathbf{V}_D^1 := \mathbf{H}_D^1(\Omega^1)$ :

$$(\boldsymbol{\sigma}^1, \boldsymbol{\varepsilon}(\boldsymbol{\eta}^1))_{\Omega^1} + \langle \mathbf{t}_C, \boldsymbol{\eta}^1 \rangle_{\Gamma_C} = (\hat{\mathbf{f}}^1, \boldsymbol{\eta}^1)_{\Omega^1} + \langle \hat{\mathbf{t}}^1, \boldsymbol{\eta}^1 \rangle_{\Gamma_N^1} \quad \forall \boldsymbol{\eta}^1 \in \mathbf{V}_0^1,$$

with  $\mathbf{V}_0^1 := \mathbf{H}_0^1(\Omega^1)$ . Note that the contact term appears with the positive sign as  $\mathbf{t}_C = \mathbf{t}^2|_{\Gamma_C} = -\mathbf{t}^1|_{\Gamma_C}$ . Together with (1.211) this gives the variational formulation in all three domains

$$\begin{aligned} \sum_{i=1}^3 (\boldsymbol{\sigma}^i, \boldsymbol{\varepsilon}(\boldsymbol{\eta}^i))_{\Omega^i} - \langle \boldsymbol{\lambda}, \boldsymbol{\eta}^2 - \boldsymbol{\eta}^3 \rangle_{\Gamma_I} - \langle \mathbf{t}_C, \boldsymbol{\eta}^2 - \boldsymbol{\eta}^1 \rangle_{\Gamma_C} &= L_F(\boldsymbol{\eta}^1, \boldsymbol{\eta}^2, \boldsymbol{\eta}^3), \\ \langle \boldsymbol{\mu}, \mathbf{u}^2 - \mathbf{u}^3 \rangle_{\Gamma_I} &= 0 \quad \forall (\boldsymbol{\eta}^1, \boldsymbol{\eta}^2, \boldsymbol{\eta}^3) \in \mathbf{V}_0^{1,2,3}, \quad \forall \boldsymbol{\mu} \in \mathcal{M}, \end{aligned} \quad (1.212)$$

where

$$L_F(\boldsymbol{\eta}^1, \boldsymbol{\eta}^2, \boldsymbol{\eta}^3) := \sum_{i=1}^3 (\hat{\mathbf{f}}^i, \boldsymbol{\eta}^i)_{\Omega^i} + \sum_{j=1,3} \langle \hat{\mathbf{t}}^j, \boldsymbol{\eta}^j \rangle_{\Gamma_N^j}.$$

In the following we use a penalty method for the contact term  $\mathbf{t}_{\epsilon_C} := \sigma_{\epsilon_N} \mathbf{n}^2 + \sigma_{\epsilon_T} \mathbf{e}^2$  with friction on  $\Gamma_C$ .

### Weak formulation with BE in the plastic domain

Using boundary integral operators (Section 1.2.2) we can proceed to the BE formulation in the plastic domain. As in Section 1.2.2 one gets

$$\begin{aligned} & (\boldsymbol{\sigma}^2, \boldsymbol{\varepsilon}(\boldsymbol{\eta}^2))_{\Omega^2} - (\hat{\mathbf{f}}^2, \boldsymbol{\eta}^2)_{\Omega^2} \\ &= \langle S\mathbf{u}^2, \boldsymbol{\eta}^2 \rangle_{\Gamma^2} + \left\langle N(\operatorname{div}[\mathbb{C}^2 : \boldsymbol{\varepsilon}^{2p}] - \hat{\mathbf{f}}^2), \boldsymbol{\eta}^2 \right\rangle_{\Gamma^2} \\ & \quad - \langle [\mathbb{C}^2 : \boldsymbol{\varepsilon}^{2p}] \cdot \mathbf{n}, \boldsymbol{\eta}^2 \rangle_{\Gamma^2} \\ & \forall \mathbf{u}^2 \in \mathbf{H}_D^1(\Omega^2), \quad \forall \boldsymbol{\eta}^i \in \mathbf{H}_0^1(\Omega^2). \end{aligned}$$

This together with the FE formulation (1.212) gives

$$\begin{aligned} & \sum_{j=1,3} (\boldsymbol{\sigma}^j, \boldsymbol{\varepsilon}(\boldsymbol{\eta}^j))_{\Omega^j} + \langle S\mathbf{u}^2, \boldsymbol{\eta}^2 \rangle_{\Gamma^2} - \langle \lambda, \boldsymbol{\eta}^2 - \boldsymbol{\eta}^3 \rangle_{\Gamma_I} - \langle \mathbf{t}_C, \boldsymbol{\eta}^2 - \boldsymbol{\eta}^1 \rangle_{\Gamma_C} \\ & + \langle N \operatorname{div}[\mathbb{C}^2 : \boldsymbol{\varepsilon}^{2p}], \boldsymbol{\eta}^2 \rangle_{\Gamma^2} - \langle [\mathbb{C}^2 : \boldsymbol{\varepsilon}^{2p}] \cdot \mathbf{n}, \boldsymbol{\eta}^2 \rangle_{\Gamma^2} = L_B(\boldsymbol{\eta}^1, \boldsymbol{\eta}^2, \boldsymbol{\eta}^3), \quad (1.213) \\ & \langle \boldsymbol{\mu}, \mathbf{u}^2 - \mathbf{u}^3 \rangle_{\Gamma_I} = 0 \quad \forall (\boldsymbol{\eta}_1, \boldsymbol{\eta}_2, \boldsymbol{\eta}_3) \in \tilde{\mathbf{V}}_0, \quad \forall \boldsymbol{\mu} \in \mathcal{M}, \end{aligned}$$

where

$$L_B(\boldsymbol{\eta}^1, \boldsymbol{\eta}^2, \boldsymbol{\eta}^3) := \sum_{j=1,3} \left\{ (\mathbf{f}^j, \boldsymbol{\eta}^j)_{\Omega^j} + \langle \hat{\mathbf{t}}^j, \boldsymbol{\eta}^j \rangle_{\Gamma_N^j} \right\} + \langle N \hat{\mathbf{f}}^2, \boldsymbol{\eta}^2 \rangle_{\Gamma^2}.$$

### 1.8.2 Discretization

We use continuous linear ( $\mathcal{P}^1$ ) or bilinear ( $\mathcal{Q}^1$ ) basis functions on a triangular or quadrilateral FE mesh  $\mathbb{T}_h^1, \mathbb{T}_h^3$  in  $\Omega^1, \Omega^3$  respectively. The boundary element discrete displacement space on  $\Gamma^2$  is given by continuous piecewise linear functions on the one dimensional mesh  $\mathcal{T}_h^2$ . Define the discrete spaces

$$\begin{aligned} {}^h\mathbf{V}^2 & := \left\{ \boldsymbol{\eta}_h \in \mathbf{H}^{1/2}(\Gamma^2) \mid \boldsymbol{\eta}_h|_{\boldsymbol{\varepsilon}} \in \mathcal{P}^1(\boldsymbol{\varepsilon}) \quad \forall \boldsymbol{\varepsilon} \in \mathcal{T}_h^2 \right\}, \\ {}^h\mathbf{V}_D^j & := \left\{ \boldsymbol{\eta}_h \in \mathbf{H}_D^1(\Omega^j) \mid \boldsymbol{\eta}_h|_{\boldsymbol{\varepsilon}} \in \mathcal{R}^1(\boldsymbol{\varepsilon}) \quad \forall \boldsymbol{\varepsilon} \in \mathbb{T}_h^j \right\}, \\ {}^h\mathbf{V}_0^j & := \left\{ \boldsymbol{\eta}_h \in \mathbf{H}_0^1(\Omega^j) \mid \boldsymbol{\eta}_h|_{\boldsymbol{\varepsilon}} \in \mathcal{R}^1(\boldsymbol{\varepsilon}) \quad \forall \boldsymbol{\varepsilon} \in \mathbb{T}_h^j \right\}, \end{aligned} \quad j = 1, 3,$$

where  $\mathcal{R}^1(\mathbf{e}) = \mathcal{P}^1(\mathbf{e})$  for a triangular mesh element  $\mathbf{e}$  and  $\mathcal{R}^1(\mathbf{e}) = \mathcal{Q}^1(\mathbf{e})$  for a quadrilateral mesh element  $\mathbf{e}$ . Define the product spaces

$$\begin{aligned} {}^h\tilde{\mathcal{V}}_D &:= {}^h\mathbf{V}_D^1 \times {}^h\mathcal{V}^2 \times {}^h\mathbf{V}_D^3, \\ {}^h\tilde{\mathcal{V}}_0 &:= {}^h\mathbf{V}_0^1 \times {}^h\mathcal{V}^2 \times {}^h\mathbf{V}_0^3. \end{aligned}$$

The discretization of the Lagrange multiplier space is given by the dual basis on one of the meshes induced on the interface  $\Gamma_I$ . Without loss of generality we choose  $\mathcal{T}_h^2$  be the mesh for the Lagrange multiplier. Let  $\{\phi_l^2\}$  be the hat-functions in the space  ${}^h\mathcal{V}^2$  which have their support on the interface boundary  $\Gamma_I$ . Define the dual basis  $\{\psi_m\}$  by

$$\langle \phi_l^2, \psi_m \rangle_{\Gamma_I} = \delta_{lm} \langle \phi_l^2, 1 \rangle_{\Gamma_I}. \quad (1.214)$$

The existence of the dual basis was shown in [49]. Then the discrete Lagrange multiplier space is given by

$${}^h\mathcal{M} := \text{span} \{\psi_i\}.$$

Note that it is possible to use the trace mesh of  $\mathcal{T}_h^3$  on  $\Gamma_I$  as well. The discrete version of (1.213) can be formulated as follows:

Find  $\mathbf{u}_h := (\mathbf{u}_h^1, \mathbf{u}_h^2, \mathbf{u}_h^3) \in {}^h\tilde{\mathcal{V}}_D, \boldsymbol{\lambda}_h \in {}^h\mathcal{M}$ :

$$\begin{aligned} \overline{F}^{int}(\mathbf{u}_h, \boldsymbol{\eta}_h) - \overline{P}\mathbf{u}_h(\boldsymbol{\varepsilon}^p, \boldsymbol{\eta}_h) + B(\boldsymbol{\lambda}_h, \boldsymbol{\eta}_h) &= \overline{F}^{ext}(\boldsymbol{\eta}_h) \quad \forall \boldsymbol{\eta}_h \in {}^h\tilde{\mathcal{V}}_0, \\ B(\boldsymbol{\mu}_h, \mathbf{u}_h) &= 0 \quad \forall \boldsymbol{\mu}_h \in {}^h\mathcal{M}. \end{aligned} \quad (1.215)$$

where

$$\begin{aligned} \overline{F}^{int}(\mathbf{u}_h, \boldsymbol{\eta}_h) &:= \sum_{j=1,3} (\boldsymbol{\sigma}^j, \boldsymbol{\varepsilon}(\boldsymbol{\eta}^j))_{\Omega^j} + \langle S\mathbf{u}^2, \boldsymbol{\eta}^2 \rangle_{\Gamma^2} - \langle \mathbf{t}_C, \boldsymbol{\eta}^2 - \boldsymbol{\eta}^1 \rangle_{\Gamma_C}, \\ \overline{P}\mathbf{u}_h(\boldsymbol{\varepsilon}^p, \boldsymbol{\eta}_h) &:= \langle N(\text{div}[\mathbb{C} : \boldsymbol{\varepsilon}^{ip}]), \boldsymbol{\eta}^2 \rangle_{\Gamma^2} - \langle [\mathbb{C} : \boldsymbol{\varepsilon}^{ip}] \cdot \mathbf{n}, \boldsymbol{\eta}^2 \rangle_{\Gamma^2}, \\ B(\boldsymbol{\lambda}_h, \boldsymbol{\eta}_h) &:= - \langle \boldsymbol{\lambda}, \boldsymbol{\eta}^2 - \boldsymbol{\eta}^3 \rangle_{\Gamma_I}, \\ \overline{F}^{ext}(\boldsymbol{\eta}_h) &:= L_B(\boldsymbol{\eta}_h^1, \boldsymbol{\eta}_h^2, \boldsymbol{\eta}_h^3), \\ (\boldsymbol{\varepsilon}^p)^i &:= \boldsymbol{\varepsilon}^p(\mathbf{u}_h^i), \quad \mathbf{t}_C^i := \mathbf{t}_C(\mathbf{u}_h^i). \end{aligned}$$

### 1.8.3 Linearization

The saddle point system (1.215) is in general nonlinear. The contact term in the functional  $\overline{F}^{int}(\mathbf{u}_h, \boldsymbol{\eta}_h)$  is nonlinear due to the constitutive contact conditions. The functional  $\overline{P}\mathbf{u}_h(\boldsymbol{\varepsilon}^p, \boldsymbol{\eta}_h)$  is nonlinear when plastic deformations occur. The Lagrange multiplier term  $B(\boldsymbol{\lambda}_h, \boldsymbol{\eta}_h)$  is linear. As in sections 1.2.1, 1.2.2, and 1.2.3 we introduce an incremental

loading process as a successive application of loading increments  $(\Delta \hat{\mathbf{f}}^i)_n, (\Delta \hat{\mathbf{t}}^i)_n, (\Delta \hat{\mathbf{u}}^i)_n$ :

$$\begin{aligned}(\hat{\mathbf{f}}^i)_{n+1} &= \hat{\mathbf{f}}^i(t_{n+1}), \\(\hat{\mathbf{t}}^i)_{n+1} &= \hat{\mathbf{t}}^i(t_{n+1}), \\(\hat{\mathbf{u}}^i)_{n+1} &= \hat{\mathbf{u}}^i(t_{n+1}),\end{aligned}$$

which defines the discrete external load

$$\overline{F}_n^{ext}(\boldsymbol{\eta}_h) := \sum_{j=1,3} \left\{ ((\mathbf{f}^j)_n, \boldsymbol{\eta}^j)_{\Omega^i} + \langle \hat{\mathbf{t}}_n^j, \boldsymbol{\eta}^j \rangle_{\Gamma_N^j} \right\} + \langle N \hat{\mathbf{f}}_n^2, \boldsymbol{\eta}^2 \rangle_{\Gamma^2}.$$

This gives a pseudo-time stepping process with the increment-dependent functional spaces

$${}^h\mathbf{V}_{D,n}^j := \{ \boldsymbol{\eta}_h \in \mathbf{H}^1(\Omega^j) \mid \boldsymbol{\eta}_h|_{\epsilon} \in \mathcal{R}^1(\epsilon) \quad \forall \epsilon \in \mathbb{T}_h^j, \quad \mathbf{u}_h^j|_{\Gamma_D} = (\mathbf{u}_D^j)_n \},$$

$$j = 1, 3,$$

$${}^h\tilde{\mathbf{V}}_{D,n} := {}^h\mathbf{V}_{D,n}^1 \times {}^h\boldsymbol{\nu}^2 \times {}^h\mathbf{V}_{D,n}^3.$$

Let  $(\mathbf{u}_h)_0$  be the initial displacement state of the body,  $(\boldsymbol{\varepsilon}^p)_0^{(0)}, \alpha_0^{(0)}, \boldsymbol{\beta}_0^{(0)}$  initial internal variables,  $(\mathbf{g}_T^p)_0^{(0)}$  initial tangential macro-displacement and let  $(\hat{\mathbf{f}}^i)_0, (\hat{\mathbf{t}}^i)_0, (\hat{\mathbf{u}}^i)_0$  be the initial load. We use *the backward Euler scheme for contact and the forward Euler scheme for plasticity*. Thus the formulation will be:

Find  $(\Delta \mathbf{u}_h)_n \in {}^h\boldsymbol{\nu}_{D,n}$ , and therefore the new displacement state  $(\mathbf{u}_h)_n = (\mathbf{u}_h)_{n-1} + (\Delta \mathbf{u}_h)_n$ , plastic strain  $(\boldsymbol{\varepsilon}^p)_n^i = \boldsymbol{\varepsilon}^p((\mathbf{u}_h^i)_n)$ , contact traction  $(\mathbf{t}_C^i)_n = \mathbf{t}_C((\mathbf{u}_h^i)_n)$  such that

$$\begin{aligned}\overline{F}^{int}((\mathbf{u}_h)_n, \boldsymbol{\eta}_h) + B(\boldsymbol{\lambda}_h, \boldsymbol{\eta}_h) &= \overline{F}^{ext}(\boldsymbol{\eta}_h) + \overline{P}_{\mathbf{u}_h}((\boldsymbol{\varepsilon}^p)_n, \boldsymbol{\eta}_h) \quad \forall \boldsymbol{\eta}_h \in {}^h\tilde{\boldsymbol{\nu}}_0, \\ B(\boldsymbol{\mu}_h, (\mathbf{u}_h)_n) &= 0 \quad \forall \boldsymbol{\mu}_h \in {}^h\mathbf{M}.\end{aligned}\tag{1.216}$$

where the contact traction is given by (1.44) and the plastic conditions are enforced by the return mapping algorithm described in boxes 1.3.1, 1.3.2.

To solve (1.216) we use Newton's method. Let  $\mathbf{U}$  be the coefficients of the expansion of  $\mathbf{u}_h$  in basis of the discrete space  ${}^h\boldsymbol{\nu}_D$ , let  $\boldsymbol{\Lambda}$  be the coefficients of the expansion of  $\boldsymbol{\lambda}_h$  in basis in the discrete space  ${}^h\mathbf{M}$ . Define

$$\begin{aligned}\overline{F}_*^{int}(\mathbf{U}, \boldsymbol{\eta}_h) &:= \overline{F}^{int}(\mathbf{u}_h, \boldsymbol{\eta}_h), \\ B_*(\boldsymbol{\Lambda}, \boldsymbol{\eta}_h) &:= B(\boldsymbol{\lambda}_h, \boldsymbol{\eta}_h)\end{aligned}$$



Therefore the first equation in (1.216) becomes

$$\overline{F}_*^{int}(\mathbf{U}_n, \boldsymbol{\eta}_h) + B_*(\boldsymbol{\Lambda}_n, \boldsymbol{\eta}_h) = \overline{F}^{ext}(\boldsymbol{\eta}_h) + \overline{P}\mathbf{u}_h((\boldsymbol{\varepsilon}^p)_n, \boldsymbol{\eta}_h) \quad \forall \boldsymbol{\eta}_h \in {}^h\tilde{\mathcal{V}}_0.$$

We perform the linearization of  $\overline{F}_*^{int}(\mathbf{U}_n, \boldsymbol{\eta}_h)$ . Choose the starting value

$$\mathbf{U}_n^{(0)} := \mathbf{U}_{n-1},$$

and introduce the Newton increment  $\Delta\mathbf{U}_n^{(k+1)}$  to proceed to the next iterate

$$\mathbf{U}_n^{(k+1)} = \mathbf{U}_n^{(k)} + \Delta\mathbf{U}_n^{(k+1)}, \quad k = 0, 1, 2, \dots$$

The Taylor's expansion provides

$$\begin{aligned} \overline{F}_*^{int}(\mathbf{U}_n^{(k+1)}, \boldsymbol{\eta}_h) &= \overline{F}_*^{int}(\mathbf{U}_n^{(k)}, \boldsymbol{\eta}_h) + \frac{\partial \overline{F}_*^{int}(\mathbf{U}_n^{(k)}, \boldsymbol{\eta}_h)}{\partial \mathbf{U}_n^{(k)}} \Delta\mathbf{U}_n^{(k+1)}, \\ B_*(\boldsymbol{\Lambda}_n^{(k+1)}, \boldsymbol{\eta}_h) &= B_*(\boldsymbol{\Lambda}_n^{(k)}, \boldsymbol{\eta}_h) + B_*(\Delta\boldsymbol{\Lambda}_n^{(k+1)}, \boldsymbol{\eta}_h). \end{aligned}$$

Now we are in the position to state the algebraic problem. Define for brevity the matrices  $\mathfrak{A}$ ,  $\mathfrak{B}$  and the right hand side vector  $\mathfrak{b}$  by

$$\begin{aligned} \mathfrak{A} &:= \frac{\partial \overline{F}_*^{int}(\mathbf{U}_n^{(k)}, \boldsymbol{\eta}_h)}{\partial \mathbf{U}_n^{(k)}}, & \mathfrak{B} &:= (B_*(\mathbf{1}, \boldsymbol{\eta}_h))^T, \\ \mathfrak{b} &:= \overline{F}_n^{ext}(\boldsymbol{\eta}_h) + \overline{P}\mathbf{u}_h((\boldsymbol{\varepsilon}^p)_n^{(k)}, \boldsymbol{\eta}_h) - \overline{F}_*^{int}(\mathbf{U}_n^{(k)}, \boldsymbol{\eta}_h) - B_*(\boldsymbol{\Lambda}_n^{(k)}, \boldsymbol{\eta}_h), \end{aligned}$$

Note, that the plastic strain from the  $(k)$ -th Newton's iteration  $(\boldsymbol{\varepsilon}^p)_n^{(k)}$  is used in the right hand side and the plastic strain has no influence on the matrix. This corresponds the forward Euler scheme for plasticity. Then the algebraic problem is: Find  $\mathfrak{x} = \Delta\mathbf{U}_n^{(k+1)}$ ,  $\mathfrak{z} = \Delta\boldsymbol{\Lambda}_n^{(k+1)}$ :

$$\begin{pmatrix} \mathfrak{A} & \mathfrak{B} \\ \mathfrak{B} & 0 \end{pmatrix} \begin{pmatrix} \mathfrak{x} \\ \mathfrak{z} \end{pmatrix} = \begin{pmatrix} \mathfrak{b} \\ 0 \end{pmatrix}. \quad (1.217)$$

The whole algorithm can be formulated now as follows.

### Solution procedure

Set initial displacement  $\mathbf{U}_0^{(0)}$ , initial internal variables  $(\boldsymbol{\varepsilon}^p)_0^{(0)}$ ,  $\alpha_0^{(0)}$ ,  $\beta_0^{(0)}$ , initial tangential macro-displacement  $(\mathbf{g}_T^p)_0^{(0)}$  and initial loads  $(\hat{\mathbf{f}}^i)_0$ ,  $(\hat{\mathbf{t}}^i)_0$ ,  $(\hat{\mathbf{u}}^i)_0$

1. for  $n = 0, 1, 2, \dots$

a) for  $k = 0, 1, 2, \dots$

i. compute the load vector

$$\mathfrak{b} := \overline{F}_n^{ext}(\boldsymbol{\eta}_h) + \overline{P}\mathbf{u}_h((\boldsymbol{\varepsilon}^p)_n^{(k)}, \boldsymbol{\eta}_h) - \overline{F}_*^{int}(\mathbf{U}_n^{(k)}, \boldsymbol{\eta}_h) - B_*(\boldsymbol{\Lambda}_n^{(k)}, \boldsymbol{\eta}_h)$$

1 Elastoplastic contact problems. Small deformations

- ii. if  $\|\mathbf{b}\|_{l_2} := \sqrt{\mathbf{b} \cdot \mathbf{b}} \leq TOL$  goto 2.
- iii. compute the matrix  $\mathfrak{A} := \frac{\partial \bar{F}_*^{int}(\mathbf{U}_n^{(k)}, \boldsymbol{\eta}_h)}{\partial \mathbf{U}_n^{(k)}}$ ,  $\mathfrak{B} := (B_*(\mathbf{1}, \boldsymbol{\eta}_h))^T$
- iv. find the next displacement increment  $\mathfrak{r} = \Delta \mathbf{U}_n^{(k+1)}$  and Lagrange multiplier increment  $\mathfrak{z} = \Delta \boldsymbol{\Lambda}_n^{(k+1)}$  by solving

$$\begin{pmatrix} \mathfrak{A} & \mathfrak{B} \\ \mathfrak{B} & 0 \end{pmatrix} \begin{pmatrix} \mathfrak{r} \\ \mathfrak{z} \end{pmatrix} = \begin{pmatrix} \mathbf{b} \\ 0 \end{pmatrix}.$$

- v. update the displacement field and Lagrange multiplier

$$\mathbf{U}_n^{(k+1)} = \mathbf{U}_n^{(k)} + \Delta \mathbf{U}_n^{(k+1)},$$

$$\boldsymbol{\Lambda}_n^{(k+1)} = \boldsymbol{\Lambda}_n^{(k)} + \Delta \boldsymbol{\Lambda}_n^{(k+1)},$$

and the internal variables  $(\boldsymbol{\varepsilon}^p)_n^{(k+1)}$ ,  $\alpha_n^{(k+1)}$ ,  $\boldsymbol{\beta}_n^{(k+1)}$ ,  $(\mathbf{g}_T)_n^{(k+1)}$ . They should satisfy the constitutive contact and plasticity conditions. We use the return mapping procedure for both contact and plastification as described in Section 1.2.

- b) set  $k = k + 1$ , goto (a)

- 2. initialize the next pseudo-time step

$$\mathbf{U}_{n+1}^{(0)} = \mathbf{U}_n^{(k)}$$

- 3. apply the next load increment

$$(\hat{\mathbf{f}}^i)_{n+1} = \hat{\mathbf{f}}^i(t_{n+1}),$$

$$(\hat{\mathbf{t}}^i)_{n+1} = \hat{\mathbf{t}}^i(t_{n+1}),$$

$$(\hat{\mathbf{u}}^i)_{n+1} = \hat{\mathbf{u}}^i(t_{n+1}),$$

if the total load is achieved exit, if not, set  $n = n + 1$  goto 1.

Next, let us consider the detailed structure of the matrix in (1.217). The total displacement increment vector  $\mathfrak{r}$  has the following form

$$\mathfrak{r} = \begin{pmatrix} \mathfrak{r}_N^1 \\ \mathfrak{r}_C^1 \\ \mathfrak{r}_C^2 \\ \mathfrak{r}_I^2 \\ \mathfrak{r}_I^3 \\ \mathfrak{r}_N^3 \end{pmatrix},$$

where the upper indexes represent coefficients belonging to  $\Omega^1, \Gamma^2, \Omega^3$  respectively, and lower indexes represent coefficients belonging to contact and interface boundary parts. Absence of the lower index means that the coefficient corresponds to the basis function lying inside the domain or on the Neumann part of the boundary. Then (1.217) can be rewritten as

$$\begin{pmatrix} A^1 & (B^1)^T & 0 & 0 & 0 & 0 & 0 \\ B^1 & C^1 + C^{11} & C^{12} & 0 & 0 & 0 & 0 \\ 0 & C^{21} & S_{CC}^2 + C^{22} & S_{CI}^2 & 0 & 0 & 0 \\ 0 & 0 & S_{IC}^2 & S_{II}^2 & 0 & 0 & -D \\ 0 & 0 & 0 & 0 & C^3 & (B^3)^T & Q^T \\ 0 & 0 & 0 & 0 & B^3 & A^3 & 0 \\ 0 & 0 & 0 & -D & Q & 0 & 0 \end{pmatrix} \begin{pmatrix} \mathbf{r}^1 \\ \mathbf{r}_C^1 \\ \mathbf{r}_C^2 \\ \mathbf{r}_I^2 \\ \mathbf{r}_I^3 \\ \mathbf{r}^3 \\ \mathfrak{z} \end{pmatrix} = \begin{pmatrix} \mathbf{b}_N^1 \\ \mathbf{b}_C^1 \\ \mathbf{b}_C^2 \\ \mathbf{b}_I^2 \\ \mathbf{b}_I^3 \\ \mathbf{b}_N^3 \\ 0 \end{pmatrix}$$

We see that the matrix  $\mathfrak{B}$  from (1.217) has the form

$$\mathfrak{B} = (0, 0, 0, -D, Q, 0).$$

The matrix  $\mathfrak{B}$  is generated by the interface mixed terms

$$B_*(\mathbf{1}, \boldsymbol{\eta}_h) := -\langle \mathbf{1}, \boldsymbol{\eta}^2 - \boldsymbol{\eta}^3 \rangle_{\Gamma_I}.$$

In the basis representation there holds

$$\mathfrak{B} \rightsquigarrow -\langle \psi_m, \phi_l^2 - \phi_k^3 \rangle_{\Gamma_I} = -\delta_{lm} \langle \mathbf{1}, \phi_l^2 \rangle_{\Gamma_I} + \langle \psi_m, \phi_k^3 \rangle_{\Gamma_I} \quad (1.218)$$

and therefore

$$D \rightsquigarrow \delta_{lm} \langle \mathbf{1}, \phi_l^2 \rangle_{\Gamma_I}, \quad Q \rightsquigarrow \langle \psi_m, \phi_k^3 \rangle_{\Gamma_I}. \quad (1.219)$$

Note that in the case of matching meshes on the interface  $\Gamma_I$  the relation (1.214) holds for the basis functions in  $\Omega^3$  as well, and therefore  $Q \equiv D$ .

### 1.8.4 Numerical simulations

As in section 1.7 we consider elastoplastic two-body contact problem, whereas in this case the domain occupied by master body is decomposed into two subdomains. The geometry of the problem is shown in Fig. 1.44. Let  $\Omega^1$  represent the elastic stamp,  $\Omega^2$  represent the plastic domain in the work piece, modelled with BEM, and  $\Omega^3$  represent the elastic domain in the work piece, modelled with FEM. The linear system within each Newton step is solved using the Generalized Minimal Residual method with the diagonal preconditioner. In average the Newton method converges after 20 iterations.

$$\Omega^1 = [-0, 5; 0, 5] \times [1; 1, 5],$$

$$\begin{aligned}\Omega^2 &= [-1; 1] \times [-1; 1], & \Gamma^2 &:= \partial\Omega^2, \\ \Omega^3 &= [-3; 3] \times [-3; 1] \setminus \Omega^2.\end{aligned}$$

The boundary parts are given by

$$\begin{aligned}\Omega^1 : & & \Gamma_D^1 &= [-0, 5; 0, 5] \times \{1, 5\}, \\ & & \Gamma_N^1 &= \emptyset, \\ & & \Gamma_C^1 &= \partial\Omega^1 \setminus \Gamma_D^1, \\ \Gamma^2, \Omega^3 : & & \Gamma_C^2 &= [-1; 1] \times 1, \\ & & \Gamma_I &= \Gamma^2 \cap \partial\Omega^3, \\ & & \Gamma_D^3 &= [-3; 3] \times \{-3\}, \\ & & \Gamma_N^3 &= \partial\Omega^3 \setminus (\Gamma_I \cup \Gamma_D^3).\end{aligned}$$

The bodies are coming into contact due to the total Dirichlet displacement  $\hat{\mathbf{u}}^1 = -1.4 \cdot 10^{-3}$  on  $\Gamma_D^1$  applied incrementally as explained in Section 1.8.3. The homogeneous displacement  $\hat{\mathbf{u}}^3 = 0$  is given on  $\Gamma_D^3$ .

In Fig. 1.45 - 1.52 we present the results of our numerical simulation. The deformed mesh is plotted in Fig. 1.45. We interpolate a FEM mesh inside  $\Omega^2$ , modelled with BEM, to show the interior deformation. The displacement in the interior points is obtained with Somigliana's representation formula. The displacements in Fig. 1.45 are multiplied with the factor 100 to make them visible. The norm  $\|\boldsymbol{\sigma}\| := \sqrt{\sum_{i,j=1}^3 \sigma_{ij}\sigma_{ij}}$  is used in the computations. The norm of the stress deviator and the norm of the plastic strain are given in Fig. 1.49 and Fig. 1.46 respectively. They show realistic plastic deformations in  $\Omega^2$ . The displacement values in  $x$ - and  $y$ -direction are presented in Fig. 1.47 and Fig. 1.48 respectively. The  $\sigma_{xx}$ ,  $\sigma_{xy}$  and  $\sigma_{yy}$  components of the stress tensor are given in Fig. 1.50 - 1.52.

## 1.9 FE/BE coupling for thermoelastic contact problems

Extending the ideas of [51], [44] we present a coupled thermoelastic formulation for contact problems with friction. The elastic material response is modelled with the boundary element (BE) method, whereas the finite element (FE) description is used for modeling the temperature field. We use constitutive equations for the normal and the tangential contact stress in terms of the penalty method, as well as constitutive equations for the heat flux on the contact boundary. As in [51] we use the operator split techniques and present an iterative solution procedure for the coupled problem.

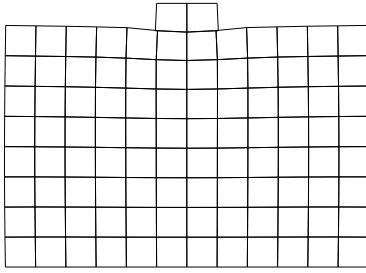


Figure 1.45: deformed mesh

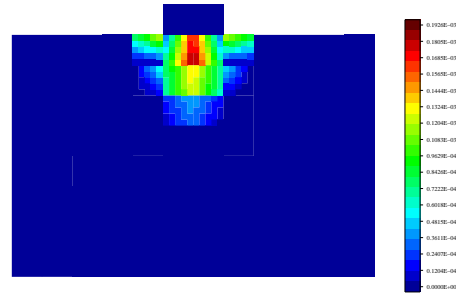


Figure 1.46:  $\|\epsilon^p\|$

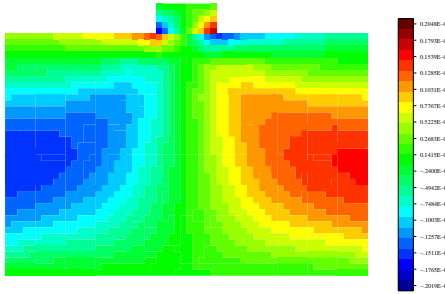


Figure 1.47:  $x$ -component of the displacement:  $u_x$

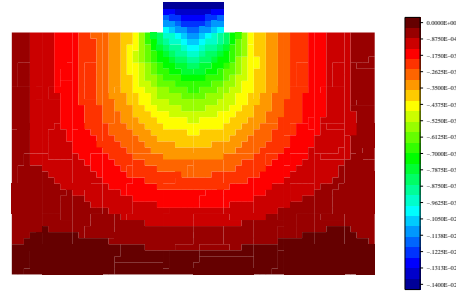


Figure 1.48:  $y$ -component of the displacement:  $u_y$

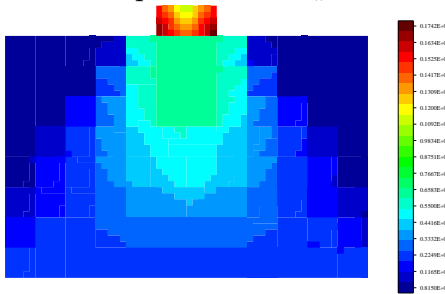


Figure 1.49:  $\|\text{dev } \sigma\|$

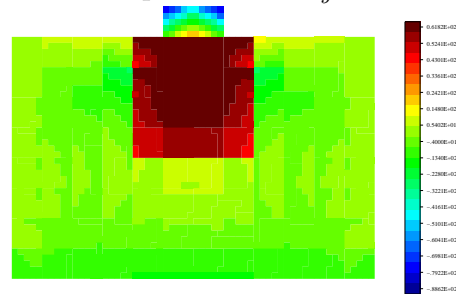


Figure 1.50:  $\sigma_{xx}$

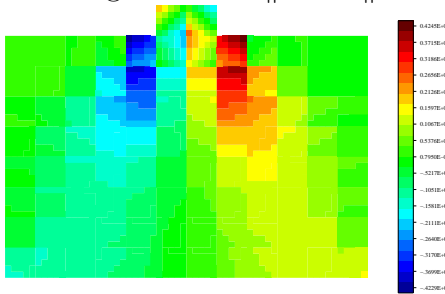


Figure 1.51:  $\sigma_{xy}$

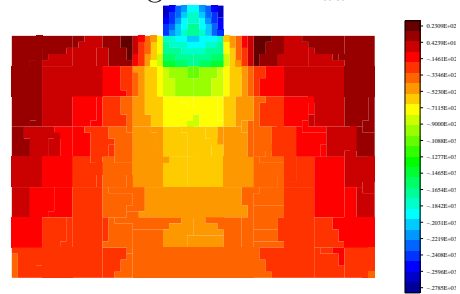


Figure 1.52:  $\sigma_{yy}$

In many industrial applications as metal forming, grinding and machining the contact interaction between a tool and a work piece plays a key role. Very often such processes can not be treated as an isothermic process. The temperature in the tool and the work piece changes much, which changes the physical properties of the bodies in contact. In

that case thermo-effects can not be neglected and should be included in the simulation, [33], [44], [51].

In Section 1.9.1 we present the continuous coupled thermo-elastic contact problem with friction and derive its penalty weak formulation. A penalty method for the mechanical contact is described in Sections 1.2, 1.3. The heat flow on the contact boundary is incorporated as in [33]. The elastic material response is modelled with the boundary element (BE) method, whereas the finite element (FE) method is used for modeling the temperature field. The first order time derivative of temperature is discretized with finite differences. Finally, in Section 1.9.2 we decompose the problem into the mechanical and the thermo-part and give an iterative fix point procedure to solve the coupled problem. In every iteration an elastic contact problem is solved with BEM under fixed temperature assumption. The thermo-contribution to the stress tensor is taken to the right hand side and is incorporated in the BEM formulation with the use of Newton potentials, as it was done in Section 1.2.2 for plastic terms. Then the temperature distribution is computed in the changed geometry.

We mention that the plastic material behavior can be easily included in the algorithm using approaches described in Sections 1.2.1, 1.2.3, 1.2.2.

### 1.9.1 Weak formulation

The classical formulation [33], [51] is given by

$$\begin{aligned}
 & \operatorname{Div} \boldsymbol{\sigma}(\mathbf{u}^i, T^i) = \hat{\mathbf{f}}^i, \\
 & \dot{T}^i = \varkappa \Delta T^i, \\
 & \boldsymbol{\sigma}(\mathbf{u}^i, T^i) = \boldsymbol{\sigma}^e(\mathbf{u}^i) - \boldsymbol{\sigma}^T(T^i), \quad \boldsymbol{\sigma}^e(\mathbf{u}^i) := \mathbb{C} : \boldsymbol{\varepsilon}(\mathbf{u}^i), \\
 & \boldsymbol{\sigma}^T(T^i) := (3\lambda + 2\mu)\alpha(T^i - T_0)\mathbf{1}, \\
 & \mathbf{u}^i = \hat{\mathbf{u}}^i, \\
 & \mathbf{t}^i = \hat{\mathbf{t}}^i, \\
 & T^i = \hat{T}_D^i, \\
 & -k\nabla T^i \cdot \mathbf{n}^i =: \hat{q}^i
 \end{aligned}
 \quad \begin{array}{l}
 \text{in } [0, T] \times \Omega^i, \\
 \\
 \text{on } [0, T] \times \Gamma_{u_D}^i, \\
 \text{on } [0, T] \times \Gamma_{u_N}^i, \\
 \\
 \text{on } [0, T] \times \Gamma_{T_D}^i, \\
 \text{on } [0, T] \times \Gamma_{T_N}^i,
 \end{array}
 \tag{1.220}$$

$$\left. \begin{aligned}
 & \sigma_{\mathcal{N}}(\mathbf{u}^B) = -\sigma_{\mathcal{N}}(\mathbf{u}^A) =: \sigma_{\mathcal{N}}, \\
 & \text{if } [u_{\mathcal{N}}] = g, \text{ then } \sigma_n < 0, \\
 & \sigma_{\mathcal{T}}(\mathbf{u}^B) = -\sigma_{\mathcal{T}}(\mathbf{u}^A) =: \sigma_{\mathcal{T}}, \\
 & \text{if } |\sigma_{\mathcal{T}}| < \mu_f |\sigma_{\mathcal{N}}|, \text{ then } u_{\mathcal{T}} = 0, \\
 & \text{if } |\sigma_{\mathcal{T}}| = \mu_f |\sigma_{\mathcal{N}}|, \text{ then } \exists \hat{\lambda} \geq 0 : [u_{\mathcal{T}}] = -\hat{\lambda} \sigma_{\mathcal{T}}
 \end{aligned} \right\} \text{on } [0, T] \times \Gamma_C,$$

$$\left. \begin{aligned}
 -k\nabla T^B \cdot \mathbf{n}^B &= \frac{\bar{\gamma}^B \bar{\gamma}^A}{\bar{\gamma}^B + \bar{\gamma}^A} |\sigma_{\mathcal{N}}| [T] + \frac{\bar{\gamma}^B}{\bar{\gamma}^B + \bar{\gamma}^A} \sigma_{\mathcal{T}} [\dot{u}_{\mathcal{T}}], \\
 -k\nabla T^A \cdot \mathbf{n}^A &= -\frac{\bar{\gamma}^B \bar{\gamma}^A}{\bar{\gamma}^B + \bar{\gamma}^A} |\sigma_{\mathcal{N}}| [T] + \frac{\bar{\gamma}^A}{\bar{\gamma}^B + \bar{\gamma}^A} \sigma_{\mathcal{T}} [\dot{u}_{\mathcal{T}}],
 \end{aligned} \right\}$$

where  $[u_j] = u_j^B - u_j^A$ ,  $j = \mathcal{N}, \mathcal{T}$ ,  $[T] = T^B - T^A$ , the symmetric gradient  $\boldsymbol{\varepsilon}(\mathbf{u}^i) := \nabla^{\text{sym}} \mathbf{u}^i := 1/2(\nabla \mathbf{u}^i + (\nabla \mathbf{u}^i)^T)$ ,  $\mathbb{C}$  is the fourth order elastic Hooke's tensor,  $\lambda, \mu$  are Lamé coefficients,  $\alpha$  is the coefficient of thermal expansion,  $T_0$  is the reference temperature,  $\varkappa := \frac{k}{\rho c}$ ,  $\rho$  - density,  $c$  - heat capacity,  $k$  - heat conductivity,  $\bar{\gamma}^B$  and  $\bar{\gamma}^A$  - heat conductances,  $\mu_f$  - friction coefficient. We write in the sequel  $\mathbf{t}_C := \sigma_{\mathcal{N}}^A \mathbf{n}^A + \sigma_{\mathcal{T}} \mathbf{e}^A$  for the boundary traction with normal and tangential vectors  $\mathbf{n}^A$  and  $\mathbf{e}^A$ .

The classical problem (1.220) yields a weak formulation in the form of a variational inequality. To avoid this inequality we employ a penalty method for the contact as described in Section 1.2. Let bodies penetrate each other slightly along the contact boundary and let us penalize the penetration  $g_{\mathcal{N}}$  (see Section 1.2 for definition) by setting the normal stress

$$\sigma_{\mathcal{N}} := -\frac{1}{\epsilon_{\mathcal{N}}} g_{\mathcal{N}},$$

where  $\epsilon_{\mathcal{N}} \ll 1$  is a penalty parameter. The regularized Coulomb's friction law is given

by

$$\sigma_{\mathcal{T}} := -\mu_f |\sigma_{\mathcal{N}}| P_{\pm 1} \left( \frac{1}{\epsilon_{\mathcal{T}}} [u_{\mathcal{T}}] \right),$$

where

$$P_{\pm 1}(x) := \begin{cases} \text{sign } x & |x| > 1, \\ x & |x| \leq 1, \end{cases}$$

see Section 1.2 for more details.

Since the bodies touch each other in the contact zone, the nonzero heat flux is initiated, if the bodies have different temperatures. The heat flux should be also proportional to the normal pressure, which has a micromechanical background, [51]. Furthermore, the heat flux should be changed by the energy dissipated due to the frictional sliding. We adopt the constitutive equations for heat flux from [33] and set as already written in (1.220)

$$\begin{aligned} -k \nabla T^B \cdot n^B &= \frac{\bar{\gamma}^B \bar{\gamma}^A}{\bar{\gamma}^B + \bar{\gamma}^A} |\sigma_{\mathcal{N}}| [T] + \frac{\bar{\gamma}^B}{\bar{\gamma}^B + \bar{\gamma}^A} \sigma_{\mathcal{T}} [\dot{u}_{\mathcal{T}}] =: q_C^B \\ -k \nabla T^A \cdot n^A &= -\frac{\bar{\gamma}^B \bar{\gamma}^A}{\bar{\gamma}^B + \bar{\gamma}^A} |\sigma_{\mathcal{N}}| [T] + \frac{\bar{\gamma}^A}{\bar{\gamma}^B + \bar{\gamma}^A} \sigma_{\mathcal{T}} [\dot{u}_{\mathcal{T}}] =: q_C^A, \end{aligned}$$

where the first term corresponds to the energy interchange due to normal contact and the second term reflects the heat produced by friction.  $\gamma^B, \gamma^A$  are experimentally defined material parameters.

The weak formulation of (1.220) is derived in two steps. First we obtain a weak form of the equilibrium equation and then the a weak form of the heat conduction equation.

Testing the equilibrium equation in (1.220) with a suitable mechanical test function  $\boldsymbol{\eta}^i$  [51] and integration by parts yields

$$\begin{aligned} \sum_{i=A,B} \left\{ (\mathbb{C} : \boldsymbol{\varepsilon}(\mathbf{u}^i), \boldsymbol{\varepsilon}(\boldsymbol{\eta}^i))_{\Omega^i} - (\boldsymbol{\sigma}^T(T^i), \boldsymbol{\varepsilon}(\boldsymbol{\eta}^i))_{\Omega^i} - \langle \mathbf{t}_C(\mathbf{u}^i), \boldsymbol{\eta}^i \rangle_{\Gamma_C} \right\} \\ = \sum_{i=A,B} \left\{ (\hat{\mathbf{f}}^i, \boldsymbol{\eta}^i)_{\Omega^i} + \langle \mathbf{t}_N^i, \boldsymbol{\eta}^i \rangle_{\Gamma_N^i} \right\}. \end{aligned} \quad (1.221)$$



Adopting notations of Section 1.2.2 and proceeding similarly we obtain with  $\Sigma^i = \Gamma_C \cup \Gamma_N^i$

$$\begin{aligned}
 & (\boldsymbol{\sigma}(\mathbf{u}^i), \boldsymbol{\varepsilon}(\boldsymbol{\eta}^i))_{\Omega^i} - (\hat{\mathbf{f}}^i, \boldsymbol{\eta}^i)_{\Omega^i} \\
 &= (\mathbb{C} : \boldsymbol{\varepsilon}(\mathbf{u}^i), \boldsymbol{\varepsilon}(\boldsymbol{\eta}^i))_{\Omega^i} - (\boldsymbol{\sigma}^T(T^i), \boldsymbol{\varepsilon}(\boldsymbol{\eta}^i))_{\Omega^i} - (\hat{\mathbf{f}}^i, \boldsymbol{\eta}^i)_{\Omega^i} \\
 &= (\mathbb{C} : \boldsymbol{\varepsilon}(\mathbf{u}^i), \boldsymbol{\varepsilon}(\boldsymbol{\eta}^i))_{\Omega^i} + (\text{Div}[\boldsymbol{\sigma}^T(T^i)], \boldsymbol{\eta}^i)_{\Omega^i} \\
 &\quad - \langle [\boldsymbol{\sigma}^T(T^i)] \cdot \mathbf{n}, \boldsymbol{\eta}^i \rangle_{\Sigma^i} - (\hat{\mathbf{f}}^i, \boldsymbol{\eta}^i)_{\Omega^i} \\
 &= (\mathbb{C} : \boldsymbol{\varepsilon}(\mathbf{u}^i), \boldsymbol{\varepsilon}(\boldsymbol{\eta}^i))_{\Omega^i} + (\text{Div}[\boldsymbol{\sigma}^T(T^i)] - \hat{\mathbf{f}}^i, \boldsymbol{\eta}^i)_{\Omega^i} \\
 &\quad - \langle [\boldsymbol{\sigma}^T(T^i)] \cdot \mathbf{n}, \boldsymbol{\eta}^i \rangle_{\Sigma^i} \\
 &= \langle S\mathbf{u}^i, \boldsymbol{\eta}^i \rangle_{\Sigma^i} + \left\langle N(\text{Div}[\boldsymbol{\sigma}^T(T^i)] - \hat{\mathbf{f}}^i), \boldsymbol{\eta}^i \right\rangle_{\Sigma^i}.
 \end{aligned}$$

Therefore the domain weak formulation (1.221) can be rewritten now in terms of a weak formulation on the boundary: Find  $\mathbf{u}_i$  on  $\Sigma^i$  such that  $\forall \boldsymbol{\eta}^i$  on  $\Sigma^i$

$$\begin{aligned}
 \sum_{i=A,B} \langle S\mathbf{u}^i, \boldsymbol{\eta}^i \rangle_{\Sigma^i} + \langle N(\text{Div}[\boldsymbol{\sigma}^T(T^i)]), \boldsymbol{\eta}^i \rangle_{\Sigma^i} - \langle [\boldsymbol{\sigma}^T(T^i)] \cdot \mathbf{n}, \boldsymbol{\eta}^i \rangle_{\Sigma^i} \\
 - \langle \mathbf{t}_C(\mathbf{u}^i), \boldsymbol{\eta}^i \rangle_{\Gamma_C} = \sum_{i=A,B} \left\langle N\hat{\mathbf{f}}^i, \boldsymbol{\eta}^i \right\rangle_{\Sigma^i} + \langle \mathbf{t}_N^i, \boldsymbol{\eta}^i \rangle_{\Gamma_N^i}.
 \end{aligned} \tag{1.222}$$

To obtain the weak formulation for the thermo-part we test the heat conduction equation in (1.220) with the thermal test function  $\varphi$  [33] and obtain

$$\sum_{i=A,B} \left\{ (\dot{T}^i, \varphi)_{\Omega^i} + \kappa(\nabla T^i, \nabla \varphi^i)_{\Omega^i} \right\} = \sum_{i=A,B} \left\{ \langle q_C^i, \varphi^i \rangle_{\Gamma_{TN}^i} + \langle q_C^i, \varphi^i \rangle_{\Gamma_C} \right\}.$$

The constitutive conditions for the heat flux provide

$$\begin{aligned}
 \sum_{i=A,B} \left\{ (\dot{T}^i, \varphi)_{\Omega^i} + \kappa(\nabla T^i, \nabla \varphi^i)_{\Omega^i} \right\} &= \sum_{i=A,B} \langle q_C^i, \varphi^i \rangle_{\Gamma_{TN}^i} \\
 &+ \frac{\bar{\gamma}^B \bar{\gamma}^A}{\bar{\gamma}^B + \bar{\gamma}^A} \langle \sigma_N[T], [\varphi] \rangle_{\Gamma_C} + \langle \sigma_T[\dot{u}_T], \{\varphi\} \rangle_{\Gamma_C},
 \end{aligned} \tag{1.223}$$

where

$$\{\varphi\} := \frac{\bar{\gamma}^B}{\bar{\gamma}^B + \bar{\gamma}^A} \varphi^B + \frac{\bar{\gamma}^A}{\bar{\gamma}^B + \bar{\gamma}^A} \varphi^A.$$

Now, the system of weak equations (1.222), (1.223) gives the coupled weak formulation for thermoelastic frictional contact problem.

## 1.9.2 Operator splitting, discretization and solution procedure

The basic idea to solve the coupled problem (1.222), (1.223) is to decompose it into a mechanical part and a thermal part [33], [51]:

1. Assume that the temperature field  $T^i$  is known. Find  $\mathbf{u}^i$  satisfying the mechanical variational equation (1.222).
2. Assume that the displacement field  $\mathbf{u}^i$  is known (and therefore  $\dot{u}_T^i$ ,  $\sigma_N$  and  $\sigma_T$ ). Find  $T^i$  satisfying the thermal variational equation (1.223).

Applying a backward Euler scheme for the time discretization the equations (1.222), (1.223) can be rewritten in a semidiscrete form ( $n = 0, 1, \dots$ )

$$\begin{aligned} \sum_{i=A,B} \langle S(\mathbf{u}^i)_n, \boldsymbol{\eta}^i \rangle_{\Sigma^i} + \langle N(\text{Div}[\boldsymbol{\sigma}^T((T^i)_n)]), \boldsymbol{\eta}^i \rangle_{\Sigma^i} - \langle [\boldsymbol{\sigma}^T((T^i)_n)] \cdot \mathbf{n}, \boldsymbol{\eta}^i \rangle_{\Sigma^i} \\ - \langle \mathbf{t}_C((\mathbf{u}^i)_n), \boldsymbol{\eta}^i \rangle_{\Gamma_C} = \sum_{i=A,B} \left\langle N \hat{\mathbf{f}}^i, \boldsymbol{\eta}^i \right\rangle_{\Sigma^i} + \langle \mathbf{t}_N^i, \boldsymbol{\eta}^i \rangle_{\Gamma_N^i}, \end{aligned} \quad (1.224)$$

$$\begin{aligned} \sum_{i=A,B} \left\{ \left( \frac{(T^i)_n - (T^i)_{n-1}}{\Delta t}, \varphi \right)_{\Omega^i} + \varkappa (\nabla(T^i)_n, \nabla \varphi^i)_{\Omega^i} \right\} = \sum_{i=A,B} \langle q_C^i, \varphi^i \rangle_{\Gamma_{TN}^i} \\ + \frac{\bar{\gamma}^B \bar{\gamma}^A}{\bar{\gamma}^B + \bar{\gamma}^A} \langle (\sigma_N)_n[(T)_n], [\varphi] \rangle_{\Gamma_C} + \left\langle (\sigma_T)_n \left[ \frac{(u_T)_n - (u_T)_{n-1}}{\Delta t} \right], [\varphi] \right\rangle_{\Gamma_C}, \end{aligned} \quad (1.225)$$

where the subindex  $n$  denotes functions evaluated in the time step  $t_n$ . Introducing the fixed point iterative process, marked with the upper index  $k$  we end up with the following algorithm inside each time step.

Set  $(\mathbf{u}^i)_n^0 := (\mathbf{u}^i)_{n-1}$ ,  $(T^i)_n^0 := (T^i)_{n-1}$ .

For  $k = 1, 2, 3, \dots$

1. Solve the mechanical problem: Find  $(\mathbf{u}^i)_n^k$ :

$$\begin{aligned} \sum_{i=A,B} \langle S(\mathbf{u}^i)_n^k, \boldsymbol{\eta}^i \rangle_{\Sigma^i} + \langle N(\text{Div}[\boldsymbol{\sigma}^T((T^i)_n^{k-1})]), \boldsymbol{\eta}^i \rangle_{\Sigma^i} - \langle [\boldsymbol{\sigma}^T((T^i)_n^{k-1})] \cdot \mathbf{n}, \boldsymbol{\eta}^i \rangle_{\Sigma^i} \\ - \langle \mathbf{t}_C((\mathbf{u}^i)_n^k), \boldsymbol{\eta}^i \rangle_{\Gamma_C} = \sum_{i=A,B} \left\langle N \hat{\mathbf{f}}^i, \boldsymbol{\eta}^i \right\rangle_{\Sigma^i} + \langle \mathbf{t}_N^i, \boldsymbol{\eta}^i \rangle_{\Gamma_N^i}, \end{aligned} \quad (1.226)$$

2. Solve the thermal problem: Find  $(T^i)_n^k$ :

$$\begin{aligned} \sum_{i=A,B} \left\{ \left( \frac{(T^i)_n^k - (T^i)_{n-1}}{\Delta t}, \varphi \right)_{\Omega^i} + \varkappa (\nabla(T^i)_n^k, \nabla \varphi^i)_{\Omega^i} \right\} = \sum_{i=A,B} \langle q_C^i, \varphi^i \rangle_{\Gamma_{TN}^i} \\ + \frac{\bar{\gamma}^B \bar{\gamma}^A}{\bar{\gamma}^B + \bar{\gamma}^A} \langle (\sigma_N)_n^k[(T)_n^k], [\varphi] \rangle_{\Gamma_C} + \left\langle (\sigma_T)_n^k \left[ \frac{(u_T)_n^k - (u_T)_{n-1}}{\Delta t} \right], \{\varphi\} \right\rangle_{\Gamma_C}, \end{aligned} \quad (1.227)$$

3. Stop, if  $\|(\mathbf{u}^i)_n^k - (\mathbf{u}^i)_n^{k-1}\| + \|(T^i)_n^k - (T^i)_n^{k-1}\| \leq TOL$ ,  
 Otherwise set  $(\mathbf{u}^i)_n^{k+1} := (\mathbf{u}^i)_n^k$ ,  $(T^i)_n^{k+1} := (T^i)_n^k$ ,  $k = k + 1$ , goto 1.

The problems (1.226), (1.227) can be discretized in space with BEM and FEM, respectively. The problem (1.226) should be also linearized, as explained in Section 1.3. Then the Newton's method can be applied to its linearized version.

### 1.9.3 Numerical simulation

The algorithm discussed in this sections has been implemented to model a thermoelastic contact problem with friction. We model an elastic punch of dimension  $30 \times 32 \text{ mm}^2$  in potential contact with an elastic foundation of dimension  $92 \times 60 \text{ mm}^2$ , a uniform quadrilateral mesh is chosen for both bodies. We use continuous, piecewise bilinear approximation for the displacement and continuous piecewise bilinear approximation for the temperature. For auxiliary variables (tractions on the contact boundary and internal plastic variables we use interpolation in Gauss quadrature nodes)

We take material data for steel [33]: Young's modulus  $E = 206\,000 \text{ MPa}$ , Poisson's ratio  $\nu = 0.3$ , density  $\rho = 7850 \text{ kg/m}^3$ , thermal expansion coefficient  $\alpha = 12 \times 10^{-6}$ , heat capacity  $c = 500 \text{ J kg}^{-1} \text{ K}^{-1}$  and thermal conductivity  $k = 43 \text{ W m}^{-1} \text{ K}^{-1}$ , thermal contact conductances  $\bar{\gamma}^1 = \bar{\gamma}^2 = 1 \text{ W N}^{-1} \text{ K}^{-1}$ , friction coefficient  $\mu_f = 0.2$ . Displacement is fixed on the lower boundary of the foundation. All boundaries are thermally insulated, the initial temperature is the reference temperature  $T_0 = 300 \text{ K}$  at all nodes. In figures the punch is pushed with constant displacement vector  $(0, -1 \text{ mm})^T$  applied at the upper edge of the punch and a tangential cycle loading is applied there with maximum deviation  $(-0.199 \text{ mm}, 0)^T$ . The load in normal direction is enforced in 4 steps, whereas each tangent cycle is performed in 64 steps. We perform 10 tangent cycles. The linear system is solved using the Conjugate Gradient method with the diagonal preconditioner.

As penalty parameters for contact we choose :  $\epsilon_{\mathcal{T}} = 1/(2E)$ ,  $\epsilon_{\mathcal{N}} = 1/(4E)$ .

In figures 1.53 and 1.54 we see the distribution of the strain norm (a), the norm of the stress deviator (b), the norm of the stress tensor (c), the second diagonal component of the stress tensor  $\sigma_{yy}$  (d), the first component of the displacement vector  $u_x$  (g), and the second component of the displacement vector  $u_y$  as well as deformed mesh (f). The figure 1.53 shows the simulation results after applying the full normal load and 5/4th of the cycle load, whereas the figure 1.54 shows the end results. Our numerical experiment (pure FE simulations) shows clearly the development of heat near the contact boundary, especially near the bottom corners of the work tool. In picture 1.54 one can clearly see the sticking along the bottom edge of the work tool, i.e. the displacements of both bodies in  $x$  direction are equal.

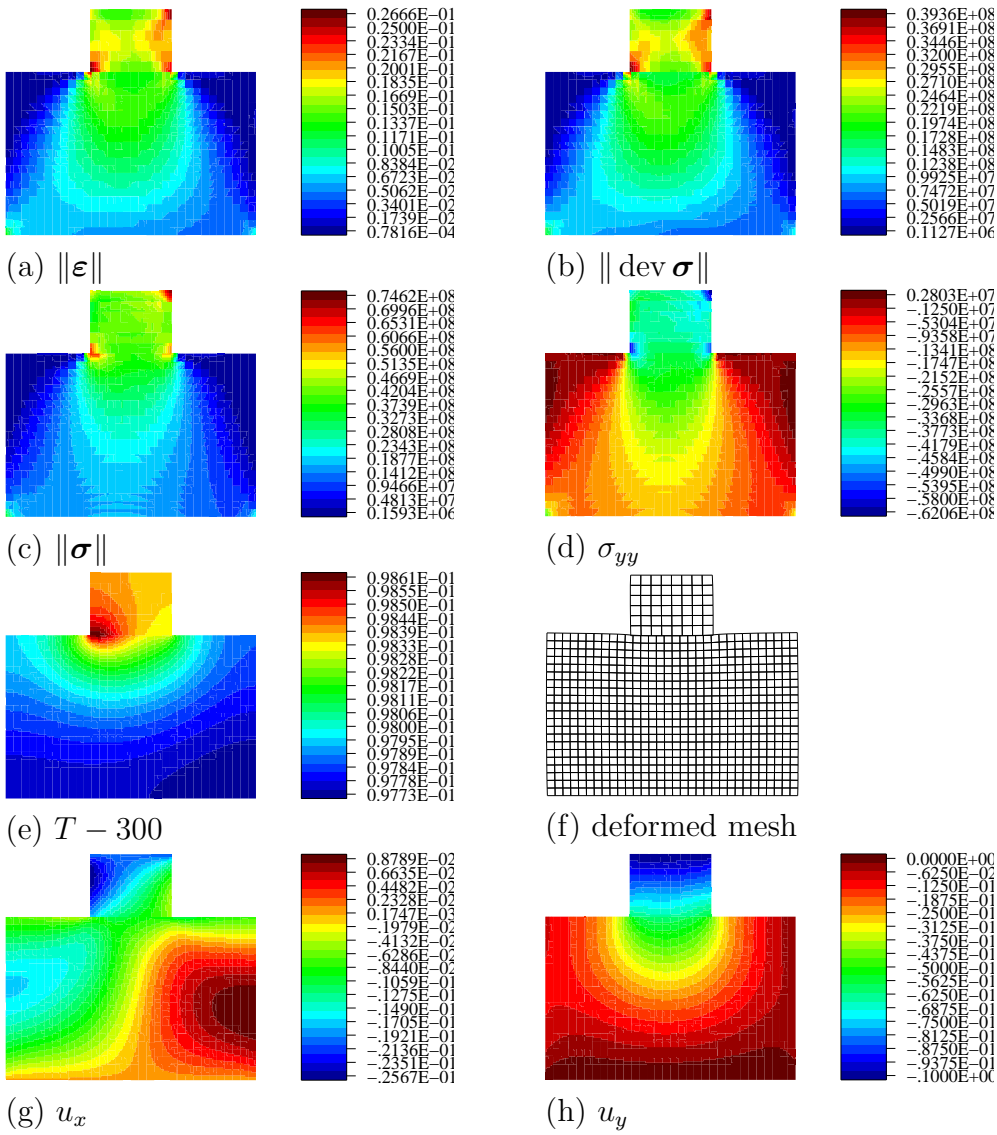


Figure 1.53: 16 increments of 2nd tangent cycle

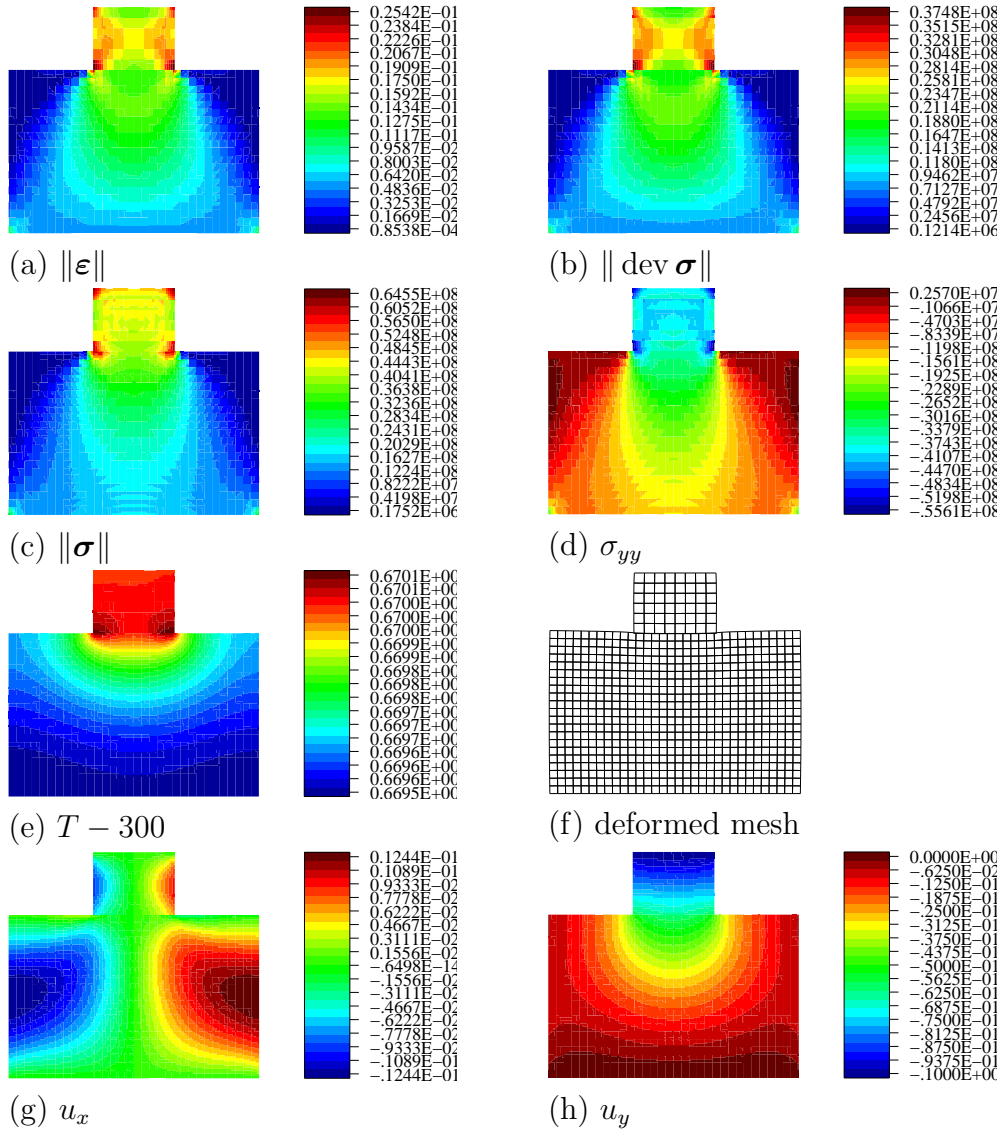


Figure 1.54: End of simulation



## 2 Hypoelasto-viscoplasticity. Large deformations

In this Chapter we extend the technique of FEM-BEM coupling that was introduced in Chapter 1 onto large deformations under hypoelasto-viscoplastic material law described by Hart's constitutive equations. We start with an introduction to continuum mechanics of large deformations subjected to Hart's model, see Section 2.2. In Section 2.5 we present numerical procedures based on the boundary element Galerkin method for hypoelasto-viscoplasticity. In Section 2.6 we present a FEM-BEM coupling procedure for the thermo-mechanical two-body contact problem. In subsections 2.5.3, 2.6.2 we present benchmarks for procedures investigated in Sections 2.5, 2.6 respectively.

### 2.1 The equilibrium equation

We consider a three-dimensional body  $\Omega \subset \mathbb{R}^2$  in a fixed given rectangular cartesian coordinate system. A material particle of the body in the reference configuration is assumed to have the coordinates  $\mathbf{X} := (X_1, X_2, X_3)^T$  and coordinates  $\mathbf{x} := (x_1, x_2, x_3)^T$  in actual (current) configuration. By  $\Omega_t \subset \mathbb{R}^2$  we will denote the volume, that body occupies at time  $t$ . So,  $\Omega_0 \equiv \Omega$ . Motion of the body is given by parameterized set of mappings  $\varphi(t) : \Omega_0 \rightarrow \Omega_t$ . We assume that for all  $t \in [0, T]$  exists  $\varphi^{-1}(t) : \Omega_t \rightarrow \Omega_0$  and both  $\varphi(t)$  and  $\varphi^{-1}(t)$  are continuous and bijective.  $\varphi_0$  is the identical mapping. We will write  $\Xi(t, \mathbf{X})$  for the value of mapping  $\Xi(t) : \Omega_0 \rightarrow Y_t$  at  $\mathbf{X} \in \Omega_0$ , where  $Y_t := \Xi(t)(\Omega_0)$ , this set may depend on  $t$ .

The displacement vector  $\mathbf{u}(t) : \Omega_0 \rightarrow \mathbb{R}^2$  is defined as follows

$$\mathbf{u}(t, \mathbf{X}) := \varphi(t, \mathbf{X}) - \mathbf{X}. \quad (2.1)$$

It is clear that  $\forall t \in [0, T]$   $\mathbf{u}(t) \circ \varphi^{-1}(t)$  is a mapping  $\Omega_t \rightarrow \mathbb{R}^2$ :

$$(\mathbf{u}(t) \circ \varphi^{-1}(t))(\mathbf{x}) = \mathbf{u}(t, \varphi^{-1}(t, \mathbf{x})) = \mathbf{x} - \varphi^{-1}(t, \mathbf{x}) \quad (2.2)$$

We will write  $\Xi(t, \mathbf{x})$  for  $(\Xi(t) \circ \varphi^{-1}(t))(\mathbf{x})$ .

**Definition 2.1.1.**

$$\begin{aligned} \forall \Xi(t), \Xi(t) &: \Omega_0 \rightarrow Y_t \text{ we use following notation :} \\ \Xi(t, \mathbf{X}) &:= \Xi(t)(\mathbf{X}), \quad \forall \mathbf{X} \in \Omega_0, \\ \Xi(t, \mathbf{x}) &:= (\Xi(t) \circ \varphi^{-1}(t))(\mathbf{x}), \quad \forall \mathbf{x} \in \Omega_t. \end{aligned}$$

Derivatives:

$$\begin{aligned} \overset{\circ}{\nabla} \Xi &:= \frac{\partial \Xi}{\partial \mathbf{X}} := \frac{\partial \Xi(t)(\mathbf{X})}{\partial \mathbf{X}}, \quad \forall \mathbf{X} \in \Omega_0. \\ \nabla \Xi &:= \nabla \frac{\partial \Xi}{\partial \mathbf{x}} := \frac{\partial (\Xi(t) \circ \varphi^{-1}(t))(\mathbf{x})}{\partial \mathbf{x}}, \quad \forall \mathbf{x} \in \Omega_t. \\ \mathbf{F} &:= \overset{\circ}{\nabla} \varphi. \end{aligned} \tag{2.3}$$

The components of the velocity vector  $\mathbf{v} := (v_1, v_2, v_3)^T$  are then defined as

$$v_i := \frac{\partial u_i(t, \mathbf{X})}{\partial t} \text{ or } v_i = \frac{du_i(t, \mathbf{x})}{dt} = \frac{\partial u_i(t, \mathbf{x})}{\partial t} + \frac{\partial u_i(t, \mathbf{x})}{\partial \mathbf{x}} \frac{\partial \varphi(t, \mathbf{X})}{\partial t}. \tag{2.4}$$

We define the symmetric part  $\mathbf{d}(t) : \Omega_t \rightarrow \mathbb{R}_{sym}^{3 \times 3}$  (rate-of-deformation) of the velocity gradient (rate of deformation)  $\frac{\partial \mathbf{v}(t, \mathbf{x})}{\partial \mathbf{x}}$  by

$$d_{ij} := \frac{1}{2} \left( \frac{\partial v_i(t, \mathbf{x})}{\partial x_j} + \frac{\partial v_j(t, \mathbf{x})}{\partial x_i} \right) \tag{2.5}$$

and the anti-symmetric part  $\mathbf{w}(t) : \Omega_t \rightarrow \mathbb{R}_{asym}^{3 \times 3}$  of the velocity gradient

$$w_{ij} := \frac{1}{2} \left( \frac{\partial v_i(t, \mathbf{x})}{\partial x_j} - \frac{\partial v_j(t, \mathbf{x})}{\partial x_i} \right), \tag{2.6}$$

where  $\mathbb{R}_{asym}^{3 \times 3} := \{\mathbf{x} \in \mathbb{R}^{3 \times 3} \mid x_{ij} = -x_{ji} \forall i, j, i \neq j\}$ . In addition to the standard time derivative  $\dot{f}(t, \mathbf{x}) := \frac{\partial f(t, \mathbf{x})}{\partial t} + \frac{\partial f(t, \mathbf{x})}{\partial \mathbf{x}} \mathbf{v}(t, \mathbf{x})$  we define the Jaumann derivative (Jaumann rate) of a symmetric tensor  $\mathbf{T}(t) : \Omega_t \rightarrow \mathbb{R}_{sym}^{3 \times 3}$  as follows

$$\overset{*}{T}_{ij} := \dot{T}_{ij} + (T_{ij} w_{kj} + T_{jk} w_{ki}). \tag{2.7}$$

For example the Jaumann rate for the Cauchy stress tensor  $\boldsymbol{\sigma}(t) : \Omega_t \rightarrow \mathbb{R}_{sym}^{3 \times 3}$  is given by

$$\overset{*}{\sigma}_{ij} = \dot{\sigma}_{ij} + (\sigma_{ik} w_{kj} + \sigma_{jk} w_{ki}), \tag{2.8}$$

where  $\dot{\sigma}_{ij}$  denotes the material derivative, given by

$$\dot{\sigma}_{ij} := \frac{\partial \sigma_{ij}(t, \mathbf{x})}{\partial t} + \frac{\partial \sigma_{ij}(t, \mathbf{x})}{\partial x_k} v_k. \tag{2.9}$$



We assume that the deformation rate is decomposed into an elastic and a non-elastic part

$$d_{ij} = d_{ij}^e + d_{ij}^n. \quad (2.10)$$

The Jaumann rate of the Kirchhoff stress tensor  $\boldsymbol{\tau}(t) : \Omega_0 \rightarrow \mathbb{R}_{sym}^{3 \times 3}$  is related to the material derivative of the 1<sup>st</sup> Piola-Kirchhoff stress tensor  $\boldsymbol{s}(t) : \Omega_0 \rightarrow \mathbb{R}^{3 \times 3}$  (see [4] Chapter 5), as follows

$$\dot{\tau}_{ij}^* = \dot{s}_{ij} + (\sigma_{ik}d_{jk} + \sigma_{kj}d_{ik}) - \sigma_{ik} \frac{\partial v_j}{\partial x_k}, \quad (2.11)$$

or in the short form

$$\dot{\tau}_{ij}^* = \dot{s}_{ij} + G_{ijkl}^{(*)} \frac{\partial v_k}{\partial x_l}, \quad (2.12)$$

where

$$G_{ijkl}^{(*)} := \frac{1}{2} (\sigma_{il}\delta_{jk} + \sigma_{ik}\delta_{jl} + \sigma_{lj}\delta_{ki} + \sigma_{kj}\delta_{li}) - \sigma_{il}\delta_{kj} \quad \delta_{ij} := \begin{cases} 0, & i \neq j, \\ 1, & i = j. \end{cases} \quad (2.13)$$

We can write the equilibrium equation of the body in actual configuration in terms of the Cauchy stress tensor  $\boldsymbol{\sigma}$ :

$$-\operatorname{div} \boldsymbol{\sigma} = \rho \boldsymbol{f} \quad \Leftrightarrow \quad \frac{\partial \sigma_{ji}}{\partial x_j} + \rho f_i = 0, \quad (2.14)$$

where  $\rho$  and  $\boldsymbol{f}$  are the density in actual configuration and the body forces respectively. Using the 1<sup>st</sup> Piola-Kirchhoff stress tensor  $\boldsymbol{s}(t) : \Omega_0 \rightarrow \mathbb{R}^{3 \times 3}$ :

$$\boldsymbol{s}(t, \boldsymbol{X}) := J(t, \boldsymbol{X}) \boldsymbol{\sigma}(t, \boldsymbol{\varphi}(t, \boldsymbol{X})) \left( \frac{\partial \boldsymbol{\varphi}(t, \boldsymbol{X})}{\partial \boldsymbol{X}} \right)^{-T} \quad (2.15)$$

in the reference configuration, (2.14) takes an equivalent form in terms of

$$\frac{\partial s_{ji}}{\partial X_j} + \rho_0 f_i = 0, \quad (2.16)$$

where  $\rho_0$  is the density in the reference configuration. It should be noted that due to the mass conservation law, the density in the reference configuration does not depend on time (the total mass of the body remains constant with time).

Later we will need the rate variant of (2.16)

$$\frac{\partial \dot{s}_{ji}}{\partial X_j} + \rho_0 \dot{f}_i = 0. \quad (2.17)$$

## 2.2 Hart's constitutive equations for hypoelasto-viscoplasticity

According to [4] the constitutive equation for arbitrary hyperelastic-plastic material admits the following representation: the Jaumann rate of Cauchy stress  $\overset{*}{\sigma}_{ij}$  is a homogeneous linear function of the elastic part  $d_{ij}^e$  of the deformation rate  $d_{ij}$  and under the assumption of material isotropy we have

$$d_{ij} = d_{ij}^e + d_{ij}^n, \quad (2.18)$$

$$\overset{*}{\sigma}_{ij} = \lambda d_{kk}^e \delta_{ij} + 2\mu d_{ij}^e \quad (2.19)$$

$$d_{ij}^n = f_{ij}(\boldsymbol{\sigma}, \mathbf{q}), \quad (2.20)$$

$$\overset{*}{q}_k = g_k(\boldsymbol{\sigma}, \mathbf{q}), \quad (2.21)$$

$$d_{kk}^n = 0, \quad (2.22)$$

where  $d_{ij}^e$ ,  $d_{ij}^n$  are the elastic and non-elastic parts of the rate-of-deformation (2.5) respectively,  $\mathbf{q}$  - inner variables,  $f_{ij}$  and  $g_k$  some functions,  $\lambda$  and  $\mu$  are Lamé coefficients from the linear elasticity theory for small deformations.

The material response in dilatation is assumed to be elastic. According to Hart's model [30, 32, 16, 39], the nonelastic strain is decomposed into two (time-dependent) components

$$d_{ij}^n = \overset{*a}{\varepsilon}_{ij} + d_{ij}^p, \quad (2.23)$$

where  $\overset{*a}{\varepsilon}_{ij}$  is the anelastic rate-of-deformation and  $d_{ij}^p$  is the completely irrecoverable and path dependent permanent part. The two state variables in the Hart's model are the anelastic part  $\overset{*a}{\varepsilon}_{ij}$  and a scalar  $\sigma^{(*)}$ , called hardness, which is similar to an isotropic strain hardening parameter or current yield stress.

The deviatoric component  $\boldsymbol{\sigma}'$  ( $\sigma'_{ij} := \sigma_{ij} - \frac{1}{3}\sigma_{kk}$ ) of the Cauchy stress tensor is decomposed into two auxiliary tensors

$$\sigma'_{ij} = \sigma'^a_{ij} + \sigma'^f_{ij}. \quad (2.24)$$

The flow rules in Hart's model for the strains and strain rates are [16, 39]

$$\overset{*a}{\varepsilon}_{ij} = \frac{\varepsilon^{(a)}}{\sigma^{(a)}} \sigma'^a_{ij}, \quad (2.25)$$

$$d_{ij}^p = \frac{d^{(p)}}{\sigma^{(a)}} \sigma'^a_{ij}, \quad (2.26)$$

$$d_{ij}^n = \frac{d^{(n)}}{\sigma^{(f)}} \sigma'_{ij}{}^f, \quad (2.27)$$

where  $d^{(n)}$ ,  $\varepsilon^{(a)}$ ,  $d^{(p)}$ ,  $\sigma^{(a)}$ ,  $\sigma^{(f)}$  are scalar invariants of the corresponding tensors, defined by

$$\begin{aligned} d^{(n)} &:= \sqrt{d_{ij}^n d_{ij}^n}, & d^{(p)} &:= \sqrt{d_{ij}^p d_{ij}^p}, & \varepsilon^{(a)} &:= \sqrt{\varepsilon_{ij}^a \varepsilon_{ij}^a}, \\ \sigma^{(a)} &:= \sqrt{\sigma'_{ij}{}^a \sigma'_{ij}{}^a}, & \sigma^{(f)} &:= \sqrt{\sigma'_{ij}{}^f \sigma'_{ij}{}^f}. \end{aligned} \quad (2.28)$$

Relationships between scalar invariants are

$$\sigma^{(a)} = \frac{2}{3} \mathcal{M} \varepsilon^{(a)}, \quad (2.29)$$

$$d^{(n)} = d_0 \left( \sqrt{\frac{3}{2}} \right)^{M+1} (\sigma^{(f)} / \sigma_0)^M, \quad (2.30)$$

$$d^{(p)} = \sqrt{\frac{3}{2}} d^{(*)} \left( \ln \frac{\sigma^{(*)}}{\sqrt{\frac{3}{2}} \sigma^{(a)}} \right)^{-1/\lambda}, \quad (2.31)$$

$$d^{(*)} = d_{sT}^{(*)} \left( \frac{\sigma^{(*)}}{\sigma_s^{(*)}} \right)^m e^{\frac{Q}{R} \left( \frac{1}{T_B} - \frac{1}{T} \right)}, \quad (2.32)$$

$$\dot{\sigma}^{(*)} = \sqrt{\frac{2}{3}} d^{(p)} \sigma^{(*)} \Gamma(\sigma^{(*)}, \sigma^{(a)}), \quad (2.33)$$

$$\Gamma(\sigma^{(*)}, \sigma^{(a)}) = \left( \frac{\beta}{\sigma^{(*)}} \right)^\delta \left( \frac{\sqrt{\frac{3}{2}} \sigma^{(a)}}{\sigma^{(*)}} \right)^{\beta/\sigma^{(*)}}, \quad (2.34)$$

where  $\mathcal{M}$ ,  $M$ ,  $m$ ,  $\lambda$ ,  $d_0$ ,  $\sigma_0$ ,  $d_{sT}^{(*)}$ ,  $\sigma_s^{(*)}$ ,  $\beta$ ,  $\delta$ ,  $R$ ,  $Q$ ,  $T_B$  are scalar parameters. Such that  $\sigma_s^{(*)}$  is the reference value of stress hardness  $\sigma^{(*)}$ ,  $T_B$  is the reference value of the temperature  $T$ ,  $d_{sT}^{(*)}$  is the reference value of the rate of strain hardening,  $R$  is the gas constant,  $Q$  is the activation energy for atomic self diffusion,  $\beta$  and  $\delta$  are strain hardening parameters.

## 2.3 Time integration

Using equations (2.24)-(2.34) one can directly obtain differential equations for  $\varepsilon_{ij}^a$  and  $\sigma^{(*)}$

$$(2.18) : d_{ij}^p = d_{ij}^n - \varepsilon_{ij}^{*a} \quad (2.35)$$

$$(2.25), (2.29) : \sigma'_{ij}^a = \frac{2}{3} \mathcal{M} \varepsilon_{ij}^a \quad (2.36)$$

$$(2.24) : \sigma'_{ij}^f = \sigma'_{ij} - \frac{2}{3} \mathcal{M} \varepsilon_{ij}^a. \quad (2.37)$$

$$\begin{aligned} d_{ij}^n &= \frac{d^{(n)}}{\sigma'^{(f)}} \sigma'_{ij}^f = \frac{d^{(n)}}{\sigma'^{(f)}} \left( \sigma'_{ij} - \frac{2}{3} \mathcal{M} \varepsilon_{ij}^a \right) \\ &= \frac{d_0}{(\sigma_0)^M} \left( \sqrt{\frac{2}{3}} \right)^{M+1} \frac{(\sigma'^{(f)})^M}{(\sigma'^{(f)})} \left( \sigma'_{ij} - \frac{2}{3} \mathcal{M} \varepsilon_{ij}^a \right) \\ &= \frac{d_0}{(\sigma_0)^M} \left( \sqrt{\frac{2}{3}} \right)^{M+1} (\sigma'^{(f)})^{M-1} \sigma'_{ij}^f, \end{aligned} \quad (2.38)$$

Starting with (2.23) and using sequently (2.26), (2.31), (2.25), (2.29) we obtain

$$\begin{aligned} \varepsilon_{ij}^{*a} &= d_{ij}^n - d_{ij}^p = d_{ij}^n - \frac{d^{(p)}}{\sigma^{(a)}} \sigma'_{ij}^a \\ &= d_{ij}^n - d^{(*)} \sqrt{\frac{2}{3}} \left[ \ln \left( \frac{\sigma^{(*)}}{\sqrt{\frac{3}{2}} \sigma^{(a)}} \right) \right]^{-1/\lambda} \frac{\sigma'_{ij}^a}{\sigma^{(a)}} \\ &= d_{ij}^n - d^{(*)} \sqrt{\frac{2}{3}} \left[ \ln \left( \frac{\sigma^{(*)}}{\sqrt{\frac{3}{2}} \sigma^{(a)}} \right) \right]^{-1/\lambda} \frac{\varepsilon_{ij}^a}{\varepsilon^{(a)}} \\ &= d_{ij}^n - d^{(*)} \sqrt{\frac{2}{3}} \left[ \ln \left( \frac{\sigma^{(*)}}{\sqrt{\frac{2}{3}} \mathcal{M} \varepsilon^{(a)}} \right) \right]^{-1/\lambda} \frac{\varepsilon_{ij}^a}{\varepsilon^{(a)}}, \end{aligned} \quad (2.39)$$

Starting with (2.33) and using (2.31), (2.32), (2.34), (2.29) we obtain

$$\dot{\sigma}^{(*)} = d^{(*)} \sigma^{(*)} \left( \ln \frac{\sigma^{(*)}}{\sqrt{\frac{3}{2}} \sigma^{(a)}} \right)^{-1/\lambda} \Gamma(\sigma^{(*)}, \sigma^{(a)})$$

$$\begin{aligned}
 &= d_{sT}^{(*)} \sigma^{(*)} \left( \frac{\sigma^{(*)}}{\sigma_s^{(*)}} \right)^m e^{\frac{Q}{R} \left( \frac{1}{T_B} - \frac{1}{T} \right)} \left( \ln \frac{\sigma^{(*)}}{\sqrt{\frac{3}{2}} \sigma^{(a)}} \right)^{-1/\lambda} \Gamma(\sigma^{(*)}, \sigma^{(a)}) \\
 &= d_{sT}^{(*)} \sigma^{(*)} \left( \frac{\sigma^{(*)}}{\sigma_s^{(*)}} \right)^m e^{\frac{Q}{R} \left( \frac{1}{T_B} - \frac{1}{T} \right)} \left( \ln \frac{\sigma^{(*)}}{\sqrt{\frac{3}{2}} \sigma^{(a)}} \right)^{-1/\lambda} \left( \frac{\beta}{\sigma^{(*)}} \right)^\delta \left( \frac{\sqrt{\frac{3}{2}} \sigma^{(a)}}{\sigma^{(*)}} \right)^{\beta/\sigma^{(*)}} \\
 &= d_{sT}^{(*)} \sigma^{(*)} \left( \ln \frac{\sigma^{(*)}}{\sqrt{\frac{2}{3}} \mathcal{M} \varepsilon^{(a)}} \right)^{-1/\lambda} \left( \frac{\sqrt{\frac{2}{3}} \mathcal{M} \varepsilon^{(a)}}{\sigma^{(*)}} \right)^{\beta/\sigma^{(*)}} e^{\frac{Q}{R} \left( \frac{1}{T_B} - \frac{1}{T} \right)} \left( \frac{\beta}{\sigma^{(*)}} \right)^\delta \left( \frac{\sigma^{(*)}}{\sigma_s^{(*)}} \right)^m. \quad (2.40)
 \end{aligned}$$

*Remark 2.3.1.* As one can see the equations (2.39), (2.40) have singularity in right-hand side as  $\sigma^{(*)} = \sqrt{\frac{3}{2}} \sigma^{(a)}$  (analog to plastic flow at the yield stress. In region  $\sigma^{(*)} \approx \sqrt{\frac{3}{2}} \sigma^{(a)}$  the equation 2.31 predicts large values of  $d^p$  and consequently very small time steps are required in a numerical computational process to capture this phenomena. For the sake of computational efficiency we impose in that region the condition  $\dot{\sigma}^{(*)} = \sqrt{\frac{3}{2}} \dot{\sigma}^{(a)}$ . Using this condition we obtain

$$d^{(p)} = \frac{\sigma_{ij}^{(a)} d_{ij}^{(n)} / \sigma^{(a)}}{1 + \sigma^{(*)} \Gamma(\sigma^{(*)}, \sigma^{(a)}) / \mathcal{M}}. \quad (2.41)$$

*Remark 2.3.2.* As one can see the equations (2.39), (2.40) have singularity in right-hand side as  $\sigma^{(a)} = 0$ . Hence, up to given tolerance we suppose material to be described by linear elastic equations.

Taking into account remarks 2.3.1 and 2.3.2 we obtain following regularization procedure for prescribed tolerance  $1 > \varrho > 0$ , that should be close to 1 and  $1 > \varrho_0 > 0$ , that should be close to 0:

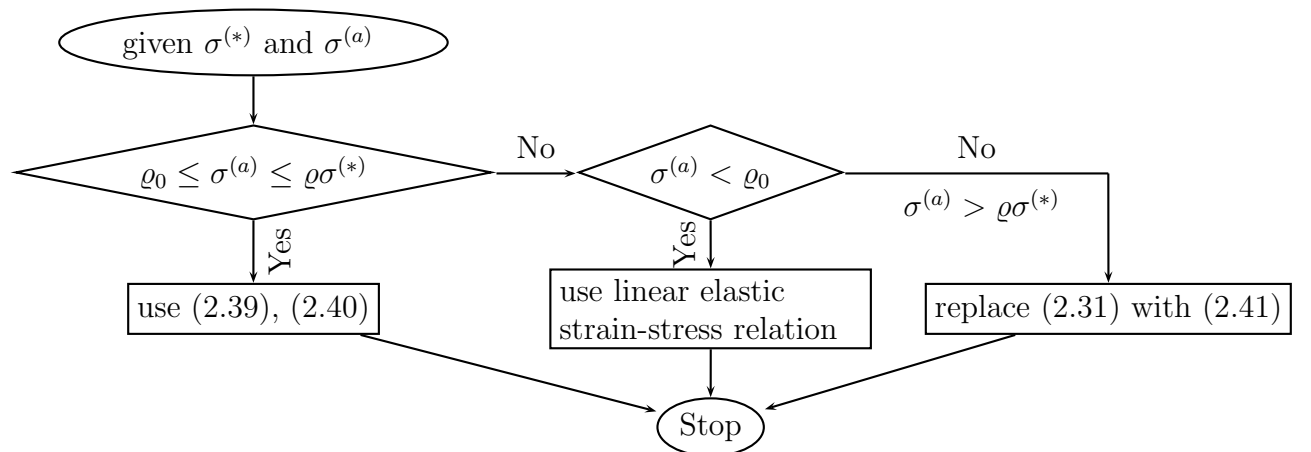


Figure 2.1: Flow chart. Hart's model regularization

## 2.4 Updated Lagrange approach

We consider the body  $\Omega \subset \mathbb{R}^d$ ,  $d=2,3$  that occupies a domain  $\Omega_t \subset \mathbb{R}^d$  at time  $t$ . Our objective is the deformation of the body due to applied forces and displacements with respect to the real time  $t$ . Using the Updated Lagrange Approach let  $\Omega_t$  be the reference configuration for the time interval  $[t, t + \Delta t]$ .

The first assumption made here is that the deformations are nearly incompressible, i.e.  $\frac{\partial v_i}{\partial x_i} \approx 0$  or  $\frac{\partial v_i}{\partial x_i} \ll 1$ . This assumption is quite reasonable in our situation since non-elastic deformations ( $\mathbf{d}^n$ ) preserve the volume by definition, see (2.22) and they are much larger than the elastic ones ( $\mathbf{d}^e$ ). Hence, the volume deformation is neglectable with respect to total one. Thus the Jacobian  $J$  of the deformation gradient  $F_{ij} = \frac{\partial x_i}{\partial X_j}$  is one, while  $\dot{J} = J \text{tr} \mathbf{d}$  (see [7] Section 3.14) and  $J(t, \mathbf{X})|_{t=0} = 1$ . Thus the deformation gradient defines an orthogonal matrix. Under this assumption one sees

$$\overset{*}{\tau}_{ij} \cong \overset{*}{\sigma}_{ij} \quad \text{since } J := \det \frac{\partial \mathbf{x}}{\partial \mathbf{X}} \cong 1 \text{ and } \tau_{ij} = J \sigma_{ij}. \quad (2.42)$$

The Green - St. Venant strain tensor  $\mathbf{E}(t) : \Omega_0 \rightarrow \mathbb{R}^{3 \times 3}$  with

$$E_{ij} = \frac{1}{2} \left( \frac{\partial u_i}{\partial X_j} + \frac{\partial u_j}{\partial X_i} + \frac{\partial u_k}{\partial X_i} \frac{\partial u_k}{\partial X_j} \right), \quad (2.43)$$

the rate of (2.43) is related to the rate-of-deformation (2.5) and deformation gradient  $F_{ij}$  as follows (see [4], p. 96)

$$\dot{E}_{ij} = d_{kl} \frac{\partial x_k}{\partial X_i} \frac{\partial x_l}{\partial X_j}. \quad (2.44)$$

Thus, in the updated Lagrangian approach it holds

$$\dot{E}_{ij} = d_{ij} \text{ at the origin of the time interval } [t, t + \Delta t]. \quad (2.45)$$

Using (2.45), (2.42) and (2.20) we obtain for the origin of the time interval  $[t, t + \Delta t]$

$$\overset{*}{\tau}_{ij} = \lambda \dot{E}_{kk}^e \delta_{ij} + 2\mu \dot{E}_{ij}^e. \quad (2.46)$$

## 2.5 A boundary element method for hypoelasto-viscoplasticity

In this chapter we use Hart's model of viscoplasticity and investigate a boundary element solution procedure. Our Galerkin approach extends the collocation procedure in [17, 39]. We describe in detail the nested loops which are necessary for our BEM implementation for details see [25]. In section 2.5.1 we present a Galerkin boundary element method for viscoplasticity and in section 2.5.3 benchmark simulations.

### 2.5.1 Integral operators

Following [17] we present a boundary element formulation for viscoplastic problems with large deformations and large strains. In order to derive a representation formula for the velocities we use the fundamental solution of the Lamé operator  $\mathcal{G}$ . Assuming that the deformation is almost incompressible then the Zaremba-Jaumann time derivative of the Cauchy stress tensor

$$\overset{*}{\boldsymbol{\sigma}} = \dot{\boldsymbol{\sigma}} - \boldsymbol{w} \cdot \boldsymbol{\sigma} + \boldsymbol{\sigma} \cdot \boldsymbol{w} \quad (2.47)$$

and of the Kirchhoff stress tensor

$$\overset{*}{\boldsymbol{\tau}} = \dot{\boldsymbol{s}} + (\boldsymbol{\sigma} \cdot \boldsymbol{d}^T + \boldsymbol{d} \cdot \boldsymbol{\sigma}) - \boldsymbol{\sigma} \cdot \frac{\partial \boldsymbol{v}}{\partial \boldsymbol{x}}, \quad (2.48)$$

satisfy the relation (see [18, 39, 52])

$$\overset{*}{\boldsymbol{\tau}} \cong \overset{*}{\boldsymbol{\sigma}}. \quad (2.49)$$

Hence, there holds (see Section 2.4)

$$\overset{*}{\boldsymbol{\tau}} \cong \mathbb{C} : \boldsymbol{d}^e \quad (2.50)$$

with the elastic part  $\boldsymbol{d}^e$  of the symmetric strain rate tensor.

We multiply the local equilibrium (2.17) in the rate formulation with the Greens function  $\mathcal{G}$  and integrate by parts yielding

$$\int_{\Omega_0} (\overset{\circ}{\nabla} \cdot \dot{\boldsymbol{s}} + \rho_0 \dot{\boldsymbol{f}}) \cdot \mathcal{G} \, d\Omega$$

with

$$\mathcal{G} \cdot (\overset{\circ}{\nabla} \cdot \dot{\boldsymbol{s}}) = \overset{\circ}{\nabla} \cdot (\dot{\boldsymbol{s}} \cdot \mathcal{G}) - (\overset{\circ}{\nabla} \circ \mathcal{G}) : \dot{\boldsymbol{s}}.$$

Integrating by parts we obtain

$$\begin{aligned}
 0 &= \int_{\Omega_0} \rho_0 \mathcal{G} \cdot \dot{\mathbf{f}} \, d\Omega + \int_{\Omega_0} \mathcal{G} \cdot (\overset{\circ}{\nabla} \cdot \dot{\mathbf{s}}) \, d\Omega \\
 &= \int_{\Omega_0} \rho_0 \mathcal{G} \cdot \dot{\mathbf{f}} \, d\Omega + \int_{\partial\Omega_0} \mathbf{n}_0 \cdot \dot{\mathbf{s}} \cdot \mathcal{G} \, d\Gamma - \int_{\Omega_0} (\overset{\circ}{\nabla} \circ \mathcal{G}) : \dot{\mathbf{s}} \, d\Omega \\
 &= \int_{\Omega_0} \rho_0 \mathcal{G} \cdot \dot{\mathbf{f}} \, d\Omega + \int_{\partial\Omega_0} \dot{\underline{\mathbf{t}}} \cdot \mathcal{G} \, d\Gamma - \int_{\Omega_0} (\overset{\circ}{\nabla} \circ \mathcal{G}) : \dot{\mathbf{s}} \, d\Omega,
 \end{aligned}$$

with  $\dot{\underline{\mathbf{t}}} := \mathbf{n}_0 \cdot \dot{\mathbf{s}}$ . The relation (2.48) can be rewritten with a suitable tensor of fourth order  $\overset{(\star)}{\mathbb{G}}$  as

$$\overset{\star}{\boldsymbol{\tau}} = \dot{\mathbf{s}} + \overset{(\star)}{\mathbb{G}} : \left( \frac{\partial \mathbf{v}}{\partial \mathbf{X}} \right)^T.$$

For  $\overset{(\star)}{\mathbb{G}}$  there holds

$$\overset{(\star)}{\mathbb{G}} = \overset{(\star)}{G}_{abcd} \mathbf{e}_a \otimes \mathbf{e}_b \otimes \mathbf{e}_c \otimes \mathbf{e}_d \quad (2.51)$$

with

$$\overset{(\star)}{G}_{abcd} := \frac{1}{2} (\sigma_{ad} \delta_{bc} + \sigma_{ac} \delta_{bd} + \sigma_{db} \delta_{ca} + \sigma_{cb} \delta_{da}) - \sigma_{ad} \delta_{cb}. \quad (2.52)$$

Thus we obtain

$$\begin{aligned}
 0 &= \int_{\Omega_0} \rho_0 \mathcal{G} \cdot \dot{\mathbf{f}} \, d\Omega + \int_{\partial\Omega_0} \dot{\underline{\mathbf{t}}} \cdot \mathcal{G} \, d\Gamma - \int_{\Omega_0} (\overset{\circ}{\nabla} \circ \mathcal{G}) : \overset{\star}{\boldsymbol{\tau}} \, d\Omega + \\
 &\quad \int_{\Omega_0} (\overset{\circ}{\nabla} \circ \mathcal{G}) : (\overset{(\star)}{\mathbb{G}} : (\nabla \mathbf{v})^T) \, d\Omega,
 \end{aligned}$$

Using (2.50) the third integral in the above equation can be written as follows:

$$\begin{aligned}
 \int_{\Omega_0} (\overset{\circ}{\nabla} \circ \mathcal{G}) : \overset{\star}{\boldsymbol{\tau}} \, d\Omega &= \int_{\Omega_0} \mathcal{E} : \overset{\star}{\boldsymbol{\tau}} \, d\Omega = \int_{\Omega_0} \mathcal{E} : \mathbb{C} : \mathbf{d}^e \, d\Omega \\
 &= \int_{\Omega_0} \mathcal{E} : \mathbb{C} : (\mathbf{d} - \mathbf{d}^n) \, d\Omega = \int_{\Omega_0} \Sigma : (\mathbf{d} - \mathbf{d}^n) \, d\Omega \\
 &= \int_{\Omega_0} \Sigma : \mathbf{d} \, d\Omega - \int_{\Omega_0} \Sigma : \mathbf{d}^n \, d\Omega \\
 &= \int_{\Omega_0} \Sigma : (\nabla \mathbf{v})^T \, d\Omega - \int_{\Omega_0} 2\mu \mathcal{E} : \mathbf{d}^n \, d\Omega \\
 &= \int_{\Omega_0} (\nabla \circ \mathbf{v}) : \Sigma \, d\Omega - \int_{\Omega_0} 2\mu (\overset{\circ}{\nabla} \circ \mathcal{G}) : \mathbf{d}^n \, d\Omega.
 \end{aligned}$$



Here we have used that the double dot product of a symmetric tensor with the antisymmetric part of a tensor as well as the double dot product of a deviator with the unit tensor vanish. Using that the reference configuration and the actual one agree, hence  $\overset{\circ}{\nabla} = \nabla$  holds, we obtain by partial integration

$$\begin{aligned}
 \int_{\Omega_0} (\overset{\circ}{\nabla} \circ \mathcal{G}) : \overset{*}{\boldsymbol{\tau}} \, d\Omega &= \int_{\Omega_0} (\nabla \circ \mathbf{v}) : \Sigma \, d\Omega - \int_{\Omega_0} 2\mu (\overset{\circ}{\nabla} \circ \mathcal{G}) : \mathbf{d}^n \, d\Omega \\
 &= \int_{\partial\Omega_0} \mathbf{n}_0 \cdot \Sigma \cdot \mathbf{v} \, d\Gamma - \int_{\Omega_0} \mathbf{v} \cdot (\overset{\circ}{\nabla} \cdot \Sigma) \, d\Omega - \\
 &\quad \int_{\Omega_0} 2\mu (\overset{\circ}{\nabla} \circ \mathcal{G}) : \mathbf{d}^n \, d\Omega \\
 &= \int_{\partial\Omega_0} \mathcal{T}_{n_Y} \mathcal{G} \cdot \mathbf{v} \, d\Gamma + \int_{\Omega_0} \mathbf{v} \cdot \underline{\mathcal{F}} \, d\Omega - \\
 &\quad \int_{\Omega_0} 2\mu (\overset{\circ}{\nabla} \circ \mathcal{G}) : \mathbf{d}^n \, d\Omega.
 \end{aligned}$$

If one inserts  $\underline{\mathcal{F}}$  by  $\delta(\mathbf{X}, \mathbf{Y}) \mathbf{e}_a$  with  $a = 1, 2, 3$  and adds the resulting three equations one obtains for  $\mathbf{v}(\mathbf{X})$ ,  $\mathbf{X} \in \Omega_0$  the following representation formula

$$\begin{aligned}
 \mathbf{v}(\mathbf{X}) &= \int_{\partial\Omega_0} \mathcal{G}(\mathbf{X}, \mathbf{Y}) \cdot \dot{\underline{\mathbf{t}}}(\mathbf{Y}) \, d\Gamma_Y - \int_{\partial\Omega_0} \mathcal{T}_{n_Y} \mathcal{G}(\mathbf{X}, \mathbf{Y}) \cdot \mathbf{v}(\mathbf{Y}) \, d\Gamma_Y + \\
 &\quad \int_{\Omega_0} \rho_0 \mathcal{G}(\mathbf{X}, \mathbf{Y}) \cdot \dot{\mathbf{f}}(\mathbf{Y}) \, d\Omega_Y + \int_{\Omega_0} 2\mu \mathcal{E}(\mathbf{X}, \mathbf{Y}) : \mathbf{d}^n(\mathbf{Y}) \, d\Omega_Y + \\
 &\quad + \int_{\Omega_0} \mathcal{E}(\mathbf{X}, \mathbf{Y}) : \left[ \overset{(*)}{\mathbb{G}}(\mathbf{Y}) : (\nabla \mathbf{v})^T(\mathbf{Y}) \right] \, d\Omega_Y,
 \end{aligned}$$

or

$$\begin{aligned}
 \mathbf{v}(\mathbf{X}) &= \int_{\partial\Omega_0} \mathcal{G}(\mathbf{X}, \mathbf{Y}) \cdot \dot{\underline{\mathbf{t}}}(\mathbf{Y}) \, d\Gamma_Y - \int_{\partial\Omega_0} \mathcal{T}_{n_Y} \mathcal{G}(\mathbf{X}, \mathbf{Y}) \cdot \mathbf{v}(\mathbf{Y}) \, d\Gamma + \\
 &\quad \int_{\Omega_0} \rho_0 \mathcal{G}(\mathbf{X}, \mathbf{Y}) \cdot \dot{\mathbf{f}}(\mathbf{Y}) \, d\Omega_Y + \int_{\Omega_0} 2\mu \left[ \overset{\circ}{\nabla} \circ \mathcal{G}(\mathbf{X}, \mathbf{Y}) \right] : \mathbf{d}^n(\mathbf{Y}) \, d\Omega_Y + \\
 &\quad + \int_{\Omega_0} \left[ \overset{\circ}{\nabla} \circ \mathcal{G}(\mathbf{X}, \mathbf{Y}) \right] : \left[ \overset{(*)}{\mathbb{G}}(\mathbf{Y}) : (\nabla \mathbf{v})^T(\mathbf{Y}) \right] \, d\Omega_Y.
 \end{aligned}$$

The last two domain integrals we again integrate by parts and obtain

$$\int_{\Omega_0} 2\mu \left[ \overset{\circ}{\nabla} \circ \mathcal{G} \right] : \mathbf{d}^n \, d\Omega = - \int_{\Omega_0} 2\mu \mathcal{G} \cdot (\overset{\circ}{\nabla} \cdot \mathbf{d}^n) \, d\Omega + \int_{\partial\Omega_0} 2\mu \mathbf{n}_0 \cdot \mathbf{d}^n \cdot \mathcal{G} \, d\Gamma,$$

or, respectively,

$$\begin{aligned} \int_{\Omega_0} [\overset{\circ}{\nabla} \circ \mathcal{G}] : \left[ \overset{(\star)}{\mathbb{G}} : (\nabla \mathbf{v})^T \right] d\Omega &= - \int_{\Omega_0} \mathcal{G} \cdot (\overset{\circ}{\nabla} \cdot \left[ \overset{(\star)}{\mathbb{G}} : (\nabla \mathbf{v})^T \right]) d\Omega \\ &+ \int_{\partial\Omega_0} \mathbf{n}_0 \cdot \left[ \overset{(\star)}{\mathbb{G}} : (\nabla \mathbf{v})^T \right] \cdot \mathcal{G} d\Gamma. \end{aligned}$$

Setting

$$\begin{aligned} \check{\mathbf{f}} &:= \rho_0 \dot{\mathbf{f}} - 2\mu (\overset{\circ}{\nabla} \cdot \mathbf{d}^n) - (\overset{\circ}{\nabla} \cdot \left[ \overset{(\star)}{\mathbb{G}} : (\nabla \mathbf{v})^T \right]), \\ \check{\mathbf{t}} &:= \dot{\underline{\mathbf{t}}} + 2\mu \mathbf{n}_0 \cdot \mathbf{d}^n + \mathbf{n}_0 \cdot \left[ \overset{(\star)}{\mathbb{G}} : (\nabla \mathbf{v})^T \right], \end{aligned}$$

we finally obtain for  $\mathbf{v}(\mathbf{X})$ ,  $\mathbf{X} \in \Omega_0$

$$\begin{aligned} \mathbf{v}(\mathbf{X}) &= \int_{\partial\Omega_0} \mathcal{G}(\mathbf{X}, \mathbf{Y}) \cdot \check{\mathbf{t}}(\mathbf{Y}) d\Gamma_Y - \int_{\partial\Omega_0} \mathcal{T}_{n_Y} \mathcal{G}(\mathbf{X}, \mathbf{Y}) \cdot \mathbf{v}(\mathbf{Y}) d\Gamma_Y + \\ &\int_{\Omega_0} \rho_0 \mathcal{G}(\mathbf{X}, \mathbf{Y}) \cdot \check{\mathbf{f}}(\mathbf{Y}) d\Omega_Y. \end{aligned} \quad (2.53)$$

In the following we use various boundary integral operators acting on the vector valued functions e.g. the single layer potential

$$V\mathbf{t}(\mathbf{X}) := \int_{\partial\Omega_0} \mathcal{G}(\mathbf{X}, \mathbf{Y}) \cdot \mathbf{t}(\mathbf{Y}) d\Gamma_Y, \quad (2.54)$$

the double layer potential

$$K\mathbf{u}(\mathbf{X}) := \int_{\partial\Omega_0} \mathcal{T}_{n_Y} \mathcal{G}(\mathbf{X}, \mathbf{Y}) \cdot \mathbf{u}(\mathbf{Y}) d\Gamma_Y \quad (2.55)$$

the adjoint double layer potential

$$K'\mathbf{t}(\mathbf{X}) := \mathcal{T}_{n_X} \int_{\partial\Omega_0} \mathcal{G}(\mathbf{X}, \mathbf{Y}) \cdot \mathbf{t}(\mathbf{Y}) d\Gamma_Y, \quad \mathbf{X} \in \partial\Omega_0 \quad (2.56)$$

and the hyper singular operator

$$W\mathbf{u}(\mathbf{X}) := -\mathcal{T}_{n_X} \int_{\partial\Omega_0} \mathcal{T}_{n_Y} \mathcal{G}(\mathbf{X}, \mathbf{Y}) \cdot \mathbf{u}(\mathbf{Y}) d\Gamma_Y, \quad \mathbf{X} \in \partial\Omega_0, \quad (2.57)$$

as well as the Newton potential

$$N_0 \mathbf{f}(\mathbf{X}) := \int_{\Omega_0} \mathcal{G}(\mathbf{X}, \mathbf{Y}) \cdot \mathbf{f}(\mathbf{Y}) d\mathbf{Y}. \quad (2.58)$$

With the integral operators we can now write for  $\mathbf{v}(\mathbf{X})$ ,  $\mathbf{X} \in \Omega_0$ :

$$\mathbf{v}(\mathbf{X}) = V \check{\mathbf{t}}(\mathbf{X}) - K \mathbf{v}(\mathbf{X}) + N_0 \check{\mathbf{f}}(\mathbf{X}). \quad (2.59)$$

For  $\mathbf{X} \rightarrow \partial\Omega_0$  there holds together with the jump relations

$$\mathbf{v}(\mathbf{X}) = V \check{\mathbf{t}}(\mathbf{X}) - K \mathbf{v}(\mathbf{X}) + \frac{1}{2} \mathbf{v}(\mathbf{X}) + N_0 \check{\mathbf{f}}(\mathbf{X}), \quad \mathbf{X} \in \partial\Omega_0. \quad (2.60)$$

We derive a second boundary integral equation by applying the boundary traction operator  $T$  on (2.59):

$$T \mathbf{v}(\mathbf{X}) = K' \check{\mathbf{t}}(\mathbf{X}) + W \mathbf{v}(\mathbf{X}) + \frac{1}{2} \check{\mathbf{t}}(\mathbf{X}) + N_1 \check{\mathbf{f}}(\mathbf{X}), \quad \mathbf{X} \in \partial\Omega_0. \quad (2.61)$$

In matrix-vector notation (2.60), (2.61) become

$$\begin{pmatrix} \mathbf{v} \\ T \mathbf{v} \end{pmatrix} = \begin{pmatrix} -K + \frac{1}{2} & V \\ W & K' + \frac{1}{2} \end{pmatrix} \begin{pmatrix} \mathbf{v} \\ \check{\mathbf{t}} \end{pmatrix} + \begin{pmatrix} N_0 \check{\mathbf{f}} \\ N_1 \check{\mathbf{f}} \end{pmatrix}.$$

From the first equation we obtain for  $\check{\mathbf{t}}$ :

$$\check{\mathbf{t}} = V^{-1} \left( K + \frac{1}{2} \right) \mathbf{v} - V^{-1} N_0 \check{\mathbf{f}}$$

and from the second equation  $T \mathbf{v}$

$$T \mathbf{v} = W \mathbf{v} + \left( K' + \frac{1}{2} \right) \check{\mathbf{t}} + N_1 \check{\mathbf{f}}.$$

If one inserts  $\check{\mathbf{t}}$  of the first equation into (2.61), there holds

$$T \mathbf{v} = W \mathbf{v} + \left( K' + \frac{1}{2} \right) V^{-1} \left( K + \frac{1}{2} \right) \mathbf{v} - \left( K' + \frac{1}{2} \right) V^{-1} N_0 \check{\mathbf{f}} + N_1 \check{\mathbf{f}},$$

with the Poincaré-Steklov operator

$$S := W + \left( K' + \frac{1}{2} \right) V^{-1} \left( K + \frac{1}{2} \right) : [H^{1/2}(\partial\Omega_0)]^2 \rightarrow [H^{-1/2}(\partial\Omega_0)]^2$$

we can write

$$T \mathbf{v} = S \mathbf{v} - \left( K' + \frac{1}{2} \right) V^{-1} N_0 \check{\mathbf{f}} + N_1 \check{\mathbf{f}}$$

or

$$S\mathbf{v} = T\mathbf{v} + (K' + \frac{1}{2})V^{-1}N_0\check{\mathbf{f}} - N_1\check{\mathbf{f}}.$$

Now we assume

$$T\mathbf{v} \cong \dot{\underline{\mathbf{t}}} = \mathbf{n}_0 \cdot \dot{\mathbf{s}} \quad (2.62)$$

and multiply the equation (2.62) with a test function  $\boldsymbol{\eta} \in [\tilde{H}^{1/2}(\partial\Omega_{0_N})]^2$ , and integrate over  $\partial\Omega_{0_N}$  and assume equality in (2.62), we obtain

$$\begin{aligned} \langle S\mathbf{v}, \boldsymbol{\eta} \rangle_{\partial\Omega_{0_N}} &= \langle \dot{\underline{\mathbf{t}}}, \boldsymbol{\eta} \rangle_{\partial\Omega_{0_N}} + \langle (K' + \frac{1}{2})V^{-1}N_0\check{\mathbf{f}}, \boldsymbol{\eta} \rangle_{\partial\Omega_{0_N}} - \langle N_1\check{\mathbf{f}}, \boldsymbol{\eta} \rangle_{\partial\Omega_{0_N}} \\ &\quad \text{for all } \boldsymbol{\eta} \in [\tilde{H}^{1/2}(\partial\Omega_{0_N})]^2. \end{aligned}$$

$\langle \cdot, \cdot \rangle_{\partial\Omega_{0_N}}$  denotes the duality pairing between the trace space  $[\tilde{H}^{1/2}(\partial\Omega_{0_N})]^2$  and the dual space  $[H^{-1/2}(\partial\Omega_{0_N})]^2$ , which is defined by

$$\langle \mathbf{v}, \mathbf{u} \rangle_{\partial\Omega_{0_N}} := \int_{\partial\Omega_{0_t}} \mathbf{v}(\mathbf{x})\mathbf{u}(\mathbf{x})d\Gamma, \quad \forall \mathbf{v} \in [\tilde{H}^{1/2}(\partial\Omega_{0_N})]^2, \quad \mathbf{u} \in [H^{-1/2}(\partial\Omega_{0_N})]^2.$$

Now we look for  $\mathbf{v} \in [H^{1/2}(\partial\Omega_0)]^2$  with

$$\begin{aligned} \mathbf{v} &= \hat{\mathbf{v}} & \text{for } \mathbf{Y} \in \partial\Omega_{0_D}, \\ \dot{\underline{\mathbf{t}}} &= \hat{\mathbf{t}} & \text{for } \mathbf{Y} \in \partial\Omega_{0_N}. \end{aligned}$$

Let  $\check{\mathbf{v}} \in [H^{1/2}(\partial\Omega_0)]^2$  be an arbitrary but fixed extension of the Dirichlet data  $\hat{\mathbf{v}} \in [H^{1/2}(\partial\Omega_{0_v})]^2$ .

Set  $\underline{\mathbf{v}} := \mathbf{v} - \check{\mathbf{v}} \in [\tilde{H}^{1/2}(\partial\Omega_{0_t})]^2$ .

Then the weak formulation of our problem reads:

Let  $\check{\mathbf{v}} \in [H^{1/2}(\partial\Omega_0)]^2$ ,  $\hat{\mathbf{t}} \in [H^{-1/2}(\partial\Omega_{0_t})]^2$  and  $\hat{\mathbf{f}} \in [\tilde{H}^{-1}(\Omega_0)]^2$  be given.

find  $\underline{\mathbf{v}} \in [\tilde{H}^{1/2}(\partial\Omega_{0_t})]^2$ , such that for all  $\boldsymbol{\eta} \in [\tilde{H}^{1/2}(\partial\Omega_{0_t})]^2$

$$\langle S\underline{\mathbf{v}}, \boldsymbol{\eta} \rangle_{\partial\Omega_{0_N}} = \langle \hat{\mathbf{t}} - S\check{\mathbf{v}} + (K' + \frac{1}{2})V^{-1}N_0\hat{\mathbf{f}} - N_1\hat{\mathbf{f}}, \boldsymbol{\eta} \rangle_{\partial\Omega_{0_N}}. \quad (2.63)$$

Note that if the Dirichlet data are given than the corresponding rate of traction  $\dot{\underline{\mathbf{t}}}$  on the whole boundary can be determined by solving the Dirichlet boundary value problem:

Let  $\mathbf{v} \in [H^{1/2}(\partial\Omega_0)]^2$  and  $\hat{\mathbf{f}} \in [\tilde{H}^{-1}(\Omega_0)]^2$  be given.

Find  $\hat{\mathbf{t}} \in [H^{-1/2}(\partial\Omega_0)]^2$ , such that for all  $\boldsymbol{\psi} \in [H^{-1/2}(\partial\Omega_0)]^2$

$$\langle V\hat{\mathbf{t}}, \boldsymbol{\psi} \rangle = \langle (K + \frac{1}{2})\mathbf{v}, \boldsymbol{\psi} \rangle - \langle N_0\hat{\mathbf{f}}, \boldsymbol{\psi} \rangle. \quad (2.64)$$

## 2.5.2 Discretization

Now we take a uniform discretization  $\mathbb{T}_h$  of the 2-dimensional domain  $\Omega_0$ , consisting of squares with maximal side-length  $h$ . Let the partitions  $\mathcal{T}_h^D$  and  $\mathcal{T}_h^N$  of the boundaries  $\partial\Omega_{0,D}$ ,  $\partial\Omega_{0,N}$  be induced by  $\mathbb{T}_h$ . If one chooses finite dimensional subspaces of test and trial functions

- $\mathbf{H}_h^{-1/2} \subset [H^{-1/2}(\partial\Omega_0)]^2$

$$\mathbf{H}_h^{-1/2} := \{ \boldsymbol{\psi}_h \in [L_2(\partial\Omega_0)]^2 \mid \forall \mathbf{e} \in \mathbb{T}_h : \boldsymbol{\psi}_h|_{\mathbf{e} \cap \partial\Omega_0} \text{ vector valued, piecewise constant}^1 \},$$

- $\mathbf{H}_h^{1/2} \subset [H^{1/2}(\partial\Omega_0)]^2$

$$\mathbf{H}_h^{1/2} := \{ \boldsymbol{\eta}_h \in [C^0(\partial\Omega_0)]^2 \mid \forall \mathbf{e} \in \mathbb{T}_h : \boldsymbol{\eta}_h|_{\mathbf{e} \cap \partial\Omega_0} \text{ vector valued, piecewise linear}^2 \},$$

- $\mathbf{H}_h^{-1} \subset [\tilde{H}^{-1}(\Omega_0)]^2$

$$\mathbf{H}_h^{-1} := \{ \boldsymbol{\phi}_h \in [L_2(\Omega_0)]^2 \mid \forall \mathbf{e} \in \mathbb{T}_h : \boldsymbol{\phi}_h|_{\mathbf{e}} \text{ vector valued, piecewise linear}^3 \},$$

and if one denotes with  $\mathbf{H}_{N,h}^{1/2}$  and  $\mathbf{H}_{N,h}^{-1/2}$  the boundary  $\mathbf{H}_h^{1/2} \cap [\tilde{H}^{1/2}(\partial\Omega_{0,N})]^2$  and  $\mathbf{H}_h^{-1/2} \cap [H^{-1/2}(\partial\Omega_{0,N})]^2$  respectively, then the Galerkin problem reads:

Let  $\hat{\mathbf{v}}_h \in \mathbf{H}_h^{1/2}$ ,  $\hat{\mathbf{t}}_h \in \mathbf{H}_{N,h}^{-1/2}$  and  $\hat{\mathbf{f}}_h \in \mathbf{H}_h^{-1}$  be given.

<sup>1</sup>On every subinterval  $\tau$  from the discretization  $\mathcal{T}_h$  of boundary  $\partial\Omega_0$  :  $\boldsymbol{\psi}_h|_{\tau}$  constant.

<sup>2</sup>On every subinterval  $\tau$  from the discretization  $\mathcal{T}_h$  of boundary  $\partial\Omega_0$  :  $\boldsymbol{\eta}_h|_{\tau}$  linear.

<sup>3</sup>In every finite element  $\nu$  from the discretization  $\mathbb{T}_h$  :  $\boldsymbol{\phi}_h|_{\nu}$  bilinear (in quadrilateral) or linear (in triangle)

Find  $\underline{\mathbf{v}}_h \in \mathbf{H}_{N,h}^{1/2}$ , such that for all  $\boldsymbol{\eta}_h \in \mathbf{H}_{N,h}^{1/2}$

$$\langle S\underline{\mathbf{v}}_h, \boldsymbol{\eta}_h \rangle_{\partial\Omega_{0N}} = \langle \hat{\mathbf{t}}_h - S\underline{\mathbf{v}}_h + (K' + \frac{1}{2})V^{-1}N_0\hat{\mathbf{f}}_h - N_1\hat{\mathbf{f}}_h, \boldsymbol{\eta}_h \rangle_{\partial\Omega_{0N}} \quad (2.65)$$

Afterwards the following discrete problem must be solved:

Let  $\mathbf{v}_h \in \mathbf{H}_h^{1/2}$  and  $\hat{\mathbf{f}}_h \in \mathbf{H}_h^{-1}$  be given.

Find  $\hat{\mathbf{t}}_h \in \mathbf{H}_h^{-1/2}$ , such that for all  $\boldsymbol{\psi}_h \in \mathbf{H}_h^{-1/2}$

$$\langle V\hat{\mathbf{t}}_h, \boldsymbol{\psi}_h \rangle = \langle (K + \frac{1}{2})\mathbf{v}_h, \boldsymbol{\psi}_h \rangle - \langle N_0\hat{\mathbf{f}}_h, \boldsymbol{\psi}_h \rangle. \quad (2.66)$$

### 2.5.3 Benchmarks

We consider a quadratic plate which is in plane strain and has side length 2 units, which is fixed on the top and a constant velocity  $v_y = 10^{-3}$ in/s is applied at its lower side in the whole time interval considered. During the deformation the lower edge can not become smaller in horizontal direction. It can be shown that in this example all components of the given boundary traction rate  $\hat{\mathbf{t}}$  remain zero during the whole deformation. A viscoplastic material law (Hart's modell) is assumed. The following initial values and material parameters are used for steel at a temperature at  $400^\circ\text{C} \equiv 673\text{K}$ . The linear system within each fix point step is solved using the Conjugate Gradient method with the diagonal preconditioner. In average we need 2-3 fix point iterations pro time step.

material parameter	value	unit
$\lambda$	0.15	-
$M$	7.8	-
$m$	5	-
$\mathcal{M}$	$0.91 \cdot 10^{11}$	Pa
$E$	$0.168 \cdot 10^{12}$	Pa
$\nu$	0.298	-
$\lambda_0$	3.15	$\text{s}^{-1}$
$\sigma_0$	$0.689 \cdot 10^8$	Pa
$\lambda_{sT}^{(*)}$	$1.841 \cdot 10^{-28}$	$\text{Pa}^{-1}$
$\sigma_s^*$	$0.689 \cdot 10^8$	Pa
$T_B$	673	K
$\beta$	$0.123 \cdot 10^{10}$	Pa
$\delta$	1.33	-

Table 2.1: Material data

Numerical results of the simulations using BE and FE methods are depicted in the

Figures 2.7 and 2.6. The BEM results correspond to the 30 sec of real time simulation, whereas FEM for 50 sec.

The domain discretization is presented in the figures 2.7.e and 2.6.e The BE discretization is done by the segmentation of the boundary  $\partial\Omega$   $16 \cdot 4$  intervals. The FE discretization is done by the decomposition of the domain  $\Omega$  in  $16 \cdot 16$  quadrilaterals. That corresponds to 30 BEM- und 255 FEM- degrees of freedom.. On the figures 2.7.a, 2.7.b and 2.6.a, 2.6.b are depicted the coefficients  $d_{yy}^n(s^{-1})$  of the rate-of-deformations tensor  $d_{yy}^n(s^{-1})$  and  $\sigma_{yy}$  of the Cauchy stress tensor  $\sigma$ . One can clearly see that the  $\sigma_{yy}$  reaches its maximum value at the corners of the plate. Consequently the non-elastic zone appears at corners and moved the center of the plate. This can be explained because of the jump of the boundary conditions at the corners from Dirichlet to Neumann. The components of the displacement in  $x$ - respectively  $y$ -direction at the end of the simulation are represented on the figures 2.7.a, 2.7.b for BEM and 2.6.a, 2.6.b for FEM. They qualitatively comply with expectations. The bottom edge of the plate is fixed in  $x$ - direction and the is shifted in  $y$ - direction by 0.03 units for BEM and by 0.05 units for FEM. These values agree with the given boundary data. On the distribution of the displacements on can see that the plate is tapered to the center in the horizontal direction.

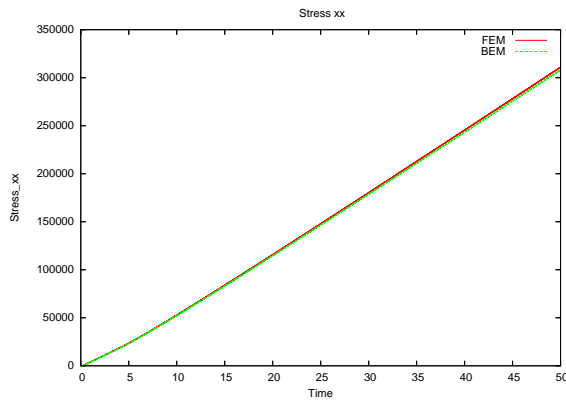


Figure 2.2: FEM-BEM comparison ( $\sigma_{xx}$ )

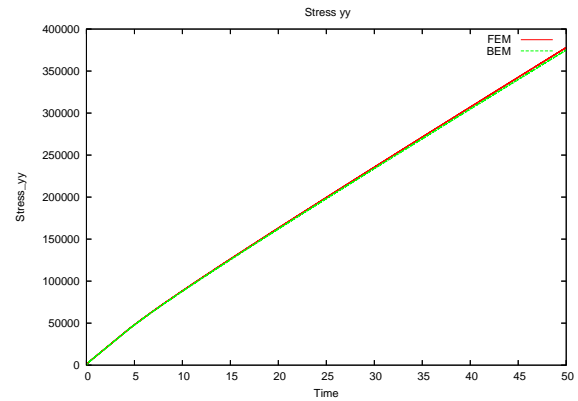


Figure 2.3: FEM-BEM comparison ( $\sigma_{yy}$ )

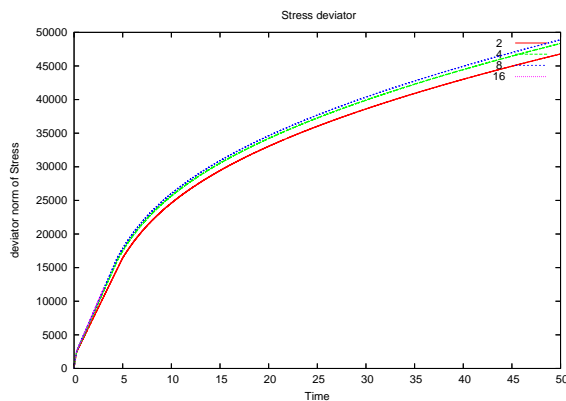


Figure 2.4: Convergence of BEM approach

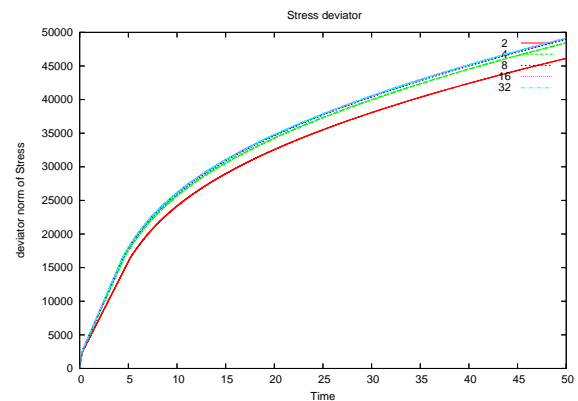


Figure 2.5: Convergence of FEM approach

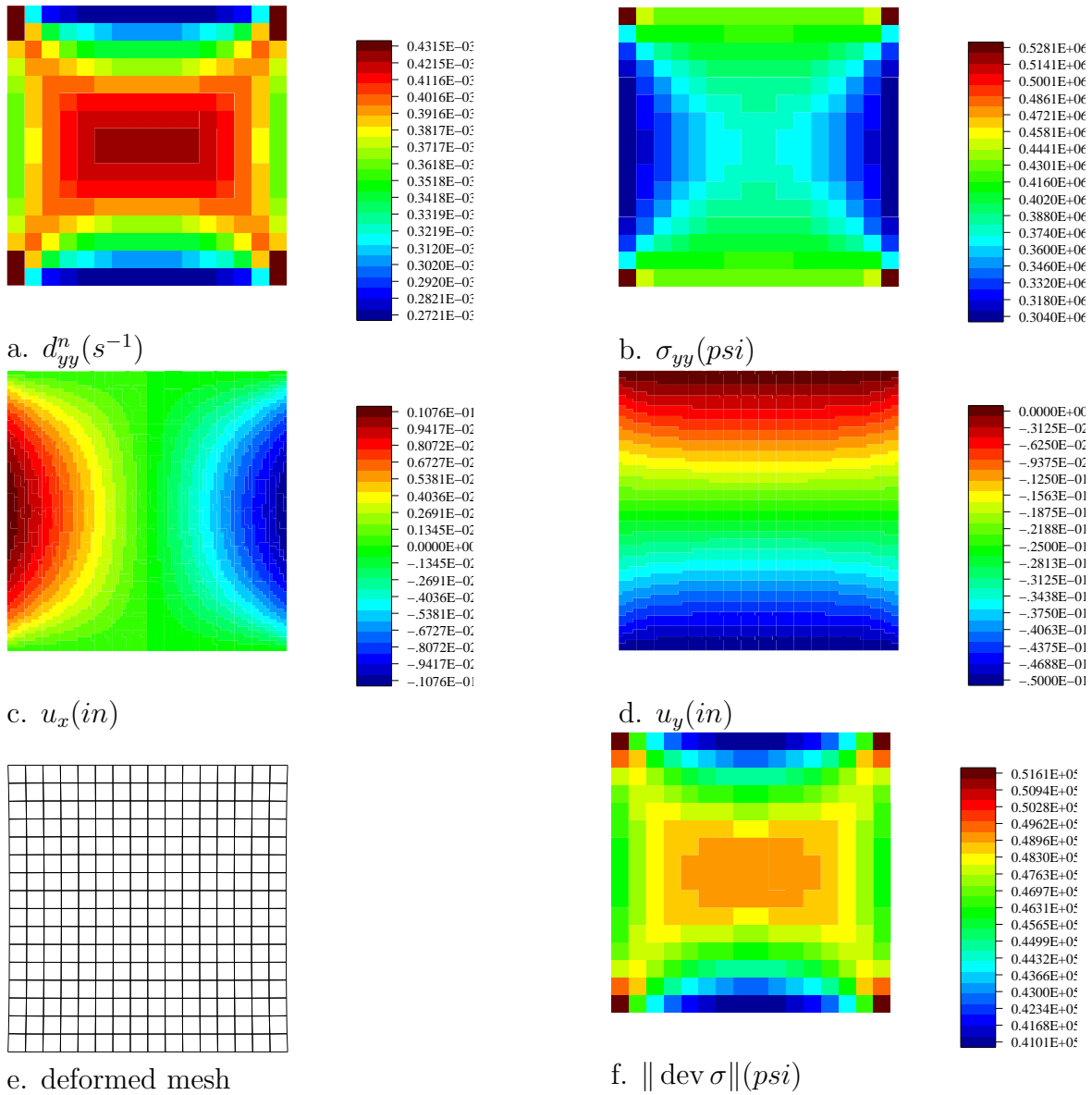


Figure 2.6: FEM (after 50 second simulation )



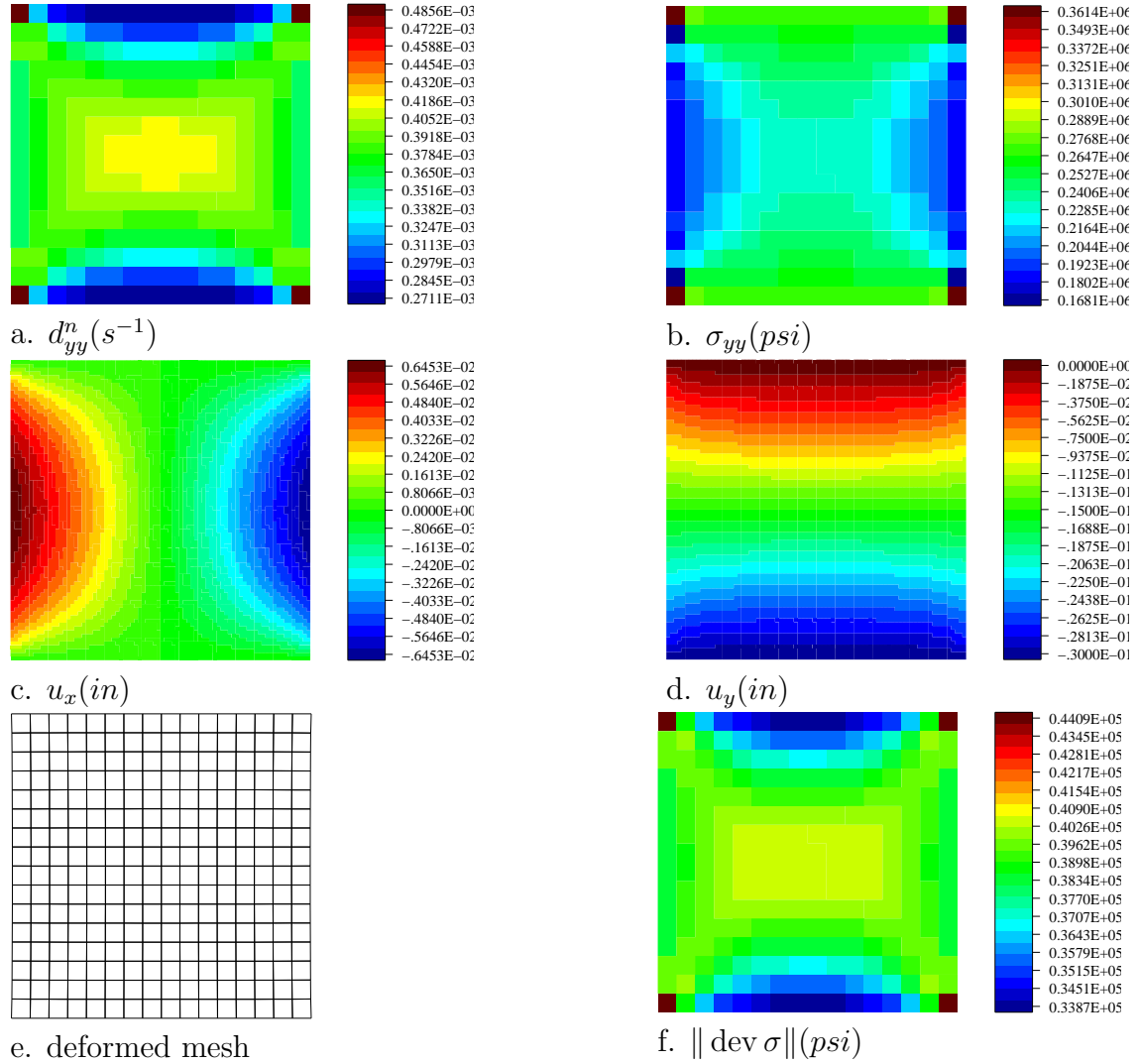


Figure 2.7: BEM (after 30 second simulation )

### 2.5.4 Implementation

The figure 2.8 shows our boundary element program, realized within the program package *maiprogs*

The BEM program consists of two nested loops. The outer loop corresponds to the time discretization and stops when the final time of simulation is obtained. Within the interior loop  ${}^t \mathbf{v}_{\tilde{\mathcal{B}}}$  is computed iteratively. The linear system (2.65) is solved using the Conjugate Gradient method yielding  ${}^t \mathbf{v}_{\partial \tilde{\mathcal{B}}_t}^{(k+1)}$ . Since for the discrete Poincré-Steklov operator the matrix  $V^{-1}$  was already used and therefore stored, it is now in our disposal. In order to compute  $\hat{\mathbf{t}}_{\partial \tilde{\mathcal{B}}}^{(k+1)}$  we therefore do not need to solve system (2.66) but only to perform a matrix vector multiplication. When  ${}^t \mathbf{v}_{\partial \tilde{\mathcal{B}}_N}^{(k+1)}$  and  $\hat{\mathbf{t}}_{\partial \tilde{\mathcal{B}}}^{(k+1)}$  are known  ${}^t \mathbf{v}_{\tilde{\mathcal{B}}}^{(k+1)}$  can be computed using the representation formula (2.53). With known  ${}^t \mathbf{v}_{\tilde{\mathcal{B}}}^{(k+1)}$  we can compute

## 2 Hypoelasto-viscoplasticity. Large deformations

$\hat{\mathbf{f}}_{\tilde{\mathcal{B}}}^{(k+1)}$  as shown in the flow chart. With this new right hand side one restarts the loop as documented. After the inner loop was completed and  ${}^t\mathbf{v}_{\tilde{\mathcal{B}}}$  is known then the actual state at time step  $t_{n+1}$  i.e.  $\{\boldsymbol{\sigma}_{n+1}, \mathbf{d}_{n+1}^n, \boldsymbol{\varepsilon}_{n+1}^a, \boldsymbol{\sigma}_{n+1}^*\}$  in  $\tilde{\mathcal{B}}$ , is computed by local integration of the constitutive equations. Afterwards  $\overset{(*)}{\mathbb{G}}_{\tilde{\mathcal{B}}}$  and  $\mathbf{u}_{\tilde{\mathcal{B}}}$  which are used for the right hand side and the Galerkin system and for the Lagrangian update procedure respectively.

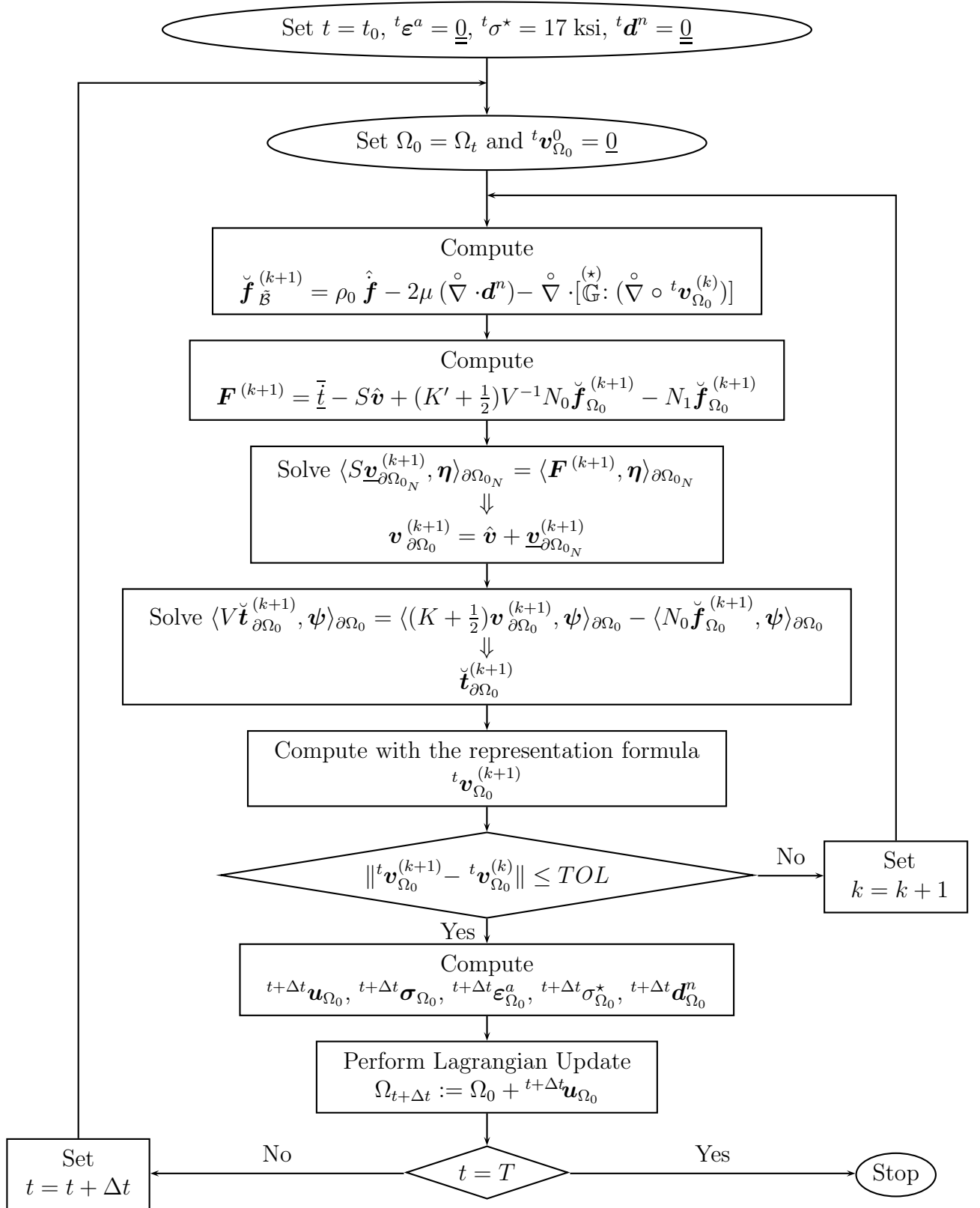


Figure 2.8: Flow chart. BEM discretization

### 2.5.5 Discretization with finite elements

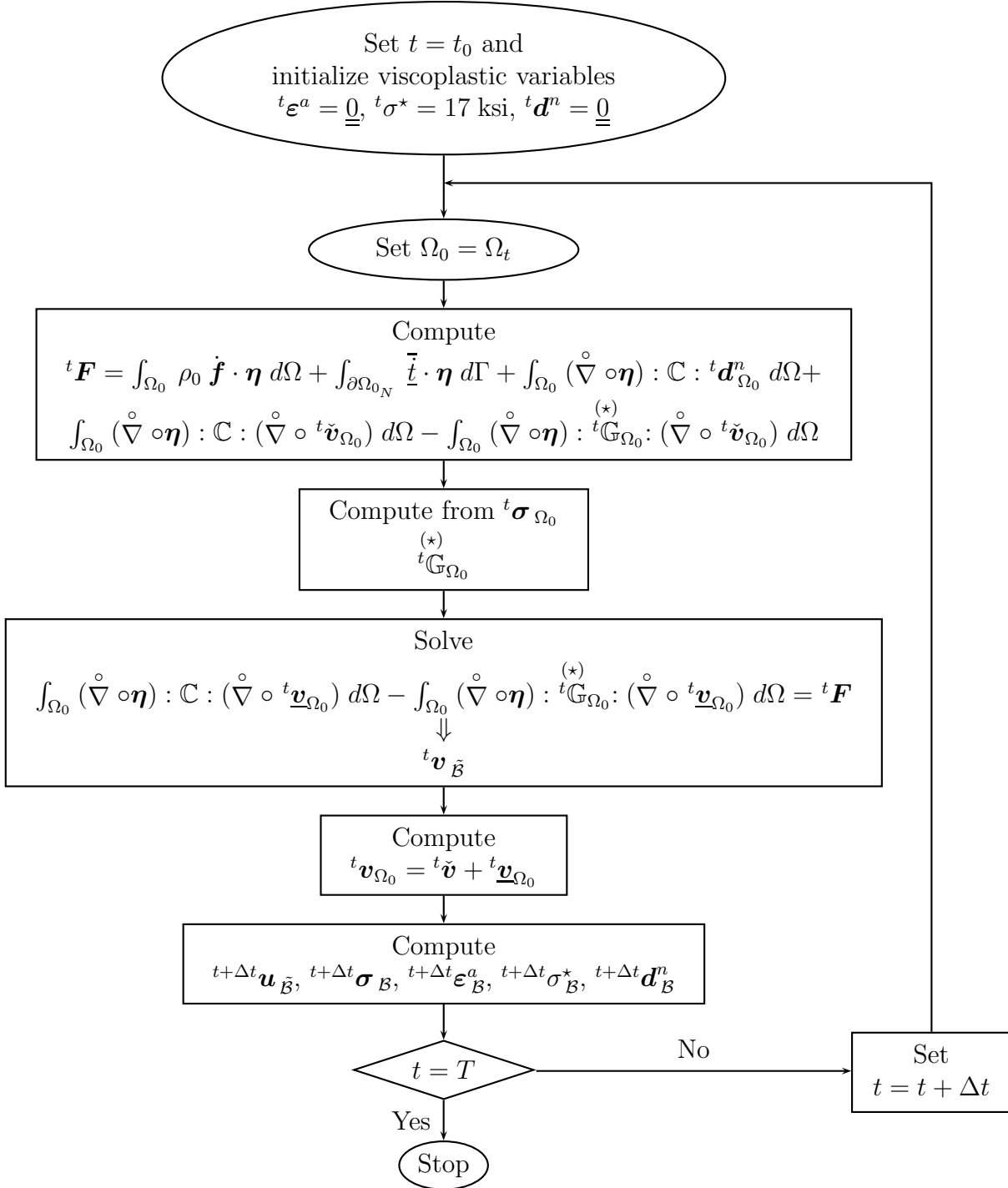


Figure 2.9: Flow chart. FEM discretization

## 2.6 Boundary element and finite element procedures for metal chipping

We present finite element/boundary element procedure for viscoplastic-thermomechanical problems and coupled thermoelastic formulation for contact problems. We consider a 2-body problem with a linear elastic worktool and viscoplastic workpiece. We allow large deformations and consider an initial boundary value problem for velocity and temperature. The viscoplastic material law under consideration is Hart's model. The mechanical equation and the heat conduction equation are solved by staggered iteration. We discretize the mechanical contact equation by finite elements for the viscoplastic material and by boundary elements for the elastic worktool. The heat conduction equation is discretized using backward Euler in time and finite elements in space. Time stepping procedure together with Lagrangian update is performed which takes care of the change of configuration.

### 2.6.1 Viscoplastic thermomechanical coupling

We consider the following initial boundary value problem for velocity and temperature. Let  $\mathbf{u}^i(0, \mathbf{X})$  denote the initial displacement,  $\mathbf{v}^i(0, \mathbf{X})$  the initial velocity and  $\Theta^i(0, \mathbf{X})$  the initial temperature ( $i=1,2$ ). Then we look for  $\mathbf{v}^B \in \mathbf{H}^1(\Omega_t^B)$ ,  $\mathbf{v}^A \in \mathbf{H}^{1/2}(\Gamma_t^A := \Gamma_{tN}^A \cup \Gamma_{tC}^A)$ ,  $\Theta := (\Theta^B, \Theta^A) \in H^1(\Omega_t := (\Omega_t^B, \Omega_t^A))$ ,  $0 \leq t \leq T$

$$\begin{aligned} \int_{\Omega_t^B} (\nabla \mathbf{v}^B) : \mathbb{C} : (\nabla \boldsymbol{\eta}^B) - \int_{\Omega_t^B} (\nabla \mathbf{v}^B) : \mathbb{G}^T(\boldsymbol{\sigma}^B) : (\nabla \boldsymbol{\eta}^B) + \langle S \mathbf{v}^A, \boldsymbol{\eta}^A \rangle_{\Gamma_t^A} \\ + \langle \dot{\mathbf{t}}_C(\mathbf{v}^B, \mathbf{v}^A), \boldsymbol{\eta}^{BA} \rangle_{\Gamma_{tC}^B} - \int_{\Omega_t^B} \mathbf{d}^n : \mathbb{C} : \nabla \boldsymbol{\eta}^B = 0, \end{aligned} \quad (2.67)$$

$$\int_{\Omega_t} \left[ \frac{\partial \Theta}{\partial t} \vartheta + \varkappa \nabla \Theta \nabla \vartheta \right] - \gamma_{12} \int_{\Gamma_{tC}^B} \mathbf{t}_C \cdot \mathbf{n}^A \Theta^{AB} \vartheta^{AB} - \int_{\Gamma_{tC}^B} \mu_f \mathbf{t}_C \cdot \mathbf{n}^A |\mathbf{v}_T^{AB}| (\gamma_1 \vartheta^B + \gamma_2 \vartheta^A) = 0 \quad (2.68)$$

with  $\boldsymbol{\eta}^B$  in  $\Omega_t^B$ ,  $\boldsymbol{\eta}^A$  on  $\Gamma_t^A$ ,  $\vartheta$  in  $\Omega_t$ ,  $\varkappa := \frac{k}{\rho c}$ ,  $\rho$  - density,  $c$  - heat capacity,  $k$  - heat conductivity. In the contact term on  $\Gamma_{tC}^B$   $\dot{\mathbf{t}}_C = \frac{\partial \mathbf{t}_C}{\partial \mathbf{u}} \mathbf{v}$  denotes the rate of the boundary traction.  $\mathbf{d}^n$  describes the viscoplasticity,  $\mu_f$  is the friction coefficient and the boundary integral operator  $S$  is the Steklov-Poincaré operator of linear elasticity. With  $\Theta^{AB}$  and  $\boldsymbol{\eta}^{AB}$  we denote the jump of the temperature and displacement between the two bodies respectively.  $\mathbf{n}^A$  is the exterior for  $\Omega_t^A$ .

Next we discretize the system (2.67)-(2.68) by using finite elements and boundary elements in space and finite differences in time. We discretize the velocity in the work piece with finite elements and in the work tool with boundary elements whereas the temperature is in both bodies discretized by finite elements. At each time step  $k = 1, \dots, N$  we look for a continuous piecewise linear function  $\mathbf{v}_{kh}^B$  in  $\Omega_{t_{k-1}}^B$  and a continuous piecewise linear function  $\mathbf{v}_{kh}^A$  on  $\Gamma_{t_{k-1}}^A$  and continuous piecewise linear function  $\Theta_{kh}$  in  $\Omega_{t_{k-1}}$  satisfying

$$\begin{aligned} \int_{\Omega_{t_{k-1}}^B} (\nabla \mathbf{v}_{kh}^B) : \mathbb{C} : (\nabla \boldsymbol{\eta}_h^B) - \int_{\Omega_{t_{k-1}}^B} (\nabla \mathbf{v}_{kh}^B) : G^{(*)T}(\boldsymbol{\sigma}_{k-1,h}) : (\nabla \boldsymbol{\eta}_h^B) + \langle S \mathbf{v}_{kh}^A, \boldsymbol{\eta}_h^A \rangle_{\Gamma_{t_{k-1}}^A} \\ + \langle \mathbf{t}_{C_{kh}}(\mathbf{v}_{kh}^B, \mathbf{v}_{kh}^A), \boldsymbol{\eta}_h^{BA} \rangle_{\Gamma_{t_{k-1}}^B} = \int_{\Omega_{t_{k-1}}^B} \mathbf{d}_{k-1,h}^{(n)} : \mathbb{C} : \nabla \boldsymbol{\eta}_h^B, \end{aligned} \quad (2.69)$$

$$\begin{aligned} \int_{\Omega_{t_{k-1}}} \left[ \frac{\Theta_{kh} - \Theta_{k-1,h}}{\Delta t} \vartheta_h + \boldsymbol{\varkappa} \nabla \Theta_{kh} \nabla \vartheta_h \right] - \gamma_{12} \int_{\Gamma_{t_{k-1}}^B} \mathbf{t}_{C_{kh}} \cdot \mathbf{n}^A [\Theta_{kh}] [\vartheta_h], \\ = \int_{\Gamma_{t_{k-1}}^B} \mu_f \mathbf{t}_{C_{kh}} \cdot \mathbf{n}^A |\mathbf{v}_{kh}^{AB}| (\gamma_1 \vartheta_h^B + \gamma_2 \vartheta_h^A) \quad (\text{backward Euler}) \end{aligned} \quad (2.70)$$

with test functions  $\boldsymbol{\eta}_h^B$  in  $\Omega_{t_{k-1}}^B$ ,  $\boldsymbol{\eta}_h^A$  on  $\Gamma_{t_{k-1}}^A$  and  $\vartheta_h$  in  $\Omega_{t_{k-1}}$ . We solve the above discretization (2.69), (2.70) with a staggered iteration as follows (see also [16]):

Start with  $\mathbf{u}^i(0, \mathbf{X})$ ,  $\mathbf{v}^i(0, \mathbf{X})$ ,  $\Theta(0, \mathbf{X})$  and initial configuration  $\Omega_0^i$ , for  $k = 1, \dots, N$  do :

1. use (2.69) to compute  $\mathbf{v}_{kh}^B$  in  $\Omega_{t_{k-1}}^B$ ,  $\mathbf{v}_{kh}^A$  on  $\Gamma_{t_{k-1}}^A$ ,  
use (2.70) to compute  $\Theta_{kh}$  in  $\Omega_{t_{k-1}}^B \cup \Omega_{t_{k-1}}^A$ .
2. apply the Lagrangian update,  $\mathbf{u}_{kh}^i := \mathbf{v}_{kh}^i \Delta t$ .

$$\begin{array}{ll} \Omega_{t_{k-1}}^i \text{ map } \Omega_{t_k}^i & \text{by setting } \mathbf{x}_k^i = \mathbf{x}_{k-1}^i + \mathbf{x}_{kh}^i, \\ \Gamma_{t_{k-1}}^A \text{ map into } \Gamma_{t_k}^A & \text{with } \mathbf{x}_k^A = \mathbf{x}_{k-1}^A + \mathbf{u}_{kh}^A. \end{array}$$

3. update  $\boldsymbol{\sigma}_{k-1,h}$  using Hart's model constitutive equations:

$$\boldsymbol{\sigma}_{k-1,h}^B \xrightarrow{\mathbf{v}_{kh}^B, \Theta_{kh}} \boldsymbol{\sigma}_{kh}^B.$$

4. return to 1.

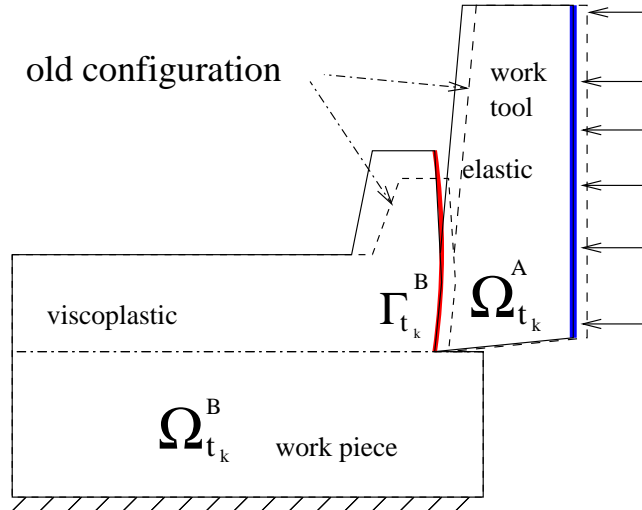


Figure 2.10: Model problem

In order to solve the contact problem (normal/tangential parts) we apply a penalty method introduced in Section 1.2 and linearized in Section 1.3 with penalty parameters  $\epsilon_{\mathcal{T}}$ ,  $\epsilon_{\mathcal{N}}$  and a gap function  $\text{Gap} - g_k$ .

$$\langle \dot{\mathbf{t}}_{khC}(\mathbf{v}_{kh}^B, \mathbf{v}_{kh}^A), [\boldsymbol{\eta}_h] \rangle_{\Gamma_C^B} = \frac{1}{\epsilon_{\mathcal{N}}} \int_{\Gamma_C^B} [\mathbf{v}_{kh}]_N^{(+)} [\boldsymbol{\eta}_h]_N + \begin{cases} \frac{1}{\epsilon_{\mathcal{T}}} \int_{\Gamma_C^B} [\mathbf{v}_{kh}]_{\mathcal{T}} [\boldsymbol{\eta}_h]_{\mathcal{T}} & \text{stick} \\ \frac{\mu}{\epsilon_{\mathcal{N}}} \int_{\Gamma_C^B} [\mathbf{v}_{kh}]_N [\boldsymbol{\eta}_h]_{\mathcal{T}} & \text{slip} \end{cases} \quad (2.71)$$

$$[\mathbf{v}_{kh}]_N^{(+)} := \begin{cases} [\mathbf{v}_{kh}]_N, & \text{if } 0 > g_{k-1}, \\ 0, & \text{if } 0 \leq g_{k-1}. \end{cases}$$

Hence, the discrete solution of problem (2.69, 2.70) depends on the discretization parameters  $h$ ,  $\Delta t$ ,  $\epsilon_{\mathcal{N}}$ ,  $\epsilon_{\mathcal{T}}$ . The optimal choice for the parameters is an open question, an indication for it can only be obtained by a series of numerical simulation. These simulations are obtained by inserting the expression (2.71) into the discretization (2.69) yields a linear system for  $\mathbf{v}_{kh}^i$ . Note that the term  $\mathbb{G}^{(*)T}(\boldsymbol{\sigma}_{k-1h})$  is explicitly computed with Hart's modell at the former time step.

Next, we introduce Hart's modell with viscoplastic interior variables [25].

## 2 Hypoelasto-viscoplasticity. Large deformations

- It uses the strain rate  $\mathbf{d}_{k-1}^{(n)}$  and the velocity gradient  $\mathbf{d}_k^{(e)} := \nabla^{sym} \mathbf{v}_k - \mathbf{d}_{k-1}^{(n)}$

- Hart's modell describes hypoelastic material law  $\boldsymbol{\sigma}_k^* := \mathbb{C} : \mathbf{d}_k^{(e)} = \mathbb{C} : (\nabla^{sym} \mathbf{v}_k - \mathbf{d}_{k-1}^{(n)}) \implies \boldsymbol{\sigma}_k \implies \boldsymbol{\sigma}'_k$

•

$$\left. \begin{aligned} \boldsymbol{\varepsilon}_k^* &:= \mathbf{d}_{k-1}^{(n)} - \sqrt{\frac{3}{2}} \lambda_{k-1}^{(*)} \left[ \ln \left( \frac{\sigma_{k-1}^*}{\sqrt{\frac{2}{3}} \mathcal{M} \|\boldsymbol{\varepsilon}_{k-1}^a\|} \right) \right]^{-1/\lambda} \frac{\boldsymbol{\varepsilon}_{k-1}^a}{\|\boldsymbol{\varepsilon}_{k-1}^a\|} \\ \dot{\sigma}_k^* &:= \sigma_{k-1}^* \lambda_{k-1}^{(*)} \left[ \ln \left( \frac{\sigma_{k-1}^*}{\sqrt{\frac{2}{3}} \mathcal{M} \|\boldsymbol{\varepsilon}_{k-1}^a\|} \right) \right]^{-1/\lambda} \left( \frac{\beta}{\sigma_{k-1}^*} \right)^\delta \left( \frac{\sqrt{\frac{2}{3}} \mathcal{M} \|\boldsymbol{\varepsilon}_{k-1}^a\|}{\sigma_{k-1}^*} \right)^{\beta/\sigma_{k-1}^*} \end{aligned} \right\} \implies \boldsymbol{\varepsilon}_k^a, \sigma_k^*$$

•

$$\mathbf{d}_k^{(n)} := \frac{\lambda_0}{(\sigma_0)^M} \left( \sqrt{\frac{3}{2}} \right)^{M+1} \|\boldsymbol{\sigma}'_k - \frac{2}{3} \mathcal{M} \cdot \boldsymbol{\varepsilon}_k^a\|^{M-1} \left( \boldsymbol{\sigma}'_k - \frac{2}{3} \mathcal{M} \boldsymbol{\varepsilon}_k^a \right),$$

where

$$\lambda_{k-1}^{(*)} := \lambda_{sT}^{(*)} \cdot \left( \frac{\sigma_{k-1}^*}{\sigma_s^*} \right)^m \exp \left[ -\frac{Q}{R} \left( \frac{1}{\Theta_{k-1}} - \frac{1}{\Theta_B} \right) \right].$$

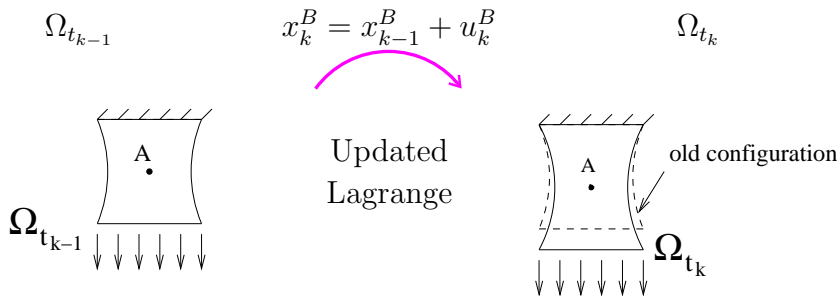
On the other hand the linear elastic work tool is modelled wit BEM using the boundary integral operators as in 1.2.2.

Substituting linearized version of (2.71) in (2.69) we obtain linear system for  $\mathbf{v}_{kh}^i$ .

The applicability of our approach is demonstrated in the following by several benchmark simulations.

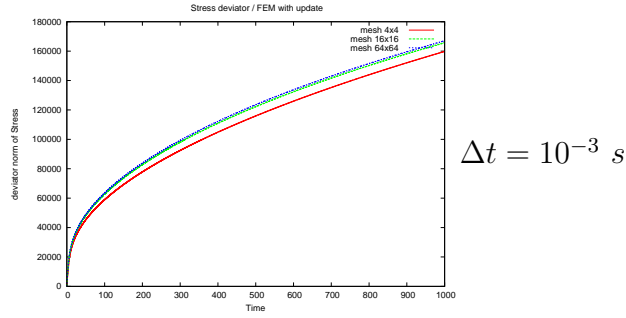
### 2.6.2 Benchmarks

#### Example 1. Tensile test: 1-Body

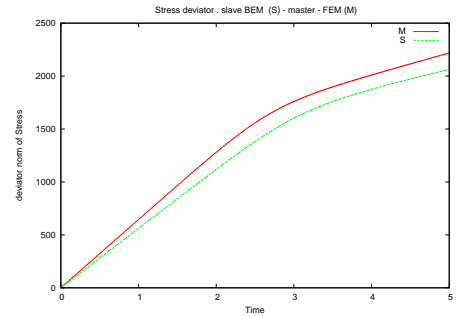
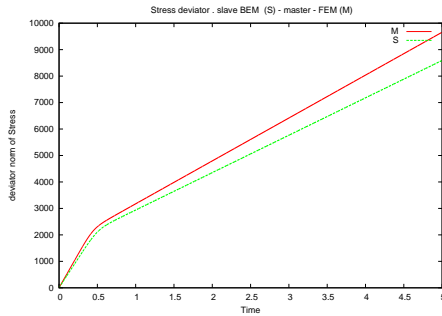
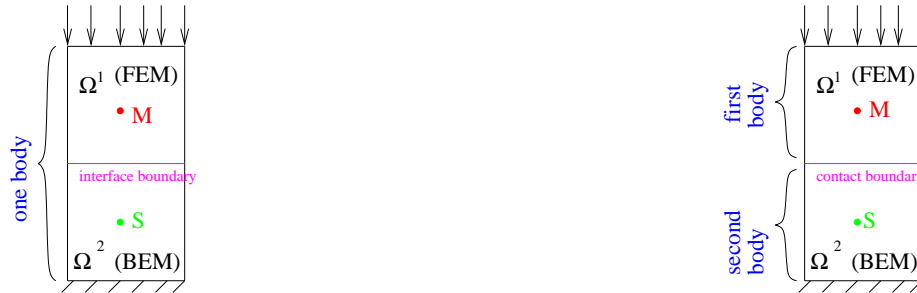




## 2.6 Boundary element and finite element procedures for metal chipping



Comparison of interface and contact modeling for viscoplastic material. We use both FEM and BEM (but without Lagrangian update) [21].



**Example 2. Metal chipping** In this section we consider an application of the FEM/BEM coupling on the metal chipping processes. Each body is discretized with finite elements: rectangles in work piece and triangles in work tool. We use Finite Element Method for approximating the displacement field with continuous piecewise bilinear shape functions in work piece and Boundary Element method for approximating the displacement field with continuous piecewise linear shape functions on the boundary of the work tool. This choice is quite reasonable, since the work tool in practice undergoes quite small deformations with respect to work piece. Therefore, we choose BEM for describing nearly linear deformations in work tool. For reasons of simplicity we use FE approach for the temperature field and approximate it with piecewise bilinear/linear functions in the work piece/tool respectively. We should mention that a replacement of a discretization procedure for temperature could be done in the same manner like for mechanical part. The Figure 2.10 shows the model problem geometry. We introduce

a prescribed line, that goes through the work piece, in order to simulate the material separation in work piece along the crack line, that is not known a-priori and actually has to be obtained. We will call the prescribed line *crack line*. Introducing the *crack line* we overcome a difficulty with determining the actual propagation path of the crack. But it is quite natural to expect that crack will propagate along the horizontal line in case of horizontally moving work tool from the right to the left (see Figure 2.10). This approach can be considered as the zero order approximation to the real case. The linear system within each fix point step is solved using the Conjugate Gradient method with the diagonal preconditioner. In average we need 2-3 fix point iterations pro time step.

On the Figure 2.11(j) depicted the initial mesh. The Cartesian norm of stress deviator ( $\|\text{dev } \boldsymbol{\sigma}\| := \sqrt{\sum_{j,i=1}^3 (\text{dev } \boldsymbol{\sigma})_{ij}^2}$ ) in both bodies is presented on Figure 2.11(a)-(i) for different time-steps..

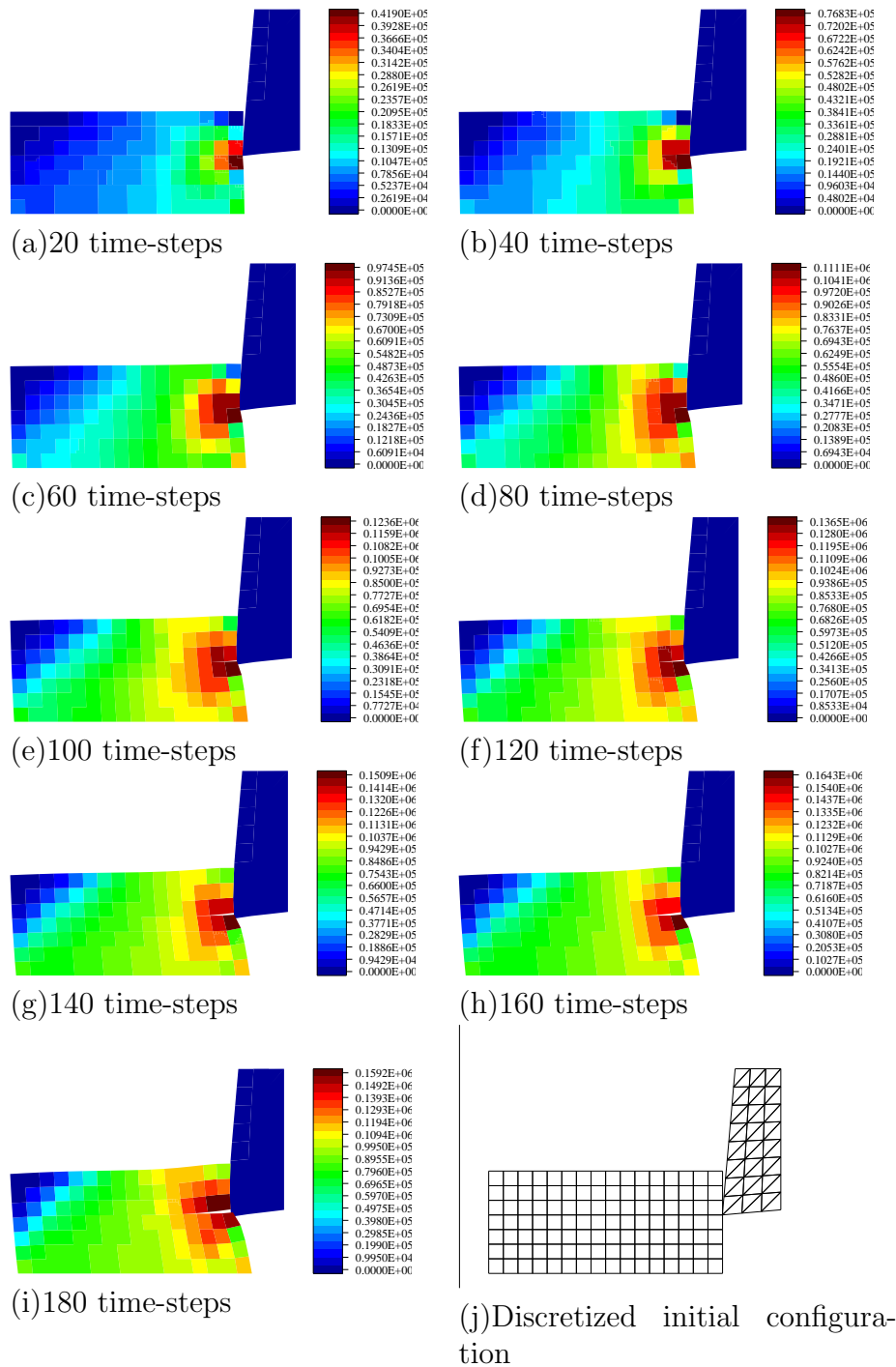


Figure 2.11: Metal chipping



# 3 Appendix

## 3.1 Implementation

In this section we present some tools necessary for the implementation of numerical methods presented in this thesis. Implementation techniques of Boundary and Volume Integral Operators needed for BEM for elastoplastic 2-body contact Section 1.2.2 discussed in Section 3.1.1. In Section 3.1.2 we explain the computation of stiffness matrixes for hypoelasto-viscoplasticity under Hart's model using software package `maiprogs`. The implementation is done by the author of this thesis as an internal library of software package `maiprogs` [38, 36, 37]. If you have an original version of the package you can find the latest documentation in the subdirectory `doku`.

### 3.1.1 Boundary operators and volume potentials

We consider an elastoplastic body occupying a Lipschitz domain  $\Omega \subset \mathbb{R}^d$ ,  $d = 2, 3$  with boundary  $\Gamma := \partial\Omega$ . If the body is in equilibrium, then for all  $x \in \Omega$  the displacement vector and the stress tensor at  $x$  are uniquely determined by displacements and tractions on the boundary  $\Gamma$ , body forces and plastic strains in the domain  $\Omega$ . These relations are given by mean of boundary integral operators and Newton volume potentials as follows (for convenience we present componentwise representation).

$$\begin{aligned} u_i(x) &= \int_{\Gamma} u_{ij}^*(x, y) p_j(y) - \int_{\Gamma} p_{ij}^*(x, y) u_j(y) + \int_{\Omega} u_{ij}^*(x, y) b_j(y) \\ &+ \int_{\Omega} \hat{\sigma}_{jki}^*(x, y) \varepsilon_{jk}^a(y) \end{aligned} \quad (3.1)$$

$$\begin{aligned} \sigma_{ij}(x) &= \int_{\Gamma} u_{ijk}^*(x, y) p_k(y) - \int_{\Gamma} p_{ijk}^*(x, y) u_k(y) + \int_{\Omega} u_{ijk}^*(x, y) b_k(y) \\ &+ \int_{\Omega} \hat{\sigma}_{ijkl}^*(x, y) \varepsilon_{kl}^a(y) + f_{ij}(\varepsilon_{kl}^a) \end{aligned} \quad (3.2)$$

$$f_{ij}(\varepsilon_{ij}^a) := -\frac{G}{4(1-\nu)} [2\varepsilon_{ij}^a + (1-4\nu)e\delta_{ij}] \quad (3.3)$$

Here and later on the summation is applied with respect to repeated index. Indexes  $i$ ,  $j$ ,  $k$ ,  $l$  runs from 1 to 3 in 3D and take values 1 and 2 in 2D. The kernels  $p_{ij}^*$ ,  $u_{ij}^*$ ,  $\hat{\sigma}_{jki}^*$ ,

### 3 Appendix

$u_{ijk}^*$ ,  $\hat{\sigma}_{ijkl}^*$  are defined in next section.  $e := \varepsilon_{11}^a + \varepsilon_{22}^a + \varepsilon_{33}^a$  in 3D case and plain strain case in 2D.

#### Definition of kernels

**Definition 3.1.1.** Kernel  $u_{ij}^*$  corresponds to the Single Layer Potential  $(V\psi)_i(x) = \int_{\Gamma} u_{ij}^*(x, y)\psi_j(y) d\Gamma_y$ , where  $\psi \in \mathbf{H}^{-1/2}(\Gamma)$ ,  $x \in \Gamma \subset \mathbb{R}^2$  and to the Newton potential  $(N_0\psi)_i(x) = \int_{\Omega} u_{ij}^*(x, y)\psi_j(y) d\Omega_y$ , where  $\psi \in \mathbf{H}^1(\Omega)$ ,  $x \in \Gamma \subset \mathbb{R}^2$

$$u_{ij}^*(x, y) := \frac{1}{16\pi(1-\nu)G|x-y|} \left\{ (3-4\nu)\delta_{ij} + \frac{(x_i-y_i)(x_j-y_j)}{|x-y|^2} \right\} \quad 3D,$$

$$u_{ij}^*(x, y) := \frac{-1}{8\pi(1-\nu)G} \left\{ (3-4\nu)\ln|x-y|\delta_{ij} - \frac{(x_i-y_i)(x_j-y_j)}{|x-y|^2} \right\} \quad 2D.$$

**Definition 3.1.2.** Kernel  $p_{ij}^*$  corresponds to the Double Layer Potential  $(K\psi)_i(x) = \int_{\Gamma} p_{ij}^*(x, y)\psi_j(y) d\Gamma_y$ , where  $\psi \in \mathbf{H}^{1/2}(\Gamma)$ ,  $x \in \Gamma \subset \mathbb{R}^2$ .

$$p_{ij}^*(x, y) := \frac{1}{4\alpha\pi(1-\nu)|x-y|^\alpha} \left\{ \left[ (1-2\nu)\delta_{ij} + \beta \frac{(x_i-y_i)(x_j-y_j)}{|x-y|^2} \right] \frac{(x_k-y_k)n_k}{|x-y|} - (1-2\nu) \frac{(x_i-y_i)n_j - (x_j-y_j)n_i}{|x-y|} \right\}.$$

Recall that  $p_{ij}^*(x, y) = (T_y G(x, y))^T$  with the fundamental solution  $G$  of the Lamé operator. Where  $\alpha = 2, 1$ ,  $\beta = 3, 2$  for three- two-dimensional plane strain, respectively.

**Definition 3.1.3.** Kernel  $\sigma_{jki}^*$

$$\sigma_{jki}^*(x, y) := \frac{1}{4\alpha\pi(1-\nu)|x-y|^\alpha} \left\{ (1-2\nu) \left( \frac{x_k-y_k}{|x-y|} \delta_{ij} + \frac{x_j-y_j}{|x-y|} \delta_{ki} - \frac{x_i-y_i}{|x-y|} \delta_{jk} \right) + \beta \frac{(x_i-y_i)(x_j-y_j)(x_k-y_k)}{|x-y|^3} \right\},$$

where  $\alpha = 2, 1$ ,  $\beta = 3, 2$  for three- two-dimensional plane strain, respectively.

Hence, Definition 3.1.3 in 2D gives

$$\sigma_{ijk}^*(x, y) = \frac{1}{4\pi(1-\nu)} \left\{ (1-2\nu) \left( -\frac{\partial}{\partial y_j} \log|x-y| \delta_{ki} - \frac{\partial}{\partial y_i} \log|x-y| \delta_{jk} + \frac{\partial}{\partial y_k} \log|x-y| \delta_{ij} \right) + \frac{\partial}{\partial y_k} \left[ \frac{(x_i-y_i)(x_j-y_j)}{|x-y|^2} \right] - \delta_{ik} \frac{\partial}{\partial y_j} \log|x-y| - \delta_{jk} \frac{\partial}{\partial y_i} \log|x-y| \right\}$$

$$\begin{aligned}
 &= \frac{1}{4\pi(1-\nu)} \left\{ -2(1-\nu) \left( \frac{\partial}{\partial y_j} \log|x-y| \delta_{ki} + \frac{\partial}{\partial y_i} \log|x-y| \delta_{jk} \right) \right. \\
 &+ \left. (1-2\nu) \frac{\partial}{\partial y_k} \log|x-y| \delta_{ij} + \frac{\partial}{\partial y_k} \left[ \frac{(x_i - y_i)(x_j - y_j)}{|x-y|^2} \right] \right\} 2D.
 \end{aligned}$$

*Remark 3.1.1.* In 3D  $\hat{\sigma}_{jki}^*(x, y) = \sigma_{jki}^*(x, y)$ . But not in 2D plain strain configuration. If the trace of nonelastic part of strain equals zero then:

$$\hat{\sigma}_{jki}^*(x, y) = \sigma_{jki}^*(x, y) - \frac{2\nu(x_i - y_i)}{4\pi(1-\nu)|x-y|^2} \delta_{jk}. \quad (3.4)$$

or

$$\hat{\sigma}_{ijk}^*(x, y) = \sigma_{ijk}^*(x, y) - \frac{2\nu(x_k - y_k)}{4\pi(1-\nu)|x-y|^2} \delta_{ij}. \quad (3.5)$$

then

$$\begin{aligned}
 \hat{\sigma}_{ijk}^*(x, y) = \frac{1}{4\pi(1-\nu)|x-y|} \left\{ (1-2\nu) \left( \frac{x_j - y_j}{|x-y|} \delta_{ki} + \frac{x_i - y_i}{|x-y|} \delta_{jk} - \frac{x_k - y_k}{|x-y|} \delta_{ij} \right) \right. \\
 \left. + 2 \frac{(x_k - y_k)(x_i - y_i)(x_j - y_j)}{|x-y|^3} \right\}
 \end{aligned}$$

or

$$\begin{aligned}
 \sigma_{ijk}^*(x, y) &= \frac{1}{4\alpha\pi(1-\nu)} \left\{ -2(1-\nu) \left( \frac{\partial}{\partial y_j} \log|x-y| \delta_{ki} + \frac{\partial}{\partial y_i} \log|x-y| \delta_{jk} \right) \right. \\
 &+ \left. \frac{\partial}{\partial y_k} \log|x-y| \delta_{ij} + \frac{\partial}{\partial y_k} \left[ \frac{(x_i - y_i)(x_j - y_j)}{|x-y|^2} \right] \right\} 2D.
 \end{aligned}$$

For pure thermal strains one has

$$\hat{\sigma}_{jki}^*(x, y) = \sigma_{jki}^*(x, y) + \frac{\nu(x_i - y_i)}{4\pi(1-\nu)|x-y|^2} \delta_{jk}. \quad (3.6)$$

**Definition 3.1.4.** Kernel  $u_{ijk}^*(x, y) := -\sigma_{ijk}^*$  corresponds to the Newton potential  $(N_1\psi)_{ij}(x) = \int_{\Omega} u_{ijk}^*(x, y) \psi_k(y) d\Omega_y$ , where  $\psi \in \mathbf{H}^1(\Omega)$ ,  $x \in \Gamma \subset \mathbb{R}^2$ .

**Definition 3.1.5.** Kernel  $p_{ijk}^*$

$$\begin{aligned}
 p_{ijk}^*(x, y) &:= \frac{G}{2\alpha\pi(1-\nu)|x-y|^\beta} \left\{ \beta \frac{(x_l - y_l) n_l}{|x-y|} \left[ (1-2\nu) \delta_{ij} \frac{x_k - y_k}{|x-y|} \right. \right. \\
 &+ \left. \left. \nu \left( \delta_{ik} \frac{x_j - y_j}{|x-y|} + \delta_{jk} \frac{x_i - y_i}{|x-y|} \right) - \gamma \frac{(x_i - y_i)(x_j - y_j)(x_k - y_k)}{|x-y|^3} \right] \right. \\
 &+ \left. \beta\nu \left( n_i \frac{(x_j - y_j)(x_k - y_k)}{|x-y|^2} + n_j \frac{(x_i - y_i)(x_k - y_k)}{|x-y|^2} \right) \right\}
 \end{aligned}$$

### 3 Appendix

$$+ (1 - 2\nu)(\beta n_k \frac{(x_i - y_i)(x_j - y_j)}{|x - y|^2} + n_j \delta_{ik} + n_i \delta_{jk}) - (1 - 4\nu)n_k \delta_{ij} \} \quad (3.7)$$

where  $\alpha = 2, 1$ ,  $\beta = 3, 2$ ,  $\gamma = 5, 4$  for three and two dimensions respectively.

**Definition 3.1.6.** Kernel  $\sigma_{ijkl}^*$

$$\begin{aligned} \sigma_{ijkl}^* &:= \frac{G}{2\alpha\pi(1-\nu)r^\beta} \{ \beta(1-2\nu)(\delta_{ij}r_{,k}r_{,l} + \delta_{kl}r_{,i}r_{,j}) \\ &+ \beta\nu(\delta_{li}r_{,j}r_{,k} + \delta_{jk}r_{,l}r_{,i} + \delta_{ik}r_{,l}r_{,j} + \delta_{jl}r_{,i}r_{,k}) - \beta\gamma r_{,i}r_{,j}r_{,k}r_{,l} \\ &+ (1-2\nu)(\delta_{ik}\delta_{lj} + \delta_{jk}\delta_{li}) - (1-4\nu)\delta_{ij}\delta_{kl} \}, \end{aligned}$$

where  $\alpha = 2, 1$ ,  $\beta = 3, 2$ ,  $\gamma = 5, 4$  for three-dimensions and plane strain, respectively, and

$$r_{,i} := \frac{\partial|x-y|}{\partial y_i} = \frac{y_i - x_i}{|x-y|}.$$

In case trace  $\varepsilon^a = 0$

$$\hat{\sigma}_{ijkl}^*(x, y) = \sigma_{ijkl}^*(x, y) + \frac{G}{2\pi(1-\nu)r^2} [4\nu r_{,i}r_{,j}\delta_{kj} - 2\nu\delta_{ij}\delta_{kl}], \quad (3.8)$$

$$f_{ij} = -\frac{G}{4(1-\nu)} [2\varepsilon_{ij}^a + (1-4\nu)\varepsilon_{ll}^a\delta_{ij}]. \quad (3.9)$$

For pure thermal strains one has

$$\hat{\sigma}_{ijkl}^*(x, y) = \sigma_{ijkl}^*(x, y) - \frac{G}{2\pi(1-\nu)r^2} [2\nu r_{,i}r_{,j}\delta_{kj} - \nu\delta_{ij}\delta_{kl}] \quad (3.10)$$

$$f_{ij} = -\frac{G(1+\nu)}{1-\nu} \alpha T \delta_{ij} \quad \alpha - \text{thermal coefficient, don't mix with another } \alpha \quad (3.11)$$

In the next two subsections we will provide regularization procedures for a boundary integral operator with the kernel  $p_{ijk}^*$  and for a volume integral operator with the kernel  $\sigma_{jki}^*$ . The aim of the regularization is to reduce the order of a singularity of the strongly singular kernels, in order to simplify an implementation procedure.

#### Regularization of $p_{ijk}^*$

We regularize a boundary integral operator in (3.2) with a hyper-singular kernel  $p_{ijk}^*$  (Definition 3.1.5) employing an integration by part as follows

$$p_{ik}^{0*}(x, y) := \frac{1}{2\pi} \frac{G}{1+\nu} \left[ -\log|x-y|\delta_{ik} + \frac{(x_i - y_i)(x_j - y_j)}{|x-y|^2} \right] \text{ see [45] p. 157,}$$



we have

$$\begin{aligned}\int_{\Gamma} p_{i0k}^*(x, y) u_k(y) &= \frac{\partial}{\partial x_1} \int_{\Gamma} \frac{\partial}{\partial s_y} p_{ik}^{0*}(x, y) u_k(y), \\ \int_{\Gamma} p_{i1k}^*(x, y) u_k(y) &= -\frac{\partial}{\partial x_0} \int_{\Gamma} \frac{\partial}{\partial s_y} p_{ik}^{0*}(x, y) u_k(y),\end{aligned}$$

or

$$\begin{aligned}\int_{\Gamma} p_{i0k}^*(x, y) u_k(y) &= -\int_{\Gamma} \left[ \frac{\partial}{\partial y_1} \frac{\partial}{\partial s_y} p_{ik}^{0*}(x, y), \right] u_k(y) \\ \int_{\Gamma} p_{i1k}^*(x, y) u_k(y) &= \int_{\Gamma} \left[ \frac{\partial}{\partial y_0} \frac{\partial}{\partial s_y} p_{ik}^{0*}(x, y), \right] u_k(y)\end{aligned}$$

*Remark 3.1.2.* In pure linear elasticity there is no big difference in 2D and 3D.

### Regularization of volume integrals

The volume integral in (3.1) with a singular kernel  $\sigma_{jki}^*$  admits straightforward implementation. The advantage of a regularization procedure, is that one can rewrite The volume integral an equivalent form as a sum of a boundary integral operator with a weakly-singular kernel  $u_{ij}^*$  and a volume integral operator with the same kernel.

$$\sigma_{jki}^*(x, y) = G (u_{ij,k}^* + u_{ik,j}^*) + \frac{2G\nu}{1-2\nu} u_{il,l}^* \delta_{jk},$$

where  $u_{il,l}^* := u_{i1,1}^* + u_{i2,2}^*$  in 2D,  $u_{il,l}^* := u_{i1,1}^* + u_{i2,2}^* + u_{i3,3}^*$  in 3D.

Hence,

$$\int_{\Omega} \sigma_{jki}^* \varepsilon_{jk}^a d\Omega = \int_{\Omega} \left\{ G (u_{ij,k}^* + u_{ik,j}^*) + \frac{2G\nu}{1-2\nu} u_{il,l}^* \delta_{jk} \right\} \varepsilon_{jk}^a d\Omega$$

and after integrating by parts

$$\int_{\Omega} \sigma_{jki}^* \varepsilon_{jk}^a d\Omega = \int_{\Gamma} u_{ij}^* 2G \left( \varepsilon_{jk}^a n_k + \frac{\nu}{1-2\nu} \varepsilon_{ll}^a \right) - \int_{\Omega} u_{ij}^* 2G \left( \varepsilon_{jk,k}^a + \frac{\nu}{1-2\nu} \varepsilon_{ll,l}^a \right),$$

$$u_i(x) = \int_{\Gamma} u_{ij}^*(x, y) \check{p}_j(y) - \int_{\Gamma} p_{ij}^*(x, y) u_j(y) + \int_{\Omega} u_{ij}^*(x, y) \check{b}_j(y), \quad (3.12)$$

where

$$\check{b}_j = b_j - 2G \left( \varepsilon_{ij,i}^a + \frac{\nu}{1-2\nu} e_{,j} \right) = b_j - \sigma_{ij,i}^a$$

### 3 Appendix

$$\check{p}_i = b_i + 2G \left( \varepsilon_{ij}^a n_j + \frac{\nu}{1-2\nu} e n_i \right) = p_i + \sigma_{ij}^a n_j$$

For plane problems (2D) these equations can also be used (i,j,k,l=1,2) with  $e = \varepsilon_{11} + \varepsilon_{22} + \varepsilon_{33}$  in plane strain and  $\nu$  replaced by  $\bar{\nu} = \frac{\nu}{1+\nu}$  with  $e = \varepsilon_{11} + \varepsilon_{22}$  in plane stress.

$$\int_{\Omega} \hat{\sigma}_{jki}^* \varepsilon_{jk}^a d\Omega = \int_{\Omega} \sigma_{jki}^* \varepsilon_{jk}^a + \int_{\Omega} \frac{2\nu \delta_{jk} r_{,i}}{4\pi(1-\nu)r} \varepsilon_{jk}^a \quad \text{if } e = 0$$

and after integrating by parts

$$\int_{\Omega} \sigma_{jki}^* \varepsilon_{jk}^a d\Omega = \int_{\Gamma} u_{ij}^* 2G \left( \varepsilon_{jk}^a n_k + \frac{\nu}{1-2\nu} \varepsilon_{ll}^a \right) - \int_{\Omega} u_{ij}^* 2G \left( \varepsilon_{jk,k}^a + \frac{\nu}{1-2\nu} \varepsilon_{ll,l}^a \right),$$

$$\sigma_{ij}(x) = \int_{\Gamma} u_{ijk}^*(x, y) \check{p}_k(y) - \int_{\Gamma} p_{ijk}^*(x, y) u_k(y) + \int_{\Omega} u_{ijk}^*(x, y) \check{b}_k(y) - C_{ijkl} \varepsilon_{kl}^a.$$

### Boundary Elements - Plasticity

' Poincaré-Steklov '

$$\begin{pmatrix} u \\ Tu \end{pmatrix}^{int} = \begin{pmatrix} -K + \frac{1}{2} & V \\ W & K' + \frac{1}{2} \end{pmatrix} \begin{pmatrix} u \\ \tilde{T}u \end{pmatrix}^{int} + \begin{pmatrix} \tilde{N}_0 f \\ \tilde{N}_1 f \end{pmatrix}^{int}$$

it follows that

$$Tu = Wu + \left( K' + \frac{1}{2} \right) V^{-1} \left( K + \frac{1}{2} \right) u - \left( K' + \frac{1}{2} \right) V^{-1} \tilde{N}_0 f + \tilde{N}_1 f$$

or

$$Tu = Su - \left( K' + \frac{1}{2} \right) V^{-1} \tilde{N}_0 f + \tilde{N}_1 f,$$

where  $N_0$ , and  $N_1$  - Newton potentials, that corresponds to the integration over a volume.

$$\begin{aligned} \langle SD, \eta \rangle_{|\Gamma \setminus \Gamma_D} &= \langle Tu, \eta \rangle_{|\Gamma \setminus \Gamma_D} + \left\langle \left( K' + \frac{1}{2} \right) V^{-1} \tilde{N}_0 f, \eta \right\rangle_{|\Gamma \setminus \Gamma_D} \\ &\quad - \langle \tilde{N}_1 f, \eta \rangle_{|\Gamma \setminus \Gamma_D} - \langle SD_0, \eta \rangle_{|\Gamma \setminus \Gamma_D}, \end{aligned} \quad (3.13)$$

where  $D$  - unknown displacement that lives on the non-Dirichlet part of the boundary.  $\eta$  - test function that lives in the same discrete subset as  $D$ .  $D_0$  - prescribed Dirichlet

data on the boundary part  $\Gamma_D$ .  $\Gamma$  - whole boundary. It should be mentioned that action of Poincaré-Steklov on the  $D_0$  has integration over  $\Gamma_D$  inside.

### Symmetric Boundary Elements with ' Poincaré-Steklov operator

$$\begin{pmatrix} u \\ Tu \end{pmatrix}^{int} = \begin{pmatrix} -K + \frac{1}{2} & V \\ W & K' + \frac{1}{2} \end{pmatrix} \begin{pmatrix} u \\ Tu \end{pmatrix}^{int} + \begin{pmatrix} \widetilde{N}_0^a \varepsilon^a \\ \widetilde{N}_1^a \varepsilon^a \end{pmatrix}^{int} - \begin{pmatrix} 0 \\ \widetilde{T}u \end{pmatrix}$$

where

$$\widetilde{T}u_i = C_{ijkl} \varepsilon_{kl}^a n_j$$

it follows that

$$Tu = Wu + \left(K' + \frac{1}{2}\right) V^{-1} \left(K + \frac{1}{2}\right) u - \left(K' + \frac{1}{2}\right) V^{-1} \widetilde{N}_0^a \varepsilon^a + \widetilde{N}_1^a \varepsilon^a - \widetilde{T}u \quad (3.14)$$

or

$$Tu = Su - \left(K' + \frac{1}{2}\right) V^{-1} \widetilde{N}_0^a \varepsilon^a + \widetilde{N}_1^a \varepsilon^a - \widetilde{T}u.$$

### Symmetric Boundary Elements with ' Poincaré-Steklov operator. Regularization

$$\begin{aligned} \begin{pmatrix} u \\ Tu \end{pmatrix}^{int} &= \begin{pmatrix} -K + \frac{1}{2} & V \\ W & K' + \frac{1}{2} \end{pmatrix} \begin{pmatrix} u \\ Tu \end{pmatrix}^{int} + \begin{pmatrix} \widetilde{N}_0 \widetilde{f} \\ \widetilde{N}_1 \widetilde{f} \end{pmatrix}^{int} \\ &+ \begin{pmatrix} \widetilde{V} \widetilde{T}u \\ (\widetilde{K}' + \frac{1}{2}) \widetilde{T}u \end{pmatrix}^{int} - \begin{pmatrix} 0 \\ \widetilde{T}u \end{pmatrix}, \end{aligned}$$

where

$$\left. \begin{aligned} \widetilde{f}_j &= -2G \left( \varepsilon_{ij,i}^a + \frac{\nu}{1-2\nu} e_{,j} \right), \\ \widetilde{T}u_i &= 2G \left( \varepsilon_{ij}^a n_j + \frac{\nu}{1-2\nu} e n_i \right), \end{aligned} \right\} \quad (3.15)$$

it follows that

$$Tu = Wu + \left(K' + \frac{1}{2}\right) V^{-1} \left(K + \frac{1}{2}\right) u - \left(K' + \frac{1}{2}\right) V^{-1} \widetilde{N}_0 \widetilde{f} + \widetilde{N}_1 \widetilde{f} - \widetilde{T}u$$

$$- \left( K' + \frac{1}{2} \right) V^{-1} \widetilde{V} \widetilde{T}u + \widetilde{\left( K' + \frac{1}{2} \right) T}u,$$

or

$$Tu = Su - \left( K' + \frac{1}{2} \right) V^{-1} \widetilde{N}_0 \widetilde{f} + \widetilde{N}_1 \widetilde{f} - \left( K' + \frac{1}{2} \right) V^{-1} \widetilde{V} \widetilde{T}u + \widetilde{\left( K' + \frac{1}{2} \right) T}u - \widetilde{T}u.$$

Using the notation (3.15) we can perform integration by part for  $\widetilde{N}_0^a, \widetilde{N}_1^a$

$$\begin{aligned} \widetilde{N}_0^a \varepsilon^a &= \widetilde{N}_0 \widetilde{f} + \widetilde{V} \widetilde{T}u, \\ \widetilde{N}_1^a \varepsilon^a &= \widetilde{N}_1 \widetilde{f} + \widetilde{\left( K' + \frac{1}{2} \right) T}u. \end{aligned}$$

Defining

$$\begin{aligned} \widehat{T}u &:= \widetilde{T}u + Tu, \\ \widehat{f} &:= \widetilde{f} + f, \end{aligned}$$

we get formulation as in Section 3.1.1.

### 3.1.2 Hypoelasto-viscoplasticity

#### Integral computation/implementation

$$\begin{aligned} \tau_{ij}^* &= \dot{s}_{ij} + (\sigma_{ik} d_{jk} + \sigma_{kj} d_{ik}) - \sigma_{ik} v_{j,k}, \\ \tau_{ij}^* &= \dot{s}_{ji} + \overset{(*)}{G}_{jikl} v_{k,l}, \end{aligned}$$

where

$$\begin{aligned} \tau_{ij}^* &= \dot{s}_{ji} + \overset{(*)}{G}_{jikl} v_{k,l} \\ d_{ij} &:= \frac{1}{2} \left( \frac{\partial v_i}{\partial x_j} + \frac{\partial v_j}{\partial x_i} \right) =: \frac{1}{2} (v_{i,j} + v_{j,i}), \end{aligned}$$

$$\begin{aligned} \sigma_{ik} d_{jk} + \sigma_{kj} d_{ik} - \sigma_{ik} v_{j,k} &= \frac{1}{2} (\sigma_{ik} v_{j,k} + \sigma_{ik} v_{k,j} + \sigma_{kj} v_{i,k} + \sigma_{kj} v_{k,i}) - \sigma_{ik} v_{j,k} \\ &= \frac{1}{2} (\sigma_{il} v_{k,l} \delta_{jk} + \sigma_{ik} v_{k,l} \delta_{jl} + \sigma_{lj} v_{k,l} \delta_{ki} + \sigma_{kj} v_{k,l} \delta_{li}) - \sigma_{il} v_{k,l} \delta_{kj}. \end{aligned}$$

We can write  $\overset{(*)}{G}_{ijkl}$  :

$$\overset{(*)}{G}_{ijkl} := \frac{1}{2} (\sigma_{il}\delta_{jk} + \sigma_{ik}\delta_{jl} + \sigma_{lj}\delta_{ki} + \sigma_{kj}\delta_{li}) - \sigma_{il}\delta_{kj}.$$

We multiply the rate of the equilibrium equation

$$\dot{s}_{ji,j} + \rho_0 \dot{F}_i^0 = 0$$

with a test function  $\tilde{v} \in H^1$ , (ansatz function  $v \in H_{DIR} + \overset{0}{H}^1$ ):

$$\int_{B^0} [\dot{s}_{ji,j}\tilde{v}_i + \rho_0 \dot{F}_i^0 \tilde{v}_i] = 0.$$

Integration by parts yields

$$\int_{B^0} \dot{s}_{ji}\tilde{v}_{i,j} - \int_{\partial B^0} \dot{s}_{ji}n_j^0\tilde{v}_i - \int_{B^0} \rho_0 \dot{F}_i^0 \tilde{v}_i = 0.$$

Using  $\dot{\tau}_i := \dot{s}_{ji}n_j^0$ , and  $\dot{s}_{ji} = \dot{\tau}_{ij} - \overset{(*)}{G}_{jikl} v_{k,l}$  we have

$$\int_{B^0} \dot{\tau}_{ij} \tilde{v}_{i,j} - \int_{B^0} \overset{(*)}{G}_{jikl} v_{k,l}\tilde{v}_{i,j} - \int_{\partial B^0} \dot{\tau}_i \tilde{v}_i - \int_{B^0} \rho_0 \dot{F}_i^0 \tilde{v}_i = 0.$$

Using  $\dot{\tau}_{ij} = \lambda d_{kk}^{(e)}\delta_{ij} + 2\mu d_{ij}^{(e)}$  and  $d_{ij} := d_{ij}^{(e)} + d_{ij}^{(n)}$  we have

$$\int_{B^0} C_{ijkl}d_{kl}^{(e)}\tilde{d}_{ij} - \int_{B^0} \overset{(*)}{G}_{jikl} v_{k,l}\tilde{v}_{i,j} - \int_{\partial B^0} \dot{\tau}_i \tilde{v}_i - \int_{B^0} \rho_0 \dot{F}_i^0 \tilde{v}_i = 0.$$

Hence,

$$\int_{B^0} C_{ijkl}d_{kl}\tilde{d}_{ij} - \int_{B^0} \overset{(*)}{G}_{jikl} v_{k,l}\tilde{v}_{i,j} - \int_{\partial B^0} \dot{\tau}_i \tilde{v}_i - \int_{B^0} \rho_0 \dot{F}_i^0 \tilde{v}_i = - \int_{B^0} C_{ijkl}d_{kl}^{(n)}\tilde{d}_{ij}, \quad (3.16)$$

where

$$\int_{B^0} C_{ijkl}d_{kl}\tilde{d}_{ij} \quad (3.17)$$

is a standard FEM matrix of the Lamé operator in the theory of linear elasticity. The subroutine **stiff2lame** located in *libfem2.f90* computes a contribution of one element to the global stiffness matrix.

Since the second integral in (3.16) is more complex we examine it more carefully.

We represent a test function and an ansatz function on the finite element  $\square$  as  $\tilde{v} = \begin{pmatrix} \tilde{v}_1 \\ \tilde{v}_2 \end{pmatrix} \tilde{\psi}(\mathbf{x})$ ,  $v = \begin{pmatrix} v_1 \\ v_2 \end{pmatrix} \psi(\mathbf{x})$  respectively. Then the second integral  $\int_{B^0} \overset{(*)}{G}_{jikl} v_{k,l}\tilde{v}_{i,j}$

### 3 Appendix

in (3.16) is a sum of local integrals having the form

$$\int_{\square} G_{j i k l}^{(*)} v_{k,l} \tilde{v}_{i,j} dx_1 dx_2 = \int_{-1}^1 \int_{-1}^1 \left| \frac{\partial x}{\partial \xi} \right| \sum_{i=1}^2 \sum_{j=1}^2 \sum_{k=1}^2 \sum_{l=1}^2 \sum_{p=1}^2 \sum_{q=1}^2 \tilde{v}_i \frac{\partial \tilde{\psi}}{\partial \xi_p} \frac{\partial \xi_p}{\partial x_j} G_{j i k l}^{(*)} \frac{\partial \xi_q}{\partial x_l} \frac{\partial \psi}{\partial \xi_q} v_k d\xi_1 d\xi_2.$$

The subroutine **stiff2lameplvijCjijklukl** located in *comp22pl.f90* computes a local matrix for one mesh element

$$\text{tmat}(p,q,i,k) := \frac{\partial \xi_p}{\partial x_j} G_{j i k l}^{(*)} \frac{\partial \xi_q}{\partial x_l}$$

The subroutine **rseiteid** located in *comp2c.f90.f90* computes a contribution of the given Neumann data to the right hand side, i.e. the integral

$$\int_{\partial B^0} \dot{\tau}_i \tilde{v}_i.$$

The subroutine **lcomp2** located in *comp22.f90* computes a contribution of the given volume data to the right hand side, i.e. the integral

$$\int_{B^0} \rho_0 \dot{F}_i^0 \tilde{v}_i.$$

The subroutine **lftgrdcomp2** located in *compstiff2.f90.f90* computes a contribution of one element to the right hand side for the volume integral

$$\int_{B^0} C_{ijkl} d_{kl}^{(n)} \tilde{d}_{ij}.$$

# Bibliography

- [1] J. ALBERTY, *Zeitdiskretisierungsverfahren für elastoplastische Probleme der Kontinuumsmechanik*, PhD thesis, Christian Albrechts Universität zu Kiel, Technische Fakultät, 2001.
- [2] O. AXELSSON, R. BLAHETA, AND R. KOHUT, *Inexact newton solvers in plasticity: theory and experiments*, Numerical Linear Algebra with Applications, 4 (1997), pp. 133–152.
- [3] F. B. BELGACEM, *The mortar finite element method with Lagrange multipliers*, Numerische Mathematik, 84 (1999), pp. 173–197. Published online September 24, 1999.
- [4] T. BELYTSCHKO, W. K. LIU, AND B. MORAN, *Nonlinear finite elements for continua and structures*, John Wiley & Sons Ltd., Chichester, 2000.
- [5] R. BLAHETA, *Convergence of newton-type methods in incremental return mapping analysis of elasto-plastic problems*, Computer Methods in Applied Mechanics and Engineering, 147 (1997), pp. 167–186.
- [6] R. BLAHETA AND O. AXELSSON, *Convergence of inexact newton-like iterations in incremental finite element analysis of elasto-plastic problems*, Computer Methods in Applied Mechanics and Engineering, 141 (1997), pp. 281–295.
- [7] J. BONET AND R. D. WOOD, *Nonlinear Continuum Mechanics For Finite Element Analysis*, Campridge University Press, 1997.
- [8] D. BRAESS, *Finite elements: Theory, fast solvers and applications in solid mechanics, 2nd edn*, Measurement Science and Technology, 13 (2002), p. 1500.
- [9] C. A. BREBBIA, *The boundary element method for engineering*, Pentech Press, second revised ed., 1980. ISBN 0-7273-0205-1.
- [10] C. A. BREBBIA, ed., *Progress in boundary element methods*, vol. 1, Pentech Press, 1981.
- [11] —, ed., *Progress in boundary element methods*, vol. 2, Pentech Press, 1983.
- [12] C. A. BREBBIA, J. C. F. TELLES, AND L. C. WROBEL, *Boundary element techniques. Theory and applications in engineering.*, Springer-Verlag, 1984.

- [13] C. A. BREBBIA AND S. WALKER, *Boundary element techniques in engineering*, Newnes-Butterworth, 1980. ISBN 0-408-00340-5.
- [14] C. CARSTENSEN AND E. P. STEPHAN, *Adaptive coupling of boundary elements and finite elements*, RAIRO Modél. Math. Anal. Numér., 29 (1995), pp. 779–817.
- [15] C. CARSTENSEN AND E. P. STEPHAN, *Coupling of fem and bem for a nonlinear interface problem: the  $h - p$  version*, Numerical Methods for Partial Differential Equations, 11 (1995), pp. 539–554.
- [16] A. CHANDRA AND S. MUKHERJEE, *Boundary element formulations for large strain-large deformation problems of plasticity and viscoplasticity*, in Developments in Boundary Element Methods, P. Banarjee and S. Mukherjee, eds., vol. 3, Elsevier Applied Science Publishers, 1984, ch. 2, pp. 27–58.
- [17] —, *Boundary element formulations for large strain-large deformation problems of viscoplasticity*, International Journal of Solids and Structures, 20 (1984), pp. 41–53.
- [18] —, *A finite element analysis of meta-forming problems with an elastic-viscoplastic material model*, International Journal for Numerical Methods in Engineering, 20 (1984), pp. 1613–1628.
- [19] A. CHERNOV, S. GEYN, M. MAISCHAK, AND E. P. STEPHAN, *Domain decomposition finite element/boundary element techniques for elastoplastic contact problems*, preprint 82, Institut für Angewandte Mathematik, Institut für Angewandte Mathematik, Universität Hannover, Welfengarten 1, D-30167 Hannover, Germany, 2005.
- [20] —, *Boundary element procedures for elastoplastic contact problems*, preprint, Leibniz Universität Hannover, IfAM, 2006.
- [21] —, *Finite element/boundary element procedures for elastoplastic contact problems*, preprint 80, Institut für Angewandte Mathematik, Institut für Angewandte Mathematik, Leibniz Universität Hannover, Welfengarten 1, D-30167 Hannover, Germany, 2006.
- [22] M. COSTABEL, *Boundary integral operators on Lipschitz domains: Elementary results*, SIAM J. Math. Anal., 19(3) (1988), pp. 613–626.
- [23] M. COSTABEL AND E. P. STEPHAN, *Coupling of finite elements and boundary elements for inhomogeneous transmission problems in  $\mathbb{R}^3$* , in MAFELAP IV, J. White-man, ed., Academic Press, London, 1988, pp. 289–296.
- [24] —, *Coupling of finite and boundary element methods for an elastoplastic interface problem*, SIAM J. Numer. Anal., 27 (1990), pp. 1212–1226.



- [25] L. DONIGA-CRIVAT, *Kopplung von randelementen und finiten elementen für visko-plastische probleme*, Master's thesis, Universität Hannover, Institut für Angewandte Mathematik, 2005.
- [26] C. ECK AND J. JARUŠEK, *Existence results for the static contact problem with Coulomb friction*, Math. Models Methods Appl. Sci., 8 (1998), pp. 445–468.
- [27] C. ECK, O. STEINBACH, AND W. L. WENDLAND, *A symmetric boundary element method for contact problems with friction*, Math. Comput. Simulation, 50 (1999), pp. 43–61. Modelling '98 (Prague).
- [28] R. GLOWINSKI, *Numerical methods for nonlinear variational problems*, Springer Series in Computational Physics, Springer-Verlag, Berlin, 2000.
- [29] W. HAN AND B. D. REDDY, *Plasticity*, vol. 9 of Interdisciplinary Applied Mathematics, Springer-Verlag, New York, 1999. Mathematical theory and numerical analysis.
- [30] E. W. HART, *Constitutive relations for the nonelastic deformation of metals*, Journal of Engineering Materials and Technology, 98 (1976), pp. 193–202.
- [31] ———, *Stress and deformation analysis of metal extrusion process*, Computer Methods in Applied Mechanics and Engineering, 10 (1977), pp. 339–353.
- [32] ———, *The effects of material rotations in tension-torsion testing*, International Journal of Solids and Structures, 18 (1982), pp. 1031–1042.
- [33] L. JOHANSSON AND A. KLARBRING, *Thermoelastic frictional contact problems: Modelling, finite element approximation and numerical realization*, Computer Methods in Applied Mechanics and Engineering, 105 (1993), pp. 181–210.
- [34] V. G. KORNEEV AND U. LANGER, *Approximate solution of plastic flow theory problems*, vol. 69 of Teubner-Texte zur Mathematik [Teubner Texts in Mathematics], BSB B. G. Teubner Verlagsgesellschaft, Leipzig, 1984. With German, French and Russian summaries.
- [35] T. A. LAURSEN, *Computational Contact and Impact Mechanics*, Springer, 2003.
- [36] M. MAISCHAK, *Technical manual of the program system maiprogs*, preprint, Institut für Angewandte Mathematik, Universität Hannover, 1996.
- [37] ———, *Book of numerical experiments (B.O.N.E.) with maiprogs*, preprint, Institut für Angewandte Mathematik, Universität Hannover, 2006. <ftp://ftp.ifam.uni-hannover.de/pub/preprints/ifam50.ps.Z>.

- [38] —, *Manual of the software package maiprugs*, technical report ifam48, Institut für Angewandte Mathematik, Universität Hannover, 2006. <ftp://ftp.ifam.uni-hannover.de/pub/preprints/ifam48.ps.Z>.
- [39] S. MUKHERJEE, *Boundary element methods in creep and fracture*, Applied Science Publishers, London and New Jersey, 1982.
- [40] D. PERIĆ AND D. R. J. OWEN, *Finite-element application to the nonlinear mechanics of solids*, Reports on Progress in Physics, 61 (1998), pp. 1495–1574.
- [41] C. POLIZZOTTO AND M. ZITO, *BIEM-based variational principles for elastoplasticity with unilateral contact boundary conditions*, Engineering Analysis with Boundary Elements, 21 (1998), pp. 329–338.
- [42] S. SAUTER AND C. SCHWAB, *Randelementmethoden. Analyse, Numerik und Implementierung schneller Algorithmen*, Teubner-Verlag, Wiesbaden, 2004.
- [43] J. C. SIMO AND T. J. R. HUGHES, *Computational inelasticity*, no. 7 in Interdisciplinary Applied Mathematics, Springer-Verlag, New York, 1998.
- [44] J. C. SIMO AND C. MIEHE, *Associative coupled thermoplasticity at finite strains: Formulation, numerical analysis and implementation*, Computer Methods in Applied Mechanics and Engineering, 98 (1992), pp. 41–104.
- [45] O. STEINBACH, *Numerische Nährungsverfahren für elliptische Randwertprobleme. Finite Elemente und Randelemente.*, Teubner, 2003.
- [46] E. P. STEPHAN, *Finite Elemente, Randelemente*. Lecture notes, 2003/2004.
- [47] —, *Numerik partieller Differentialgleichungen I/II*. Lecture notes, 2003/2004.
- [48] E. P. STEPHAN, *Coupling of boundary element methods and finite element methods*, in Encyclopedia of Computational Mechanics, E. Stein, R. de Borst, and T. J. Hughes, eds., John Wiley & Sons, 2004. Volume 1, Chapter 13: Fundamentals.
- [49] B. WOHLMUTH, *A mortar finite element method using dual spaces for the lagrange multiplier*, SIAM Journal on Numerical Analysis, 38 (2000), pp. 989–1012.
- [50] P. WRIGGERS, *Computational contact mechanics*, John Wiley & Sons Ltd, 2002.
- [51] P. WRIGGERS AND C. MIEHE, *Contact constraints within coupled thermomechanical analysis — a finite element model*, Comput. Methods Appl. Mech. Engrg, 113 (1994), pp. 301–319.
- [52] Y. YAMADA AND H. HIRAKAWA, *Large deformation and instability analysis in metal forming process*, in Applications of Numerical Methods to Forming Processes, vol. AMD 28, ASME, 1978, pp. 27–38.

- [53] D. ZARRABI, *Beiträge zur Numerik und Modellierung elastoplastischer Kontaktprobleme*, PhD thesis, Technische Fakultät, Christian-Albrechts-Universität zu Kiel, 2004.

# Curriculum Vitae

## Personal Details:

Name: Sergey Geyn  
Email: gein@ifam.uni-hannover.de  
Born: 8th Mai 1981, Tula, Russia  
Family Status: single

## Education:

since 10/2003 Ph.D. Student and Junior Researcher at Institute of Applied Mathematics, University of Hanover, Germany  
09/1998 - 06/2003 Student of Mathematics and Mechanics at Department of Computational Mechanics, Faculty of Mechanics and Mathematics, Moscow State Lomonosov University, Russia  
09/1997 - 06/1998 Specialized Educational and Research Center, M.V. Lomonosov Moscow State University - A.N. Kolmogorov School, Moscow, Russia  
09/1993 - 06/1997 Secondary School N 73, Tula, Russia  
09/1988 - 06/1993 Secondary School N 25, Tula, Russia

## Examinations:

25/06/2003 Honours Diploma in Mechanics and Applied Mathematics  
25/06/1998 State Examination (School-Leaving Certificate)

## Professional history:

01/2006-12/2006 Junior Researcher; DFG grant no. STE 573/7-1  
"Randelemente- / Finite Elemente-Verfahren bei Zerspanprozessen"  
University of Hanover, Germany  
10/2003 - 12/2005 Junior Researcher; DFG grant no. STE 573/5-1,  
"Kopplung von Randelementen und Finiten Elementen für Inkrementelle Umformverfahren"  
University of Hanover, Germany  
09/1998-06/2003 Student of Mathematics and Mechanics at Department of Computational Mechanics, Faculty of Mechanics and Mathematics, Moscow State Lomonosov University, Russia

## Research Interests:

Finite Elements, Boundary Elements and their Coupling, Frictional Contact, Thermomechanical coupling, Software Development

## Language Skills:

native language Russian, English, German